New Perspectives on Post-Transcriptional Regulation Mechanisms in *Pseudomonas aeruginosa*

Von der Fakultät für Lebenswissenschaften

der Technischen Universität Carolo-Wilhelmina zu Braunschweig

zur Erlangung des Grades eines

Doktors der Naturwissenschaften

(Dr. rer. nat.)

genehmigte

D i s s e r t a t i o n

von Stephan Brouwer

aus Steinfurt

1. Referent: Professor Dr. Michael Steinert

2. Referentin: Professorin Dr. Susanne Häußler

eingereicht am: 20.04.2015

mündliche Prüfung (Disputation) am: 09.07.2015

Druckjahr 2015

Vorveröffentlichungen der Dissertation

Teilergebnisse aus dieser Arbeit wurden mit Genehmigung der Fakultät für Lebenswissenschaften, vertreten durch den Mentor der Arbeit, in folgenden Beiträgen vorab veröffentlicht:

Publikationen

Brouwer, S., Pustelny, C., Ritter, C., Klinkert, B., Narberhaus, F., & Häußler, S. The PqsR and RhlR transcriptional regulators determine the level of Pseudomonas quinolone signal synthesis in Pseudomonas aeruginosa by producing two different pqsABCDE mRNA isoforms. Journal of Bacteriology 196(23):4163-4171 (2014)

Pustelny, C.†, **Brouwer, S.**†, Müsken, M., Bielecka, A., Dötsch, A., Nimtz, M., & Häußler, S. The peptide chain release factor methyltransferase PrmC is essential for pathogenicity and environmental adaptation of Pseudomonas aeruginosa PA14. Environmental Microbiology 12(2):597-609 (2013)

† Authors made an equal contribution to the work

Tagungsbeiträge

Brouwer, S., Hoßmann, J., & Schuster, F. Regulation of gene expression in pathogenic bacteria. 5th Public Retreat HZI Graduate School, Goslar Hahnenklee (2014)

Posterbeiträge

Gödeke, J., **Brouwer, S.**, Preuße, M., & Häußler, S. Genetic and metabolic adaptation mechanisms in Pseudomonas aeruginosa towards environmental perturbations. 4. Joint Conference of the Association for General and Applied Microbiology (VAAM) and the Society of Hygiene and Microbiology (DGHM), Dresden (2014)

Brouwer, S., Pustelny, C., Müsken, M., Bielecka, A., Dötsch, A., Nimtz, M., & Häußler, S. Novel post-transcriptional regulation mechanisms in Pseudomonas aeruginosa. 4th Public Retreat HZI Graduate School, Goslar Hahnenklee (2013)

Brouwer, S., Pustelny, C., & Häußler, S. The putative methyltransferase HemK is essential for pathogenicity of Pseudomonas aeruginosa. 5th International PhD Symposium, HZI, Braunschweig (2011)

What is a scientist after all?

It is a curious man looking through a keyhole,

the keyhole of nature,

trying to know what's going on.

Jacques-Yves Cousteau

Abstract

Regulation of gene expression plays a key role in bacterial adaptability to changes in the environment. Quorum sensing (QS) systems constitute an integral part of this gene regulatory network and coordinate bacterial responses under high cellular densities. In the nosocomial pathogen *Pseudomonas aeruginosa*, a sophisticated QS network exists controlling virulence factor synthesis important for pathogenesis.

The overall aim of this thesis was to gain insight into novel regulation mechanisms of QS-based gene expression at the post-transcriptional level. In this context, we characterized the S-adenosyl-L-methionine-dependent methyltransferase (PrmC), specifically methylating a conserved GGQ motif of peptide chain release factors. Mutation of *prmC* was shown to predominantly affect the expression of major virulence-associated factors and caused attenuation of virulence in a *Galleria mellonella* larvae infection model. Furthermore, a previously unrecognized post-transcriptional regulation mechanism in bacteria was characterized. This involved an RhlR-mediated transcriptional induction of a secondary structure in the 5' untranslated region of the *pqs* operon transcript. The resulting hairpin-like structure sterically hinders ribosomal access to the ribosome binding site thus repressing *pqs* signaling. Another important focus of the work was to establish ribosome profiling (Ribo-Seq). The technique Ribo-Seq is based on deep sequencing of ribosome-protected mRNA fragments and provides a global snapshot of translation *in vivo*. This powerful tool opens up wide-ranging prospects to the developing picture of post-transcriptional regulation in *P. aeruginosa*.

Finally, the present thesis focuses on the role of PqsE as part of the *pqs* QS system in regulating QS-dependent virulence factor production. We provide evidence that PqsE is an enzyme that interferes with carbon flow at the chorismate branching point in the complex metabolic network of *P. aeruginosa*. By using a multi-methodological approach, we suggest that PqsE is involved in the biosynthesis of phenylpyruvate, being a possible signal molecule for the *rhl* QS system.

Zusammenfassung

Regulation der Genexpression spielt eine zentrale Rolle in der bakteriellen Anpassungsfähigkeit an sich verändernde Umweltbedingungen. Quorum sensing (QS) Systeme sind ein wesentlicher Bestandteil dieses regulatorischen Netzwerkes und koordinieren bakterielle Reaktionen bei hoher Zelldichte. In dem nosokomialen Pathogen *Pseudomonas aeruginosa* existiert ein komplexes QS Netzwerk, welches die Synthese von Virulenzfaktoren kontrolliert die wichtig für die Pathogenese sind.

Allgemeines Ziel dieser Dissertation war es, Einblicke in neuartige Regulationsmechanismen auf QS-basierender Genexpression auf dem post-transkriptionellen Level zu gewinnen. In diesem Zusammenhang haben wir die S-Adenosyl-L-Methionin-abhängige Methyltransferase (PrmC) charakterisiert, die spezifisch ein konserviertes GGQ Motif der Terminationsfaktoren methyliert. Es wurde gezeigt, dass *prmC* Mutation vorwiegend die Expression wichtiger Virulenz-assoziierter Faktoren betraf und eine Abschwächung der Virulenz in einem *Galleria mellonella* Larven Infektionsmodel zur Folge hatte. Zudem wurde ein zuvor unerkannter post-transkriptioneller Regulationsmechanismus charakterisiert. Dieser umfasst eine RhlR-vermittelte transkriptionelle Induktion einer Sekundärstruktur in der 5‘ nicht-codierenden Region des *pqs* Operon Transkripts. Die daraus resultierende Haarnadel-ähnliche Struktur verhindert sterisch den Zugang des Ribosoms an die ribosomale Bindungsstelle und unterdrückt auf diese Weise das *pqs* Signalsystem. Ein weiterer wichtiger Fokus dieser Arbeit bestand darin, ribosome profiling (Ribo-Seq) zu etablieren. Die Ribo-Seq Technik basiert auf dem deep sequencing von Ribosom geschützten mRNA Fragmenten, und verschafft eine globale Momentaufnahme der Translation *in vivo*. Dieses leistungsfähige methodische Werkzeug eröffnet umfangreiche Perspektiven im Hinblick auf das sich entwickelnde Bild der post-transkriptionellen Regulation in *P. aeruginosa*.

Schließlich liegt ein Fokus dieser Dissertation auf der Rolle von PqsE als wichtiger Bestandteil des *pqs* QS Systems in der Regulation QS-abhängiger Virulenzfaktorproduktion. Wir konnten zeigen, dass PqsE ein Enzym ist, welches in den Kohlenstoffstrom an dem Chorisminsäure Verzweigungspunkt des komplexen metabolischen Netzwerkes von *P. aeruginosa* eingreift. Durch den Einsatz eines multi-methodischen Ansatzes schlagen wir vor, dass PqsE in der Phenylpyruvat Biosynthese involviert ist, welches ein mögliches Signalmolekül für das *rhl* QS System darstellt.

Table of Contents

List of Figures

List of Tables

Abbreviations

% (v/v)	percentage volume per volume
% (w/v)	percentage weight per volume
λ	wavelength
3-oxo-C_{12}-HSL	N-(3-oxododecanoyl)-L-homoserine lactone
Abs	absorbance
AHL	N-acyl-L-homoserine lactone
AQ	2-alkyl-4-quinolone
ATP	adenosine triphosphate
bp	base pair
c-di-GMP	cyclic dimeric guanosine monophosphate
cDNA	complementary DNA
CF	cystic fibrosis
CFU	colony forming units
C_4-HSL	N-butanoyl-L-homoserine lactone
CoA	coenzym A
DMSO	dimethyl sulphoxide
DNA	deoxyribonucleic acid
DTT	dithiothreitol
EDTA	ethylenediaminetetraacetic acid
et al.	et alia
FAD	flavin adenine dinucleotide
g	grams
GC	gas chromatography
gfp	green fluorescent protein

GTP	guanosine triphosphate
h	hour
HHQ	2-heptyl-4-quinolone
HPLC	high-performance liquid chromatography
HSL	homoserine lactone
IPTG	isopropyl ß-D-L-thiogalactopyranoside
kb	kilobase
kDa	kilodalton
l	litre
LB	Luria Bertani broth
LC-MS/MS	liquid chromatography – tandem mass spectrometry
lux	bioluminscence
M	molar concentration
MCS	multiple cloning site
mg	milligram
µg	microgram
min	minute
ml	milliliter
µl	microlitre
mM	millimolar concentration
µm	micrometer
mRNA	messenger RNA
MS	mass spectroscopy
NAD	nicotinamide adenine dinucleotide
NADP	nicotinamide adenine dinucleotide phosphate
nd	not determined
nm	nanometer

NMR	nuclear magnetic resonance
nt	nucleotide
OD	optical density
PBS	phosphate buffered saline
PCR	polymerase chain reaction
PQS	Heptyl-3-hydroxy-4(1H)-quinolone (or *Pseudomonas* quinolone signal)
QS	quorum sensing
RBS	ribosome binding site
RF	peptide chain release factor
RLU	relative luminescence unit
RNA	ribonucleic acid
rpm	revolutions per minute
rRNA	ribosomal RNA
s	second
SAM	S-adenosyl-L-methionine
SD	Shine-Dalgarno
SDS	Sodium dodecyl sulphate
SDS-PAGE	sodium dodecyl sulphate polyacrylamide gel electrophoresis
T3SS	type III secretion system
TCA	tricaboxylic acid
TLC	thin layer chromatography
Tris	tris(hydroxymethyl)aminomethane
tRNA	transfer RNA
TSS	transcriptional start site
UV	ultraviolet
UTR	untranslated region
wt	wild-type

Three letter and single letter abbreviation for the amino acids

Ala	A	alanine
Arg	R	arginine
Asn	N	asparagine
Asp	D	aspartic acid (aspartate)
Cys	C	cysteine
Gln	Q	glutamine
Glu	E	glutamic acid (glutamate)
Gly	G	glycine
His	H	histidine
Ile	I	isoleucine
Leu	L	leucine
Lys	K	lysine
Met	M	methionine
Phe	F	phenylalanine
Pro	P	proline
Ser	S	serine
Thr	T	threonine
Trp	W	tryptophane
Tyr	Y	tyrosine
Val	V	valine

1 Introduction

1.1 *Pseudomonas aeruginosa* – A leading nosocomial pathogen

Pseudomonas aeruginosa is a well-studied pathogen belonging to the *Pseudomonads* branch of the gamma group of the proteobacteria. Like all proteobacteria, *P. aeruginosa* is a gram-negative bacterium with a cell wall composed of two distinct lipid layers: an inner and outer membrane. It is a free-living microbe which has a comparably large genome averaging 6.6 Mbp in size with a high GC content (~66.6 %). In total, the core genome of *P. aeruginosa* contains ~5,320 coding sequences (1). Together, the core and accessory genome contain a disproportionately large number of genes predicted to encode outer membrane proteins that function in adhesion, motility, antibiotic efflux, virulence factor export, environmental sensing by two-component systems, transport systems and enzymes involved in nutrient uptake and metabolism (2). The *P. aeruginosa* genome additionally has an unusually high percentage of regulatory genes (8.4 %), a significantly larger proportion than in other bacterial genomes (3). This illustrates the need for genetic regulation to ensure that appropriate virulence and acclimatization factors are produced at the right moment.

Nowadays, *P. aeruginosa* has become one of the most commonest cause of nosocomial infections being responsible for 10–20 % of hospital infections worldwide (4). Although it seldom poses a significant threat to healthy individuals, *P. aeruginosa* is an opportunistic pathogen that can cause serious acute and chronic infections in immunocompromised patients. *P. aeruginosa* infection is a severe complication in cystic fibrosis (CF) patients where it is found to be the leading cause of morbidity and mortality (5). Patients with CF suffer from a chronic, progressively destructive bronchitis resulting in mucus hypersecretion. It is believed that a defective mucus clearance, a key mechanism of the host to defend the respiratory tract from bacterial challenge, enables pathogenic bacteria to thrive within this environment. While the lungs of CF patients are often initially colonized by *Staphylococcus aureus* during childhood, an estimated 80 % of adult people carrying this hereditary disease do develope a chronic infection with *P. aeruginosa* (6). Chronic colonization throughout the course of disease is due to the ability of *P. aeruginosa* to form highly-organized, multicellular three-dimensional structures known as biofilms. Biofilms, in addition to the high intrinsic antibiotic resistance, protect the bacteria from antibiotics. The slime matrix has barrier properties rendering antibiotics unable to diffuse the matrix to deeper cell layers. In combination with the unusually restricted outer-membrane permeability and various multidrug efflux systems

that pump antibiotics out of the cell, these resistance mechanisms of *P. aeruginosa* are associated with serious complications in treatment of persistent infection.

Moreover, *P. aeruginosa* is equipped with a large repertoire of virulence factors which also contributes to the pathogenesis of acute and chronic infections. Both, virulence and biofilm formation are controlled by signal molecule-dependent cell–cell communication systems, which are used by *P. aeruginosa* to monitor its own population density in a process known as quorum sensing (QS) (7). Since new resistant strains emerge at a faster rate than novel antibiotics are discovered, alternative treatments of infections need to be developed.

1.1.1 Environmental adaptability

P. aeruginosa is a ubiquitous bacterium thriving in a variety of environments. It is commonly found in soil, plant and animal tissues as well as in aqueous solutions including coastal marine habitats. As an exceptionally versatile organism it can tolerate a wide range of habitat conditions (e.g. temperatures of up to 45 °C (8)), and in contrast to its limited ability to grow on sugars, *P. aeruginosa* can use multiple other carbon and nitrogen sources (3, 9).

While *P. aeruginosa* is an obligate aerobe, it is also capable to perform denitrification utilizing N-oxides as alternative terminal electron acceptors for respiration under anaerobic growth conditions. *P. aeruginosa* harbors gene clusters for all four reductases (*nar*, *nir*, *nor*, and *nos*) required for the complete reduction of nitrate to molecular nitrogen. Expression of denitrifying genes has recently been shown to be essential for growth in the lung and sputum of CF patients (10). Besides denitrification, fermentation is another central metabolic process that allows growth under hypoxic and anoxic conditions and ensures survival when faced with oxygen depletion. *P. aeruginosa* has the ability to ferment arginine and pyruvate anaerobically (11–15). These pathways do not involve redox reactions and energy yields are comparably low, thus, in the presence of N-oxides fermentation is generally repressed (16). More recently, Glasser and colleagues could show that phenazine redox cycling also renders *P. aeruginosa* able to carry out anaerobic glycolysis (a process where glucose is broken down to acetate without the use of oxygen) facilitating generation of ATP and a proton-motive force (17). Thus, phenazine redox cycling can serve as an alternate pathway for ATP synthesis and long-term survival during hypoxia.

Besides its very versatile energy metabolism, *P. aeruginosa* can secrete iron-chelating siderophores to sequester iron in an iron-limiting environment. Iron-loaded siderophores are then transported back into the cell and confer significant selective advantage for growth. Siderophores are amongst the strongest soluble iron-binding agents known and allow pathogenic bacteria like *P. aeruginosa* to acquire iron tightly bound to proteins such as hemoglobin, transferrin and lactoferrin (18). In addition, *P. aeruginosa* is also able to carry out chemotaxis which may provide a significant fitness advantage in nutrient-poor environments. Chemotactic organisms that can locomote toward a desirable nutrient have an increased chance of survival and could outcompete co-habitant microbes in a polymicrobial population. Polymicrobial infections are increasingly being recognized as clinically important in cystic fibrosis lung disease, and a facultative anaerobic lifestyle in combination with a motile phenotype and biofilm-forming abilities clearly contribute to the ecological success of *P. aeruginosa* (19).

1.1.2 Motility

Motility is a remarkable feature in microbial physiology. The active movement of a bacterial cell allows the organism to reach new resources in a favorable environment. Such movement is a reaction to particular stimuli, which either attract cells, as in case of nutrients and light, or repel them from adverse conditions. *P. aeruginosa* is capable of three types of motility: flagellum-mediated swimming, type IV pilus-dependent twitching and swarming which requires both flagella and type IV pili (20–24).

Flagella are thin appendages anchored in the cell envelope and enable bacterial cells to swim in aqueous environments and low-viscosity media. These helical filaments function by rotation and propel cells forward in a corkscrew-like motion. The energy required for such mechanical work is generated by proton translocation across the cell membrane, and *P. aeruginosa* is able of actively maintaining its proton motive force even under anaerobic conditions during fermentation (17). Flagella are, however, not only important for motility but likewise play a critical role in pathogenesis. They are involved in the adherence to surfaces and human respiratory mucin during biofilm formation (25, 26). Furthermore, the presence of flagella was reported to facilitate initiation of infection while being dispensable once the infection is established (27).

When attached to a surface, *P. aeruginosa* switches to a flagellum-independent gliding movement known as twitching motility (20). Twitching, unlike swimming, is mediated by type IV pilli and is believed to result from repeated extension, tethering, and retraction of pilli which drags bacterial cells along a surface (20). These long protein fibers have functional characteristics in common with flagella as they are equally important for biofilm development and also provide the ability to adhere to diverse surfaces, including epithelial cells (26). According to Burrows, the primary function of twitching motility is likely exploration of surfaces via chemotaxis (28). If environmental conditions are unsuitable, bacterial cells can again detach from surfaces using a pilli-driven motility behavior in a so-called launch sequence (29).

Besides swimming and twitching, *P. aeruginosa* exhibits a coordinated locomotion on semisolid surfaces, denoted as swarming motility (30). On agar plates, swarming cells migrate in complex patterns from the point of inoculation in defined groups, referred to as tendrils, in all directions. This movement presumably helps bacteria to sense the local environment and trace nutrient availability to colonize a potential suitable habitat (31). Unlike all other swarming bacteria, swarming of *P. aeruginosa* is not dependent exclusively on flagella, but additionally requires type IV pilli (22, 24). Further, rhamnolipids play a decisive role in swarming behavior as they have surface wetting properties and allow cells to move across a hydrated, viscous semisolid surface. Recently it was demonstrated that swarming is an adaptation to a viscous environment and entails a substantial change in virulence gene expression and antibiotic resistance (32). There also exists a complex relationship between swarming motility and biofilm formation which were shown to be inversely regulated in *P. aeruginosa* (33). While swarming contributes to initial adherence steps, it is repressed during biofilm maturation. Contrary to other motility behaviors, swarming is controlled by a regulatory network involving transcriptional regulators of quorum sensing systems (32), highlighting the dynamic complex interplay among bacterial motility and virulence.

1.1.3 Biofilm formation

In most natural settings, bacteria are found predominantly in sessile, multicellular microcolonies rather than as planktonic cells that live in a floating existence (34, 35). This mode of life is an adaptive response to environmental signals that trigger the attachment of a

few cells to a surface, which in turn induces the expression of biofilm-associated genes and enables bacteria to coordinate group behavior. Cells may thus form complex three-dimensional structures surrounded by an extracellular matrix that serves as structural scaffolding for the cells (36). The extracellular matrix is a typical feature of biofilm communities and it mainly consists of exopolysaccharides, proteins and nucleic acids (37). Bacteria assembled in a biofilm are usually less susceptible to antibiotics than their free-living counterparts (38–40). This phenotype of increased antibiotic tolerance arises from the protective barrier surrounding the biofilm, resulting in a reduced diffusivity of antibiotics. In addition, there is also an accumulation of antibiotic-degrading enzymes, such as β-lactamases, within the extracellular matrix (41). Moreover, there are subpopulations of non-replicating cells in biofilms which can serve as reservoirs for recurrent infections (42). This microbial stasis within biofilms is thought to further complicate the treatment of many persistent infections.

The developmental process from single planktonic cells to multicellular structures is characterized by five stages (Fig.1.1) (43, 44). At first, free-living cells reversibly attach to a surface. Some cells then anchor themselves irreversibly to the surface by means of adhesion molecules. During further maturation, biofilms show a more complex architecture including the formation of pillar-like structures traversed by channels which allow for nutrient influx and waste efflux (45). Bacterial communities at this stage are composed of subpopulations of different metabolic activity and, depending on the oxygen concentration gradient within the biofilm, have similar gene expression patterns to stationary-phase or anaerobically grown cells (46, 47). In the final stage, motile cells disperse from the biofilm, mainly in response to changes in the environment, to spread and colonize new surfaces.

Biofilm formation is a dynamic and complex process involving multiple signaling pathways. Quorum sensing as well as the nearly ubiquitous bacterial second-messenger molecule cyclic di-GMP are of particular importance for biofilm development and facilitate the response and adaptation to divergent environments by modulating the expression of key transcriptional regulators (48, 49). The complexity of single-species biofilms was illustrated by Müsken et al. who screened a PA14 transposon mutant library for genes affecting the biofilm phenotype of *P. aeruginosa* (50). It was shown that approximately 10% of all annotated genes altered biofilm formation *in vitro*. However, *in vivo* things are even more complicated as chronic biofilm infections are typically polymicrobial and complex interspecies interactions occur

within these diverse microbial populations, an important factor in pathogenesis (19, 51). Interbacterial metabolite transfer between co-habitant microbes is a common feature, and fermentation products like 2,3-butanediol were shown to significantly increase virulence factor production, antimicrobial activity and biofilm formation of *P. aeruginosa* (52).

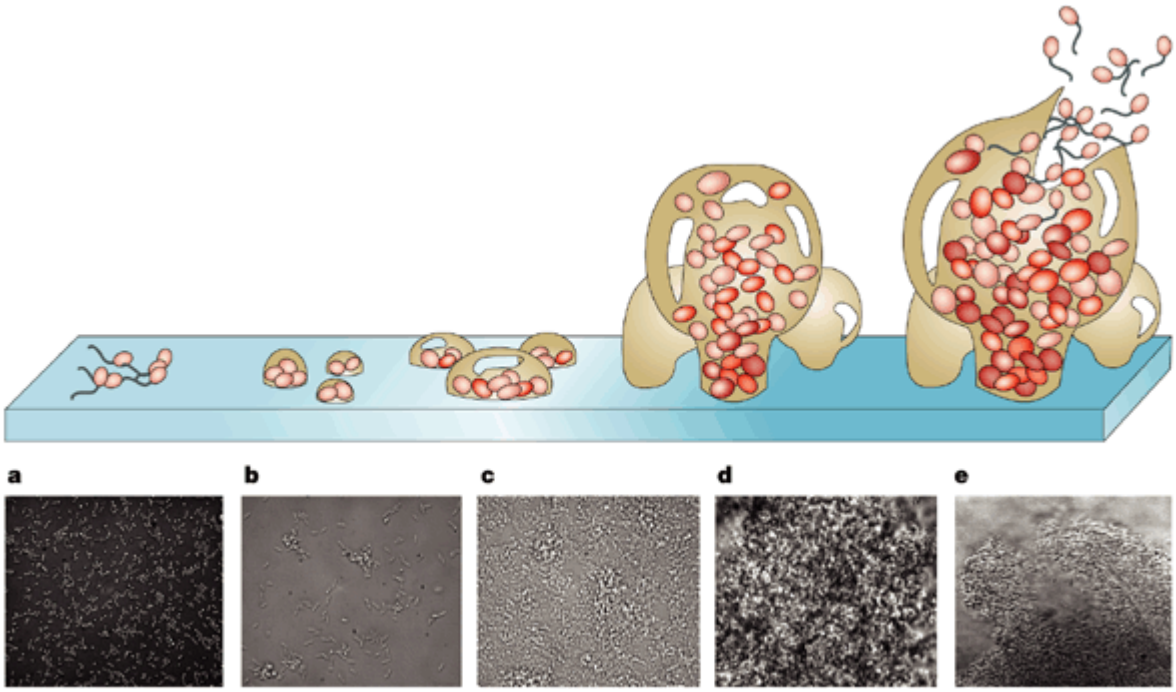

Figure 1.1: Development of bacterial biofilms. The various stages of the complex developmental cycle of biofilm formation are depicted. After initial attachment of planktonic cells to a surface, bacterial cells irreversibly adhere to the surface and generate multiple layers of cell clusters (a c). After attachment to a surface, bacteria undergo further adaptation to life in a biofilm and form more complex three-dimensional structures (d), before motile cells are finally dispersed from the biofilm to colonize new surfaces (e). The figure is taken from (53).

1.1.4 Virulence factor production

It is not without reason that *P. aeruginosa* causes a wide range of devastating acute and chronic infections. This opportunistic pathogen produces a large variety of exoproducts many of which are responsible for its pathogenesis. *P. aeruginosa* is able to secrete several extracellular virulence factors capable to defend bacterial cells against cellular components of the immune system. Lipase, alginate and rhamnolipids, for example, all play a crucial role in

the persistence of infection and confer protection from phagocytosis (54–56). Amphiphilic rhamnolipids are further essential for the elimination of polymorphonuclear neutrophilic leukocytes, which dominate the immune response to infections in CF lungs (57). They also act as biosurfactants responsible for the solubilisation of lung phospholipids, thereby making them more accessible to cleavage by phospholipase C (58). Phospholipase C is a hemolysin that induces vascular permeability and it has been shown to cause organ damage and death in various animal models (59).

Moreover, *P. aeruginosa* produces a range of toxins and exoenzymes which modify eukaryotic targets and thus may cause extensive damage to the host. Probably the most toxic and thoroughly studied extracellular product associated with *P. aeruginosa* is exotoxin A (60). This potent bacterial toxin is an inhibitor of protein synthesis as it modifies the elongation factor 2 in eukaryotes, causing death of infected host cells (61). In contrast to the majority of released virulence factors, the bi-functional exoenzymes ExoS, ExoT, both of which function as ADP-ribosyltransferase and as Rho GTPase activator (reviewed by (62)), the adenylate cyclase ExoY (63) and the phospholipase ExoU (64) are injected directly into the host cells. Within the eukaryotic cells, ExoS/T plays a role in the ribolysation of ADP and increased intracellular GTPase activity, thereby affecting host-cell division, wound healing, exocytosis and cell apoptosis (65, 66). Another virulence determinant of *P. aeruginosa* is elastase LasB, which is implicated in the destruction of connective tissue thus e.g. facilitating invasion of epithelial cells (58, 59). Additional virulence-associated factors include alkaline protease (60), hydrogen cyanide (61), catalase and superoxide dismutases as well as lectins (68).

A characteristic feature of fluorescent *Pseudomonads* is the capability to produce a large group of redox-active antibiotics known as phenazines (67). The most intensively studied phenazine is pyocyanin, a soluble blue-green pigmented secondary metabolite that contributes to the virulence and ecological fitness of *P. aeruginosa*. Pyocyanin causes the typical blue-greenish coloration of many laboratory and clinical isolates and is recovered in large quantities from the lungs of CF patients who suffer from *P. aeruginosa* infection (68). It exerts diverse cytotoxic effects which are mediated mainly through its ability to redox cycle by accepting electrons from the reducing agents NADH and NADPH with subsequent electron transfer to oxygen, thereby generating reactive oxygen species (69). However, there

is also indication that the redox activity of pyocyanin can as well affect the carbon flux through central metabolic pathways (70).

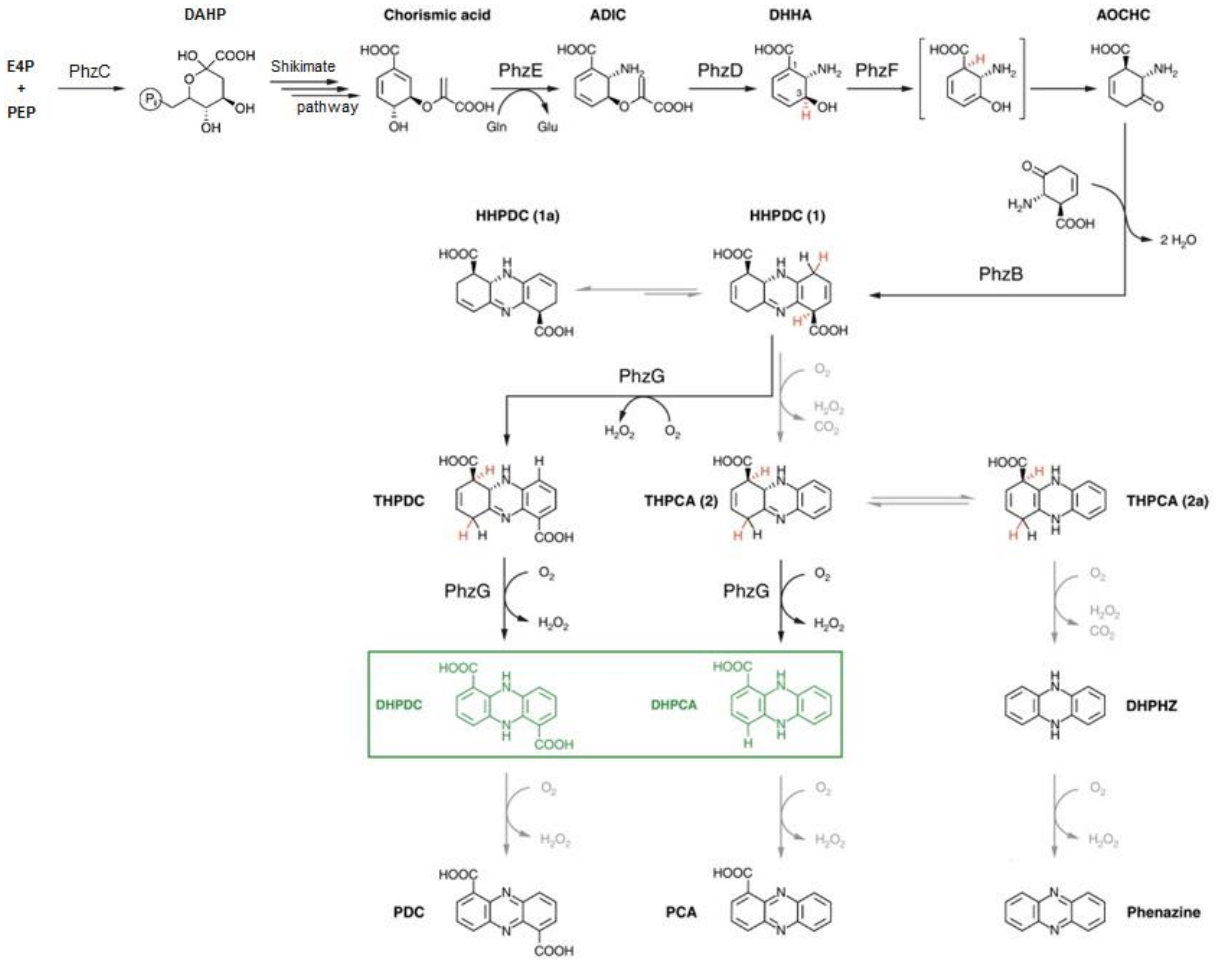

Figure 1.2: Phenazine biosynthesis in *P. aeruginosa*. The final products of the core biosynthetic pathway of phenazines are indicated in green, and grey arrows indicate uncatalyzed reactions. Abbreviations: (E4P) erythrose-4-phosphate; (PEP) phosphoenolpyruvic acid; (DAHP) 3-deoxy-7-phosphoheptulonate; (ADIC) 2-amino-2-desoxyisochorismic acid; (DHHA) (5S,6S)-6-amino-5-hydroxy-1,3-cyclohexadiene-1-carboxylic acid; (AOCHC) 6-amino-5-oxocyclohex-2-ene-1-carboxylic acid; (HHPDC) hexahydrophenazine-1,6-dicarboxylic acid; (THPCA) tetrahydrophenazine-1,6-carboxylic acid; (THPDC) tetrahydrophenazine-1-carboxylic acid; (DHPCA) 5,10-Dihydro-PCA; (DHPDC) 5,10-Dihydro-PDC; (PCA) phenazine-1-carboxylic acid; (PDC) phenazine-1,6dicarboxylic acid. This is a modified figure taken from (71)**.**

Phenazine genes are widespread among eubacteria, many of which produce multiple phenazine derivatives. The core biosynthetic genes (*phzA-G*) are often flanked by accessory genes encoding terminal-modifying enzymes that alter the substituent added to the basic phenazine structure (67, 72). In case of *P. aeruginosa*, these accessory genes comprise a transamidase (*phzH*), a methyltranferase (*phzM*) and a flavin-containing monooxygenase (*phzS*) responsible for the conversion of phenazine-1-carboxylic acid (PCA), the common biosynthetic precursor for strain-specific phenazine derivatives in all *Pseudomonads* (64). Figure 1.2 shows our current understanding of the biosynthetic pathway of core phenazines in *P. aeruginosa* (71). The first step of this pathway, involving the condensation of erythrose-4-phosphate and phosphoenolpyruvic acid by a type II 3-deoxy-d-arabinoheptulosonate-7-phosphate (DAHP) synthase (*phzC*), is a primary site for stringent regulation and guarantees sufficient substrate levels for phenazine synthesis (72). Unlike other prokaryotic DAHP synthases, PhzC is not subject to feedback inhibition by any of the three aromatic amino acids as it lacks the common structural basis for allosteric control (72). Interestingly, *P. aeruginosa* was found to contain two redundant copies of the core *phzA-G* operon (73), and could possibly explain why it is one of the most active phenazine producers. But despite considerable functional redundancy, these operons, *phzA-G1* and *phzA-G2*, were recently shown to exhibit differential regulation of gene expression and to play distinctive roles in pathogenicity (74).

1.2 Quorum sensing: bacterial small talk

For a long time bacteria were regarded solely as unicellular microbes that reproduce by binary fission and are subject to natural selection to compete with their neighbors for space and resources. Until the early 1980's, it was hardly imaginable that recognition and cooperation between cells could exist in the bacterial world. The following quotation from Francois Jacob (1973) nicely illustrates this way of thinking (75): 'It is perfectly possible to imagine a rather boring universe without sex, without hormones and without nervous systems peopled only by individual cells reproducing *ad infinitum*. This universe in fact exists. It is the one formed by a culture of bacteria.' However, the widely accepted view on the universe of bacterial life eventually proved wrong.

The discovery of coordinated activity and intercellular communication among bacteria was a significant breakthrough in microbiology. It has fundamentally altered our perception of the complex, cooperative interactions that occur between bacterial cells. The ‘language’ used for this collective behavior is based on small, self-generated signal molecules called autoinducers and enables bacteria to coordinate gene expression in a cell density-dependent manner (7). Cell-to-cell communication in bacteria was given the generic term ‘quorum sensing’ (QS) to describe the capability of bacteria to sense and respond to these pheromones. QS systems are in fact all very similar as they rely on the activation of specific transcriptional regulators by their corresponding autoinducers produced by a respective autoinducer synthase (Fig.1.3).

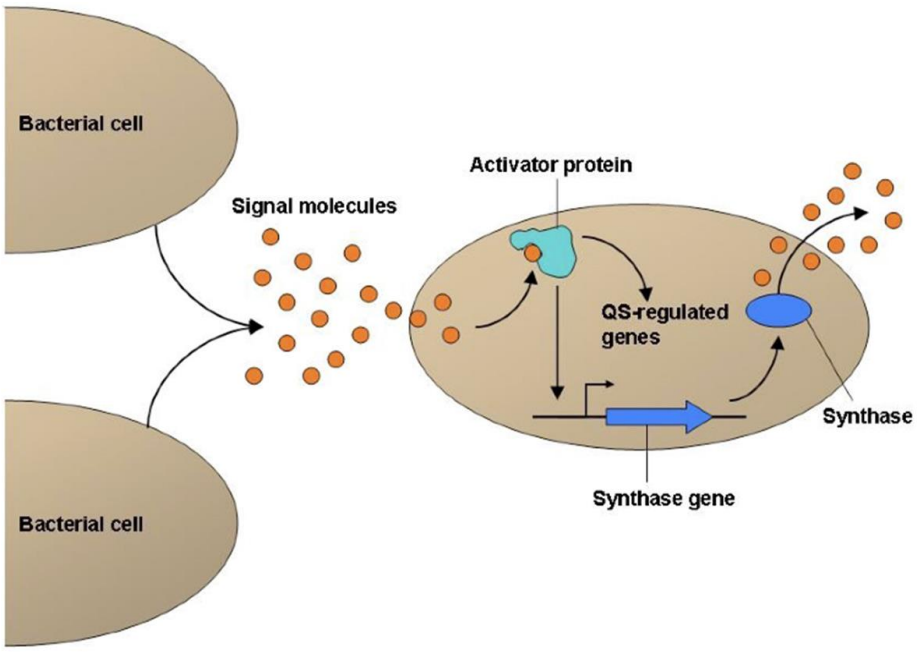

Figure 1.3: Signal transduction cascades of bacterial cells. Bacterial cells release different pheromones into the environment in a cell density dependent manner. These signal molecules may be sensed by the bacterial population in the vicinity, and upon binding to transcriptional activator proteins induce the expression of QS-regulated genes as well as expression of the signal molecule synthase gene.

QS was first observed in the luminous marine bacterium *Vibrio fischeri*, a symbiont of certain fish and squid (76). Autoinduction of bacterial luciferase requires acylated homoserine lactones (AHL), which bind to the LysR-type regulatory protein LuxR inducing the

transcription of the *luxCDABE* genes. In the course of luciferase expression, light is produced in special organs of marine animals and luminous bacteria like *V. fischeri* are thus thought to be involved in the attraction of prey, or predator avoidance with camouflage. In return, the host provides a nutrient-rich and protected environment for these bacteria (77). This symbiosis illustrates the practical use of bacterial communication. Since its discovery, QS has been confirmed for many bacterial species including opportunistic pathogenic bacteria like *P. aeruginosa* whose complex QS network architecture will be further addressed below.

1.2.1 AHL-dependent signaling

The remarkable ecological success of *P. aeruginosa* can be attributed to its large metabolic versatility and its sophisticated QS network. QS enables *P. aeruginosa* to control expression of numerous virulence factors and it is involved in biofilm formation, thereby facilitating establishment of chronic infections.

The complex communication mechanisms in many gram-negative bacteria rely upon the utilization of AHLs as signal molecules. LuxI-like enzymes synthesize these pheromones in a sequentially ordered NADH-dependent reaction using two substrates; (1) S-adenosyl-L-methionine (SAM) which serves as the amino donor for the homoserine lactone ring, and (2) acyl chains that are derived from lipid metabolism and are provided as acylated-acyl carrier protein (ACP) conjugates (78, 79). *P. aeruginosa* possesses at least two canonical inter-connected AHL-dependent QS systems, termed *las* and *rhl*, which regulate the expression of various exoenzymes and secondary metabolites (Fig. 1.4). The *las* system is considered to stand at the top of the hierarchy. It is composed of the LuxR/I homologues LasR and LasI. The signal synthase LasI directs the synthesis of *N*-(3-oxododecanoyl)-L-homoserine lactone (3-oxo-C_{12}-HSL), which is the ligand of the LasR receptor (80, 81). The *las* system is interconnected with the *rhl* system as LasR bound to its autoinducer 3-oxo- C_{12}-HSL induces transcription of *rhlR* (82). The transcriptional regulator RhlR then binds to N-butanoyl-L-homoserine lactone (C_4-HSL) synthesized by RhlI (83, 84). Together, these pathways were shown to regulate expression of ~10 % of the *P. aeruginosa* transcriptome including several virulence factors such as pyocyanin, rhamnolipids, hydrogen cyanide and exotoxin A (84–86).

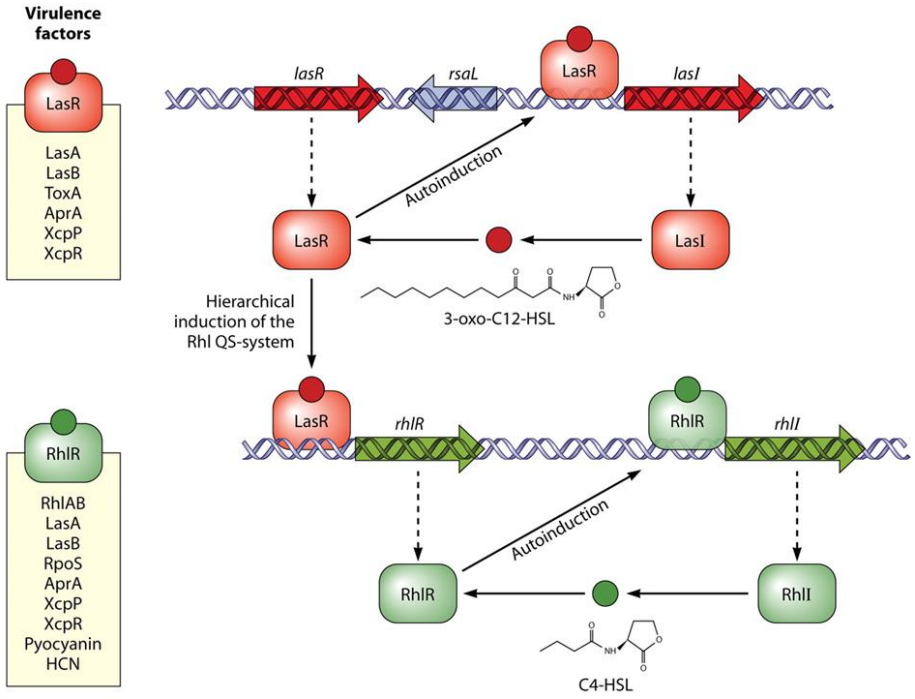

Figure 1.4: AHL-dependent QS in *P. aeruginosa*. *P. aeruginosa* possesses two AHL-dependent QS systems (*las* and *rhl*) which regulate the expression of numerous virulence factors. These systems are organized in a hierarchical manner such that the *las* system exerts transcriptional control over *rhlR*. Both systems consist of a transcriptional regulator (LasR and RhlR) and a synthase (LasI and RhlI) which directs the synthesis of the cognate signal molecule. Binding of the signal molecules to LasR and RhlR creates an autoinduction feedback loop. The figure is taken from (87).

QS in *P. aeurginosa* is object of ever-growing scientific interest and led to the identification of a large plethora of global regulators modulating AHL-dependent gene expression. Vfr is a long-known regulator of QS (88), and was shown to directly activate transcription of *lasR* (89). Further, Vfr-binding to several binding sites present in the *rhlR* promoter region was recently verified by Croda-García et al. (90). By contrast, the orphan QS regulator QscR acts as an inhibitor of both *las* and *rhl* systems (91–93). Like LasR, activation of QscR was recently demonstrated to rely on specific binding to 3-oxo- C_{12}-HSL (94). In fact, QscR is part of a regulatory cascade in which the global regulator VqsR inhibits *qscR* expression (95), thereby relieving QscR-mediated inhibition of QS. The *vqsR* gene, in turn, was initially thought to be under transcriptional control of VqsM (96), but binding of VqsM to the *vqsR* promoter region could not be confirmed *in vitro* (97). Instead, VqsM directly bound to the *lasI* promoter as well as to promoter regions of the antibiotic resistance regulator (*nfxB*) and the master type III secretion system (T3SS) regulator (*exsA*) (97). Other transcriptional

regulators of *lasI* include RsaL (98, 99), itself an integral part of the *las* QS system (Fig.3), CzcR (100) and MvaT (101).

However, there are also protein–protein interactions that exert a profound influence on modulation of cell-density dependent gene expression. For example, QsIA was shown to block QS by directly interacting with the transcription factor LasR, preventing dimerization and binding of LasR to its target DNA (102). In addition, stability of both transcriptional regulators, LasR and RhlR, was previously shown to rely on the presence of a protein named QteE, via an as yet unknown mechanism (103). More recently, Köhler and colleagues identified a novel genetic locus comprising *qsrO* whose gene product is capable of repressing QS in *P. aeruginosa* (104).

1.2.2 AQ-dependent signaling

At the turn of the new millennium, Pesci and colleagues discovered a previously unrecognized QS system in *P. aeruginosa* that is not dependent on AHLs but on 2-alkyl-4-quinolone signal molecules (AQs) (105). The major synthase genes were found to be arranged in a polycistronic operon (*pqsA-E*), whose transcription is dependent on the adjacent *pqsR* gene (also known as *mvfR*) encoding the LysR-type transcriptional regulator of the *pqs* system (106–109). Homologues of the *pqs* genes were identified in only a few other bacteria, of which the human pathogens *Burkholderia pseudomallei* and *B. thailandensis* exclusively contain a complete *pqsA–E* operon termed *hhqA–E* (110). Like AHL-dependent signaling, AQs play an important role in the expression of numerous virulence factors, and these signal molecules itself are known to induce a protective stress response towards deteriorating environmental conditions (111, 112).

The *Pseudomonas* quinolone signal (PQS) and its direct precursor 2-heptyl-4-quinolone (HHQ) are active members of over 50 different AQs produced by *P. aeruginosa* (113). AQ biosynthesis requires the biosynthetic genes *pqsA*, *pqsB*, *pqsC*, and *pqsD* (but not *pqsE*), and involves the following steps (Fig. 1.5): (i) First, the acyl-coenzyme A ligase homolog PqsA catalyzes the formation of anthraniloyl-CoA from anthranilate (114). Both, the kynurenine pathway of tryptophane degradation as well as the anthranilate synthase PhnAB are critical sources of anthranilate in *P. aeruginosa* (115). (ii) Although the precise contribution of PqsBCD to AQ biosynthesis is not yet fully understood, there is evidence that these proteins

are responsible for the ‘head-to-head’ condensation of anthraniloyl-CoA and a 3-oxo-fatty acid to form HHQ (106, 116–118). (iii) In a final step, an NADH-dependent flavin monooxygenase (PqsH) oxidizes HHQ to PQS by introducing a hydroxyl group to HHQ (106, 119, 120). Interestingly, the two AQs can act both as classical QS autoinducers capable to induce their own production upon binding to the transcriptional regulator PqsR, although PQS is ~100-fold more potent than HHQ in driving *pqsA–E* transcription (107, 109, 121). Activated PqsR furthermore exerts positive control on the neighbouring *phnAB* locus to guarantee sufficient anthranilate for AQ synthesis (107). While most AHLs diffuse passively across the cell membrane, AQs are actively transported out of the cell through various mechanisms: the MexEF-OprN efflux pump is responsible for HHQ export (122) and membrane vesicles serve to traffic PQS within a population (123, 124).

It can be assumed that the production of multiple AQs entail advantages for *P. aeruginosa* under different environmental conditions. The ability of PqsR to also use HHQ as signal molecule, for instance, could be important in anaerobic environments to ensure basal transcription of the HHQ-biosynthetic genes *pqsA-D* in the absence of PQS (120), as sufficient levels of HHQ are produced anaerobically to induce *pqsA-E* transcription (109). PQS, on the other hand, plays multifunctional roles in QS and iron entrapment (125, 126), and thereby differs greatly from HHQ and AHLs which appear to solely function as autoinducer molecules. Furthermore it was shown that the presence of PQS substantially promotes adherence and biofilm formation of *P. aeruginosa* and it is involved in the production of large amounts of extracellular DNA, an important factor for the stability and structure of biofilms (111, 127). Likewise, PQS affects the production of exoproducts such as pyocyanin (106) and elastase (105), and it plays a role in the persistence of *P. aeruginosa* in long-term infections by inhibiting human T-cell proliferation (128).

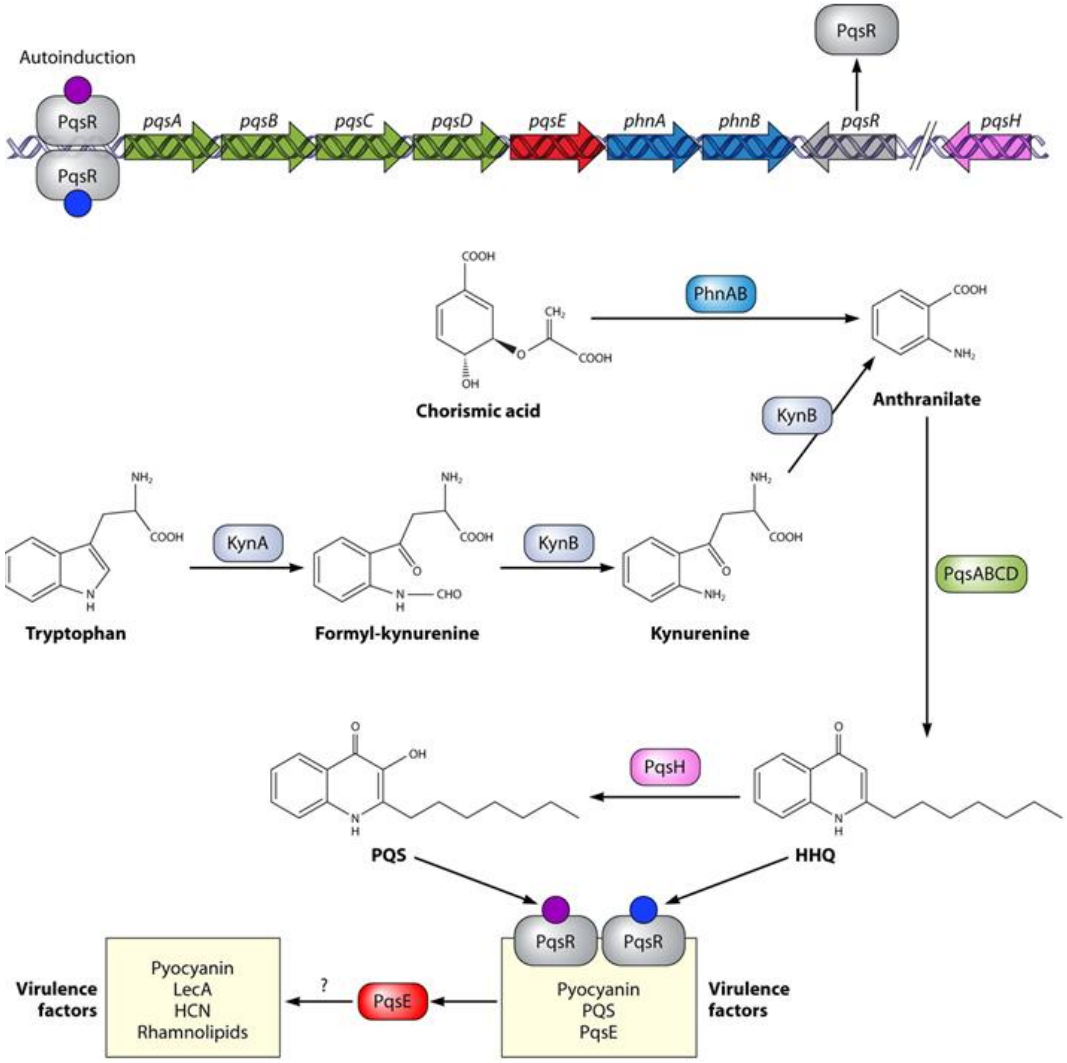

Figure 1.5: AQ-dependent QS in *P. aeruginosa*. The biosynthetic precursor of all AQs is anthranilate, provided by either tryptophane degradation via the kynurenine pathway or the PhnAB anthranilate synthase. In the next step, PqsABCD produce HHQ from anthranilate, the substrate for PqsH and immediate precursor of PQS. Both HHQ and PQS are co-inducers of the transcriptional regulator PqsR that drives the expression of the *pqsA-E* and *phnAB* biosynthetic operons as well as expression of other virulence factors. The fifth gene product of the *pqs* locus, PqsE, is not involved in the AQ biosynthetic pathway but, in concert with RhlR, is essential for virulence. The figure is taken from (87).

1.2.3 The complex interrelationships between QS systems of *P. aeruginosa*

Evidently, there exists a delicate and finely tuned cross-linkage of the different QS systems in *P. aeruginosa*. The complex network is organized in a hierarchical fashion with the *las* system being the very top of the hierarchy as it exerts regulatory control over both, the *rhl* and

the *pqs* signaling system (83, 105, 129). Besides acting as an activator of *rhlR* transcription (82), LasR furthermore increases PQS formation by inducing transcription of *pqsA-E*, *pqsH* and *pqsR* (108, 119, 121). However, there is an extra level of control in the *pqs* system owing to the binding of RhlR to *pqsA-E* and *pqsR* promoter regions, accompanied by repression of PQS signaling (129). Interestingly, PQS itself has been shown to be integral to the functioning of the *rhl* QS system in a negative feedback regulatory loop by promoting *rhlI* transcription (111, 130). On the other hand, PQS may thereby regulate its own solubility considering that the biosurfactant rhamnolipid increases the solubility of PQS in aqueous solutions and that rhamnolipid biosynthesis depends on a functional *rhl* system (131).

Another important aspect of the interconnected relationship within the QS circuitry of *P. aeruginosa* which has received a lot of interest in the past is the codependency between the *rhl* system and the final gene of the *pqs* operon, *pqsE*. In contrast to the other genes of the *pqs* locus, *pqsE* is not involved in the biosynthetic pathway of AQ production, instead the PqsE enzyme has positive regulatory function in *rhl* signaling and controls various virulence functions, whereby PqsE was shown to act independently of AQs (132). While PqsE does not majorly affect the production of C_4-HSL or the transcription of *rhlR/I*, PqsE significantly enhances the responsiveness of RhlR to its cognate signal molecule (132). Intriguingly, the same effect is observed in an *E. coli* background; however, the exact mechanism by which PqsE affects the *rhl* system and achieves its regulatory function still remains an unsolved mystery. In any event, by stimulating *rhl* signaling PqsE negatively regulates its own expression as well as expression of the entire *pqs* operon. The essential contribution of PqsE to the virulence of *P. aeruginosa* is however of undisputed importance and evidently requires RhlR (132–134).

1.3 Post-transcriptional control of gene expression in *Pseudomonas aeruginosa*

While regulation of gene transcription is central to the cellular metabolism, post-transcriptional regulation of bacterial gene expression has also gained significant attention in recent years. The importance of these post-transcriptional regulatory processes is highlighted (among other features) by the general weak correlation between transcript and protein abundances in prokaryotes (135). Most mRNAs are subject to considerable post-transcriptional modification. Hundreds of proteins and small non-coding RNAs participate in

such processes, and truncation or inclusion of extra sequences can also strongly affect the translation as well as the degradation rate of mRNAs (136).

Post-transcriptional repression events in prokaryotes mainly occur either by binding of small regulatory RNAs to target mRNA molecules or by formation of secondary structures in the mRNA, which play an important role in post-transcriptional regulation of gene expression in bacteria (137, 138). One common form of an RNA regulatory element is the so called riboswitch. These regulatory elements usually reside in the non-coding region of the mRNA and regulate gene expression by forming alternative structures in response to binding of a specific metabolite (139). Bacteria commonly mask the Shine-Dalgarno (SD) sequence to block access of the 30S ribosomal subunit. With this, translation initiation becomes highly dependent on the folding structure of the initiation region of the mRNA (140). A well-studied example of such a regulatory mechanism includes RNA thermosensors. They form a zipper-like structure which unwinds with increasing temperature allowing successful binding of the ribosome (141). Recently, the small heat shock protein IbpA was found to be under control of two temperature-sensitive hairpin structures in the 5' untranslated region (UTR) of *ibpA* in *P. aeruginosa* (142).

In *P. aeruginosa*, post-transcriptional processes appear to play a decisive role in biofilm-associated infections. An integral part of *P. aeruginosa* biofilms constitute extracellular polysaccharides such as alginate, Pel and Psl, whose expression is also controlled at the post-transcriptional level. *algC* is one of the essential alginate biosynthetic genes and presumably contains structural features in its 5' UTR that regulate mRNA translation efficiency (143, 144). Translation initiation of the *psl* locus, by contrast, is under control of an RNA-binding protein. RsmA, a homologue of the *Escherichia coli* carbon storage regulator CsrA, represses *pcl* expression by binding to the mRNA leader resulting in the formation of a hairpin structure in the region spanning the Shine-Dalgarno (SD) sequence and preventing ribosome binding (145). Similar to RsmA, the Crc global regulator is involved in the repression of translation of several genes of catabolic pathways and was shown to be essential for biofilm development and virulence of *P. aeruginosa* (146, 147). Crc itself, however, is devoid of any RNA binding activity (148). Another level of post-transcriptional control takes place during translation of *lasB* mRNA, and encompasses two regulatory elements in the 5' UTR: a translational enhancer and a second iron responsive element (149). This regulation is independent of LasR

and represents an additional level at which a virulence factor known to promote biofilm formation is subject to post-transcriptional control (149, 150).

1.3.1 Small regulatory RNAs as modulators of gene expression

Small non-coding RNAs represent a significant, ubiquitous and ever-growing class of regulatory RNAs that are engaged in a wide variety of molecular tasks and functions in all organisms. They usually regulate gene expression by base pairing to target mRNAs which can lead to inhibition of translation and/or alteration of mRNA stability (151). Despite recent progress in identifying novel small RNA candidates in *P. aeruginosa* (152–156), the function of only a few has actually been revealed.

One of the most well studied class of small RNAs are those involved in carbon catabolite repression (157), which allows bacteria the assimilation of a preferred carbon source when they are exposed to more than one carbohydrate (158, 159). Considering the metabolical versatility and flexibility of *P. aeruginosa*, it is of no surprise that there exist various mechanisms that regulate carbon metabolism. Recently, the mode of action of the regulatory RNA CrcZ has been characterized by Sonnleitner and colleagues, who present evidence that CrcZ does in fact not exert its regulatory effect by directly binding to target mRNA but binds to and sequesters Hfq, which in turn results in abrogation of Hfq-mediated translational repression of mRNAs (160). The post-transcriptional RsmA/RsmZ system of *P. aeruginosa* constitutes another example of protein binding RNAs that antagonize the function of the riboregulator RsmA to modulate the production of several virulence determinants (161–163).

On the other hand, the small RNAs PhrS (164) and PrrF (165–167) act by base-pairing with target mRNAs, but while PhrS acts as an activator of translation, PrrF pairing causes rapid degradation of mRNA in response to iron. Just recently, the small RNA ErsA of *P. aeruginosa* was shown to impact the pathogenesis by directly operating in a negative post-transcriptional regulation of the *algC* gene (168). Together, these few examples illustrate the regulatory complexity and future research on small RNAs will help to further decipher their role in the pathogenesis of *P. aeruginosa*.

1.3.2 Implications of post-transcriptional regulation for QS

Post-transcriptional regulation is also known to play a pivotal role in QS-controlled gene expression in *P. aeruginosa*. As mentioned above, the small RNA PhrS can enhance translation upon binding to the 5' UTR of target genes (164). One such target gene is *pqsR*, and PhrS was shown to stimulate synthesis of AQs in response to oxygen depletion (164). Transcription of *phrS* relies on the oxygen-responsive regulator ANR, and oxygen limitation leads to activation of ANR which results in enhanced levels of PhrS. Consequently, PhrS increases *pqsR* translation indirectly by inducing structural rearrangements at the ribosomal binding site of the adjacent gene *uof* of the *uof-pqsR* operon. Recently, an additional layer of control over PQS signaling was published by Tipton et al. (169), who verified a translational coupling of a transcriptional regulator, QapR, to a functional protein, PA5507. PA5507 has sequence homology to isochorismateses and was shown beforehand to negatively affect PQS production (170). The authors postulate a model of translational repression of PA5507 through SD occlusion by the formation of a secondary structure at the 3' end of *qapR* mRNA, resulting in increased concentrations of PQS (169).

The two AHL-dependent QS systems *las* and *rhl* of *P. aeruginosa* were also shown to be subject to post-transcriptional modification. Of particular importance seems to be thermoregulation of *rhlR* and *lasI*, both of which contain a thermosensor in their 5′ UTR (171). Interestingly, in case of *rhlR* expression and translation was highest at body temperature (171), which may reflect host-specific behavioral adaptation of *P. aeruginosa*. Furthermore, the tRNA modification enzyme GidA exerts post-transcriptional control on *rhlR* while it had no impact on *lasR* and AHL production (172). *rhl* QS is also under control a novel post-transcriptional regulatory cascade, Crc-Hfq/Lon/RhlI, where the catabolite repression control (Crc) protein binds *lon* mRNA in the presence of Hfq which results in the repression of *lon* gene expression at a post-transcriptional level (173). Reduced levels of the Lon protease, in turn, lead to an increased stability and abundance of the RhlI protein that synthesizes C_4-HSL. Moreover, the global repressor RsmA impairs AHL-dependent signaling by reducing translation efficiency of *lasI* and *rhlI* mRNA (162). However, QS-regulated genes and proteins are not always directly targeted for post-transcriptional modification. The DksA protein, for instance, was shown to be required for translation of the *lasB* elastase gene and the rhamnosyltransferase encoding *rhlAB* gene, but it did not majorly affect transcription or translation of *rhlRI* and *lasRI* (174).

1.4 Aims of the thesis

The ability of *P. aeruginosa* to evoke various life-threatening infections and the flexibility to face the challenge of changing environments can partially be attributed to an intact QS system. Recent studies have demonstrated that the phenotypic plasticity (the genetically mediated response to external environmental changes) is particularly complex in this nosocomial pathogen, and can largely be explained by effects at transcriptional or post-transcriptional levels.

The overarching aim of this work was to shed light on mechanisms of post-transcriptional regulation and how they control virulence of *P. aeruginosa*. On one hand, we were interested in characterizing previously undescribed candidate virulence-associated genes participating in QS regulation. On the other hand, we aimed at elucidating the regulatory mechanism by which the QS transcriptional activator RhlR represses AQ biosynthesis. Besides concentrating on individual-level relations, another focal point of this thesis was to establish a recently developed method for the global evaluation of translation efficiency, termed ribosome profiling (175). Genome-wide translational profiling is a powerful tool to identify global-scale features of translational control. Furthermore, we seeked to investigate the molecular function of PqsE that intricately links PqsE to the *rhl* QS system.

2 The peptide chain release factor methyltransferase PrmC is essential for pathogenicity and environmental adaptation of *P. aeruginosa* PA14

2.1 Objective

To unravel new genes involved in the regulation of virulence factor production, Dr. Mathias Müsken previously screened for *P. aeruginosa* PA14 mutants, unable to upregulate the AQ-dependent virulence factor pyocyanin after exogenous addition of organic extract containing AQ signal molecules (PA14-extract) to the growth media. Several AQ-non responding mutants were identified by the screen. Here, we focused our interest on a mutant carrying a transposon insertion within a gene, coding for the putative methyltransferase HemK.

The PA14 HemK homologue in *E. coli*, PrmC, has been identified as an enzyme that post-translationally methylates a critical amino acid of the release factors RF-1 and RF-2. Inactivation of *prmC* leads to increased stop codon read-through, growth retardation and induction of oxidative stress response (176, 177). In *E. coli* and in *Porphyromonas gingivalis* it was shown, that *prmC* and its cognate homologue were upregulated during infections or in host environment respectively (178, 179). In this study we show, that HemK has a methyltransferase activity (and is therefore referred to as PrmC) and plays an essential role for *P. aeruginosa* motility, regulation of virulence factors and adaptation to anaerobic growth. Furthermore, we observed that PrmC is important for the type III secretion system (T3SS) and virulence of *P. aeruginosa* in the host infection model *Galleria mellonella*. Enhanced by transcriptomic and proteomic analyses our results indicate that PrmC exerts an intense effect on global regulatory processes and is significantly involved in calibrating pathogenicity in *P. aeruginosa*.

2.2 Results

2.2.1 Identification of AQ-non responding mutants

To identify new genes involved in AQ-dependent pyocyanin production, Dr. Mathias Müsken previously screened all 5833 mutants of the PA14NR library (180) for their capability to produce pyocyanin and analyzed their responsiveness towards the exogenous addition of concentrated PA14-extract. Excluding transposon mutants within genes well-known to be involved in pyocyanin biosynthesis (86, 106), 26 AQ-non responder were detected (without

any growth limitation) with impaired pyocyanin production despite addition of PA14-extracts (Tab. 2.1).

Table 2.1: Pyocyanin restoration by *pqsE* in PA14 transposon mutants that did not respond with an enhanced pyocyanin production after exogenous addition of AQ extracts.

PA14	Mutant-ID	Gene	Product name	Pyocyanin restoration
PA14_04390	25921	*ygdP*	dinucleoside polyphosphate hydrolase	+
PA14_07170	26710	*epd*	D-erythrose 4-phosphate dehydrogenase	+
PA14_13410	31568	*prfC*	Peptide chain release factor 3	++
PA14_16730	53059		hypothetical protein	+
PA14_23090	41014		2-keto-3-deoxy-6-phosphogluconate aldolase	+
PA14_23110	41779		Putative RNA pseudouridine synthase	+
PA14_23480	38372		hypothetical protein - DNA uptake protein and related DNA-binding proteins	+
PA14_25100	41384		hypothetical protein - Uncharacterized protein conserved in bacteria	-
PA14_30360	38757		putative anthranilate phosphoribosyltransferase	++
PA14_35430	5764	*pvcA*	pyoverdine biosynthesis protein PvcA	+
PA14_40510	4840	*ccoN-2*	putative cytochrome c oxidase, cbb3-type, subunit	+
PA14_41880	37666		universal stress protein	++
PA14_46080	53031		hypothetical protein - Ketosteroid isomerase homolog	+
PA14_46840	47948		conserved hypothetical protein	+
PA14_52630	30633	*aruE*	Arginine and proline metabolism	+
PA14_52990	45960	*phhA*	phenylalanine 4-monooxygenase - phenylalanine catabolic process	++
PA14_53970	37002		probable aconitate hydratase	+
PA14_53980	38302		hypothetical protein - propionate catabolic process, 2-methylcitrate cycle	-
PA14_61680	46240	*hemK*	Putative methyl transferase	-
PA14_64180	33692		putative tRNA-dihydrouridine synthase	++
PA14_65320	46697	*miaA*	Delta 2-isopentenylpyrophosphate transferase	++
PA14_66320	45771		hypothetical protein - cyclase activity	++
PA14_68370	40356	*cysQ*	3'(2'),5'-bisphosphate nucleotidase	+
PA14_68730	42600	*gshA*	glutamate--cysteine ligase - glutathione biosynthetic process	+
PA14_72390	35639		putative two-component sensor	-
PA14_73370	34284	*gidA*	Glucose-inhibited division protein A	++

Each AQ extract-non-responding mutant was transformed with the expression vector pUC20*pqsE* and pyocyanin production levels were assayed. (-) no pyocyanin production; (+) restored wild-type level; (++) more than wild-type level as compared to the empty vector pUCP20 control.

Since pyocyanin production is strongly influenced by the activity of PqsE encoded from the last gene of the *pqsA-E* operon (132–134), together with Dr. Christian Pustelny I next investigated whether the AQ-non responding mutants still display a reduced pyocyanin

production when complemented with plasmid borne *pqsE* (pUC20*pqsE*). Despite over-expression of *pqsE*, 4 out of 26 mutants were not capable of increasing the pyocyanin level in our experimental conditions. Those 4 genes were PA14_25100 and PA14_53980 (both coding for a hypothetical protein), PA14_72390 (the PA14 orthologue of *kinB* in *P. aeruginosa* PAO1), and the hypothetical methyltransferase PrmC. A detailed analysis of the latter mutant showed that PA14Δ*prmC* was not able to restore pyocyanin production independent of *pqsE*. However, also vice versa, overexpression of *prmC* (pUCP20*prmC*) in a PA14Δ*pqsE* mutant did not restore synthesis of the virulence factor (Fig. 2.1). These results clearly demonstrate that the presence of both proteins, PrmC and PqsE, is essential for *P. aeruginosa* PA14 to produce pyocyanin.

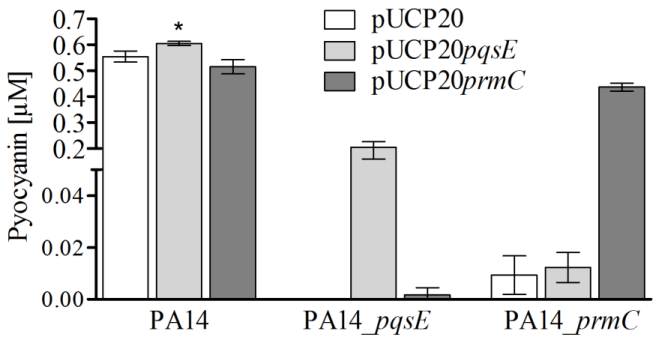

Figure 2.1: Pyocyanin production by PA14 wild-type and the *prmC* and *pqsE* transposon mutants. All strains harbored the empty plasmid vector pUCP20 (white), pUCP20*pqsE* (grey) or pUCP20*prmC* (dark grey). Bacterial cultures were grown in BM2 medium and pyocyanin was extracted after 24 h growth (late stationary phase). Error bars represent one standard deviation of the mean value from three independent experiments, * $p \leq 0.05$ PA14 pUCP20 versus PA14 pUCP20*pqsE*.

2.2.2 Methyltransferase activity of PrmC

In the last decade it was demonstrated, that the PmrC homologues in *E. coli* (PrmC), *Yersinia pseudotuberculosis* (VagH) and in *Chlamydia trachomatis* (PrmC) showed N5-Glutamine-S-adenosyl-L-methionine-dependent methyltransferase activity. By methylation at the glutamine residue of a conserved GGQ motif of peptide chain release factors (RFs) the PmrC homologues were demonstrated to impact on translational termination and therefore on the

global translational pattern (177, 181, 182). A protein alignment of PA14 PmrC with various previously described methyltransferases is depicted in Fig. 2.2 and revealed that PA14 PmrC exhibits identity to the various homologues from 25.08 % (PrmC from *C. trachomatis*) and 48.55 % (VagH from *Y. pseudotuberculosis*) to 50.09 % (PrmC from *E. coli*).

Figure 2.2: Multiple protein sequence alignment between *P. aeruginosa* PrmC and various homologues. Protein sequence alignment was created with ClustalW2 and visualized with Boxshade 3.31 (Mobyle@Pasteur-v1.0.4). Background color indicate different residues (white), similar residues (grey) and identical residues (black) in direct comparison to *P. aeruginosa* PrmC.

Consequently, we wanted to investigate, whether PrmC also displays a methyltransferase activity. Since the knockout of *prmC* in *E. coli* (*E. coli* CK783) comes along with a significant growth defect (177), I analyzed if expression of the *P. aeruginosa* PA14 PrmC protein in *E. coli* CK783 can overcome the growth deficiency. The heterologous expression of PrmC restored the growth rate in *E. coli* CK783 to almost wild-type levels (Fig. 2.3), indicating that PrmC can complement the defective PrmC methyltransferase activity in *E. coli* CK783.

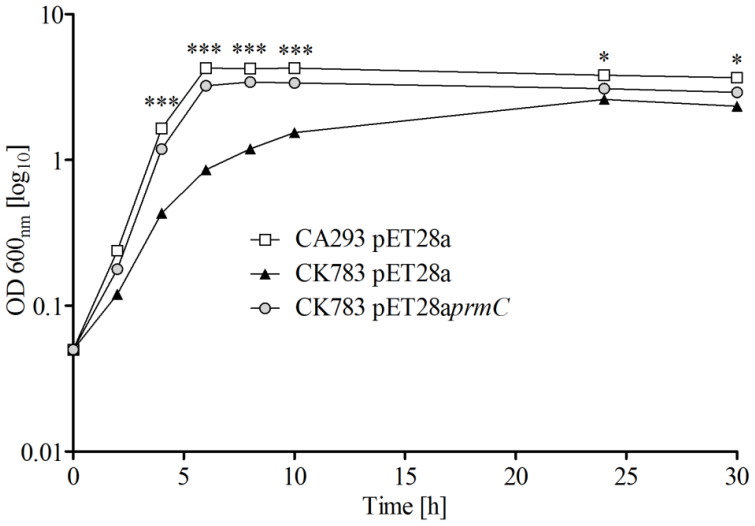

Figure 2.3: Growth of the *E. coli*Δ*prmC* knockout mutant CK783 complemented with PrmC from PA14. Growth of *E. coli* wild-type strain CA293 (square), the *prmC* mutant strain CK783 (filled triangle) both harboring the empty plasmid vector pET28a and CK783 overexpressing *prmC* via pET28a*prmC* (grey circle). The growth media LB broth was supplemented with 1mM IPTG. Data represent the mean from three independent experiments, * $p \leq 0.05$ and *** $p \leq 0.001$ CK783 pET28a versus CA293 pET28a.

In addition, with the help of Dr. Christian Pustelny, I measured the PrmC methyltransferase activity *in vitro*, as previously described for *Y. pseudotuberculosis* (182). Purified PrmC was incubated with radioactive labeled [^{3}H-methyl]-SAM and cell lysate from *P. aeruginosa* PA14 wild-type and the respective *prmC* transposon mutant. When PrmC was incubated with PA14Δ*prmC* mutant lysate the incorporation rate was 2-fold higher as compared to PA14 wild-type lysate (Fig. 2.4), suggesting that in contrast to the PA14Δ*prmC* mutant, the putative PrmC targets, such as the peptide chain release factors PrfA and PrfB, are already methylated in the PA14 wild-type. To demonstrate that the methylation targets of PrmC are the RFs, we increased the RF concentration by generating cell lysates of *P. aeruginosa* PA14 wild-type and PA14Δ*prmC*, both overexpressing *prfA*. As expected, cell lysates with high levels of PrfA remarkably increased the PrmC-dependent incorporation of radioactive ^{3}H-methyl (Fig. 2.4).

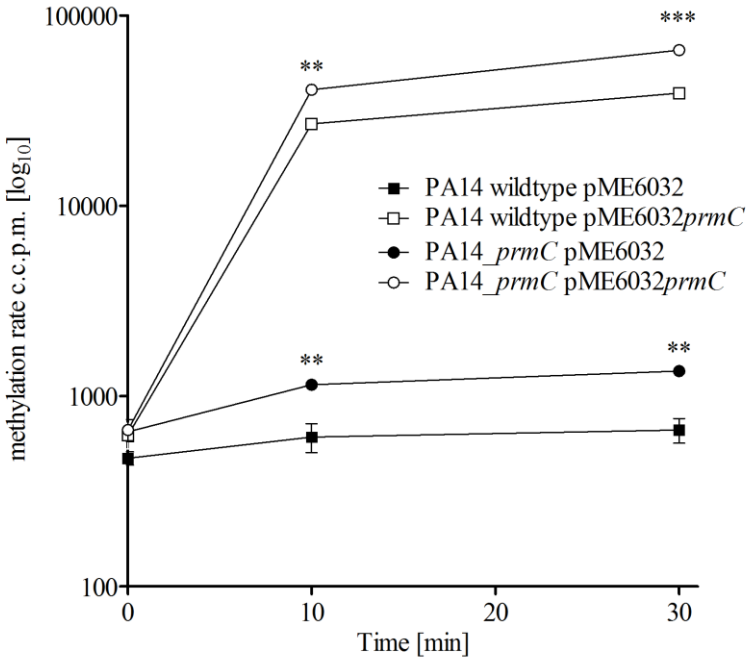

Figure 2.4: SAM-dependent methyltransferase activity of PrmC. Cell lysates from PA14 wild-type and PA14Δ*prmC* carrying the empty plasmid pME6032 or pME6032*prfA* were incubated with purified PrmC and [^{3}H-methyl]-SAM. Methylation was quantified using a microplate liquid scintillation counter (1450 MicroBeta TriLux, Wallac). Data represent the mean from three independent experiments, ** $p \leq 0.01$ and *** $p \leq 0.001$ PA14 wild-type pME6032 versus PA14Δ*prmC* pME6032 and PA14 wild-type pME6032*prfA* versus PA14Δ*prmC* pME6032*prfA*.

Furthermore, PrmC-dependent methylation of PrfA in cell lysates of PA14Δ*prmC* pUCP20 and PA14Δ*prmC* pUCP20*prmC* was confirmed by SDS-gel autoradiography. The auto-radiogram shown in Fig. 2.5 illustrates that PrmC specifically methylates PrfA since no incorporation of ^{3}H-methyl was detected in the control sample lacking PrmC. However, this method was not sensitive enough to visualize methylation of endogenous RFs of PA14Δ*prmC* pUCP20. In addition, with the help of Dr. Manfred Nimtz, we performed a parallel in-gel digestion and LC-MS/MS analysis of the fragment containing PrfA and the methylation at the glutamine residue of the GGQ motif (peptide sequence SSGAGGQHVNK, amino acids 231 to 241) was clearly confirmed (data not shown).

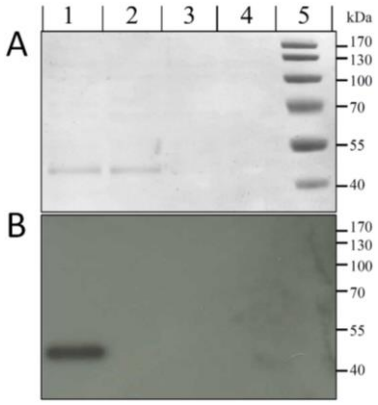

Figure 2.5: Autoradiogram of PrmC-dependent methylated PrfA. Cell lysates from PA14Δ*prmC* pME6032*prfA* + purified PrmC (1); PA14Δ*prmC* pME6032*prfA* (2); PA14Δ*prmC* pME6032 + purified PrmC (3) and PA14Δ*prmC* pME6032 (4) were mixed with 0.6 µM [^{3}H-methyl]-SAM and incubated at 37 °C for 30 min. Lane 5 shows the PageRuler Prestained Protein Ladder from Thermo Scientific. On the top panel (A) a NuPAGE 10 % Bis-Tris gel was used to separate each reaction. The lower panel (B) shows the corresponding autoradiogram illustrating an intensive methylation reaction of PrfA in the presence of PrmC.

2.2.3 The influence of PrmC on the *P. aeruginosa* QS systems

The production of pyocyanin is highly complex and influenced by various different regulatory genes including those involved in the QS circuit of *P. aeruginosa* (73, 106, 111, 119). Since pyocyanin production was almost abolished in the PA14Δ*prmC* mutant and could not be restored by *pqsE* overexpression, we aimed at investigating whether PrmC is modulating the interconnected QS network of *P. aeruginosa*. First I measured the PrmC-dependent protein levels of the AQ-effector protein PqsE and the transcriptional regulator RhlR in late stationary phase. In comparison to the wild-type, the *prmC* mutation had just a marginal effect on RhlR protein level and no significant difference in extracellular C_4-HSL levels could be detected by performing a bioreporter analysis (data not shown). Interestingly, complementation with *prmC* increased the RhlR production about 2-fold. Overexpression of *pqsE* in the *prmC* mutant background clearly increased the RhlR protein level; however, as demonstrated beforehand (Fig. 2.1), this does not lead to a restored pyocyanin production in the *prmC* mutant.

Unlike RhlR, the protein level of PqsE was significantly decreased in a PA14Δ*prmC* mutant and complementation with *prmC* or *pqsE* restored wild-type PqsE protein levels (Fig. 2.6).

These results indicate that PrmC affects pyocyanin production independent of the level of RhlR and PqsE. The *pqsE* gene is encoded by the *pqsA-E* operon involved in PQS biosynthesis, so we were interested in whether a reduction in PqsE level is a direct consequence of a decreased expression of the entire operon. I compared the PQS production of a *prmC* mutant with the wild-type strain but could not detect any significant differences in quinolone signal molecule level (data not shown). Therefore it is likely, that PrmC affects expression of *pqsE* post-transcriptionally.

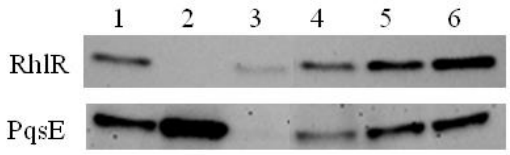

Figure 2.6: Western blot analysis of PrmC-dependent RhlR and PqsE production. Proteins were extracted from (1) PA14 pUCP20, (2) PA14Δ*rhlR* pUCP20, (3) PA14Δ*pqsE* pUCP20, (4) PA14Δ*prmC* pUCP20, (5) PA14Δ*prmC* pUCP20*prmC* and (6) PA14Δ*prmC* pUCP20*pqsE*. Cultures were grown for 20 h (stationary phase of growth) in BM2 medium. Extracts from (2) PA14Δ*rhlR* and (3) PA14Δ*pqsE* were used as negative controls.

2.2.4 Global identification of PrmC-regulated genes and proteins in *P. aeruginosa* PA14

To identify genes regulated by PrmC, I used a RNA sequencing technology as recently described (183). Comprehensive analysis of RNA-Seq data was performed in collaboration with Dr. Andreas Dötsch. Under the experimental conditions employed, the transcriptomic data revealed that the expression of 147 genes (p-value ≤ 0.01), equivalent to 2.3 % of all annotated *P. aeruginosa* genes, was affected more than 4-fold by the loss of PrmC (Tab. 2.2). About one third of genes was upregulated (52 genes) and mainly comprised hypothetical and putative proteins. Among the 95 downregulated genes, we found many genes involved in the production of virulence determinants, such as pyocyanin (*phzA-G1*, *phzA-G2*, *phzM*, *phzS*), the chitinolytic enzyme ChiC (*chiC*) and genes involved in pyochelin biosynthesis or uptake respectively (*pchA-G* and *fptA*) (73, 111, 119, 184–187). Furthermore, we found many genes involved in T3SS and the production of secretion factors (*pscB*, *pscE*, *pscF*, *pscG*, *pscH*,

pscK, *pscN*, *pscQ*, *pscU*, *popB*, *popD*, *popN*, *pcrH*, *pcrG*, *pcrV*, *exsC*, *exoT*, *exoY*, *exoU*), a key gene enabling denitrification (*norB*- nitric-oxide reductase subunit B) and genes associated with resistance (*opmD*, *mexI*, *mexH*, *mexG*) (188–192).

Table 2.2: List of selected genes affected by PrmC identified by RNA-Seq.

PA14[a]	Gene	wt vs *prmC*[b]	Product name[a]
PA14_00560	*exoT*	-6.639	exoenzyme T
PA14_00600		6.690	putative transcriptional regulator
PA14_00620		4.374	conserved hypothetical protein
PA14_00640	*phzH*	-5.271	potential phenazine-modifying enzyme
PA14_01080		4.547	conserved hypothetical protein
PA14_01270		5.173	conserved hypothetical protein
PA14_01510		5.696	putative plasmid stabilisation system protein
PA14_01720	*ahpF*	-4.904	alkyl hydroperoxide reductase subunit F
PA14_01930	*pcaR*	4.432	transcriptional regulator PcaR
PA14_02110		9.931	putative GGDEF domain
PA14_02140		4.576	conserved hypothetical protein
PA14_04970		6.203	thiamine biosynthesis protein ThiS
PA14_05450		4.350	conserved hypothetical protein
PA14_05600		-4.121	conserved hypothetical protein
PA14_06180		-4.350	putative RNA polymerase sigma-70 factor. ECF subfamily
PA14_06240		4.747	putative transcriptional regulator. LysR family
PA14_06430		15.791	putative biotin-requiring enzyme
PA14_06830	*norB*[*]	-12.960	nitric-oxide reductase subunit B
PA14_08420		4.219	putative HIT family protein
PA14_09220	*pchB*	-7.301	salicylate biosynthesis protein PchB
PA14_09230	*pchC*	-5.318	pyochelin biosynthetic protein PchC
PA14_09240	*pchD*	-4.757	pyochelin biosynthesis protein PchD
PA14_09290	*pchG*	-4.061	pyochelin biosynthetic protein PchG
PA14_09320		-5.119	putative ATP-binding component of ABC transporter
PA14_09400	*phzS*	-8.311	flavin-containing monooxygenase
PA14_09410	*phzG1*	-9.044	phenazine biosynthesis protein PhzG1
PA14_09420	*phzF1*	-11.135	phenazine biosynthesis protein PhzF1
PA14_09440	*phzE1*	-22.565	phenazine biosynthesis protein PhzE1
PA14_09450	*phzD1*	-12.510	phenazine biosynthesis protein PhzD1
PA14_09460	*phzC1*	-7.912	phenazine biosynthesis protein PhzC1
PA14_09490	*phzM*	-4.417	probable phenazine-specific methyltransferase
PA14_09500	*opmD*	-25.124	outer membrane protein
PA14_09520	*mexI*	-23.507	probable RND efflux transporter
PA14_09530	*mexH*	-47.275	RND efflux membrane fusion protein precursor
PA14_09540	*mexG*	-89.202	putative membrane protein
PA14_10320		4.767	putative transcriptional regulator

PA14_10360		-9.139	conserved hypothetical protein
PA14_11140		-7.685	putative nonribosomal peptide synthetase
PA14_12560		4.485	conserved hypothetical protein
PA14_12970	*tauD*	6.580	TauD
PA14_14320		-5.162	conserved hypothetical protein
PA14_14330		-10.000	probable chaperone
PA14_14540		-5.913	hypothetical protein
PA14_16010		5.602	putative ong-chain acyl-CoA thioester hydrolase
PA14_16100		-4.167	conserved hypothetical protein
PA14_16250	*lasB*	-4.955	elastase LasB
PA14_16310		-6.552	putative MFS permease
PA14_16380		9.299	putative LysR-family transcriptional regulator
PA14_17920	*glpM*	6.489	membrane protein GlpM
PA14_18120	*mmsA*	-10.696	methylmalonate-semialdehyde dehydrogenase
PA14_18140	*mmsB*	-13.232	3-hydroxyisobutyrate dehydrogenase
PA14_18870		5.571	conserved hypothetical protein
PA14_19570		4.945	putative aliphatic sulfonates transport permease protein
PA14_22100		-4.767	hypothetical protein
PA14_22710		4.311	putative nitroreductase family protein
PA14_23440	*orfL*	-4.050	putative group 1 glycosyl transferase
PA14_26020		-6.046	putative aminopeptidase
PA14_26360		9.494	putative permease of ABC transporter
PA14_27370		4.925	putative ATP-dependent RNA helicase. DEAD box family
PA14_28020		20.322	hypothetical protein
PA14_28470		-4.266	hypothetical protein
PA14_28560		9.311	conserved hypothetical protein
PA14_29070		22.675	putative membrane protein
PA14_30900		-4.047	TrbJ-like protein
PA14_31420		5.583	hypothetical protein
PA14_32290		4.636	conserved hypothetical protein
PA14_32470		-5.922	hypothetical protein
PA14_34460		-5.971	putative alkylhydroperoxidase
PA14_34490		-6.160	putative acyl-CoA dehydrogenase
PA14_34500		-4.783	putative ATP-binding component of ABC transporter
PA14_34510		-5.123	putative sulfonate ABC transporter
PA14_34520		-5.449	putative sulfonate ABC transporter.
PA14_34870	*chiC*	-6.004	chitinase
PA14_35160		-6.391	hypothetical protein
PA14_35430	*pvcA*	10.726	pyoverdine biosynthesis protein PvcA
PA14_36830		-4.928	hypothetical protein
PA14_37170		4.320	conserved hypothetical protein
PA14_38130		6.148	putative lysine-specific permease
PA14_38310		-9.376	conserved hypothetical protein
PA14_39000		17.497	conserved hypothetical protein
PA14_39320	*rbsC*	-5.018	ribose ABC transporter. permease protein
PA14_39570		4.630	hypothetical protein

PA14_39880	*phzG2*	-9.305	phenazine biosynthesis protein PhzG2
PA14_39890	*phzF2*	-9.938	phenazine biosynthesis protein PhzF2
PA14_39910	*phzE2*	-16.370	phenazine biosynthesis protein PhzE2
PA14_39925	*phzD2*	-11.624	phenazine biosynthesis protein PhzD2
PA14_39945	*phzC2*	-9.196	phenazine biosynthesis protein PhzC2
PA14_39960	*phzB2*	-7.563	phenazine biosynthesis protein PhzB2
PA14_40290	*lasA*	-5.032	staphylolytic protease preproenzyme LasA
PA14_42260	*pscK*	-4.073	PscK type III export protein
PA14_42310	*pscF*	-5.274	type III export protein PscF
PA14_42360	*pscB*	-5.116	type III export apparatus protein
PA14_42380		-4.411	conserved hypothetical protein
PA14_42390	*exsA*	-5.116	transcriptional regulator ExsA
PA14_42400	*exsB*	-7.653	exoenzyme S synthesis protein B
PA14_42430	*exsC*	-4.830	exoenzyme S synthesis protein C precursor
PA14_42440	*popD*	-10.541	translocator outer membrane protein PopD precursor
PA14_42450	*popB*	-10.875	translocator protein PopB
PA14_42470	*pcrV*	-6.598	type III secretion protein PcrV
PA14_42480	*pcrG*	-11.543	regulator in type III secretion
PA14_42510		-5.426	conserved hypothetical protein
PA14_42520		-4.928	conserved hypothetical protein
PA14_42570	*pscN*	-7.669	ATP synthase in type III secretion system
PA14_42580	*pscO*	-9.305	translocation protein in type III secretion
PA14_42610	*pscQ*	-4.928	translocation protein in type III secretion
PA14_42630		-4.365	putative translocation protein in type III secretion
PA14_42660	*pscU*	-6.360	translocation protein in type III secretion
PA14_42890	*stp1*	-4.966	serine/threonine protein phosphatase
PA14_42940		-8.398	putative lipoprotein
PA14_43910		6.169	conserved hypothetical protein
PA14_44520		28.345	putative drug efflux transporter
PA14_45120		4.853	hypothetical protein
PA14_46380		4.585	hypothetical protein
PA14_47410		4.237	conserved hypothetical protein
PA14_48060	*aprA*	-4.255	alkaline metalloproteinase precursor
PA14_48140		-4.506	conserved hypothetical protein
PA14_49260	*napB*	-6.713	cytochrome c-type protein NapB precursor
PA14_51520	*spcU*	-5.053	SpcU
PA14_51530	*exoU*	-9.673	ExoU
PA14_52080		6.964	hypothetical protein
PA14_52730		7.978	hypothetical protein
PA14_53290	*trxB2*	-6.769	thioredoxin reductase 2
PA14_54850		13.114	hypothetical protein
PA14_55820		-6.038	putative membrane protein
PA14_55890		-7.255	putative type II secretion system protein
PA14_55900		-7.428	putative pilus assembly protein
PA14_55920		-4.263	putative type II secretion system protein
PA14_55940		-4.064	putative pilus assembly protein

PA14_56530		4.554	putative beta-lactamase
PA14_56540		4.061	putative flavoprotein
PA14_58110		4.255	putative Maf-like protein
PA14_59380		-5.035	conserved hypothetical protein
PA14_60400	*rpsT*	5.070	ribosomal protein S20
PA14_60620		4.196	tRNA-Arg
PA14_63320		5.363	conserved hypothetical protein
PA14_63910		-7.584	putative membrane protein
PA14_64990		4.767	putative phospholipase
PA14_66875	*phaF*	-7.372	polyhydroxyalkanoate synthesis protein PhaF
PA14_68390		6.034	putative hydrolase
PA14_71300		5.144	putative electron transfer flavoprotein. alpha subunit
PA14_71890		4.767	putative coenzyme A transferase
PA14_72360		-5.088	conserved hypothetical protein
PA4704.1	*prrF1*	-4.823	nd

a. Gene number. gene name and product name are from the *Pseudomonas* genome project (193). **b**. Fold change in gene expression of (wt) *P. aeruginosa* PA14 wild-type compared with (*prmC*) *P. aeruginosa* PA14Δ*prmC* transposon mutant (mutant ID 46240). Adjusted p-value is ≤ 0.01 and when indicated with an asterix, the p-value is ≤ 0.05.

Since we expected PrmC to affect translation rather than transcription, Agata Bielecka performed a proteomic analysis which partially overlapped with the transcriptomic data. We found 163 proteins to be differentially regulated in PA14Δ*prmC*, but were just able to identify 26 candidates (Tab. 2.3). Among them we detected several downregulated proteins of which the coding genes were already identified in the transcriptomic analysis, such as PhzS, PhzB2, PhzD1, PhzE1 and PhzF1, all involved in phenazine biosynthesis and the chitinolytic enzyme ChiC. GroEL, described as the heat shock 60 kD chaperonin, was also significantly down-regulated in PA14Δ*prmC*. GroEL is known to be involved in the folding, assembly and transport of newly synthesized proteins in *E. coli* (194). The proteome data shows that up-regulated proteins identified by the analysis were mainly involved in translation such as the 30S ribosomal protein S2, energy metabolism, nucleotide biosynthesis (PpiB, PurT, Tal) and iron acquisition (PA14_64520).

Table 2.3: List of differentially expressed proteins in PA14Δ*prmC* as compared to the wild-type.

PA14 number	PAO1 ortholog	Protein name	Fold change	Description
PA14_05230	PA0400	--	- 5.3	cystathionine gamma-lyase
PA14_09150	PA4236	KatA	- 9.4	Catalase
PA14_09400	PA4217	PhzS	- 18.2	phenazine biosynthesis protein PhzS
PA14_09420	PA1904	PhzF1	- 10.4	phenazine biosynthesis protein phzF1
PA14_09440	PA1903	PhzE1	- 30.3	phenazine biosynthesis protein PhzE1
PA14_09450	PA1902	PhzD1		phenazine biosynthesis protein PhzD1
PA14_09470	PA4211	PhzB1		phenazine biosynthesis protein phzB1
PA14_11810	PA4022	--	- 7.0	putative aldehyde dehydrogenase
PA14_15890	PA3751	PurT	+ 5.9	phosphoribosylglycinamide formyltransferase 2
PA14_17060	PA3656	RpsB	+ 7.179	30S ribosomal protein S2
PA14_27960	PA2796	Tal	+ 4.705	transaldolase B
PA14_25390	PA2991	Sth	- 10.4	soluble pyridine nucleotide transhydrogenase
PA14_34870	PA2300	ChiC		chitinolytic enzyme
PA14_35490	PA2250	lpdV	- 2.7	dihydrolipoamide dehydrogenase (Energy metabolism)
PA14_35500	PA2249	--	- 4.9	branched-chain alpha-keto acid dehydrogenase subunit E2
PA14_39960	PA1900	PhzB2	- 20.8	phenazine biosynthesis protein PhzB2
PA14_41390	PA1793	PpiB	+ 2.4	peptidyl-prolyl cis-trans isomerase B
PA14_50290	PA1092	FliC	+ 2.3	flagellin type B
PA14_54660	PA0744	--	- 3.8	enoyl-CoA hydratase/isomerise
PA14_56240	PA4329	PykA	- 4.4	pyruvate kinase
PA14_57010	PA4385	GroEL	- 12.34	chaperonin GroEL
PA14_57275	PA4407	FtsZ	+ 5.232	cell division protein FtsZ
PA14_60800	PA4595	--	- 4.3	putative ABC transporter ATP-binding protein
PA14_61780	PA4671	--	- 3.6	50S ribosomal protein L25/general stress protein Ctc
PA14_64520	PA4880	--	+ 5.4	putative bacterioferritin
PA14_68340	PA5172	ArcB	- 9.6	ornithine carbamoyltransferase

In PA14Δ*prmC* 26 proteins were identified to be differentially expressed. A positive value indicates a higher expression in the absence of PrmC as compared to the wild-type. When the fold change was indicated with a dash (--) the protein was not identified in PA14Δ*prmC*.

2.2.5 PrmC-dependent growth, virulence factor production and motility

The growth rate of PA14Δ*prmC* in various defined media displayed no significant differences in comparison to the wild-type strain (data not shown). But we observed an intense growth defect in an anaerobic environment. PA14Δ*prmC* was not able to grow in the absence of oxygen (Fig. 2.7), probably due to the diminished production of key proteins involved in denitrification such as NorB (Tab. 2.2).

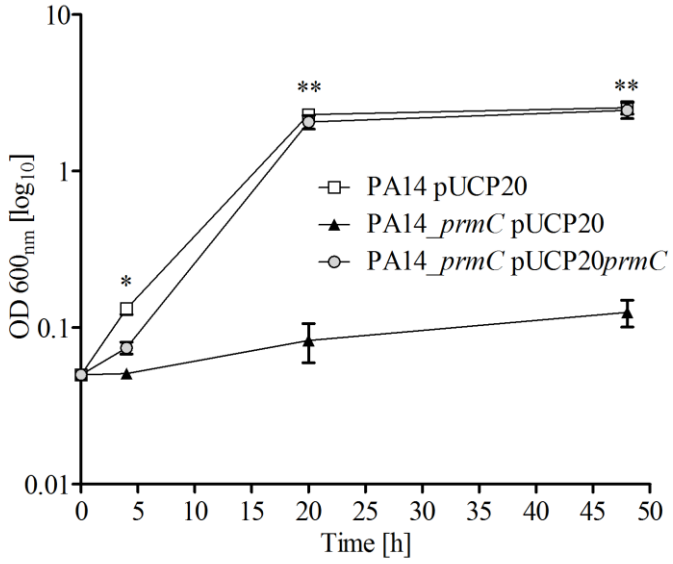

Figure 2.7: PrmC-dependent growth of PA14 in anaerobic environment. Anaerobic growth of PA14 wild-type (square), *prmC* mutant (filled triangle) both harboring the empty plasmid pUCP20 and PA14Δ*prmC* complemented with pUCP20*prmC* (circle) was measured in PYG-KNO_3. Data is reported with standard deviation of the mean from three independent experiments. * $p \leq 0.05$ and ** $p \leq 0.01$ PA14Δ*prmC* versus PA14Δ*prmC* pUCP20*prmC*.

Since PrmC exerts an intensive effect on pyocyanin production and positively influences the RhlR protein concentration, together with Dr. Christian Pustelny I examined if PrmC has a more global effect on bacterial virulence factor production, motility and biofilm formation. The *rhl* system is essential for the regulation of rhamnolipid production (*rhlAB*), which occurs during stationary phase of growth (195, 196). Therefore, we first measured the influence of the *prmC* mutation on rhamnolipid levels. Fig. 2.8 shows that loss of PrmC is attended by a reduction of rhamnolipids, whereby complementation of *prmC* restores rhamnolipid levels. These results demonstrate that the presence of *prmC* influences the RhlR-dependent production of rhamnolipids.

In addition to the results revealed by the trancriptomic analysis, a recent report by Garbom et al. showed that the PrmC homologue VagH in *Y. pseudotuberculosis* is involved in the regulation of the T3SS (182). Hence, I determined the PrmC-dependent expression of the secreted adenylatecyclase *exoT* by introducing the reporter plasmid pUC20P*exoT-gfp* into

PA14 wild-type and PA14Δ*prmC* mutant, respectively. Indeed, absence of PrmC led to decreased *exoT* expression as compared with the wild-type strain (Fig. 2.9).

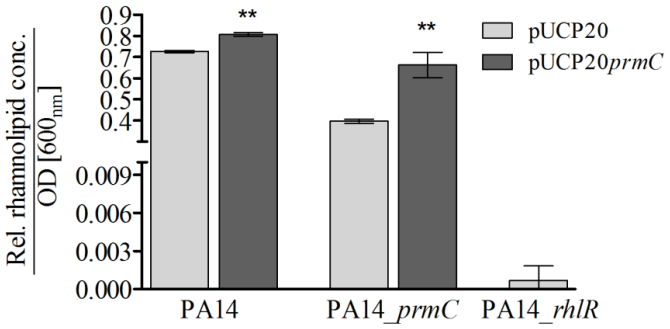

Figure 2.8: Rhamnolipids production by PA14 and *prmC* mutant. PA14 wild-type and PA14Δ*prmC* harbored the empty plasmid pUCP20 (grey bars) and pUCP20 constitutively expressing *prmC* (black bars). PA14Δ*rhlR* pUCP20 was used as negative control. Bacterial cultures were grown in BM2 medium and rhamnolipids were extracted after 48 h growth (late stationary phase). Error bars represent one standard deviation of the mean value from three independent experiments. ** $p \leq 0.01$ PA14 and PA14Δ*prmC* carrying the empty plasmid pUCP20 versus pUCP20*prmC*.

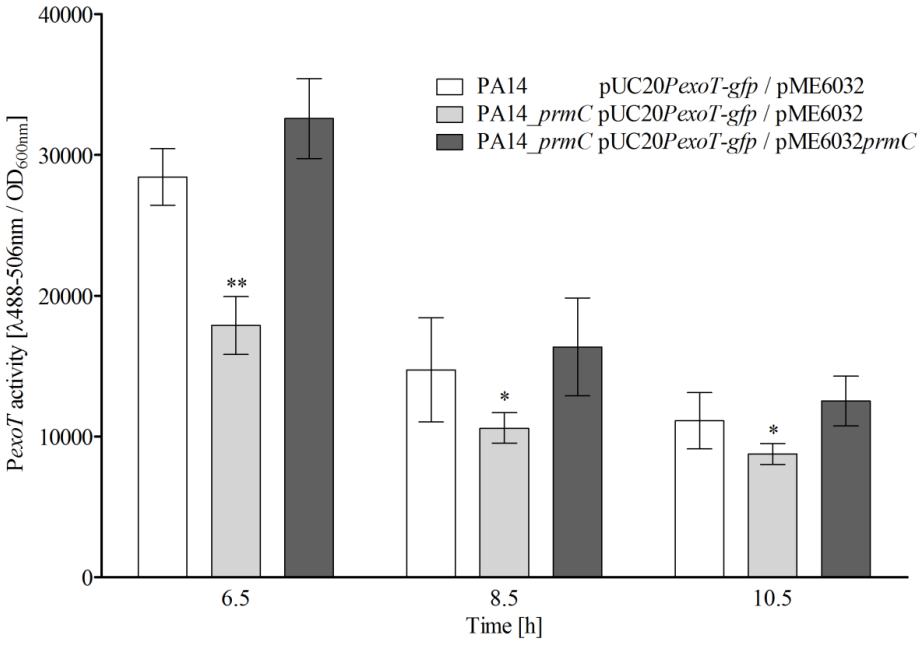

Figure 2.9: Effects of PrmC on *exoT* promoter activity. All strains harbored the *exoT* reporter plasmid pUCP20P*exoT-gfp* and activation of the *exoT* promoter was measured by fluorescence

(ex./em.: 488/506 nm) using a microplate reader (Synergy4; Bio-Tek) and fluorescence was divided by the respective OD600 of the cultures (relative luminescence). PA14 wild-type (white bars) and PA14Δ*prmC* (grey bars) were both transformed with the empty plasmid pME6032 and PA14Δ*prmC* was complemented with pME6032*prmC* (black bars). Bacterial cultures were grown in SM medium to stimulate secretion of ExoT. The average of three independent replicates is reported with standard deviation. * $p \leq 0.05$ and ** $p \leq 0.01$ PA14Δ*prmC* pUCP20P*exoT-gfp* / pME6032 versus PA14Δ*prmC* pUCP20P*exoT-gfp* / pME6032*prmC*.

It is known that all three modes of motility in *P. aeruginosa* are dependent on the *rhl* system (24, 197, 198). Since our results indicate that PrmC affects RhlR-dependent rhamnolipid production, we analyzed if PA14Δ*prmC* is as well attenuated in swimming, swarming or twitching. As expected, PA14Δ*prmC* displayed a significant impaired swimming and twitching phenotype (Fig. 2.10 B; C). PrmC was also essential for swarming motility, as the *prmC* mutant completely lost the ability to swarm under the experimental conditions used (Fig. 8 A). Interestingly, overexpression of *prmC* in the wild-type and the *prmC* mutant did not lead to an increased swarming and twitching phenotype. Conversely, we observed an enhanced swimming motility once PrmC was overproduced in both, the wild-type and the *prmC* mutant strain. Swarming motility was reported to be inversely related to the capability to form biofilms (33). Thus, in collaboration with Dr. Mathias Müsken, we investigated if PrmC also affects biofilm formation in a static 96-well assay. However, we were unable to detect any differences in biofilm formation between the wild-type and the PA14Δ*prmC* mutant (data not shown).

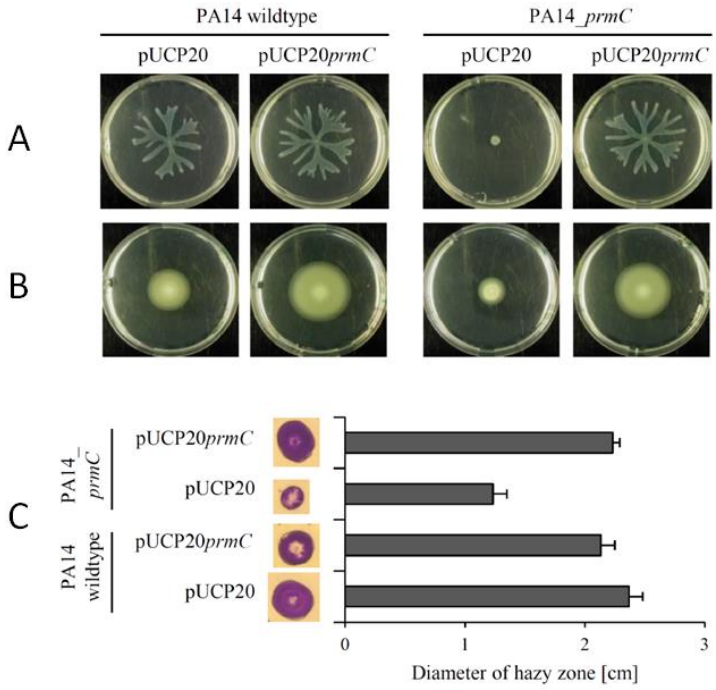

Figure 2.10: PrmC-dependent modulation of PA14 motility. Motility assays were performed with PA14 and PA14Δ*prmC* harboring pUCP20*prmC* and the respective empty vector. (A) Swarming motility; (B) Swimming motility; (C) Twitching motility.

2.2.6 The role of PrmC in pathogenicity of *P. aeruginosa* PA14

Considering the fact that PrmC is essential for pyocyanin, rhamnolipid and ExoT production and further affects motility, we investigated the impact of *prmC* mutation on *P. aeruginosa* pathogenicity using the vertebrate infection animal model *Galleria mellonella* (greater wax moth). The larvae of *G. mellonella* are sensitive to *P. aeruginosa* infections (199) and extensively used as a mini-host model for pathogenic bacteria and fungi, that are responsible for severe human diseases such as: *Bacillus cereus* (200), *Candida albicans* (201), *Cryptococcus neoformans* (202), *Enterococcus faecalis* (203), *Francisella tularensis* (204), *Listeria monocytogenes* (205), *Staphylococcus aureus* (206), and *Y. pseudotuberculosis* (207). It was also reported, that the T3SS in *P. aeruginosa* plays a significant role in *G. mellonella* killing (208). As expected, in *G. mellonella* the PA14Δ*prmC* mutant was significantly attenuated in virulence. With a median survival of 50 hours, PA14Δ*prmC* infected *G. mellonella* survived about 4 times longer than *G. mellonella* infected with PA14 wild-type which died after 14 hours. Plasmid-mediated complementation of *prmC* mutation restored the pathogenicity of PA14, as the median survival with 20 hours was close to wild-type levels

(Fig. 2.11 A). To scrutinize the significant higher survival rate of *G. mellonella* infected with PA14Δ*prmC*, we investigated if the decreased pathogenicity was a possible consequence of growth deficiency *in vivo*. The results obtained from the CFU analysis showed that PA14Δ*prmC* is not able to proliferate after injection into the host organism (Fig. 2.11 B), which in turn could reflect a restrained growth effect correlating with the growth deficiency observed in oxygen limiting conditions (Fig. 2.7).

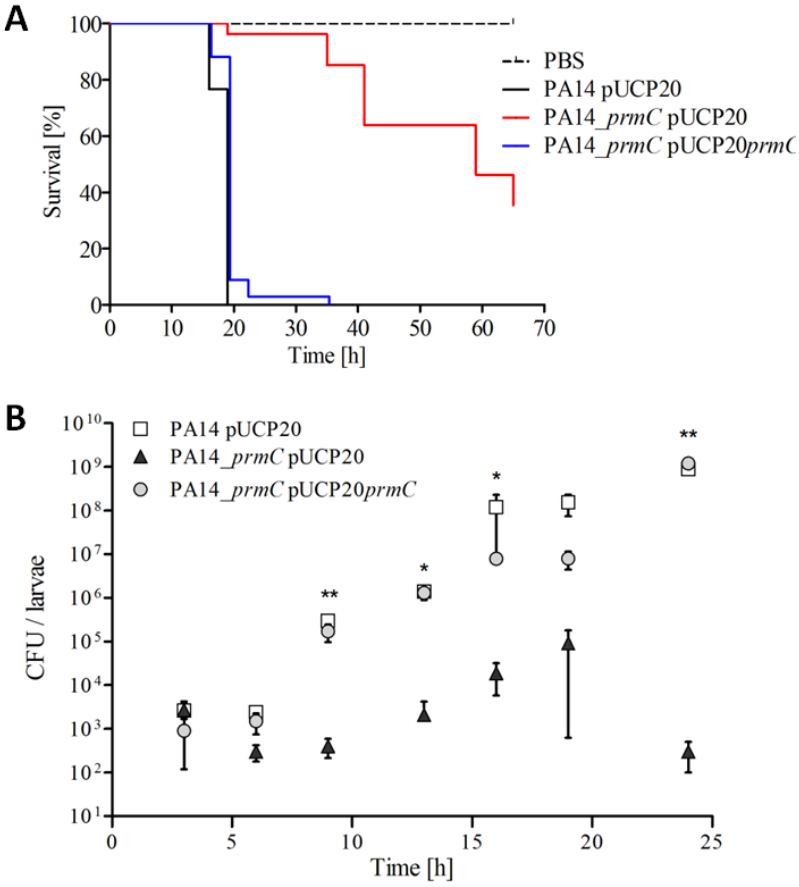

Figure 2.11: *G. mellonella* pathogenicity assay. *G. mellonella* larvae were inoculated with PA14 and PA14Δ*prmC* both harboring the empty plasmid pUCP20 and PA14Δ*prmC* complemented with pUCP20*prmC*. PBS was used as a negative control. (A) Survival rates of the infected *G. mellonella* larvae; 20 larvae for PBS and 30 larvae for each strain. (B) Bacterial growth within each larvae was monitored for 1 day; 5 larvae for each timepoint. Error bars represent one standard deviation of the mean. * $p \leq 0.05$ and ** $p \leq 0.01$ PA14Δ*prmC* pUCP20 versus PA14Δ*prmC* pUCP20*prmC*.

2.3 Discussion

In this study, we looked for new genes affecting QS and virulence factor production in *P. aeruginosa* PA14, such as the phenazine pigment pyocyanin. Pyocyanin synthesis is facilitated by an intact QS system and induced by exogenous addition of AQs. By screening the transposon mutant library (180) towards AQ-responsiveness, we identified a new set of AQ-non responding mutants with a decreased pyocyanin production.

We focused our studies on one mutant affected in the *prmC* gene. PrmC was demonstrated to be essential for pyocyanin production even in the presence of exogenously added extract containing QS-signal molecules and independent of the AQ effector protein PqsE. By performing western blot analysis, we obtained evidence that in the PA14Δ*prmC* background PqsE is still active since overexpression leads to increased RhlR level. PrmC exhibits high homology to the SAM-dependent methyltransferase in various Gram-positive and Gram-negative bacteria including *E. coli*. Various proteins of the HemK family were shown to methylate RFs modulating translational regulation *in vitro* and *in vivo* (177, 181, 182, 209, 210).

In this study, heterologous expression of PA14 *prmC* in *E. coli* was demonstrated to overcome and complement the growth defect of the *E. coli*Δ*prmC* knockout mutant CK783, suggesting a similar enzymatic activity as *E. coli* PrmC. Using autoradiography and LC-MS/MS analysis, it was clearly shown that PrmC specifically methylates the peptide chain release factor PrfA and that the methylation occurs at the conserved GGQ motif.

Since previous reports indicate that proteins of the PrmC family exhibit a decisive role in gene expression and post-transcriptional regulation, we analyzed the global regulatory effects of PrmC by generating a transcriptional profile and by conducting a proteomic study of *P. aeruginosa* PA14Δ*prmC* (177, 182). Our results showed that loss of PrmC affected ~ 2.3 % of the annotated genes in *P. aeruginosa* and caused repression of 95 genes (p-value ≤ 0.01), including a high proportion of virulence-associated genes and genes involved in the T3SS. However, this impact of PrmC on gene expression may not in all cases be a direct consequence of inefficient translation due to non-methylation of RFs, but may likewise represent an indirect result of a decrease in levels of positive regulators. Our proteomic analysis revealed just 26 proteins to be differentially regulated in PA14Δ*prmC*. This was a surprising finding, since PrmC-dependent methylation of RFs strongly affects their

translational termination efficiency and thus, we expected to see major differences at the protein level. However, one interesting protein negatively affected by the loss of PrmC was GroEL, a chaperon involved in the correct assembly of expressed proteins. Therefore, some phenotypic effects triggered by PrmC might be assigned to the impaired synthesis of GroEL. Among the proteins which were upregulated in PA14Δ*prmC* we found the flagellar filament structural protein FliC. Since PA14Δ*prmC* displayed a non-motile phenotype, the accumulation of FliC might reflect a defective flagellar assembly leading to an increased intracellular protein level. The marginal effect of PrmC on the proteome has raised the question of whether the few identified proteins are directly affected through under-methylation of RFs and share any commonalities on the gene level. To address this question we analyzed the 26 genes with regard to similarities in their termination codon sequence context but could not identify any common features.

During infection and colonization it is crucial for *P. aeruginosa* to adapt to various environmental changes and to circumvent hostile conditions by moving towards beneficial places. Loss of *prmC* comes along with a non-motile phenotype and the bacterium was no longer able to grow in an anaerobic atmosphere. Despite the obvious functional similarities of PrmC (*E. coli*) and PrmC (*P. aeruginosa*), their regulation of genes involved in respiration and denitrification is different. The loss of *prmC* in *E. coli* leads to repression of genes related to aerobic respiration and induction of genes involved in anaerobic growth, whereas in this study we demonstrate that the presence of PrmC in *P. aeruginosa* PA14 conversely is essential for anaerobic growth (177).

The inability of the PA14Δ*prmC* mutant to adapt in a sufficient way to various environmental changes is reflected in restrained infection efficiency in the *G. mellonella* host infection model. Pathogenicity of *P. aeruginosa* PA14Δ*prmC* in this infection model was impaired and fully restored after *prmC* complementation. Hereby, PrmC played a significant role in proliferation since *P. aeruginosa* PA14Δ*prmC* rarely achieved a critical bacterial mass (CFU of ~1 x 10^5) to kill the larvae. The reduced growth rate within the host may be explained by the lack of virulence factors important for nutrition utilization, or it may be a result of the previously described importance of PrmC for survival in the absence of oxygen considering the bacteria face a microaerophilic or anaerobic environment during infection.

Taken together, in this study we demonstrate that the methyltransferase PrmC in *P. aeruginosa* PA14 is essential for virulence, plays an important role in adaptation to various

environmental conditions, and the functional activity of PrmC is crucial for *P. aeruginosa* pathogenicity. Thereby, the regulation of various virulence factors such as pyocyanin, ExoT and rhamnolipids can partially be explained by a reduced QS activity. Although the absence of PrmC led to pronounced changes in motility and anaerobic growth, we were not able to detect a detrimental effect on biofilm formation. Nevertheless, further investigations may help to understand if RF-methylation creates a bias to affect preferential genes important for the bacterium to survive under certain stress conditions, and if PrmC is a potential target for anti-virulence drug development.

2.4 Experimental procedures

Bacterial strains, media and growth conditions

Unless otherwise noted, bacterial strains listed in Tab. 2.4 were routinely grown in Luria broth (LB) medium at 37 °C and shaking at 180 rpm. Growth kinetics were monitored by taking OD_{600} measurements. Anaerobic growth of *P. aeruginosa* was monitored in an anaerobic workstation at 37 °C in PYG-KNO_3 medium [DSMZ_Medium 104 supplemented with 100 mM KNO_3 (www.dsmz.de/microorganisms/medium/pdf/DSMZ_Medium104.pdf)]. Antibiotics were added at the following final concentrations [µg/ml]: for *E. coli*, kanamycin 50; ampicillin 100; tetracycline 12.5; for *P. aeruginosa*, carbenicillin 400; tetracaycline 100. Isopropyl-β-D-thiogalactopyranosid (IPTG) was added to the medium at a concentration of 1 mM (*E. coli*) and 0.1 mM (*P. aeruginosa*).

Table 2.4: Strains, plasmids and primers used in this work.

Strain/plasmid	Relevant characteristics[a]	Source
Strains		
E. coli DH5α	F$^-$ *endA1 gln*V44 *thi-1 recA1 relA1 gyr*A96 *deoR nupG* Φ80d*lacZ*ΔM15 Δ(*lacZYA-argF*) U169, *hsdR*17 ($r_K^- m_K^+$), λ-	(211)
E. coli BL21 [DE3]	F- *ompT hsdS*$_B$ ($r_B^- m_B^-$) gal dcm	Stratagene
E. coli CA293	HfrC *lacZ*$_{oc659}$ *trp*$_{am8}$ *relA1 spoT1*	(212)
E. coli CK783	CA293 Δ*prmC*::Cm^R	(177)
PA14	Wild-type	(180)
PA14Δ*pqsA*	*pqsA* transposon mutant from the NR PA14 transposon mutant library; ID 23621, Gm^R	(180)
PA14Δ*pqsE*	*pqsE* transposon mutant from the NR PA14 transposon mutant library; ID 45262, Gm^R	(180)
PA14Δ*prmC*	*prmC* transposon mutant from the NR PA14 transposon mutant library; ID 46240, Gm^R	(180)

PA14Δ*rhlR*	*rhlR* transposon mutant from the NR PA14 transposon mutant library; ID 37943, Gm^R	(180)
Plasmids		
pUCP20	*Escherichia-Pseudomonas* shuttle vector with beta-lactamase (*bla*) and LacZ alpha peptide (*lacZ* alpha) genes, $Amp^R/Carb^R$	(213)
pUC20*pqsE*	pUCP20 containing PAO1 *pqsE*	(214)
pUC20*prmC*	pUCP20 containing PA14 *prmC* cloned into the EcoRI/SacI site	This study
pUC20P*exoT-gfp*	PAO1 *exoT* promoter-*gfp* fusion construct from pExoT-*gfp* (210) was cloned into the EcoRI site of pUCP20 in opposite direction of the *lac* promoter	This study
pET28a	*E. coli* expression vector with N- and C-terminal His_6-tag, Km^R	Novagen
pET28a*prmC*	pET28a containing PA14 *prmC* cloned into the NdeI/HindIII site	This study
pME6032	pVS1-p15A shuttle expression vector, Tc^R	(215)
pME6032*prmC*	pME6032 containing PA14 *prmC* cloned into the EcoRI/SacI site	This study
pME6032*prfA*	pME6032 containing PA14 *prfA* cloned into the EcoRI/Acc65I site	This study
Primer[b]		
*prmC*_EcoRI_fw	5'- TATGAATTCGACATGACCACTATCTGTACC	This study
*prmC*_SacI_rv	5'- TATGAGCTCTCAGCATGCCCATTGTCCGA	This study
*prmC*_NdeI_fw	5'- TATCATATGAATACCAGGCCGATCAACTGG	This study
*prmC*_HindIII_rv	5'- TATAAGCTTAGCAGGATCTGGCGACTGTA	This study
*prfA*_EcoRI_fw	5'- TATGAATTCATGAAAGCTTCTCTGCTGAAAAAGCTGGATGTCCTCAGC	This study
*prfA*_Acc65I_rv	5'- TATGGTACCTCAGTCGCCCAGGGCCGCCAGTTGATC	This study

a. Cm^R, chloramphenicol resistant; Gm^R, gentamycin resistant; Amp^R, ampicillin resistant; $Carb^R$, carbenicillin resistant; Km^R, kanamycin resistant; Tc^R, tetracycline resistant. **b**. Engineered restriction sites are underlined.

Preparation of concentrated organic extract including AQs (PA14-extract)

A volume of 250 ml Brain Heart Infusion (BHI) medium was inoculated with an overnight *P. aeruginosa* PA14 culture and incubated in an orbital shaker for 24 h with 180 rpm at 37 °C. To extract AQs, equal amounts of dichloromethane (250 ml) and culture (250 ml) were mixed, shaken for 1 min and added to a separating funnel. The lower organic phase was collected and filtered by a paper filter to eliminate slimy interphase residues followed by evaporation under a hood. The dried concentrate was resuspended in 10 ml methanol and frozen in 2 ml aliquots at -20 °C.

AQ screen of the PA14NR library

96-well plates with 200 µl LB per well were inoculated from the deep-frozen 96-well stock of the non-redundant PA14 transposon mutant library (in total 63 plates) by use of a 96-pin replicator (180). The microtiter plates were inserted in a box with humid atmosphere and incubated in an orbital shaker for approx. 4 h with 180 rpm at 37 °C. Following a defined schema, the 96 samples were split to eight 24-well plates: 5 µl of each mutant preculture was used to inoculate both 500 µl LB and 500 µl LB containing 1 µl/ml PA14-extract. The 24-

well plates were inserted in boxes with humid atmospheres and incubated in an orbital shaker with 180 rpm for approx. 16 h at 37 °C. After incubation pyocyanin levels were analyzed by eye to judge the differences between cultures with and without exogenously added AQs.

Immunoblotting

Bacterial cultures were grown for 20 h in BM2 minimal medium [7 mM $(NH_4)_2SO_4$, 40 mM K_2HPO_4 and 22 mM KH_2PO_4 with 0.5 % casamino acids] at 37 °C to an OD_{600} of 3.0. Whole cell lysates were normalized for protein content and 10 µl of an OD_{600} of 10.0 were separated by SDS-PAGE (10 % acrylamide) after 15 min incubation at 95 °C. Primary antibodies: Rabbit polyklonal antisera α-RhlR and a polyclonal antibody α-PqsE (Biogenes) were used at dilutions of 1:20.000 and 1:5.000 respectively. B4c goat anti-rabbit IgG (Dianova) were used as the secondary antibody at a dilution of 1:4.000. The blot was developed using Lumi-Light Western Blotting Substrate (Roche) and chemiluminescence was detected using Las-3000 Imager (Fujifilm).

Galleria mellonella infection assay

Bacterial strains were grown to exponential growth phase in LB supplemented with carbenicillin. Cells were harvested by centrifugation at 13.000 rpm for 4 min. resuspended in sterile phosphate buffered saline (10 mM PBS, pH 7.5) to an OD_{600} of 1.0 and 10-fold serially diluted in PBS. *G. mellonella* larvae were inoculated with 20 µl of a 1:20.000 dilution containing 5 x 10^2 ± 40 colony-forming units (CFUs) by injection into the haemocoel of the hindmost proleg with a 100 µl Hamilton syringe and a 30G needle. The larvae were placed in Petri-dishes and incubated in the dark at 37 °C. Mortality rates of 30 larvae per treatment were monitored for 65 h. Larval death was assessed by the lack of movement of larvae in response to stimulation together with melanization of the cuticle. To determine bacterial growth in infected larvae, five larvae of each treatment were homogenized individually in eppendorf tubes at seven different time points in 500 µl PBS by vortexing for 30 sec. A volume of 10 µl drops of serial dilutions in PBS were plated on *Pseudomonas* isolation agar (Fluca Analytical/Sigma-Aldrich) containing carbenicillin to select for pUCP20-carrying *P. aeruginosa*. CFUs were determined after 14 – 24 h incubation at 37 °C. PBS was used as a negative control in the experiment.

Transcription analysis

Preparation of RNA and comparative analysis of gene expression was performed as previously described by (183). RNA was extracted from *P. aeruginosa* cultures grown in BM2 medium at 37 °C to late exponential growth phase (OD_{600} of 1.9 – 2.1). For each strain two biological replicates were used.

Proteomics

P. aeruginosa PA14 wild-type and PA14Δ*prmC* mutant were grown in LB medium at 37 °C. Cultures were harvested at an OD_{600} of 2.0. washed twice with PBS and the pellet was resuspended in 10 ml lysis buffer (7 M Urea, 2 M Thio-urea, 4 % Chaps, 20 mM Tris base, DTT) and protease inhibitors (Complete mini, EDTA free, Roche). Disruption of the cells was performed by sonication. Lysate was precipitated using the 2D Clean-Up Kit (GE Healthcare) and pellets were resuspended in urea buffer. The protein concentration was determined using a Bradford reagent (BIO-RAD). Samples were passively rehydrated for 12 h and run on IPG strips (pH 3-10. 18 cm) using an Ettan IPGpfor system (GE Healthcare). Each sample contained in total 150 µg of proteins. After first dimension, proteins distributed on IPG strip were reduced with DTT and alkylation was performed with idodoceamide. The second dimension separation was performed using gradient SDS-PAGE gels (10-15 %). Gels were fixed with 10 % TCA, stained with Commassie brilliant blue, scanned with ImageScanner III (GE Helathcare) and matched using a Compugen Z3 software. Differentially expressed proteins were cut out from the gel and digested with trypsin and further sequenced using MALDI-TOF.

Pyocyanin quantification

Pyocyanin levels were determined as previously described (216) using cell-free supernatants of *P. aeruginosa* cultures grown in BM2 medium for 24 h at 37 °C. After centrifugation at 13.000 rpm for 10 min, 1 ml of cell-free supernatant was mixed with an equal volume of chloroform. Samples were centrifuged at 13.000 rpm for 5 min. and the organic phase was mixed with 1 ml of 0.2 M HCl by brief vortexing. After centrifugation at 13.000 rpm for 1 min. the pink/red top layer was used for spectrophotometrical analysis at 520 nm. Pyocyanin concentrations were calculated by multiplication with 17.072 and standardized by dividing the OD_{520} through the respective OD_{600} of the cultures.

Rhamnolipid quantification

Relative rhamnolipid levels in the supernatant of *P. aeruginosa* cultures grown in BM2 medium for 48 h at 37 °C were quantified indirectly using a 1.6 % orcinol assay previously described (217). After centrifugation at 13.000 rpm for 10 min. a volume of 600 µl of the culture supernatants was mixed with 3.4 ml diethylether by brief vortexing. Samples were centrifuged at 13.000 rpm for 5 min and 2 ml of the upper fraction was evaporated to a final volume of 1 ml. After addition of 600 µl 20 mM HCl and vigorous vortexing, samples were centrifuged for 3 min at 13.000 rpm and 500 µl of the organic phase was evaporated to dryness. The remainder was dissolved in 100 µl 1.6 % orcinol and 800 µl of 60 % H_2SO_4 and after 30 min incubation at 80 °C rhamnolipids were measured spectrophotmometrically at an OD_{421}.

Extraction and quantification of P. aeruginosa AQ metabolites

AQs were extracted from *P. aeruginosa* cultures grown in BM2 medium at 37 °C for 24 h with dichlormethane as described previously (111). Briefly, the bacterial cultures were normalized to an OD_{600} of 3.0 and mixed with 2 volumes of dichlormethane by vigorous shaking. After centrifugation at 13.000 rpm for 5 min, the lower organic phase was evaporated to dryness, before being dissolved in methanol.

TLC was perfomed using a silica gel 60 F254 plate which had been previously soaked for 30 min in 5 % KH_2PO_4 and activated at 80 °C for 1 h. The *P. aeruginosa* extracts were separated by TLC using a 95:5 dichlormethane-methanol mobile phase until the solvent front reached the top of the plate. Fluorescent spots were visualized under UV light and photographed. Synthesized PQS (2 µl of a 2 mg/ml standard) was used as standard.

GC-MS analysis was performed by derivatization with trimethylsilylation (50 % pyridine, 50 % BSTFA [bistrimethylsilyltrifluoroacetamide] containing 1 % TMC [trimethyl-chlorosilane]). (70 °C. 1 h) with a Thermo-Finnigan GCQ ion trap mass spectrometer (Finnigan MAT Corp.) running in the positive-ion electron impact (EI) mode equipped with a 30-m DB5 capillary column as described by (117). Quantification was performed by electronic integration of the most abundant fragment ion traces at m/z: 304 (PQS) and correction of the integrals by the relative intensities of the respective fragment ions

Motility assay

Swimming motility of *P. aeruginosa* was evaluated by seeding stationary-phase cells (1 µl of an OD_{600} of 2.0) onto the agar surface of swimming agar plates (BM2, 1.5 % agar, 0.4 % glucose, 2 mM $MgSO_4$ and 10 µM $FeSO_4$), which were air dried 15 min directly before use. Plates were incubated at 37 °C, and the diameter of the circular turbid zone formed by bacterial cells migrating from the point of inoculation was measured 16 h postinoculation.

Swarming migration was analyzed by inoculating precultured bacteria (1 µl of an OD_{600} of 2.0) carefully onto the surface of swarming agar plates [BM2 without $(NH_4)_2SO_4$, 1.5 % agar, 0.4 % glucose, 2 mM $MgSO_4$ and 10 µM $FeSO_4$]. The plates were incubated at 37 °C for 12 h. Swarming motility was assessed by examining the colony sizes and the branch-spreading patterns on the semisolid agar medium.

Twitching motility was assessed by stab inoculating cells to the bottom of LB-agar plates (1.5 %) with a toothpick and subsequent 24 h incubation at 37 °C. Strains capable of twitching motility form a light haze zone of growth at the interface between the agar and the petri plate surrounding the colony, whereas strains defective in twitching motility are supposed to remain clustered in the area of initial inoculation. Attached cells were stained with 1 % crystal violet and the characteristic flat, spreading colony morphology was used as a measure of twitching motility.

Fluorescence assay

To analyze the *in vivo* expression level of *exoT* in *P. aeruginosa*, the vector p*exoT-gfp* (218) was digested with EcoRI and cloned in the opposite orientation to the *lac* promoter in pUCP20. The resulting plasmid pUCP20P*exoT-gfp* was transformed into the PA14 wild-type and PA14Δ*prmC* mutant strain both harboring the empty vector pME6032, or pME6032*prmC* respectively. *P. aeruginosa* cultures were grown in SM-Medium supplemented with the respective antibiotics and IPTG at 37 °C and shaking at 180 rpm to stimulate the T3SS. After 6 h growth, nine aliquots of 200 µl of each strain were transferred to the wells of a 96-well plate. Growth and fluorescence kinetics were monitored using a Varioskan Flash (Thermo Scientific) with an excitation λ 488 nm and an emission λ 508 nm.

PrmC purification

A volume of 500 ml LB supplemented with kanamycin was inoculated 1:25 with an overnight culture of *E. coli* BL21 cells harboring the *prmC* expression vector pET28a*prmC*. The culture was grown at 37 °C and PrmC expression was induced at OD_{600} of 0.5 – 0.8 by addition of 1 mM IPTG. Subsequently, the culture was shaken overnight at 20°C before harvesting the cells by centrifugation. Bacterial cells were resuspended in lysis buffer (50 mM NaH_2PO_4 pH 8.0, 300 mM NaCl, 10 mM imidazole) containing 1 mM DTT, 1 mg/ml lysozyme, protease inhibitors (Complete mini, EDTA free, Roche) and Benzonase Nuclease (Novagen). After ribolyzing the cells for 60 s and subsequent centrifugation at 13.000 rpm for 15 min at 4 °C, the supernatant was incubated with nickel-nitrilotriacetic acid agarose resin (Qiagen) for 1 h at 4 °C. The resin was washed with lysis buffer and proteins were eluted with 50 mM NaH_2PO_4 pH 8.0, 300 mM NaCl containing 1 mM DTT with a stepwise increase in imidazole concentration (50, 100, 150, 250 mM). After SDS-PAGE analysis, the fraction containing pure protein PrmC-His_6 (elution with 250 mM imidazol) was dialyzed for 16 h at 4 °C in 50 mM NaH_2PO_4 pH 8.0 and 300 mM NaCl.

Methylation assay

In vitro methylation assays were performed as previously described with minor modifications (182, 219). For the preparation of PA14 cell lysates, the wild-type and *prmC* mutant strain, each carrying the PA14 *prfA* expression vector pME6032*prfA* and the empty vector as control, were grown overnight in LB supplemented with tetracycline. Expression of the release factors was induced by addition of 1 mM IPTG. The cultures were equalized to an OD_{600} of 20.0 in a volume of 1 ml, centrifuged and cells were washed once in reaction buffer (50 mM Tris, 100 mM NaCl, 10 mM EDTA, 20 % (v/v) glycerol, pH 8.0) containing protease inhibitors (Complete mini, EDTA free, Roche). Bacterial pellets were finally resuspended in an equal volume of the same buffer. Cells were ribolyzed for 60 sec and after centrifugation at 13.000 rpm for 15 min at 4 °C the supernatants were directly used for the methylation assay. Protein concentrations were determined using a Bradford reagent (BIO-RAD). The reaction mixture was adapted to a final concentration of 30 µg/ml PA14 cell lysates, 6 µg/ml purified PrmC-His_6, 0.6 µM [^{3}H-methyl]-SAM (specific activity 1 mCi/ml, Hartman analytics) and incubated at 37 °C. At several timepoints, 10 µl aliquots were removed, spotted on presoaked and dried filter paper (1 cm^2, Rotilabo, Roth) and quenched with 10 % (w/v) trichloroacetic acid (TCA). The filters were washed twice with 10 % (w/v) TCA for 15 min and once with 95

% EtOH for 10 min. Air-dried filters were transferred into a 24-well sample plate, covered with 1 ml scintillation fluid and radioactivity was quantified using a microplate liquid scintillation counter (1450 MicroBeta TriLux, Wallac). For autoradiography analysis 20 µl aliquots were removed after 30 min incubation and directly transferred to a NuPAGE 10 % Bis-Tris gel. After electrophoresis and Coomassie staining (acetic acid 10 %, methanol 25 %, Coomassie brilliant blue R250 0.2 %). proteins were washed for 90 min and incubated for 30 min in amplification reagent (Amersham AmplifyTM Fluorographic Reagent, GE Healthcare), dried and exposed to a high performance autoradiography film (Amersham HyperfilmTM MP, GE Healthcare) for 24 h at -70 °C before developing. In parallel, protein samples were separated by SDS-PAGE and bands corresponding to PrfA were digested with trypsin and further analyzed by MALDI-TOF.

3 The PqsR and RhlR transcriptional regulators determine the level of PQS synthesis in *P. aeruginosa* by producing two different *pqsABCDE* mRNA isoforms

3.1 Objective

Regulation of gene expression plays a key role in bacterial adaptability to changes in the environment. An integral part of this gene regulatory network is achieved via QS systems that coordinate bacterial responses under high cellular densities. In *P. aeruginosa* the *pqs* signaling pathway is crucial for bacterial survival under stressful conditions. Biosynthesis of the *Pseudomonas* Quinolone Signal (PQS) is dependent on the *pqsA-E* operon, which is positively regulated by the LysR-family regulator PqsR and repressed by the transcriptional activator protein RhlR. However, the molecular mechanisms underlying this inhibition have remained elusive. Interestingly, RhlR was found to inhibit *pqsA-E* expression by binding to a *las/rhl* box centred at -311 bp upstream of the *pqsA* transcriptional initiation site (129). Dötsch and colleagues have recently shown that there is an alternative transcriptional start site (*pqsA*-339) just downstream of the RhlR-binding site (183), indicating that repression of PqsA production via RhlR might be post-transcriptional. To affirm this hypothesis, the influence of RhlR on the translation efficiency of the *pqsA-E* mRNA was analyzed in more detail.

3.2 Results

3.2.1 RhlR induces transcription of the PQS biosynthetic operon via an alternative transcriptional start site

In an early attempt to investigate regulation of PQS synthesis, RhlR-C_4-HSL was found to negatively regulate *pqsR* transcription and thus to inhibit PQS synthesis (121). Later, Xiao and colleagues showed binding of RhlR to a *las/rhl* box in the 5' leader sequence of *pqsA* (Fig. 3.1 A) (109). Deletion of the entire *las/rhl* box significantly increased *pqsA* transcription in *P. aeruginosa* wild-type but not in *rhlR* mutant cells. It was therefore suggested that binding of RhlR to the *las/rhl* box lowers *pqsA* transcription (129).

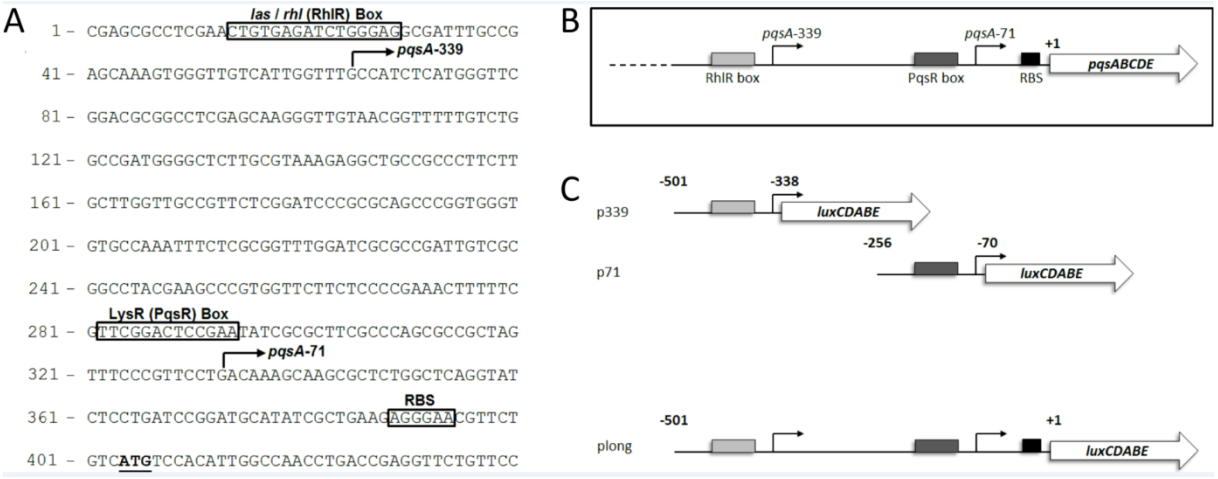

Figure 3.1: Regulatory elements within the 5' UTR of the *pqsA* gene and constructs used in this study. (A) Promoter region of *pqsA*. The *pqsA* transcriptional start sites are indicated by bent arrows at *pqsA*-339 and *pqsA*-71, and the *pqsA* ATG start codon is underlined. The binding sites of RhlR, PqsR and the ribosome are boxed and labeled. (B) Model of the *pqsA* promoter region. (C) *pqsA* promoter-fusion (p339 and p71) and translational (plong) constructs used in the present study. (-) and (+) indicate position to the start codon of *pqsA*. Lines are not drawn to scale.

To address this further, I generated *luxCDABE* promoter fusions that contained the recently predicted *pqsA*-339 (183) (p339), and the *pqsA*-71 (p71) transcription initiation site of the *pqsA-E* operon respectively (Fig. 3.1 B,C). Expression of *lux* in the *P. aeruginosa* PA14 wild-type strain and *rhlR* and *pqsR* mutant strains was monitored during exponential growth phase (183). Consistent with Dötsch and colleagues (183), I found expression from the region containing *pqsA*-339 as well as *pqsA*-71 (Fig. 3.2). While *pqsA*-339-induced luminescence was mostly detected in PA14Δ*pqsR* and silent in the absence of RhlR, *pqsA*-71 was active in PA14Δ*rhlR* but silent in the absence of PqsR. This demonstrates that induction of *pqsA*-339 is strictly dependent on RhlR, whereas induction of *pqsA*-71 is dependent on PqsR. Interestingly, activity of the *pqsA*-71 fusion doubled in the *rhlR* mutant as compared to the wild-type strain. Since it has previously been shown that RhlR is a transcriptional repressor of *pqsR* (14), the increased activity of *pqsA*-71 could be a consequence of an elevated level of PqsR in PA14Δ*rhlR*.

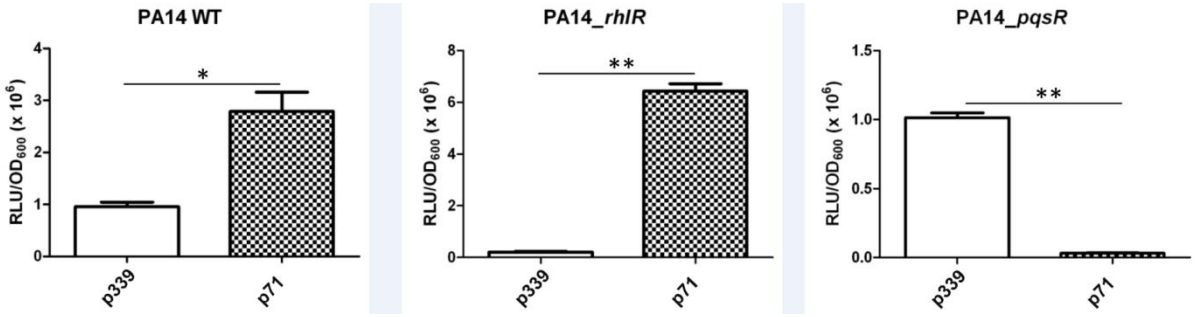

Figure 3.2: Promoter activities of the two alternative transcriptional start sites of *pqsA*. *P. aeruginosa* strains PA14 WT, *pqsR* and *rhlR* mutants containing plasmids p339 and p71 were cultured as described in experimental procedures and assayed for *lux* expression. Data are presented in relative luminescence and error bars represent one standard deviation of the mean value from three biological replicates (*$p \leq 0.05$ and **$p \leq 0.01$).

3.2.2 The RhlR-dependent long 5' UTR of *pqsA* blocks the translation initiation site

I next tested if *pqsA*-339 might be the transcriptional start site of a novel small regulatory RNA responsible for inhibition of PQS synthesis. Small RNAs involved in gene regulation often share sequence complementarity to their target mRNA to form a RNA-RNA duplex occluding the ribosome binding site. However, sequence alignment did not reveal any complementary regions between a *pqsA*-339 transcript and the PqsR-induced mRNA of *pqsA*. Nonetheless, we introduced nucleotide sequences into an IPTG-inducible *tac* promoter vector comprising the nucleotides -342 to -73 and -342 to -1 of the 5' end of *pqsA*, respectively. To prevent partial read-through at an endogenous terminator due to high activity of the *tac* promoter, I used a transcriptional terminator placed upstream of the inserts. The constructs were introduced into the PA14 wild-type strain and pyocyanin production, as a read out for AQ signaling, was monitored after induction of the *tac* promoter. None of the constructs caused a significant difference in pyocyanin production (data not shown), which argues against the presence of a small regulatory RNA that inhibits transcription/translation of the *pqsA-E* operon, but suggests an alternative mechanism of regulation by RhlR.

I could demonstrate that RhlR is an activator of *pqsA* transcription, but simultaneously represses PQS production. We hypothesized that base-pairing in the translation initiation region of the longer transcript might result in gene silencing due to inaccessibility of the SD sequence to the 30S ribosomal subunit. To test this hypothesis, I predicted the secondary

structures of the *pqsA*-71 induced 5' leader sequence (Fig. 3.3 A, short) and of a longer construct containing six additional nucleotides present in the *pqsA*-339 transcript (Fig. 3.3 A, long). In contrast to the short mRNA, the long RhlR-induced transcript is predicted to sequester the SD domain.

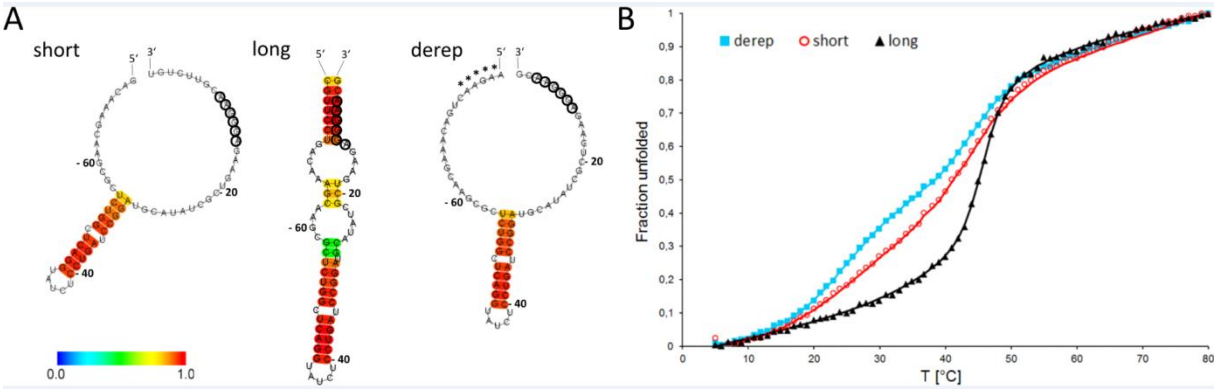

Figure 3.3: Folding dynamics and stability of secondary structures formed by the 5' UTR of *pqsA*. (A) Predicted secondary structures in the 5' leader sequence of the mRNA induced by PqsR (short; -14.10 Kcal/mol), RhlR (long; -29.80 Kcal/mol) and a derepressed RNA variant (derep; -14.10 Kcal/mol). Secondary structures were generated using the CONTRAfold method (45). The color-code represents base-pairing probabilities in the structure ensemble, whereby high values (red) close to 1 are the most probable. Numbers indicate nucleotide positions relative to A of the AUG start codon. The Shine-Dalgarno sequence AGGGAA is encircled and mutated nucleotides are emphasized by an asterisk (*). (B) Thermal unfolding behavior of 71–mer single-stranded DNA oligonucleotides equivalent to the RNA sequences shown in (A) monitored by UV-absorption at 255 nm. Markers represent the raw data recalculated to the fraction of unfolded DNA. Continuous lines represent the data fits used to calculate the melting temperatures.

In collaboration with Prof. Christiane Ritter, we next analyzed the thermal stability of 71–mer single-stranded DNA oligonucleotides equivalent to the sequence of the mRNAs (Fig. 3.3 B). To equate the expansion at the 5' end of the 'long' RhlR-induced primer (which comprises the entire sequence predicted to participate in hairpin formation), six nucleotides (TTCTGT) were added to the 3' end of the 'short' primer. Both unfolding curves can be best explained by two separate unfolding events. Strikingly, the 'long' primer underwent thermal unfolding at significantly higher temperatures (44 °C and 46 °C) and with greater cooperativity than the 'short' oligonucleotide (26 °C and 44 °C). This strongly supports formation of a stable

secondary structure in the RhlR-mediated transcript of *pqsA-E*. This effect could be reversed by site-specific mutagenesis of five nucleotides upstream of *pqsA*-71 responsible for base pairing with the SD region with random non-complementary nucleotides (CGTTC replaced by AAGAA).

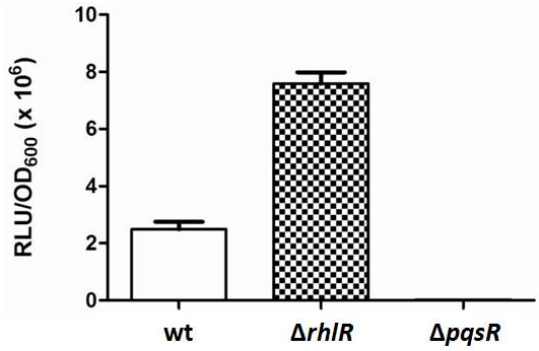

Figure 3.4: Translational control of *pqsA* expression. *P. aeruginosa* strains PA14 wild-type, *pqsR* and *rhlR* mutants containing the plasmid plong were cultured as described in experimental procedures and assayed for *lux* expression. Data are presented in relative luminescence and error bars represent one standard deviation of the mean value from three biological replicates.

To examine a potential inhibitory role of the secondary structure in the 5' UTR of *pqsA*, I generated an additional *lux*-fusion construct (Fig. 3.1 C). The plong construct is a translational fusion and harbors both promoter regions and the additional 70 nucleotides downstream of *pqsA*-71containing the *pqsA* ribosomal binding site (RBS). As with the transcriptional reporters, exponentially grown cells were monitored for luminescence expression levels. A significant decrease in luminescence (up to 3-fold) in the wild-type strain was detected in comparison to the *rhlR* mutant (Fig. 3.4). Although activity of *pqsA*-339 has been verified in PA14Δ*pqsR* (Fig. 3.2), I was unable to measure any luminescence signals in the translational fusion construct. Hence, the present data support our hypothesis, that RhlR mediates post-transcriptional control on the *pqs* operon by producing an alternative transcript which leads to alterations in the folding pattern of the 5' UTR in a way that inhibits efficient translation.

3.2.3 RhlR-induced transcription of the *pqs* operon abolishes efficient translation of the mRNA

Our data imply that formation of a secondary structure within the RhlR-induced long *pqsA* transcript may inhibit *pqsA* translation. This effect should be reversed by site-specific mutagenesis liberating the SD sequence as depicted in Fig. 3.3 A. To test this, I analyzed PqsA production *in vivo* using His_6-tagged *pqsA* whose transcription was under control of the *lac* promoter but dependent on accessibility of the native SD sequence. Levels of PqsA-His_6 were monitored during exponential growth in both *P. aeruginosa* PA14 and *E. coli* BL21 (Fig. 3.5 A). Strikingly, I was unable to detect PqsA-His_6 in cells harboring the native RhlR-induced sequence while secondary structure destabilization in the derepressed construct drastically restored PqsA production in both bacterial strains, indicating that it is a general phenomenon not dependent on a *Pseudomonas*-specific factor. I also performed Western blot analysis by the use of an anti-PqsE antibody (221) to monitor PqsE production. No PqsE could be detected in the PA14Δ*pqsR* mutant, indicating that translation of not only *pqsA* but also the whole *pqsA-E* operon is hindered in the RhlR-induced long *pqsA* transcript (data not shown).

To further assess the exact molecular role of the hairpin loop we performed primer extension inhibition (toeprinting) experiments (in collaboration with Prof. Franz Narberhaus, Ruhr-Universität Bochum) to examine binding of the 30S ribosomal subunit to an mRNA molecule. In this method, ribosome-mRNA complex formation inhibits the primer extension reaction resulting in a terminated product (toeprint) around position +17 with respect to the translational start site. We used the assay to investigate the ability of the ribosome to recognize the SD sequence and to form a translation initiation complex upstream of *pqsA*. Efficiency of ribosome binding was compared between the following *in vitro* transcribed mRNAs: (1) PqsR-induced *pqsA* transcript, (2) RhlR-induced *pqsA* transcript, and (3) a mutated RhlR-induced mRNA exhibiting a destabilized secondary structure (Fig. 3.5 B). Consistent with impaired translation from the long transcript, a toeprint at position +17 was detectable in the PqsR-induced *pqsA* transcript but absent in the RhlR-induced *pqsA* transcript (Fig. 3.5 C). Binding of the ribosome was partially restored upon destabilization of the secondary structure. This clearly demonstrates that the secondary structure of the RhlR-induced *pqsA* transcript, which comprises the SD sequence, prevents formation of the pre-initiation complex. Additional reverse transcription products are indicative of additional

double-stranded regions able to terminate reverse transcription (structures 1 and 2 in Fig. 3.5 C). Together these data demonstrate that RhlR mediates post-transcriptional repression of PQS synthesis by initiating a long *pqsA* transcript, in which the SD sequence is sequestered in a secondary structure.

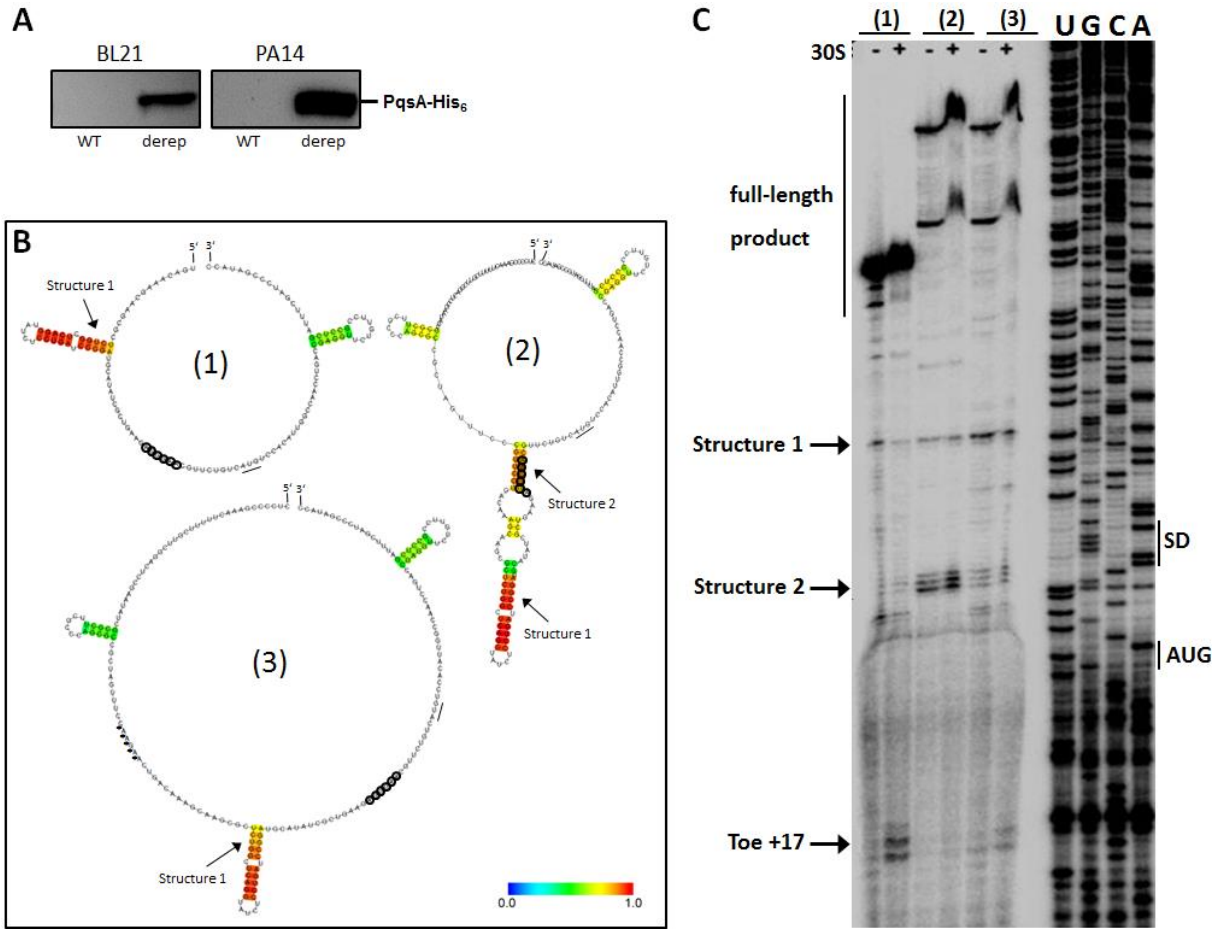

Figure 3.5: Implication of a secondary structure at the translation initiation site on PqsA production. (A) Analysis of His_6-tagged PqsA expressed under *lac* promoter control but in dependence of the native translation initiation site in *E. coli* BL21 and PA14. *In vivo* levels of PqsA-His_6 were compared between the wild-type 5' UTR comprising -80 nucleotides relative to the start codon and a derepressed 5' UTR causing liberation of the SD sequence. (B) Predicted folding patterns of the *in vitro* transcribed *pqsA* constructs used for the toeprint assay: (1) PqsR-induced *pqsA* transcript (-22.70 Kcal/mol), (2) RhlR-induced *pqsA* transcript (-46.40 Kcal/mol), and (3) a mutated RhlR-induced mRNA exhibiting a destabilized secondary structure (-29.80 Kcal/mol). Folding dynamics of the mRNA constructs were predicted using the CONTRAfold method (220). Secondary structures are color-coded according to base-pairing probabilities in the structure ensemble, whereby high values (red) close to 1 are the most probable. The Shine-Dalgarno (SD) sequence AGGGAA is

encircled and the AUG start codon is indicated by a black line. Site-specific mutated nucleotides are emphasized by an asterisk (*). (C) Primer extension inhibition assay of the *pqsA* mRNAs drawn in (B), including the 5' UTR and the first 60 nucleotides of the *pqsA* coding sequence. Addition (+) or absence (-) of *E. coli* 30S ribosomal subunits is indicated. The AUG start codon and the SD sequence are marked on the right and full-length products, structure 1 and structure 2 and the toeprint are indicated on the left-hand side.

3.3 Discussion

Pathogens have developed mechanisms to persist and survive in various environments including the human host. In *P. aeruginosa*, the production of the inter-bacterial signal molecule PQS is critical for survival under deteriorating conditions. PQS itself is a multifunctional molecule acting as a QS signal molecule (222), it has an iron-chelating activity and is essential for biofilm formation (86, 126). Furthermore, PQS plays a pivotal role in tuning cellular physiology and has been implicated in cell death under stressful conditions (86, 223). Recently, PQS was suggested to act as both a pro-oxidant and an inducer of an anti-oxidative stress response (112), emphasizing the importance of this molecule in environmental adaptation of *P. aeruginosa*. Therefore, production of PQS needs to be strictly controlled.

The complex regulatory circuit of PQS synthesis involves the LysR-type transcriptional regulator protein PqsR, which recognizes and binds the signal molecule PQS and subsequently enhances transcription of the AQ biosynthetic operon *pqsA-D* thus forming a positive autoregulatory loop (121). Expression of *pqsR* in turn is controlled by the *las* and *rhl* QS systems, interconnecting all three QS systems of *P. aeruginosa*. However, the transcriptional regulator of the *rhl* system, RhlR, was also shown to directly exert control on PQS biosynthesis by binding to the *pqsA-E* promoter region (129). The present study provides molecular insights into this mechanism.

The discovery of an alternative transcriptional start site (*pqsA*-339) of the *pqsA-E* operon suggested an additional level of direct transcriptional regulation of the PQS system in *P. aeruginosa* (183). The fact that a RhlR-binding box is located just upstream of this transcriptional start site lead us to hypothesize that RhlR might be the transcriptional regulator of this promoter. Indeed, in the present study I demonstrated that RhlR is actually a

transcriptional activator of *pqsA-E* and initiates transcription from *pqsA*-339. Further analyses revealed that RhlR binding to the *pqsA* promoter region induces the transcription of a *pqsA-E* mRNA with an extended 5´ UTR that exhibits a stable secondary structure, which sequesters the SD sequence and inhibits translation initiation of *pqsA*. As a consequence, a PA14Δ*pqsR* mutant displayed transcriptional activation of *pqsA*-339 but failed to efficiently induce production of PqsA (Fig. 3.5). By inducing a longer *pqsA-E* transcript, RhlR prevents translation of the *pqsA* gene, whose product is responsible for priming anthranilate for entry into the PQS biosynthetic pathway and whose deletion is known to impede PQS production (114, 224). Translation of not only *pqsA* but also of the whole operon was abolished. I could not detect PqsE, encoded by the last gene on the operon, in a *pqsR* mutant suggesting that the *pqsA*-339-induced transcript might be unstable as a consequence of ribosomes failing to load on its 5' end. Hence, depending on the presence of sufficient intra- and extracellular concentrations of the signal molecules C_4-HSL and/or PQS, the *pqs* signaling pathway can either be induced by PqsR or inhibited by RhlR. The control of PQS production by two transcriptional regulators of different QS systems thus allows *P. aeruginosa* to fine-tune *pqs* signaling in response to cell density and environmental stimuli (Fig. 3.6).

Many bacterial mRNAs have been described to harbor structured elements in their 5′ leader sequence that control translation (225). Here, to our knowledge, we report for the first time on the modulation of bacterial protein levels via the production of two mRNA isoforms which form variable secondary structures at the translation initiation site and thus are translated at variable efficiency. We found that two transcriptional factors induce alternative transcripts that have profound effects on cell-signaling dependent phenotypes. Recently, a similar regulatory mechanism has been described for the *crl* gene in *E. coli.* Overlapping promoters produce similarly sized mRNAs, but only one harbors a ribosomal binding site (226).

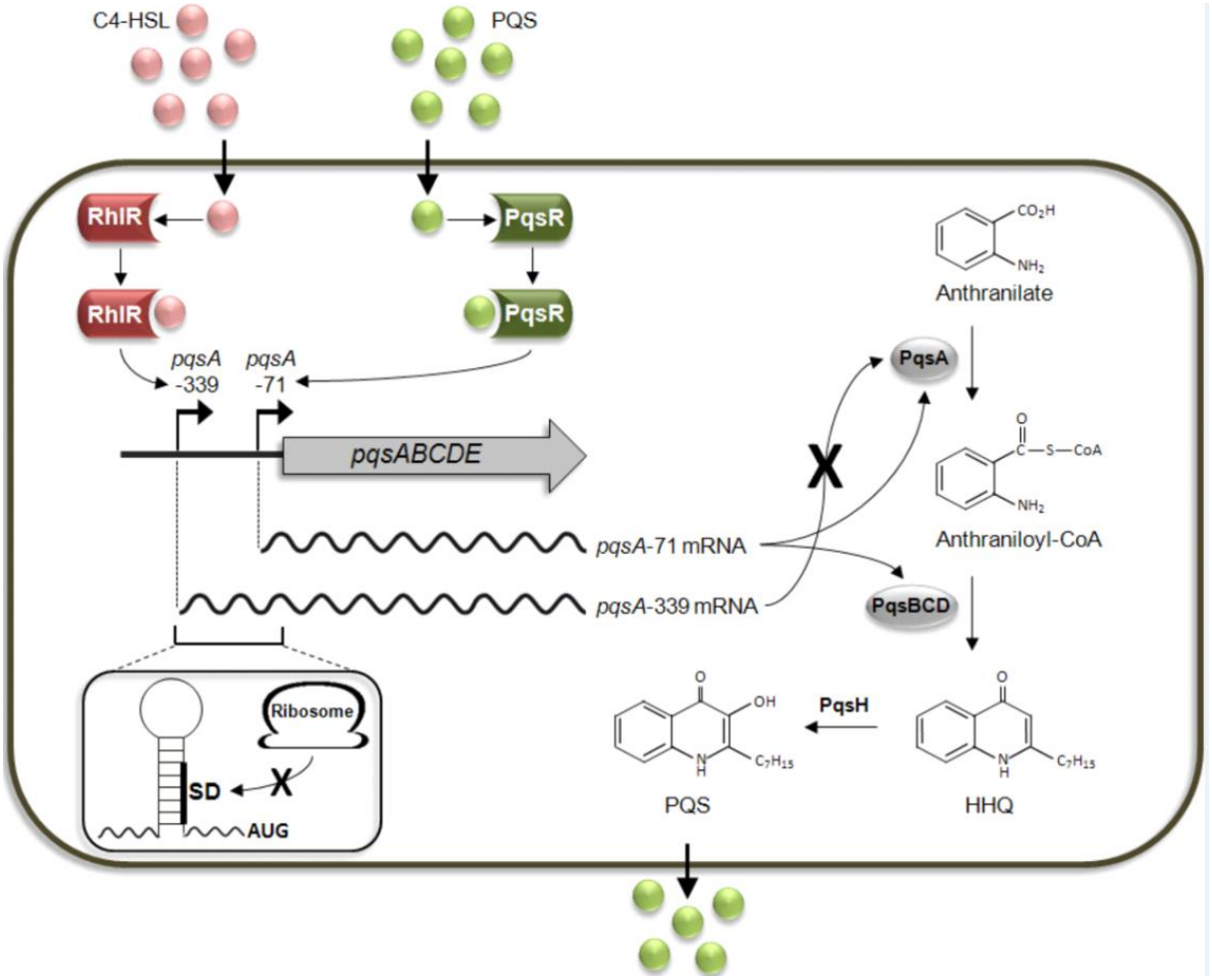

Figure 3.6: Model of transcriptional and translational control of the *pqs* operon. *P. aeruginosa* releases the signal molecules C_4-HSL and PQS in a cell-dependent manner. Upon binding to their cognate ligand, the transcriptional regulators RhlR- C_4-HSL and PqsR-PQS induce transcription of the *pqs* operon from the transcription start sites *pqsA*-339 and *pqsA*-71, respectively. In the *pqsA*-339-induced mRNA the formation of a hairpin at the translation initiation site of *pqsA* blocks access of the ribosome to the SD-sequence. As a consequence, production of the anthranilate-coenzyme A ligase PqsA is hindered rendering *P. aeruginosa* unable to generate HHQ/PQS.

Although not well described in bacteria, different mRNA isoforms are known to play an important role in the regulation of translation in eukaryotes. In mammalians, up to 10-18 % of all genes use multiple promoters (227). For instance, the *axin2* gene, which is involved in early post-natal development and tumor suppression, has three promoters whose expression is strictly tissue-specific (228, 229). The 5´ UTR of each mRNA isoform affects translation efficiency and mRNA stability due to the formation of different secondary structures. Another example in eukaryotes is the tumor suppressor gene *brca1* where transcription is induced from

two separate promoters. Here, as observed for *pqsA* mRNA translation, a longer 5´ UTR of the *brca1* mRNA is translated at lower efficiency due to formation of a stable secondary structure (230). Taken together, this study sheds light on the post-transcriptional regulation of PQS synthesis and illustrates that the promoter region of *pqsA* represents a major site of transcriptional and translational control. Differential secondary structures in mRNA isoforms that directly impact on translational efficiency of genes - a common mechanism of regulation in eukaryotes - might represent an underestimated mechanism of post-transcriptional control in bacteria and might play a more important role in bacterial adaptation than previously anticipated.

3.4 Experimental procedures

Bacterial strains and growth conditions

Unless otherwise noted, bacterial strains listed in Tab. 3.1 were grown in LB medium at 37°C and shaking at 180 rpm. *E. coli* DH5*α* was routinely used for subcloning and propagation. For plasmid selection and maintenance, antibiotics were added at the following final concentrations (µg/ml): for *E. coli*, ampicillin 100; tetracycline 12.5; gentamicin 15; for *P. aeruginosa*, carbenicillin 400; tetracycline 100; gentamicin 30.

Table 3.1: Bacterial strains and plasmids.

Strain/plasmid	Relevant characteristics[a]	Source
Strains		
E. coli DH5α	F⁻ *endA1 gln*V44 *thi-1 recA1 relA1 gyr*A96 *deoR nupG* Φ80d*lacZ*ΔM15 Δ(*lacZYA-argF*) U169, *hsdR*17 ($r_K^-m_K^+$), λ-	(211)
E. coli BL21 [DE3]	F- *ompT hsdS*$_B$ (r_B^- m_B^-) gal dcm	Stratagene
E. coli S17-1	Mobilizing strain for RP4 Mob-containing plasmids	(231)
PA14	Wild-type	(180)
PA14Δ*pqsR*	*pqsR* knockout mutant	This study
PA14Δ*rhlR*	*rhlR* knockout mutant	This study
Plasmids		
pEX18Ap	Gene replacement vector with MCS from pUC18, *oriT*$^+$ *sacB*$^+$, Amp^R	(232)
pEX18Ap2	pEX18TAp derivative. 845bp fragment containing 5S rRNA and lacZ-alpha genes and MCS removed by inverse PCR, novel MCS generated with unique restriction sites for XhoI, PstI, SmaI/XmaI, XbaI, SacI, HindIII, NheI, NotI, MluI, KpnI, BamHI, EcoRI, Amp^R	(233)
pEX18Ap-Δ*pqsR*::FRT-Gm	Gene replacement vector for PA14 *pqsR* containing a FRT-Gm cassette, Amp^R	This study
pEX18Ap2-Δ*rhlR*::FRT-Gm	Gene replacement vector for PA14 *rhlR* containing a FRT-Gm cassette, Amp^R	This study

pFLP3	FLP expression vector, *sacB*$^{+}$ *oriT*$^{+}$, Amp^{R} Tc^{R}	(234)
pBBR1-MCS5-Terminator-RBS-Lux (pMTRL)	Broad-host-range low-copy-number vector pBBR1-MCS5 harboring *luxCDABE* and terminators lambda T0 rrnB1 T1 for plasmid-based transcriptional fusions, Gm^{R}	(235)
p339	-501 to -338 fragment upstream of *pqsA* cloned into pMTRL using SpeI and PstI sites, Gm^{R}	This study
p71	-256 to -70 fragment upstream of *pqsA* cloned into pMTRL using SpeI and PstI sites, Gm^{R}	This study
plong	-501 to +1 fragment upstream of *pqsA* cloned into pMTRL using SpeI and PstI sites, Gm^{R}	This study
pUCP20	*Escherichia-Pseudomonas* shuttle vector with beta-lactamase (*bla*) and LacZ alpha peptide (*lacZ* alpha) genes; Amp^{R}/Carb^{R}	(213)
pUCP20-TOE*pqsA*_(1)	-72 to +60 fragment of *pqsA* containing a T7 promoter (5'-GAA ATTAATACGACTCACTATAGG-3') and a EcoRI restriction site at the 3' end cloned into pUCP20 using the SmaI site, Amp^{R}	This study
pUCP20-TOE*pqsA*_(2)	-140 to +60 fragment of *pqsA* containing a T7 promoter (5'-GAA ATTAATACGACTCACTATAGG -3') and a EcoRI restriction site at the 3' end cloned into pUCP20 using the SmaI site, Amp^{R}	This study
pUCP20-TOE*pqsA*_(3)	pUCP20-TOE*pqsA*_long containing a mutation in the 5' UTR of *psqA* where CGTTC was replaced by AAGAA, Amp^{R}	This study
pUCP20_ΔRBS	Plasmid-borne ribosomal binding site AGGAAA of pUCP20 was replaced by CCTCGC, Amp^{R}	This study
pUCP20_ΔRBS-*pqsA*-His6	Fragment containing -80 bp of the 5' UTR and the entire coding sequence of *pqsA* was cloned into pUCP20_ΔRBS using KpnI and HindIII sites, Amp^{R}	This study
pUCP20_ΔRBS-Δ*pqsA*-His6	pUCP20_ΔRBS-pqsA-His6 containing a mutation in the 5' UTR of *psqA* where CGTTC was replaced by AAGAA, Amp^{R}	This study

a. Cm^{R}, chloramphenicol resistant; Gm^{R}, gentamycin resistant; Amp^{R}, ampicillin resistant; Carb^{R}, carbenicillin resistant; Tc^{R}, tetracycline resistant.

Construction of knockout mutants

To create the single knockout mutants in the wild-type PA14 parental strain we used an adapted version of the gene replacement method by (232) with use of plasmid pEX18Ap for *pqsR* and pEX18Ap2 (233) for *rhlR*, and a gentamicin resistance cassette flanked by Flipase Recombination Target (FRT-Gm) originating from plasmid pPS856. The mutant fragments were constructed by PCR extension overlap (236) with the following primers for *pqsR*: upstream region *pqsR*up2FEcoRI/*pqsR*up2RBamHI, downstream region *pqsR*dwFcompup/ *pqsR*dwRHindIII; and for *rhlR*: upstream region up*rhlR*NotI-fw/up*rhlR*NheI-rv, downstream region do*rhlR*NheI-fw/do*rhlR*HindIII-rv (Tab. 3.2). The BamHI site was introduced between the upstream and downstream region of *pqsR* and the NheI site for *rhlR* respectively. These restriction sites were used to insert the FRT-Gm cassette. In case of *pqsR*, the primers were designed to target for deletion the 529 bp upstream region of *pqsR*, which comprise of all promoter binding sites, as well as 487 bp part of the coding sequence, while for *rhlR* the primers were designed to delete the entire coding sequence of the gene. The resulting plasmids pEX18Ap-Δ*pqsR*::FRT-Gm and pEX18Ap2-Δ*rhlR*::FRT-Gm were transferred into *P. aeruginosa* PA14 by two-parental mating using the donor strain *E. coli* S17-1. *P. aeruginosa* cells were selected on nalidixic acid (20 μg/ml) and gentamicin (50 μg/ml). The

occurrence of the double cross-over was checked by plating at least 30 colonies from the mating result on gentamicin and carbenicillin (400 µg/ml) containing agar plates. Gentamicin resistant and carbenicillin sensitive bacteria were isolated and the insertion of the FRT-Gm cassette ensured by PCR. Finally the FRT-Gm cassette was removed from the chromosomal DNA with help of flipase encoded on pFLP3 plasmid (234). The knockout mutation was confirmed by PCR using primers annealing outside of any pEX18Ap/pEX18Ap2 mediated deletion regions.

Bioluminescence assays

To generate *luxCDABE* (*lux*) reporter fusion plasmids, *pqsA* 5' leader sequence fragments were PCR-amplified from PA14 chromosomal DNA, digested with SpeI and PstI. and subcloned into pMTRL (235). p339 was generated from primers *pqsA*-339-SpeI-fw/*pqsA*-339-PstI-rv, p71 from primers *pqsA*-71-SpeI-fw/*pqsA*-71-PstI-rv and plong from primers *pqsA*-339-SpeI-fw/*pqsA*-ATG-PstI-rv (Table 2). The resulting plasmids were transferred into the *P. aeruginosa* strains PA14 wild-type, PA14Δ*pqsR* and PA14Δ*rhlR*. The reporter strains were grown overnight with the appropriate antibiotic, then subcultured from an OD_{600} of 0.05 in BM2 medium containing 0.01 % casamino acids and 10 µM $FeSO_4$, and grown to mid-exponential growth phase at 37 °C (OD_{600} ~ 2.0). Bioluminescence was monitored using an EnSpire Multimode Plate Reader (PerkinElmer). Promoter activities are given as the relative luminescence of 200 µl of the cultures measured in a 96-well plate divided by the OD_{600} (relative light units [RLU] OD_{600}^{-1}). All results represent the mean of at least three independent replicates.

Overexpression of a potential small regulatory RNA

Fragments comprising the sequence information of a potential small regulatory RNA encoded by *pqsA*-339 were PCR-amplified using the primer set Seq_pqsA-339do2f/Seq_A-71term_rv (-342 to -73 fragment of pqsA) and Seq_pqsA-339do2f/Seq_pqsAterm_rv (-342 to -1 fragment of *pqsA*), of which the reverse primers contain a palindromic transcriptional termination motif (5'-GGGAGGAAGGGGTGACCCTTCCTCCCTTTTTTTATCCTTCT-3') at the N-terminus. The PCR products were subcloned into the EcoRI and Acc65I sites of pME6032 and the resulting plasmids were introduced into the PA14 wild-type strain. Bacterial cultures were grown in LB medium in the presence of 1 mM IPTG and production

of the phenazine pigment pyocyanin was monitored over time as a read out for quinolone signaling.

Thermal unfolding of DNA oligonucleotides

UV absorption spectra of 71 bp-long oligonucleotides (Tab. 3.2) were recorded on a JASCO J-815 CD spectrometer at a concentration of 10 µM in 50 mM potassium phosphate buffer pH 7.2. Thermal unfolding of secondary structure was monitored as an increase in absorption at 255 nm as a function of temperature in intervals of 1 °C and a ramp rate of 4 °C per minute. To determine the melting temperatures, raw data were fitted with an equation for a dual step unfolding of a monomer with corrections for linear changes of the CD signal before and after the unfolding transition (237).

Generation of His_6-tagged fusion pqsA and Immunoblotting

The impact of folding structures in the 5' UTR on the *in vivo* translation efficiency of *pqsA* in *E. coli* and *P. aeruginosa* was analyzed by cloning C-terminal his-tagged *pqsA* from nucleotide -80 to the stop codon into the KpnI/HindIII sites of pUCP20_ΔRBS, a pUCP20 derivate lacking the plasmid-borne ribosomal binding site generated by site-specific mutagenesis (QuikChange II Site-Directed Mutagenesis Kit. Agilent Technologies) using the primer set pUCP20_RBSmut-fw/pUCP20_RBSmut-rv (Tab. 3.2), according to the manufacturer's instructions. pUCP20_ΔRBS-*pqsA*-His_6 was generated using the primer set *pqsA*_KpnI-fw/*pqsA*_6His-rv and primers *pqsA*_mut_KpnI-fw/*pqsA*_6His-rv were used for generation of pUCP20_ΔRBS-Δ*pqsA*-His_6 (Tab. 3.2). To prepare samples for Western Blot analysis, whole-cell lysates of cultures grown to exponential growth phase in LB medium were normalized for protein content and 10 µl of an OD_{600} of 10.0 were separated by SDS-PAGE (10 % acrylamide) after 15 min incubation at 95 °C. As primary antibody we used a His-Tag mouse IgG_1 monoclonal antibody (Novagen) at a dilution of 1:1000. A4a goat anti-mouse IgG & IgM (Dianova) was used as secondary antibody at a dilution of 1:2000. Blots were developed using Lumi-Light Western Blotting Substrate (Roche) and chemiluminescence was detected using a Las-1000 Luminscent Image Analyzer (Fujifilm).

Toeprinting analysis

Primer extension inhibition (toeprinting) assays were performed as described previously (238). Plasmid templates were generated by cloning PCR-amplified fragments comprising a

T7 promoter sequence (5'-GAAATTAATACGACTCACTATAGG-3') at the 5´ end, a EcoRV site at the 3' end, and -140 (2) and -72 (1) to +60 nucleotides of *pqsA*, with usage of primers T7-*pqsA*200nt-fw/Toe_EcoRV-rv and T7-*pqsA*132nt-fw/Toe_EcoRV-rv (Tab. 3.2), into SmaI cut pUCP20 (blunt-end treated) resulting in pUCP20-TOE*pqsA*_(2) and pUCP20-TOE*pqsA*_(1), respectively. To generate pUCP20-TOE*pqsA*_(3) site-specific mutagenesis of pUCP20-TOE*pqsA*_(2) was carried out using the QuikChange II Site-Directed Mutagenesis Kit (Agilent Technologies) with the primers 5'UTR*pqsA*_mut-f /5'UTR*pqsA*_mut-r (Tab. 3.2), according to the manufacturer's instructions. For *in vitro* transcription with T7 RNA polymerase plasmids were linearized by digestion with EcoRV and the primer Toe_short-rv was used for reverse transcription. The experiments were carried out at 37 °C in the presence and absence of *E. coli* 30S ribosomal subunits.

Table 3.2 Oligonucleotides.

Primer	Sequence (5'-3' direction)[a]
Mutagenesis	
*pqsR*up2FEcoRI	GAGAATTCATCCACCGGGCAGCCCAG
*pqsR*up2RBamHI	CGGGATCCGTTAGCGTAGCCACCGGCCAGGC
*pqsR*dwFcompup	TGGCTACGCTAACGGATCCCGTCGGCTACACCAAGGCGTTC
*pqsR*dwRHindIII	CCCAAGCTTGAGAACGCTCTACTCTGGTGCG
up*rhlR*NotI-fw	TATGCGGCCGCTGCAGCGCGCCTACGCG
up*rhlR*NheI-rv	TCAGTCAGTCAGCTAGCTGCAGTAAGCCCTGATCGATAAAATGCA
do*rhlR*NheI-fw	GCTAGCTGACTGACTGAAGCGCAGGGCGCGCCG
do*rhlR*HindIII-rv	TATAAGCTTGGCGGCGTAGCGCGAAAGC
Promoter-*lux* fusions	
pqsA-339-SpeI-fw	TCAGACTAGTGGAGGCTGCAAATGGCA
pqsA-339-PstI-rv	ATACTGCAGGCAAACCAATGACAACCCACTTTGC
pqsA-71-SpeI-fw	TCAGACTAGTTGCCGCCCTTCTTGCTTG
pqsA-71-PstI-rv	ATACTGCAGTCAGGAACGGGAAACTAGCGG
pqsA-ATG-PstI-rv	ATACTGCAGGACAGAACGTTCCCTCTTCAGC
Small regulatory RNA	
Seq_pqsA-339do2f	TATGAATTCTTTGCCATCTCATGGGTTCGGACGC
Seq_A-71term_rv	TATGGTACCAGAAGGATAAAAAAAGGGAGGAAGGGTCACCCCTTCCTCCCGGAACGGGAA ACTAGCGGCGCT
Seq_pqsAterm_rv	TATGGTACCAGAAGGATAAAAAAAGGGAGGAAGGGTCACCCCTTCCTCCCGACAGAACGTT CCCTCTTCAGCGATAT
CD Spectroscopy	
short	TGACAAAGCAAGCGCTCTGGCTCAGGTATCTCCTGATCCGGATGCATATCGCTGAAGAGGG AACGTTCTGT
long	CGTTCCTGACAAAGCAAGCGCTCTGGCTCAGGTATCTCCTGATCCGGATGCATATCGCTGAA GAGGGAACG
derep	AAGAACTGACAAAGCAAGCGCTCTGGCTCAGGTATCTCCTGATCCGGATGCATATCGCTGA AGAGGGAACG
His_6-tagged *pqsA*	

pUCP20_RBSmut-fw	GGAATTGTGAGCGGATAACAATTTCACACCCTCTGCAGCTATGACCATGATTACGAATTCCCCG
pUCP20_RBSmut-rv	CGGGGAATTCGTAATCATGGTCATAGCTGCAGAGGGTGTGAAATTGTTATCCGCTCACAATTCC
*pqsA*_KpnI-fw	TATCGGTACCCCCGTTCCTGACAAAGCAAGCG
*pqsA*_mut_KpnI-fw	TATCGGTACCCCAAGAACTGACAAAGCAAGCGCTCTGGC
*pqsA*_6His-rv	TATCAAGCTTTCATCATCAGTGGTGGTGGTGGTGGTGACATGCCCGTTCCTCCGGAAGGTT
Toeprinting	
T7-*pqsA*200nt-fw	GAAATTAATACGACTCACTATAGGCTCCCCGAAACTTTTTCGTTCGGACTC
T7-*pqsA*132nt-fw	GAAATTAATACGACTCACTATAGGTGACAAAGCAAGCGCTCTGGC
Toe_EcoRV-rv	TAAGATATCGGTATCGGGATCGAAATCGAGGCG
Toe_short-rv	TCGAAATCGAGGCGGAACAGAACC
5'UTR*pqsA*_mut-f	CCAGAGCGCTTGCTTTGTCAGTTCTTGGAAACTAGCGGCGCTGGGC
5'UTR*pqsA*_mut-r	GCCCAGCGCCGCTAGTTTCCAAGAACTGACAAAGCAAGCGCTCTGG

a. Restriction sites are underlined.

4 Ribosome profiling in *P. aeruginosa*

4.1 Objective

Recent technical developments allow monitoring of global gene expression and protein production in a living organism. This has drastically increased our knowledge on fundamental biological processes. But even though transcriptomic and proteomic approaches are indisputable valuable tools they are usually inappropriate to study dynamics of post-transcriptional regulation. For a long time, research on such regulations has been focused on an individual level as high-throughput molecular analyses of mRNA translation profiles were hardly applicable on a genome-wide scale.

Recently a new alternative technique has been developed by Ingolia and Weissmann who successfully applied ribosome profiling to monitor translation in *Saccharomyces cereviseae*. *in vivo* (175). Ribosome profiling (in the following Ribo-Seq) takes advantage of the novel RNA high-throughput sequencing technologies that have emerged during the past years. This powerful approach involves the deep sequencing of ribosome-proteceted mRNA fragments at a given timepoint and, in comparison to RNA-Seq, Ribo-Seq not only provides information on mRNA abundance but also on the number and position of ribosomes on cellular mRNAs. These discrete footprints usually comprise ~30 nucleotides and, dependent on the ribosome-targeting antibiotic used, allow for profiling of initiating or elongating ribosomes. To date, Ribo-Seq is well established in eukaryotes (commercially available Kits) and is generally the method of choice to accomplish the needs for integrative analyses of post-transcriptional regulation.

Information on the translatome in bacteria, however, is sparse and to our knowledge Ribo-Seq has so far only been applied for *E. coli* and *B. subtilis* (239–241). The relatively small number of studies focusing on the translational landscape of bacterial cells could be due to the fact that the in eukaryotes commonly used nuclease RNase I is inactive in bacteria (242). Here, micrococcal nuclease (MNase) has been used instead which, however, is associated with a substantial loss in resolution. An important disadvantage of MNase is its reported sequence specificity having a 30-fold greater catalytic activity at the 5′ side of A or T (243). This results in more heterogeneous fragment lengths than eukaryotic mRNA-ribosome complexes treated with RNase I (242). An accurate measurement of the ribosome position at a sub-codon resolution is thus usually not possible. Nevertheless, Ribo-Seq in prokaryotes still provides an

in-depth analysis of translation. As an example, it could be shown that internal SD-sequences have the potential to stall bacterial elongation, a previously unknown regulatory mechanism (239). Under conditions of fast growth, internal SD site-containing mRNA regions had a significant impact on the length and symmetry of ribosomal footprints in bacteria (239, 244). This so-called 'caterpillar model' implies that ribosomes stalling at SD sequences in close proximity to the 5' end of a gene tend, on average, to result in longer footprints than non-SD sites (244). The extension was shown to occur unidirectional at the 3' footprint end and exemplifies that the precise position of the A-site codon in a footprint can be variable and strongly depends on the sequence context of bacterial mRNA, as well as on environmental factors such as growth phase (244). By using Ribo-Seq, Kannan and colleagues could also shed light on the general mode of action of macrolides, clinically important antibiotics widely used for the treatment of serious bacterial infections (241).

4.2 Results

4.2.1 Exploring inherent mRNA features that may affect translation efficiency in *P. aeruginosa*

Next to transcript structure and tRNA abundance, codon usage as well as the amino acid sequence are well-known factors that have the potential to modify translation efficiency, but it has proved challenging to decipher their subtle effects on translation *in vivo*. The role of biased codon usage in translation dynamics is subject to a particularly controversial debate (reviewed by 244). Usually synonymous codons are not used in equal frequencies, and this synonymous codon bias is widely known to have an impact on e.g. heterologous protein production. Yet, other large-scale systematic studies could not find a significant correlation between codon usage and translation efficiency (). The exact role of codon bias in translation still remains unresolved at the moment. In *P. aeruginosa*, a first attempt has already been made to elucidate the relationship between codon usage variation and translation efficiency (246). To further refine this relationship, general features in codon and amino-acid usage within the *P. aeruginosa* genome were initially analyzed in this study.

Codon bias

With the help of Matthias Preuße, codon usage patterns of the *P. aeruginosa* PA14 genome were screened for variations in frequency among annotated protein-coding genes. Using

principal component analysis, the relative abundance of codons was analyzed and genes were found to cluster into three distinct groups (Fig. 4.1 A). The vast majority of genes grouped together on the basis of relatively uniform codon composition (group 1). The other two groups, however, comprised genes which differed in their codon composition: group 2 assembled genes having on average higher frequencies of rare codons, whereas genes of group 3 primarily contained more frequently used codons. Further analysis was carried out to identify the genes and revealed that group 2 consisted almost exclusively of a set of horizontally acquired genes (Fig. 4.1 B).

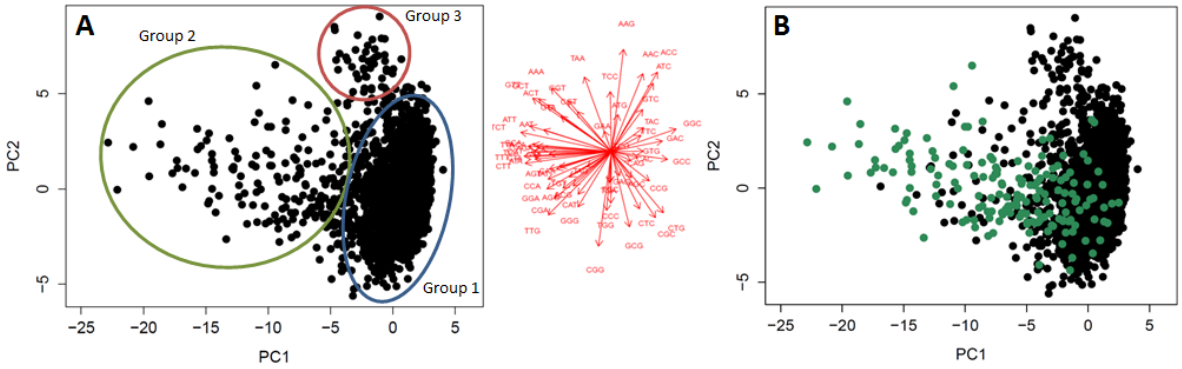

Figure 4.1: Codon usage in *P. aeruginosa*. Principal component analysis was used to organize annotated protein-coding genes of *P. aeruginosa* according to their codon composition. Positioning of the genes in feature space was determined by the frequency of codons as indicated by red arrows. (A) Genes were grouped into three clusters: Group 1 comprises genes with common patterns of codon bias (blue circled), genes with a high percentage of rare codons clustered in group 2 (green circled), and genes with an unusual high percentage of frequently used codons clustered in group 3 (red circled). (B) Distribution of horizontally acquired genes depicted in green.

Out of the 40 genes that clustered in group 3, a large number encode ribosomal proteins that make up the translational apparatus. Ribosomal protein genes are well-known to contain an unusually high number of codons that are frequently used, relative to the entire genome (247, 248). These codons are typically C-ending and represent a nonrandom feature of codon usage (249). Other genes of group 3, also depleted in codons rarely utilized, were previously predicted to be highly expressed in *E. coli* (250). Cold shock proteins are good examples for preferential usage of optimal codons. The synthesis of most cellular proteins is inhibited after

a decrease in temperature (251, 252), and the adapted codon usage of bacterial cold-shock proteins presumably allows to cope with such a deteriorating environment.

Amino acid sequence

Next, we were interested if there are any amino acid preferences of proteins in *P. aeruginosa* with respect to their functionality. Again, principal component analysis was used for mapping genes into feature space (Fig. 4.2). Two groups clustered in the matrix (Fig. 4.2 A), of which one group contained protein-coding genes solely enriched in membrane-associated functions (Transport of small molecules, energy metabolism, and cell envelope). These proteins are composed primarily of hydrophobic (Leucine, tryptophane, and phenylalanine) or non-polar (Glycin) amino acids (Fig. 4.2 B). As expected, acquired genes are equally distributed in the matrix with no distinctive features (Fig. 4.2 C). Potentially highly expressed genes, by contrast, showed very strong bias towards the charged amino acids lysine and aspartate (Fig. 4.2 D). This is in line with previous observations that bacterial ribosomal proteins have a significantly high percent of positive residues which is mainly due to the high content of lysine residues (253).

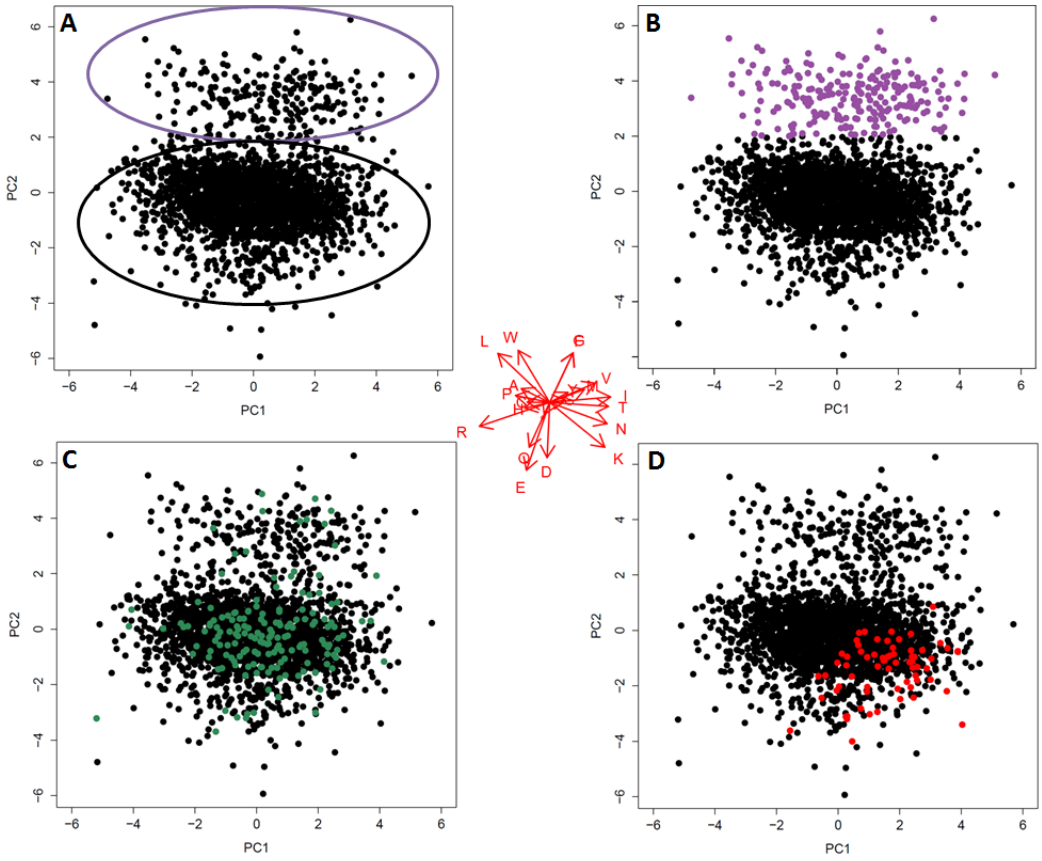

Figure 4.2: Amino acid composition in the genome of *P. aeruginosa*. Principal component analysis was used to organize annotated protein-coding genes of *P. aeruginosa* according to their amino acid composition. Positioning of the genes in feature space was determined by the frequency of amino acids as indicated by red arrows. (A) General separation of genes in two groups. (B) Genes encoding membrane-associated proteins cluster separately (violet). (C) Distribution of horizontally acquired genes (green). (D) Distribution of genes enriched in frequently used codons of group 3 (Fig. 4.1 A).

4.2.2 Establishment of Ribo-Seq as a tool for monitoring the translatome of *P. aeruginosa*

Comparing the ratio of ribosome densities over mRNA abundance is the commonly applied approach to gain information about translation efficiency. This requires parallel analysis of both the transcriptome and translatome on a genome-wide scale of the same sample at a given timepoint. Therefore, I took advantage of a well-established RNA-Seq protocol in our lab (183), and used this in combination with a modified version of a ribosome profiling protocol for prokaryotes to allow for a direct comparison to RNA-Seq data (242).

Briefly (as depicted in Fig. 4.3): late exponential/early stationary phase cultures in M9 minimal medium were initially challenged with chloramphenicol to arrest elongating ribosomes. Chloramphenicol is a potent inhibitor of translation as it binds to the A site of ribosomes and thereby blocks the peptidyl transfer step. After antibiotic treatment, bacterial cells were pelleted onto a nitrocellulose membrane and washed off using ice-cold lysis buffer. Repeated flash-freezing and thawing cycles have been applied to gently gain access to intact ribosome-mRNA complexes. Next, total RNA fragments not associated with ribosomes were digested using MNase. The resulting ribosome-protected mRNA fragments were purified through 1 M sucrose and separated on agarose gels. In addition to nucleic acid digestion, the actual size range of 20-50 nt RNA excised from these gels is a major determinant of footprint length distribution. Fragments of footprinted regions were subsequently used for preparation of a 5’ barcoded cDNA library, according to Dötsch and colleagues (183). Importantly, the cDNA library was prepared without removing rRNA to avoid non-specific binding and unintended removal of short mRNA transcripts. The library was then subjected to Illumina HiSeq 2000 single end sequencing occupying half of a lane per flow-cell. The resulting data were analyzed with the help of Matthias Preuße, who performed bioanalytical analyses.

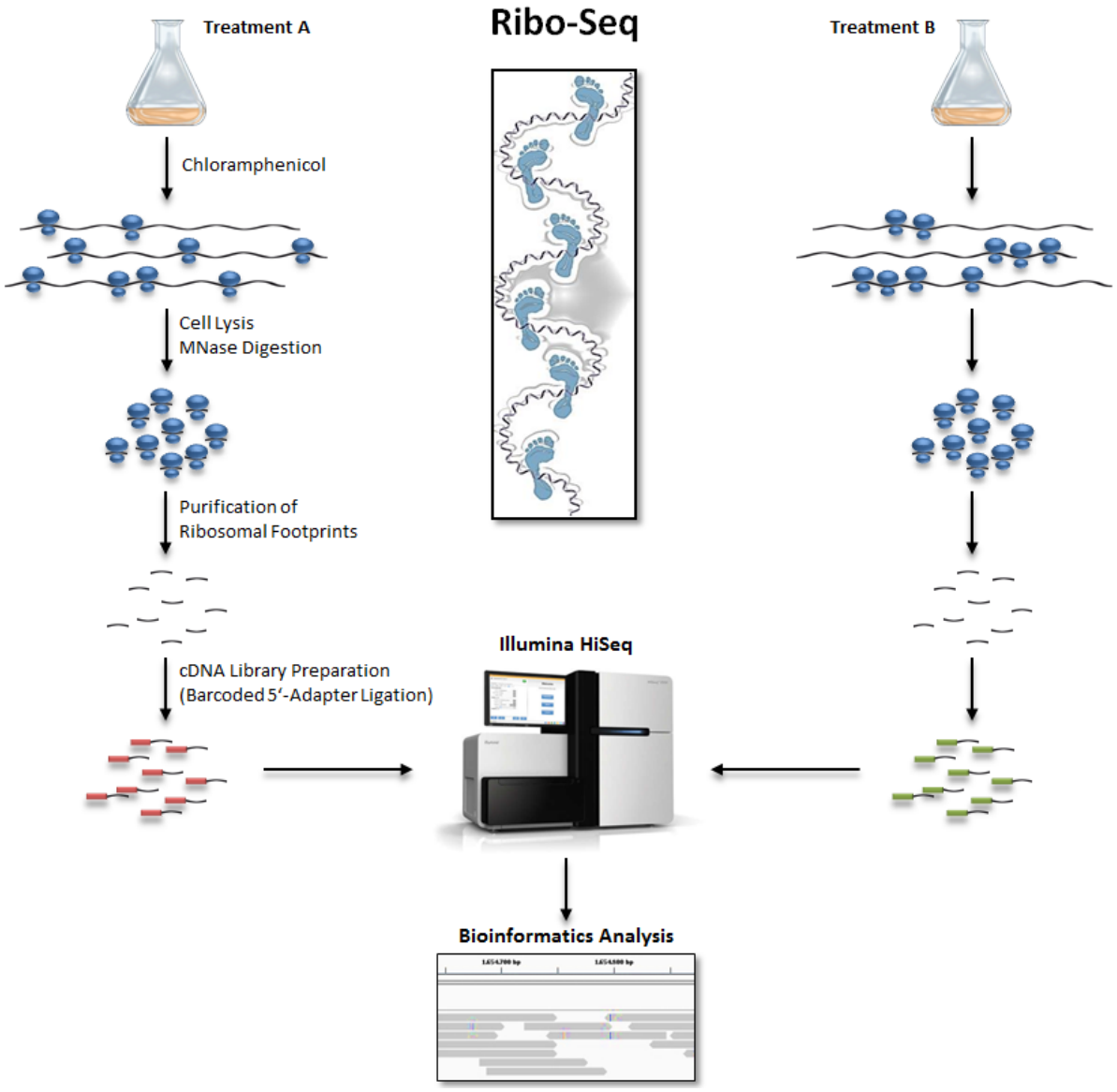

Figure 4.3: Ribo-Seq in *P. aeruginosa*. *P. aeruginosa* cultures were routinely grown to the onset of stationary growth phase. Translating ribosomes were stalled by the addition of chloramphenicol blocking the peptidyl transfer step of elongation on the large (50S) ribosomal subunit. After digestion of RNA with MNase, ribosome-protected mRNA molecules were purified and cDNA libraries were prepared (183), using 5' adapters containing a barcode sequence at the 3' end (indicated by a red/green box). Final cDNA libraries of different treatments were pooled and sequenced with the Illumina HiSeq 2000 system. Raw sequence data obtained were first separated by their barcode sequence and reads with a length of 20 – 50 nt were mapped to a PA14 reference genome. The illustrated ribosomal footprints are a modified version of the original image from (254).

In general, the number of mRNA sequencing reads differed considerably between Ribo-Seq and RNA-Seq. Total RNA of the Ribo-Seq data generated mostly contained rRNA (~ 87 %) and tRNA (~ 9 %). Consequently, just 4 % of total RNA could be assigned to protein-coding mRNA molecules, which is sufficient for a reasonable comparison with transcriptomic data but obviously insufficient for cost-effective multiplex sequencing of Ribo-Seq samples. The significant difference in mRNA content is however due to the fact that Ribo-Seq samples were not subject to any rRNA removal procedure. Deep sequencing of the transcriptome yielded ~6.7 million consistently good quality reads which covered about 90 % of the genome (Tab. 4.1). By contrast, merely 40 % of the genome was covered by the ~1.15 million mRNA fragments obtained from Ribo-Seq (Tab. 4.1). It is difficult at the moment to state if the difference in genome coverage is mainly due to the lower number of total mRNA reads of the Ribo-Seq approach or, alternatively, if the 40 % coverage is a rough approximation for the actual translational activity in the bacterial cells.

Table 4.1 Genome coverage of RNA- and Ribo-Seq reads.

			% Coverage[a]		
	total mapped reads	**mRNA reads**	**1 read[b]**	**5 reads[b]**	**10 reads[b]**
RNA-Seq	12,706,763	6,692,955	90.69	71.84	56.54
Ribo-Seq	27,368,303	1,152,892	38.87	17.62	10.33

a. Coverage of a PA14 reference genome. **b**. Minimum coverage of reads.

4.2.3 Pattern of ribosome distribution along mRNA

In yeast, ribosomes showed a greater mean density in the first 100-150 codons of genes, a phenomenon described and referred to as ‘ramp’(175). The ‘ramp hypothesis’ attributes higher ribosome densities to slow down translation speed at rare codons enriched at the N terminus of genes in most organisms, which supposedly reduces the risk of ribosomal traffic jams during further elongation (175). In *P. aeruginosa*, we could confirm an increased usage of rare codons within the first 50 codons of genes (Fig. 4.4). While rare codons like AGA (arginine), TCT and TCA (serine) are significantly enriched in this region, more frequently used codons tend to be underrepresented. We next focused on possible effects of this codon bias on the density of ribosomes and their allocation.

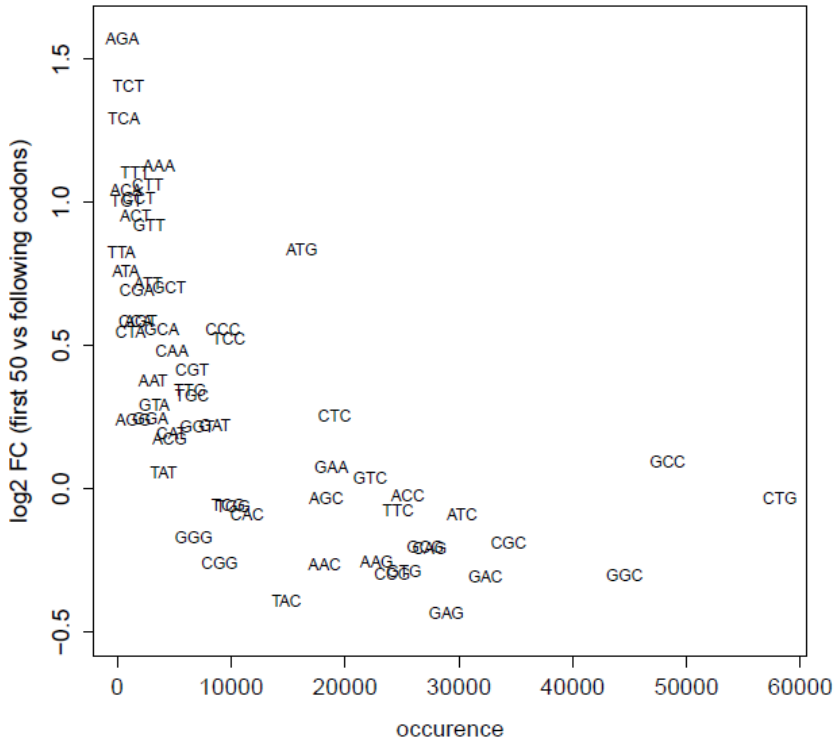

Figure 4.4: Global codon usage at the 5' end of genes of *P. aeruginosa* strain PA14. The general number of codons (occurrence) in genes of the PA14 genome (x axis) is plotted against their abundance at the 5' end of the coding sequence (y axis). The 5' end was defined as the first 50 codons of the coding sequence. The abundance of codons in this region was compared to the abundance within the following codons of the coding sequence (log2 fold ratio). Stop codons are not shown but were highly underrepresented at the 5' end.

Gene-specific ribosome density profiles revealed that, indeed, the majority of footprints mapped to 5' region of genes (Fig. 4.5 A). However, there was no direct correlation between the codon bias and footprint density. For instance, genes containing a particularly large number of the rare codons AGA, TCT and TCA within the first 50 nt region did not have the most pronounced ramp. In addition, genes with a higher number of codons in this region that are used far more frequently, such as CTG, GCC and GGC, likewise created a ramp at the 5' end of the coding sequence.

More recently, Shah and colleagues proposed a computational model where the 5'-to-3' ramp may be explained by increased translation initiation properties of shorter genes (255, 256). The ribosomal footprints of these shorter genes possibly cause a putative ramp in the

transcriptome-wide average ribosome density. To test this possibility, we compared ribosome distribution along the mRNA of genes greater than or equal to 100 nt in length having a minimum number of 1000 sequencing reads within the first 100 nt to have a meaningful ribosome coverage in this region. Interestingly, shorter genes seem not to be the cause of the ramp in our analysis. There was no significant difference in gene length of the total 1112 genes considered in the evaluation with respect to the number of reads within the first 50 nt or 50-100 nt respectively (Fig. 4.5 B). In both cases, the length of genes was more or less the same irrespective of a putative ramp. Therefore, an influence of short genes on the observed accumulation of ribosomes at the 5' end of mRNA molecules can most likely be excluded.

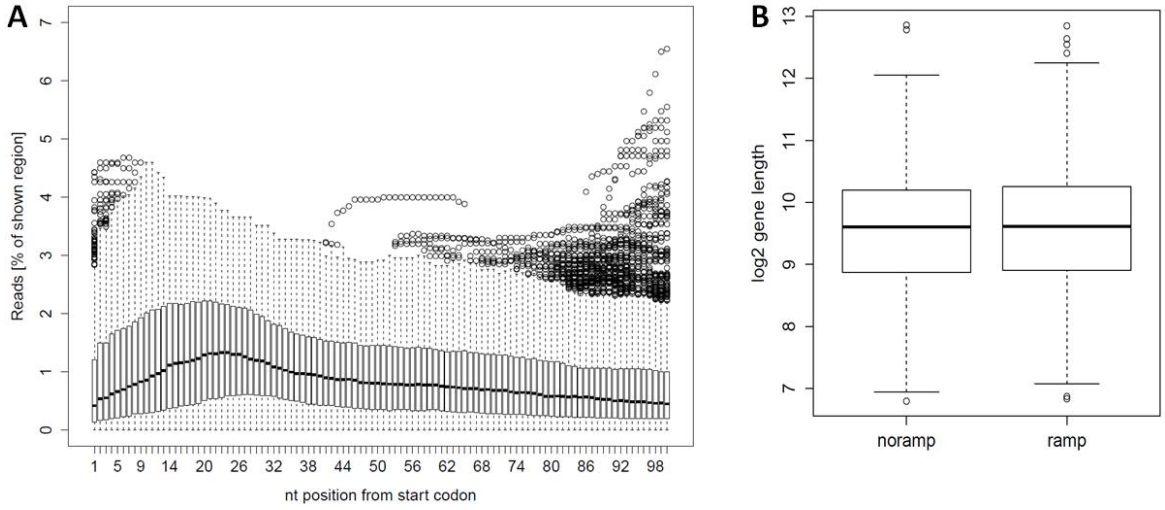

Figure 4.5: 5' reading frame distribution of ribosome footprints. (A) Read density as a function of position within the first 100 nt of coding sequence. (B) Comparison of the length of genes with and without a ramp. A ramp was considered present if the mean number of reads within the first 50 nt was higher than the 50-100 nt region, and vice versa.

Another explanation for the reduced speed of ribosomes at the beginning of genes might be the N-terminal positive charge environment of proteins. Charneski and Hurst, however, could show that this pattern is created by the length distribution of N-cytosolic tails of transmembrane proteins and supposedly may not play a role in the elongation speed ramp (257). In agreement with this finding, no obvious trends of charged amino acids at translational starts of genes with and without the ramp capability were detected in our profile (data not shown). Hence, the actual cause of the ramp remains unclear.

4.2.4 A first application of the integrative '-omics' approach

Transcriptomic and translatomic data were generated from a single sample of the PA14 wild-type strain grown to early stationary growth phase (OD_{600} of 3.0) in M9 minimal medium. Comparison between Ribo-Seq and RNA-Seq data gave a preliminary but valid impression on translation efficiency. The following assumptions and procedures were used for the interpretation of the data: (i) only annotated protein-coding genes were considered for comparison; (ii) genes with a low expression level (less than 20 RNA-Seq reads) were not considered for inclusion into the study; (iii) exclusively ribosome footprint fragments between 20-50 nt sequencing read length have been taken into account; (v) a minimum number of 20 sequence reads per gene in both approaches was estimated to be required for relevant results. Footprints of genes with less than 20 reads, but with simultaneous RNA-Seq reads greater than 60 were permitted as an exception and were incorporated into the analysis.

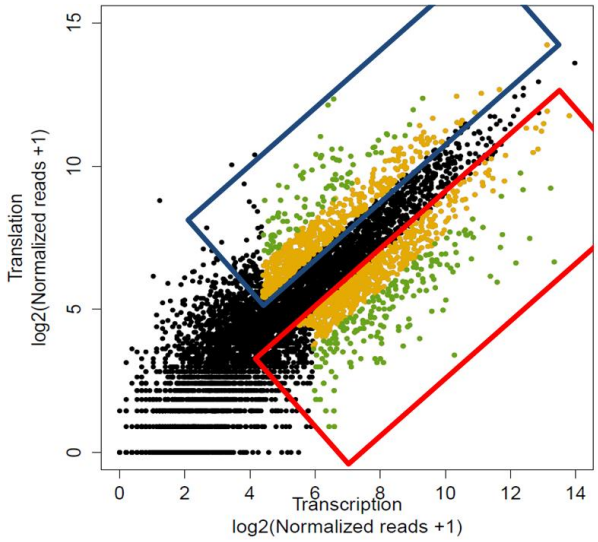

Figure 4.6: Comparison between transcriptome and translatome. Scatterplot showing the correlation between normalized RNA- and Ribo-Seq sequencing reads. Genes that were differentially regulated by ≥|2|-fold in Ribo-Seq are highlighted by boxes: highly translated genes (blue box), poorly translated genes (red box). Yellow points: ≥|2|-fold change in translation efficiency; Green points: ≥|5|-fold change in translation efficiency.

Overall, the Ribo-Seq data showed good correlation with the RNA-Seq data (Fig. 4.6). In this experiment, transcription and translation had a linear relationship where less abundant

transcripts were less efficiently translated, and vice versa. However, there were as well exceptions to this transcriptome-translatome correlation. Analysis identified mRNA of in total 1318 genes that demonstrated a ≥|2|-fold change in translation efficiency (Fig. 4.6). Of these, 521 gene transcripts were highly translated (98 genes with ≥5-fold change), while transcripts of 797 genes were poorly translated (193 genes with ≥5-fold change). It must be mentioned that almost 8 % of all ribosomal footprints mapped to the gene PA14_45410, an uncharacterized homolog of flagellar biosynthesis protein FlhB (193), which is an obvious disproportionate high amount. Given that transcription and translation are tightly coupled in bacterial cells and that this gene was only weakly expressed in RNA-Seq, this finding appears rather questionable and may be an outlier. A multiple repetition of the experiment could provide evidence of this concern.

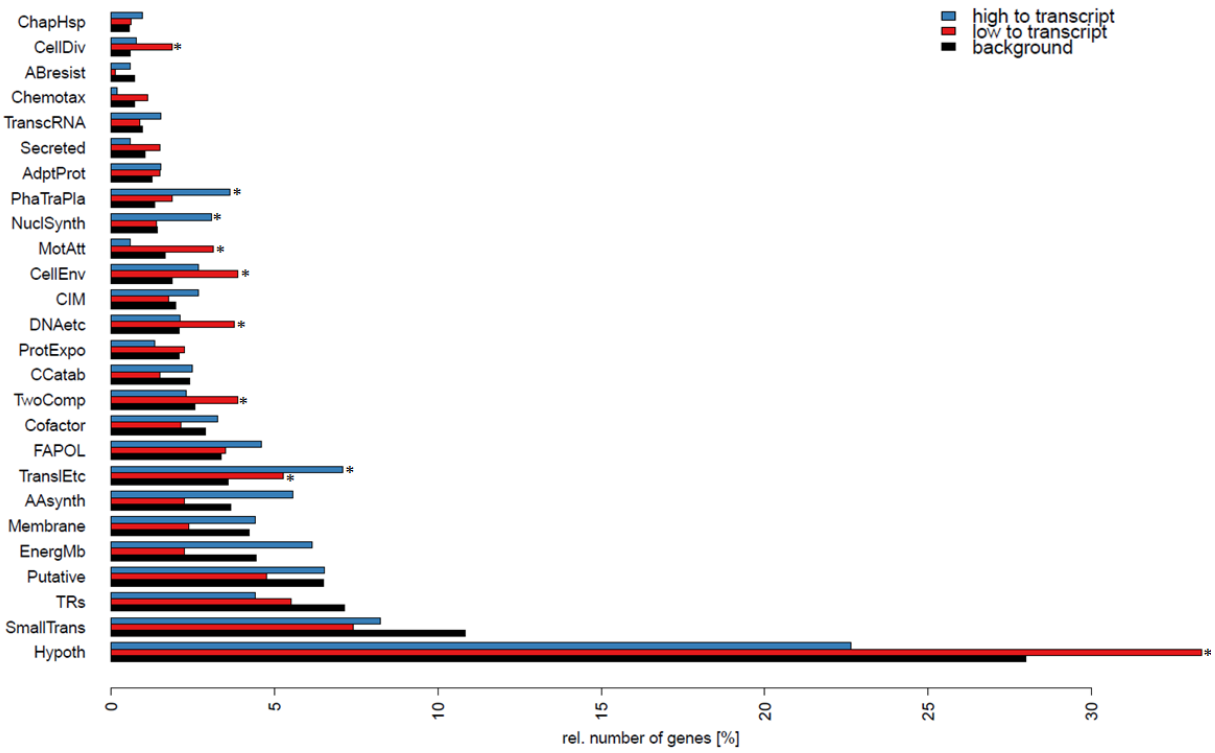

Figure 4.7: Classification of differentially regulated genes into functional groups. Information of the protein function were derived from the *P. aeruginosa* community annotation project (PseudoCAP) database (193). Significant overrepresentation (asterisk) was determined by the hypergeometric test, and an FDR adjusted p-value ≤ 0.05 was considered significant if at least two genes belonged to a PseudoCAP.

Further analysis of the data revealed that enriched footprints in Ribo-Seq were not randomly distributed. The affected genes were classified according to their function using PseudoCAP functional classifications. As depicted in Fig. 4.7, potentially highly translated transcripts primarily constituted protein-coding genes involved in housekeeping processes (translation and nucleic acid synthesis) but also phage-related functions. Overrepresented genes with low ribosome density mainly encode for proteins with unknown function, or for proteins participating in cell division, signaling and motility (PseudoCAP functional classes: 'DNAetc', 'TranslEtc', 'TwoComp', 'CellDiv', 'CellEnv', and 'MotAtt'). Such functions are especially important during exponential growth and needed for maintaining maximal viability, but they are dispensable during stationary phase.

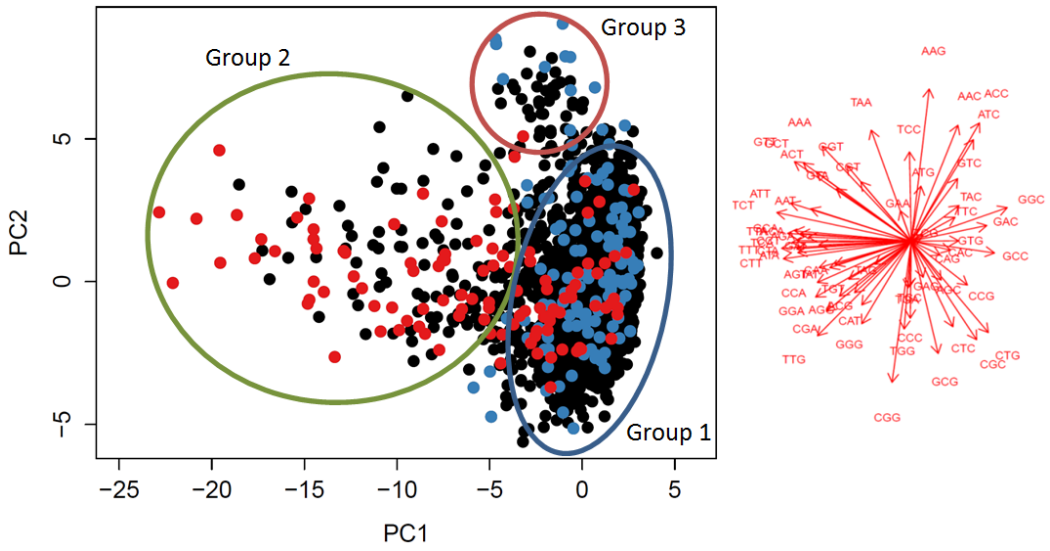

Figure 4.8: The effect of codon composition on translation efficiency. Principal component analysis was used to organize protein-coding genes as previously described (Fig. 4.1). Genes that were either enriched or depleted in Ribo-Seq by ≥|5|-fold change compared to RNA-Seq are shown in blue and red, respectively.

The main objective of this analysis was of course to investigate the molecular mechanisms controlling the translational efficiency. One of the factors known to play a role in translation efficiency is synonymous codon bias (258). Intriguingly, genes which contain on average more rare codons were exclusively less efficiently translated (group 2, Fig. 4.8). On the contrary, genes containing an unusually high number of codons that are frequently used in *P.*

aeruginosa were found to be predominantely enriched in Ribo-Seq (group 3, Fig. 4.8). This finding suggests that codon usage might play an important role in translation efficiency in *P. aeruginosa*. However, numerous genes with different absolute translation efficiency belonged to group 1 (Fig.8), and did not show any particular preference for codon usage. This may indicate that there are other critical factors affecting the efficiency of translation.

4.2.5 The Shine-Dalgarno sequence determines translational efficiency

One of the - if not the - most important determinant of translation efficiency is the proper assembly of the translation initiation apparatus. The rate-limiting step in this process is the binding of the 30S ribosomal subunit to the SD sequence, a central control point in the regulation of translation initiation. To consider this fundamental aspect in post-transcriptional regulation of expression, a search was made for SD sequence motifs in the 5' leader sequence of differentially translated mRNAs.

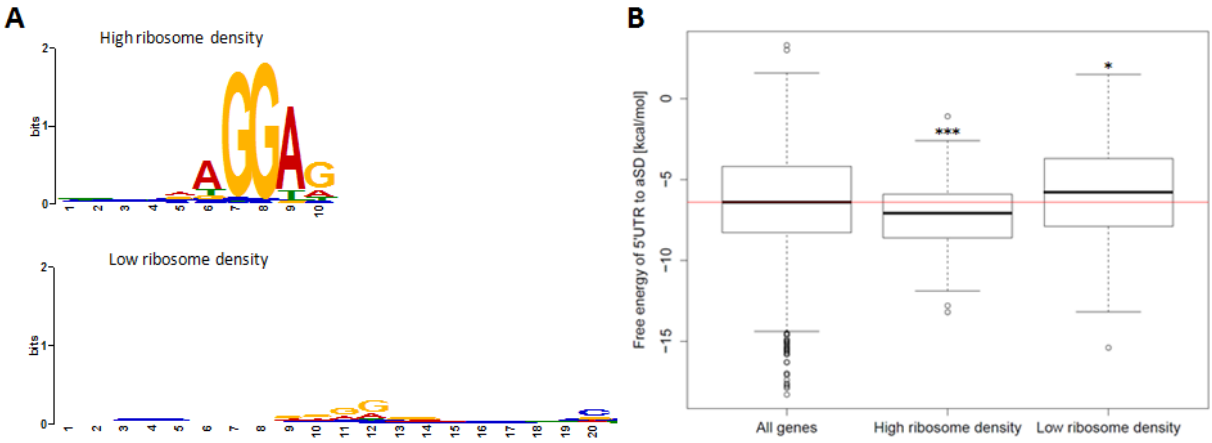

Figure 4.9: The effect of the SD sequence on translation. (A) The SD motifs in the 5' leader of 20 nt of differentially translated mRNAs (≥|5|-fold change) using the motif-based sequence analysis tool MEME Suite (259). Test of statistical significance (asterisk) was performed with the use of unpaired Welch's t-test.

The effectiveness of a SD sequence is determined by its base-pairing potential with the small ribosomal subunit and its spacing to the translation initiation codon (260, 261). As a very

general rule of thumb, the stronger the free energy of a given SD sequence the more efficiently it base-pairs with the anti-SD sequence found at the 3′ end of 16S rRNA. Consequently, it was not surprising that nearly all genes with a high ratio of ribosome footprint density to mRNA abundance are preceded by a strong SD sequence, AGGAG (E-value 2.7e-030; Fig. 4.9 A). The free energy gain upon binding of the rRNA to this SD sequence significantly increases (p-value = 0.001425) in these genes compared to the average SD free energy value of *P. aeruginosa* (Fig. 4.9 B). The mRNAs with low ribosome density, on the other hand, did not share a highly conserved motif (E-value 1.1e-022; Fig. 4.9 A), and the calculated free energy of SD pairing was significantly weaker (p-value = 0.02552) than for average genes (Fig. 4.9 B). These results indicate that the SD sequence was of major importance in driving translational efficiency under our experimental settings.

4.3 Discussion

Genome-wide profiling techniques have emerged as a powerful strategy to study regulatory and molecular aspects of gene expression. Unfortunately, there is often limited correlation of transcript expression and protein production, with the result that in-depth analysis of the transcriptome is only a proxy for the actual synthesis of proteins and vice versa. This is due to various reasons: varying half-lives of mRNAs and proteins, post-transcriptional regulation mechanisms, post-translational modifications of proteins, differences in resolution capability between different approaches, just to name a few. Recent studies have therefore used Ribo-Seq to quantitatively monitor protein production whilst simultaneously profiling mRNA abundance, which has greatly increased our knowledge of post-transcriptional dynamics.

In the present work, I describe a preliminary design of an adapted protocol for Ribo-Seq (242), which was successfully applied in an integrated transcriptome and translatome analysis for complementary profiling of gene expression in *P. aeruginosa*. Our analysis of Ribo-Seq data resulted in relatively low genome coverage compared to RNA-Seq. In bacteria, the process of transcription and translation are tightly coupled. Therefore it appears rather unlikely that less than 50 % of actively transcribed genes were effectively translated. At the same time we cannot rule out the possibility that the 40% coverage was a rough approximation for the actual translational activity in the bacterial cells. Considering that cells were grown to entry into stationary phase in minimal medium, it can be assumed that this

growth phase results in an extensive reprogramming of physiology and protein synthesis, such as has been described for *E. coli* (262, 263). Despite the low genome coverage, Ribo-Seq data showed good concordance with gene expression patterns from RNA-Seq. However, there were notable exceptions that provide an indication of post-transcriptional regulation.

Codon bias and the SD sequence both drive translational efficiency in P. aeruginosa

We identified a subset of genes that contain features in their cognate mRNAs affecting translation efficiency in the experimental setup. Arguably, the SD sequence had a major influence on translation. Protein-coding sequences preceded by a strong SD consensus sequence (AGGAG) were found to be more efficiently loaded with ribosomes than genes having a comparably poor SD sequence. A large part of AGGAG-preceded mRNAs encode for housekeeping or phage-related proteins. In bacteria, highly expressed genes such as ribosomal protein genes are generally more likely to possess a strong SD sequence than average genes (264), and are thus favored to be constitutively expressed even under starvation-like conditions. This is apparently also true for genes of probable phage origin. Interestingly, expression of these genes has been found to be strongly induced in *P. aeruginosa* biofilms (265). The underlying reasons remain unknown, but it can be speculated that an optimized SD sequence is commonly used by phages to ensure expression under stressful environmental conditions. Genes with a weak SD sequence were mostly composed of putative uncharacterized genes and genes with function in cell division, signaling and motility. From a cellular point of view, it makes sense to slow down rates of protein production of such metabolically expensive functions under conditions of restricted growth. Furthermore, we give experimental evidence that certain codon bias can also affect protein synthesis in *P. aeruginosa*. This especially applies for genes that are enriched in rarely used codons. Many of these genes were acquired through horizontal gene transfer and were generally poorly translated. Hence, it appears as if under the experimental setup used in this preliminary study both the SD sequence as well as codon usage bias were important features governing translation efficiency.

Increased ribosomal trafficking at the 5' end of transcripts

Read coverage peaks in the ribosomal footprint data provide experimental evidence for a greater mean density of ribosomes at the 5' end of genes. This is consistent with previous observations and indicates that post-initiation pausing of ribosomes appears to be a universal

feature of translation (175). Advanced search revealed that positively charged amino acids at protein N-termini as well as the gene length both seemed essentially unrelated to this ramp. Despite an enrichment of rare codon at the 5' end of genes in *P. aeruginosa* PA14 (Fig. 4.4), there appeared to be no obvious relationship between this codon bias and the increased accumulation of ribosomes at translation post-initiation sites. Interestingly, in a more recent study sequence-independent stalling of ribosomes at the 5th codon position has been identified in mammalian cells (266). Pausing of ribosomes was shown to be governed by the geometry of the ribosomal exit tunnel. The authors surmise that the stalling allows the first amino acids to be positioned correctly within the large ribosomal subunit to emerge from the exit tunnel, which ensures productive translation. It is imaginable that the time required for this process can vary depending on the physiochemical properties of the amino acids. This may as well have caused enhanced accumulation of ribosomes at the beginning of genes in our study. At present, the actual cause(s) of the putative ramp still remains to be determined.

As of this writing, this is the first time that Ribo-Seq has been used to assess translation in a bacterial species other than *E. coli* and *B. subtilis* (239–241). The results provide initial indications that Ribo-Seq is a suitable tool to study translational events and its implications for dynamics of *P. aeruginosa* infection. Ribo-Seq might also be applicable to identify novel translated open reading frames and may help to identify functional micropeptides. Proteins as short as 11 amino acids have been shown to possess molecular activity, a sequence length generally not characterized as coding sequence (62). Moreover, Ribo-Seq could be used to study translation initiation and principles of its regulation by using appropriate antibiotics. In this respect, it may also serve as a platform to identify the mode of action of novel antibiotics targeting bacterial translation. as recently demonstrated for macrolide antibiotics (241). However, there are currently still some unsolved problems and limitations of this approach, which will be addressed in the following section.

4.4 Trouble shooting

The main open question is whether the 40 % genome coverage of the Ribo-Seq library is real or due to an insufficient number of mRNA copies. Increasing the amount of mRNA would, however, require more sequencing depth which is hardly applicable. Sequencing of the Ribo-

Seq library occupied already half of a lane per flow-cell, far too expensive to be used for multiple sample analysis. This problem could be solved by using sucrose density-gradient centrifugation to fractionate functionally active ribosomes from total ribosomal proteins. The conversion of 70S ribosomes to 100S ribosome dimers has been shown to be a characteristic feature in bacterial cells entering stationary growth phase (267). Analysis of ribosomal proteins at different stages of growth, mainly during the transition between exponential and stationary phase, revealed a close relationship between the ribosome profile and the life cycle of *E. coli* (268). Formation of 100S dimers in the early stationary phase is accompanied by translational inactivation and has thus been termed the 'hibernation' stage of ribosomes (269, 270). Purified ribosomes in our Ribo-Seq approach therefore, supposedly, were mainly composed of inactive 100S dimers. Targeted fractionation of active 70S ribosomes from 100S ribosome dimers and ribosomal subunit proteins would presumably significantly increase the yield of mRNA. Alternatively, efficient removal of rRNA (with a share of ~ 87 % of total RNA) could help to increase the mRNA content using *Pseudomonas*-specific oligonucleotides prior to cDNA synthesis. RNA-Seq typically begins with the removal of abundant rRNAs, but in case of Ribo-Seq this might be problematic because of the short fragment length of footprints which may result in an unintended removal of certain mRNAs. Therefore one would need to compare the datasets to assess the degree of loss and/or bias of mRNA levels. In case the bias is neglectable, it should be straight-forward to remove rRNA by means of subtractive hybridization before sequencing.

Like many other molecular profiling techniques Ribo-Seq also has limitations: For example, the sequencing reads of footprints are particularly short and are therefore more prone to incorrect mapping and assignment. Further, harvesting and lysis of cells are potential sources of error. MNase treatment is another risk of bias with its high sequence specificity (243), and important regulatory information in the 5' and 3' UTRs of transcripts gets lost during nuclease digestion. When comparing the ratio of ribosome densities over mRNA abundance as a measure of actively translated mRNAs, slow translation at e.g. internal SD sites may be misleading and result in false interpretation of the data. The combination of proteomic and translatomic data might help to interpret the results correctly. One important aspect that has to be taken into consideration to the effect of biases is the possibility of sequence bias intrcoduced during Ribo-Seq library construction. This technical bias might explain the high level of mRNA of the uncharacterized gene PA14_45410 in the Ribo-Seq sample (~ 8 % of all ribosomal footprints). Another key consideration concerning library construction is

whether or not different sample preparation methods introduce bias in the analysis. Last but not least, adequate bioinformational analysis has to be developed to cope with the huge amount of data generated (271, 272).

4.5 Experimental procedures

Bacterial strains and growth conditions

For RNA- and Ribo-Seq, the PA14 wild-type strain (180) was grown in 30 ml of M9 minimal medium [42.2 mM Na_2HPO_4, 22 mM KH_2PO_4, 18.7 mM NH_4Cl, 8.6 mM NaCl, 1 mM $MgSO_4$, 0.1 mM $CaCl_2$, 20 mM glucose, 0.01 mM $Fe(II)SO_4$, 1.368 mM Lysin, and 0.1 mM of the other 19 amino acids] at 37 °C and 180 rpm to an OD_{600} of 3.0. Therefore, the M9 medium was inolculated with an OD_{600} of 0.05 from an overnight culture grown in 10 ml of the same medium.

RNA-Seq

For RNA-Seq, a volume of 2 ml of the culture was mixed with an equal volume of RNA-Protect Bacteria Reagent (Qiagen) and incubated for 10 min at room temperature. Aliquots of twice 1 ml were centrifuged at 8.000 rpm for 5 min and pellets were stored at -70 °C. RNA was extracted from bacterial pellets by using the ScriptSeq Complete Kit for bacteria (Epicenter, Illumina), according to the manufacturer's instructions.

Ribo-Seq

For Ribo-Seq, the remaining culture was treated with 0.1 mg/ml chloramphenicol for 2 min under normal growth conditions before further processing. After antibiotic treatment, bacterial cells were pelleted onto a MF-Millipore membrane under vacuum. The membrane was carefully transferred to a 50 ml Falcon tube and cells were immediately shock-frozen in liquid nitrogen for 20 sec. Semi-thawed cells were washed off the membrane using 1 ml lysis buffer [10 mM $MgCl_2$, 100 mM NH_4Cl, 20 mM Tris pH 8.0, 0.4 % Triton X-100, 1 mM chloramphenicol, and 100 U/ml DNaseI]. 2 Aliquots of 350 µl lyzed cells were subject to repeated freezing (liquid nitrogen) and thawing (room temperature) to gain access to ribosome-mRNA complexes. Samples were centrifuged for 5 min at 10.000 rpm at 4 °C. The supernatants were pooled, flash-frozen in liquid nitrogen and stored at -70 °C. After gentle thawing on ice, 350 µl of the supernatants were digested with 1 µl micrococcal nuclease

(MNase, 300 U/µl) for 1 h at 25 °C in a thermocycler with continuous shaking at 600 rpm. MNase digestion was stopped by the addition of 6 mM EGTA pH 8.0. Ribosome-mRNA complexes were carefully loaded onto 900 µl of 1 M sucrose and centrifuged in a Beckman Optima TLX ultracentrifuge at 70.000 rpm at 4 °C for 4 h, using a TLA100.4 rotor. The supernatant was discarded and pellets were stored at -70 °C overnight.

Pellets were first reuspended in 50 µl Nuclease-free water before addition of 700 µl Qiazol. The samples were incubated for 5 min at room temperature and further purified using miRNeasy Mini Kit (Qiagen). After DNaseI treatment, RNA was further processed as previously described (183), except for the following differences: RNA was separated in a 3 % agarose gel and fragments with ~50 nt in size were extracted and transferred to a Spin-X polypropylene centrifuge tube filter (Corning, Costar). Samples were frozen at -20 °C for 20 min (to disrupt the gelstructure), squeezed in 300 µl 0.3 M NaCl with an inoculation loop, incubated for 5 min at room temperature, and centrifuged for 10 min at 13.000 rpm at 4 °C. The supernatants were discarded, RNA pellets washed in ice-cold 70 % ethanol and after a repeated cycle of centrifugation the pellets were dried and resuspended in 16 µl RNase-free water (samples can be stored at -70 °C). After 5’ adapter ligation, RNA frgaments of ~75-100 nt were extracted from a 3 % agarose gel and treated as described above. RNA pellets were finally resuspended in 8 µl RNase-free water (samples can be stored at -70 °C). 4 µl of this RNA pool was then used for cDNA library preparation.

5 Elucidation of the molecular function(s) and the regulatory role of PqsE

5.1 Objective

The QS circuitry of the opportunistic pathogen *P. aeruginosa* is extremely complex. In addition to the AHL-dependent signaling systems, *las* and *rhl*, *P. aeruginosa* possesses a third QS system that utilizes alkyl quinolones (AQs) and that is interwoven in the hierarchical QS cascade (222). The two signal molecules HHQ and PQS are the best studied AQs in *P. aeruginosa* and are essential for the production of various virulence factors and biofilm formation (113, 273). Biosynthesis of AQs is accomplished by the *pqsABCD* operon genes. *pqsH* encoding for a FAD-dependent monooxygenase is responsible for catalyzing the conversion of HHQ to PQS. The transcriptional activator of these genes, PqsR, binds AQ signal molecules and, as a consequence, induces expression of the biosynthetic genes (109, 121, 273, 274). Interestingly, the fifth gene of the *pqs* operon, *pqsE*, is co-transcribed with the AQ biosynthetic genes *pqsA-D*, but is not involved in the biosynthetic pathway. In fact, a negative autoregulatory role has been described for PqsE by repressing both *pqsA* expression and AQ biosynthesis (133). Moreover, PqsE is indispensable for synthesis of numerous virulence factors, including the phenazine pyocyanin, and this regulation was shown to be disconnected from AQ signaling (132, 134). In contrast to its self-inhibitory function, PqsE-mediated induction of pyocyanin and rhamnolipid production is strictly dependent on the downstream acting RhlR transcriptional regulator (133). However, to date, little is known about this interdependence.

It is undisputed that PqsE is a key regulator within the QS circuitry of *P. aeruginosa*. PqsE is predicted to belong to the metallo-hydrolase/oxidoreductase and possesses the characteristic metal ion-binding HXHXDH amino acid motif of this protein family. Notably, in two independent studies PqsE has been co-crystallized in presence of small organic chorismate-like compounds (214, 275). Although this suggests that such a molecule might be the substrate - or product - of PqsE, a significant turnover of chorismate-derived molecules has not yet been verified. PqsE was shown to exhibit a very weak enzymatic activity to hydrolyze phosphodiesters (214), but the natural substrate(s) of PqsE still remain elusive. The aim of this study was to identify the enzymatic activity of this protein to better understand how PqsE facilitates the environmental adaptation and enhanced virulence factor production of *P. aeruginosa*.

5.2 Results

5.2.1 Auto-inhibitory role of PqsE in AQ signaling

PqsE is known to repress transcription of *pqs* biosynthetic genes thus exhibiting a negative autoregulatory role (133). This inhibitory role of PqsE is comparable to RsaL of the *las* QS system whose expression is under transcriptional control of the regulator LasR. When the respective signal molecule C_{12}-HSL (one of the numerous AHLs produced by *P. aeruginosa*) reaches a certain physiological threshold concentration, RsaL binds to the *rsaL-lasI* bidirectional promoter blocking transcription of both genes (98, 276). Although PqsE exerts its regulatory role rather indirectly, its role in repressing AQ signaling can be considered analogous. There have been many attempts to decipher the enzymatic activity of PqsE. Binding and turnover of various substances, including PQS and AHLs, has been assayed previously (214). Of these molecules, only anthranilate and benzoate showed weak binding to PqsE, although the authors postulate that the substrate binding site of PqsE seems perfectly suited for a PQS-shaped molecule.

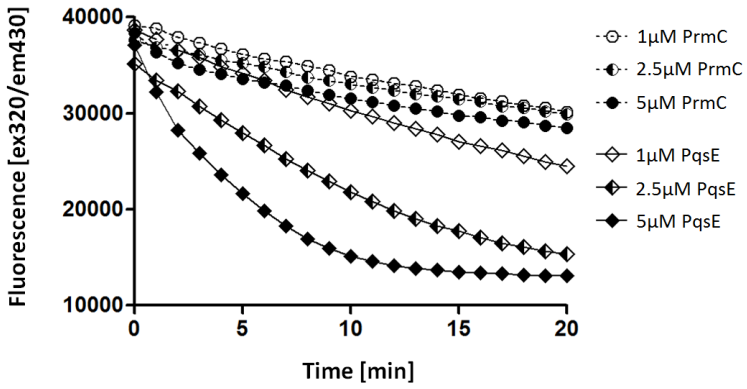

Figure 5.1: Fluorometric analysis of *P. aeruginosa* PA14 metabolite extract degradation. Freshly prepared PA14 extract was incubated *in vitro* with purified PqsE and PrmC (negative control) using protein concentrations as given. All 100 µl reactions were carried out at 37 °C in 50 mM NaH_2PO_4 pH 7.5. The assay was monitored continuously by measuring fluorescence intensities under 320 nm excitation and 405 nm emission. The presented data represent the result of several independent experiments.

To address this further, I initially extracted AQs from the supernatant of a PA14 wild-type culture. Since AQs are known to show autofluorescence, I monitored fluorescence of the extract in the presence of purified PqsE in an *in vitro* assay. To exclude non-specific binding/turnover, the previously characterized peptide chain release factor methyltransferase protein (PrmC) of *P. aeruginosa* was used as a negative control (221). Depending on the protein concentration used, a dramatic decrease of the fluorescence intensity of the PA14 extract was observed when incubated with PqsE (Fig. 5.1). While this decrease in fluorescence was linear to increasing PqsE concentrations, PA14 extract fluorescence remained roughly constant in the negative controls.

Next, I analyzed the metabolic composition of the fluorescent PA14 extract by using thin layer chromatography (TLC), which allows for an easy semi-quantitative comparison of metabolic profiles. AQs were extracted with dichlormethane as described previously (chapter 2). The extract contained a vast number of fluorescent metabolites including the AQs HHQ and PQS. To investigate if the reduction in fluorescence of the extract was due to PqsE-mediated degradation of one of these AQs, the extract was incubated with 5 µM PqsE and PrmC for either 1 h or overnight for approximately 12 h at 37 °C. After re-extraction of the metabolites, the samples were loaded onto an analytical TLC plate. To our surprise, there was no significant difference in the metabolic profile between the samples, irrespective of the incubation time (data not shown).

Notably, while negative control samples (PrmC and protein-free control) maintained the yellowish-green color of the extract, PqsE-treated extract turned light red after prolonged incubation. This color change might have been caused by formation of either a red colored PQS+Fe^{3+} complex or pyochelin+Fe^{3+} complex. Both fluorescent siderophores were shown to chelate ferric iron with similar affinity (PQS: pFe^{3+} value of 16.6 at pH 7.4 (273); Pyochelin: pFe^{3+} value of 16.0 at pH 7.4 (277)) and to turn red upon chelation of Fe^{3+}. The PQS+Fe^{3+} complex conferred a lethal phenotype in *Caenorhabditis elegans* in the ‘red death’ response of *P. aeruginosa* during phosphate depletion (278). Recombinant PqsE possess an Fe^{2+}/Fe^{3+} center (214), and the relative importance of active-site positions of the iron atoms for *P. aeruginosa* virulence was verified in a recent study (275). Additionally, the binding site of PqsE seems perfectly suited for a PQS-shaped molecule (10). Thus, it is quite possible that PQS, as an ferric iron chelator (126), bound to or removed the ferric iron from the active site of PqsE which could as well account for the observed reduction of extract fluorescence. To

test this, I treated AQ extract samples with Fe^{3+}. Addition of 10 µM Fe^{3+} indeed drastically lowered fluorescence intensity of the extract comparable to the effect of PqsE (data not shown). This effect could not be reversed by supplementation with EDTA.

5.2.2 Reviewing the role of PqsE as the PQS response regulator

To further assess the PqsE-specific effect on the PA14 extract, and to validate a potential specific interaction of PQS with the active site of PqsE, I next generated metabolite extracts from the supernatant of overnight cultures of a PA14Δ*pqsR* mutant (deficient in AQ production) and a PA14Δ*pchA-D* mutant strain (deficient in pyochelin production), following the same procedure as previously used for the wild-type strain. Fluorescence intensity of the obtained extracts was again monitored *in vitro*, with or without PqsE. Interestingly, the extract of the PA14Δ*pchA-D* mutant showed similar fluorescence values to those of the wild-type strain with a strongly decreasing intensity in PqsE-treated samples (data not shown). The extract of the PA14Δ*pqsR* mutant, on the other hand, did not show any fluorescence at all, although it contained large amounts of fluorescent pyochelin (Fig. 5.2).

The same samples were then subjected to HPLC-MS for quantitative analysis of AQ composition (in collaboration with Dr. Kathrin Wittstein, HZI - group microbial drugs). Therefore, acidified metabolites were extracted using ethyl acetate as organic solvent. As depicted in Fig. 5.2, the extract of the wild-type strain largely comprised a mixture of two interconvertible isomers of pyochelin, the AQs HHQ and PQS, and an unknown compound(s) which occurred as a double peak in the HPLC chromatogram with a retention time of 10-11 min. Since the double peak was absent in PA14Δ*pqsR*, it is likely to be one of the numerous AQs produced by *P. aeruginosa*. Overall, the HPLC chromatograms of samples (a) PrmC, and (b) PqsE showed good coincidence. However, notably, there was a significant decrease in the PQS peak height after incubation with PqsE. The direct precursor of PQS, HHQ, on the other hand was unaffected by PqsE suggesting a PqsE-specific effect on PQS. It should be noted that, unlike PQS, HHQ is unable to chelate Fe^{3+} (273). This effect of PqsE was most pronounced in the PA14Δ*pchA-D* mutant extract which is unable to produce the siderophore pyochelin, but evidently produces increased levels of PQS. Remarkably, despite the capacity of pyochelin to chelate ferric iron, levels of the siderophore were not modified. Also, no additional peaks indicative of a potential PqsE-catalyzed reaction product were detectable in

any of the samples supporting the hypothesis of PQS-specific interaction with the Fe^{2+}/Fe^{3+} center of PqsE.

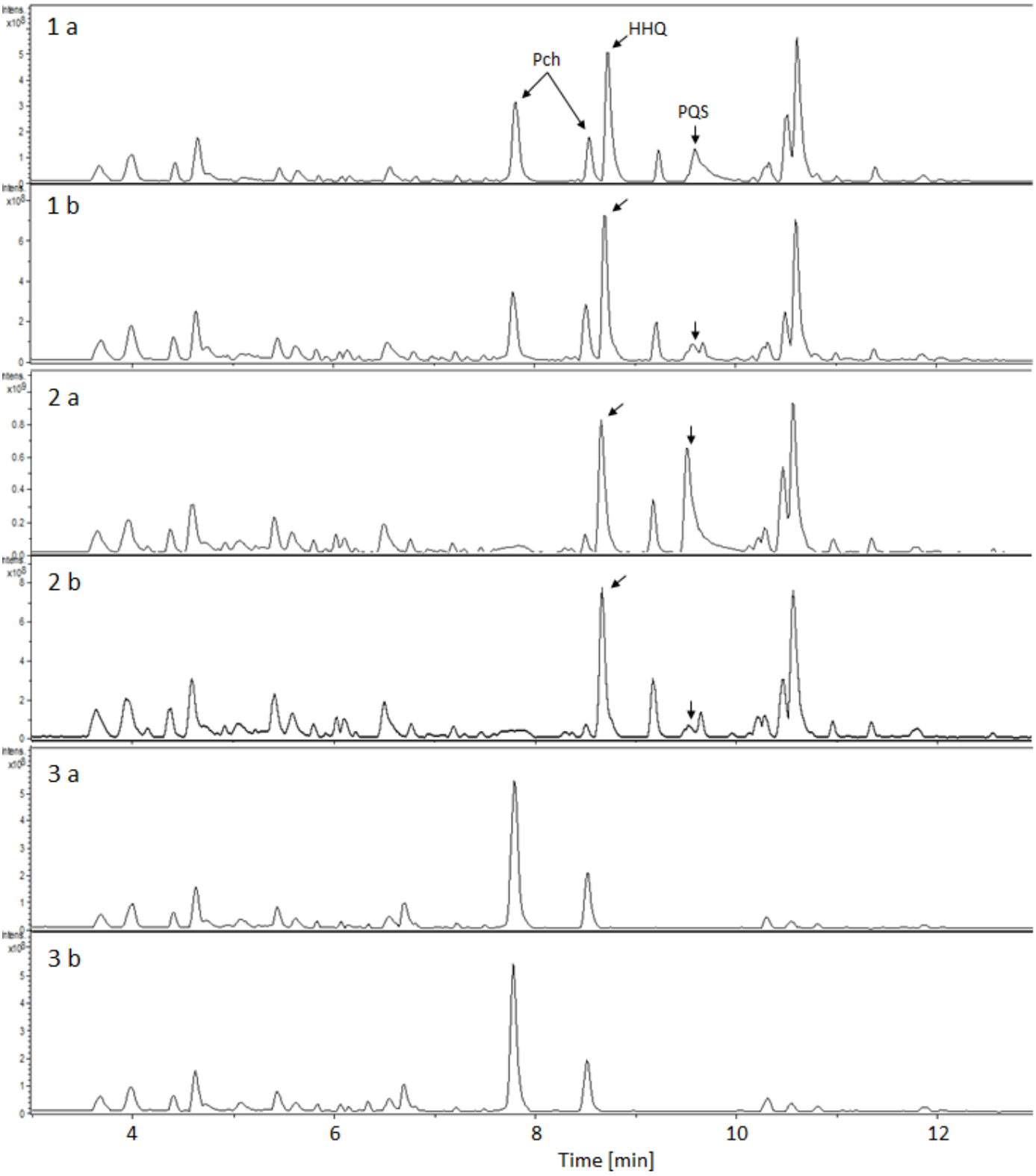

Figure 5.2: Quantitative HPLC-MS analysis of extracts from different *P. aeruginosa* PA14 strains incubated with PqsE. Metabolite extracts of PA14 strains were incubated for 20 min in 2 ml

50 mM NaH_2PO_4 pH 7.5 at 37 °C with **(a)** 5 µM PrmC (negative control) and **(b)** 5 µM PqsE. Acidified metabolites were selectively extracted using polymeric weak anion exchange sorbent (Strata-X-AW 33u, Phenomenex) prior to HPLC-MS analysis. For guidance, clearly identified compounds comprising pyochelin (Pch), HHQ and PQS are indicated by an arrow in the chromatograms. Extracts: **(1)** PA14 wild-type; **(2)** PA14Δ*pchA-D* mutant; **(3)** PA14Δ*pqsR* mutant.

To further examine the finding of the HPLC-MS analysis, purified PQS was purchased and likewise tested for interaction with recombinant PqsE. Surprisingly, PQS itself did not display the fluorescence of the extract. However, it is likely that the concentration of PQS used in the assay was not sufficient to show the characteristic fluorescence of the extract since the peak height of purified PQS in the assay was obviously lower than in PA14 extracts (Fig. 5.3). Unfortunately, purified PQS cannot be solubilized at higher concentrations without precipitation. Nevertheless, there was a striking decrease of soluble PQS in PqsE-treated sample eluates compared to the PrmC negative control. The two major peaks for PQS with a characteristic mass (m/z: 260) were described previously (279), but why reduction was always restricted to only the lefthand peak is unclear.

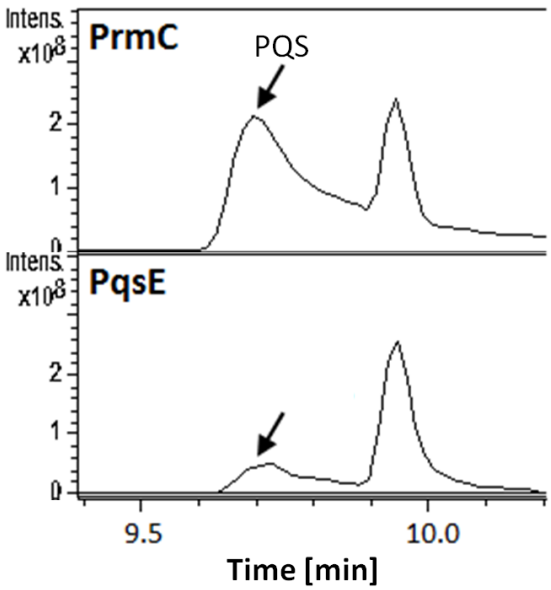

Figure 5.3: Quantitative HPLC-MS analysis identifies PqsE-specific interaction with PQS. Purified PQS was incubated in reaction buffer (50 mM NaH_2PO_4 pH 7.5) with a final concentration of ~ 40 µM for 20 min at 37 °C with 5 µM protein, whereby PrmC served as negative control. Acidified PQS was selectively extracted using polymeric weak anion exchange sorbent (Strata-X-AW 33u,

Phenomenex) prior to HPLC-MS analysis. The two major peaks for PQS had a characteristic mass of m/z: 260 (279).

5.2.3 The co-dependency between PqsE and the *rhl* system

As already mentioned, PqsE controls phenazine biosynthesis in cooperation with the *rhl* system (in particular via action of RhlR) and this interaction was shown to be AQ-independent (132, 133). Expression of *pqsE* is not sufficient to complement the pyocynain-deficient phenotype of an *rhlR* mutant. Vice versa, *rhlR* expression can partially restore pyocyanin production in *pqsE* mutant cells (see Fig.5.4 and 134). These findings illustrate that both *pqsE* and *rhlR* are essential for phenazine biosynthesis and that PqsE depends on the downstream acting RhlR to positively regulate pyocyanin production. To date, only two scenarios have been described where pyocyanin production could partially be restored in a *pqsE* mutant; either by overexpression of *rhlR* or by addition of large amounts of C_4-HSL (132, 134), again demonstrating the significance of RhlR in PqsE-mediated induction of pyocyanin production. The co-dependency between PqsE and RhlR is probably not reflected on a transcriptional level, since *rhlR* expression was found to be downregulated by only ~2-fold in a *pqsE* mutant, hardly sufficient to explain the striking phenotypic effects mediated by PqsE (134).

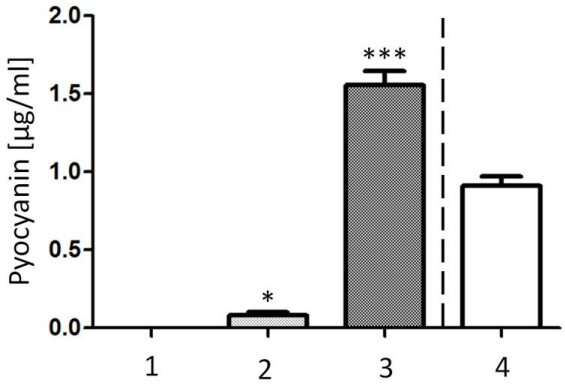

Figure 5.4: Effect of *rhlR* and *pqsE* expression on production of pyocyanin in PA14Δ*pqsE*. The levels of pyocyanin were determined in the supernatants from overnight cultures of *P. aeruginosa* PA14Δ*pqsE* carrying (1) the empty vector pUCP20, (2) pUCP20*rhlR*, and (3) pUCP20*pqsE*. The PA14 wild-type harbouring pCUP20 (4) served as a reference. All strains were grown in BM2

minimal medium supplemented with 0.01 % (w/v) casamino acids and carbenicillin at 37 °C. Statistical significance values are stated (paired t-test).

To gain further insight into the relationship between the two proteins and to investigate a potential role in dynamic regulation, fluorescence intensity of an *rhlR-gfp* translational fusion under control of the native *rhlR* promoter was monitored in dependence of *pqsE in vivo*. As depicted in Fig. 5.5, there was a significantly delayed production of RhlR in the absence of *pqsE*. Co-expression with *pqsE* enhanced fluorescence by ~ 2-fold in early log-phase cells and, interestingly, fluorescence values in the complemented strain did not change over time. In contrast, RhlR production was lowest during early growth in *pqsE* mutant cells, but steadily increased reaching comparable levels of fluorescence to the complemented strain at mid- to late log growth-phase. These results demonstrate that PqsE is dispensable for RhlR production, although it evidently can be considered as an important enhancer (132).

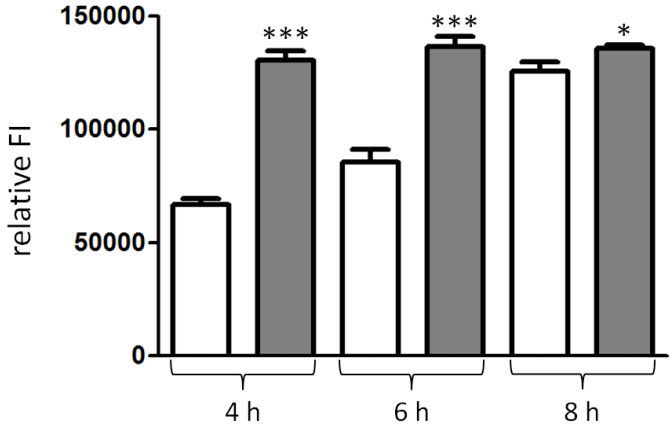

Figure 5.5: Expression of an *rhlR-gfp* translational fusion in dependence of *pqsE*. Growth-dependent *rhlR* translation was monitored in a PA14Δ*pqsE* transposon mutant carrying two plasmids: pUCP20*rhlR-gfp* in combination with either pME6032*pqsE* (grey bars), or the empty vector pME6032 as control (white bars). Production of GFP is under control of the *rhlR* promoter. Fluorescence intensity (ex./em.: 488/508 nm) of the strains, grown in BM2 minimal medium supplemented with 0.01% (w/v) casamino acids and 1 mM IPTG, is given relative to the OD_{600} after substraction of background fluorescence from pyocyanin. Statistical significance values are stated (paired t-test).

5.2.4 PqsE has a potential dual-enzymatic activity of the bifunctional P-protein PheA

To decipher the exact relationship between PqsE, RhlR and pyocyanin production, I next sought to identify other physiological compounds than PQS able to interact with recombinant PqsE. Since chorismate is the direct precursor for both AQs and pyocyanin (see Fig. 5.6), and a chorismate-derived molecule has been co-crystallized with PqsE (214, 275), we were wondering if PqsE might display similar substrate specificity as other chorismate-utilizing enzymes. In *P. aeruginosa* and other bacteria, chorismate is an important branch-point metabolite that serves as a precursor for the synthesis of aromatic amino acids (phenylalanine, tyrosine, and tryptophane), but also for other products such as AQs, siderophores and phenazines. Chorismate itself is synthesized from shikimate in a multi-enzymatic cascade reaction pathway only to be found in bacteria, fungi and plants. During the last decades, there have been various studies focusing on chorismate-utilizing enzymes illustrating the biological relevance of this key metabolic intermediate (reviewed by (280)). *P. aeruginosa* possesses the following enzymes (Fig. 5.6): (1) A periplasmic chorismate mutase (AroQ) catalyzing a pericyclic Claisen rearrangement reaction from chorismate to prephenate; (2) The cytosolically active and bifunctional PheA (also referred to as P-Protein) possessing catalytic domains of chorismate mutase and prephenate dehydratase, which rearranges chorismate to prephenate and phenylpyruvate in the pathway of phenylalanine biosynthesis; (3) The anthranilate synthase (PhnAB) catalyzes the conversion of chorismate to anthranilate, the direct substrate for PQS synthesis; (4) The aminodeoxyisochorismate synthase (PhzE) converts chorismate into aminodeoxy-isochorismate, the first step in pyocyanin biosynthesis; (5) During salicylate biogenesis, the isochorismate synthase (PchA) catalyzes the conversion of chorismate to isochorismate which is further processed by the isochorismate pyruvate-lyase (PchB), a bifunctional enzyme also displaying chorismate mutase activity; and (6) putative chorismate lyase (UbiC) removing pyruvate from chorismate to produce 4-hydroxybenzoate in the ubiquinone biosynthetic pathway.

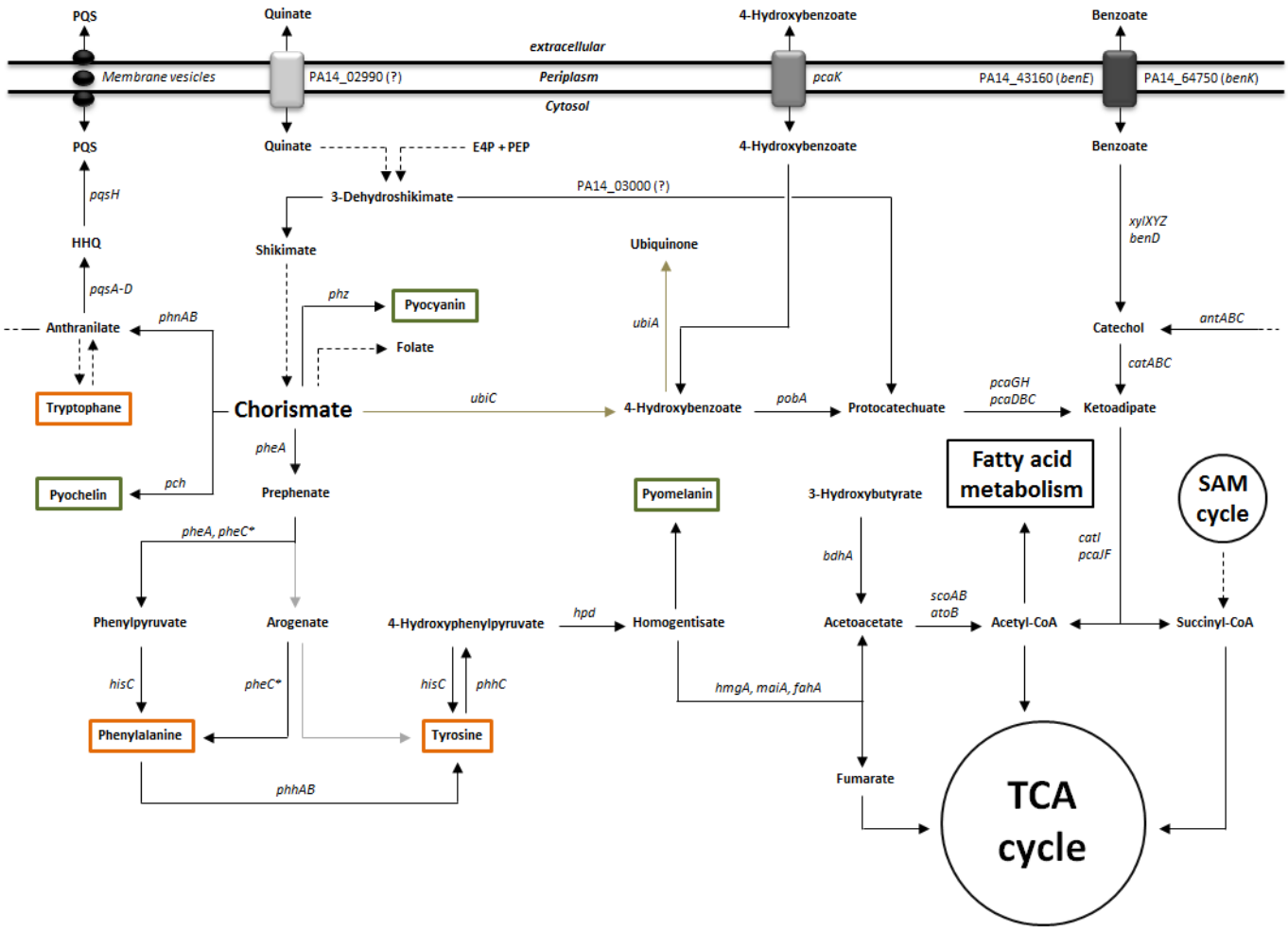

Figure 5.6: Schematic of the metabolic network of *P. aeruginosa*. Aromatic amino acids are boxed in orange and secretory products in green. Operone-encoded UbiCA catalyze the first steps in the ubiquinone biosynthetic pathway (shown in brown). Accumulating homogentisate was shown to spontaneously oxidize and polymerize to the dark-brown pigment pyomelanin often found in the lungs of chronically infected patients (42), if not degraded via the homogentisate central pathway whose products finally enter the tricarboxylic acid (TCA) cycle. The flow route from prephenate to arogenate and tyrosine is shown in grey because it is a minor route in *P. aeruginosa* (281). Complex multi-enzymatic reactions are shown as a dashed line. PheC-catalyzed periplasmic reactions are indicated by an asterisk. E4P, Erythrose-4-phosphate; PEP, Phosphoenolpyruvate.

I initially tested purified PqsE for its ability to utilize chorismate as substrate for a potential enzymatic catalysis *in vitro*. Therefore, PqsE was incubated with chorismate at 37 °C and the lyophilized reaction mix was analyzed by Prof. Dr. Christaine Ritter (HZI), who performed NMR spectroscopy on the samples to investigate chorismate turnover and to search for

potential reaction products. Indeed, preliminary results indicated a conversion of chorismate to phenylpyruvate with prephenate as intermediate reaction product (data not shown). In *P. aeruginisa*, and most other proteobacteria, these subsequent reactions are generally catalyzed by PheA, a bifunctional fusion protein which redirects carbon flow from chorismate to phenylalanine biosynthesis (281). The actual reaction product phenylpyruvate is the immediate precursor of phenylalanine. To confirm these preliminary data, I quantitavely measured production of both prephenate and phenylpyruvate spectrophotometrically following an adopted version of a well-established protocol (282). Metal ions are common cofactors for members of the metallo-hydrolase/oxidoreductase family and in case of PqsE a previously measured weak phosphodiesterase activity was highest with Co^{2+} (214). Considering these previous observations, I tested a potential role of different doubly charged metal ions (Fe^{2+}, Mn^{2+} and Co^{2+}) on the putative chorismate-utilizing activity of PqsE. As depicted in Fig. 5.7, turnover of chorismate to prephenate and phenylpyruvate could be confirmed and appeared to be specific to PqsE. No significant amounts of prephenate and phenylpyruvate, intermediates of the phenylalanine biosynthetic pathway, were detectable in any of the samples containing the peptide chain release factor methyltransferase PrmC which served as a negative control. Interestingly, while the chorismate mutase activity of PqsE was independent of the tested metal ions (Fig. 5.7 A), the prephenate dehydratase activity was approximately 2- to 3-fold increased with Co^{2+} compared to Mn^{2+} and Fe^{2+} respectively (Fig. 5.7 B), both of which had no significant effect on conversion of prephenate to phenylpyruvate. However, these data should be interpreted with care and need to be confirmed by using another independent pool of purified PqsE to exclude cross-contamination with *E. coli* PheA.

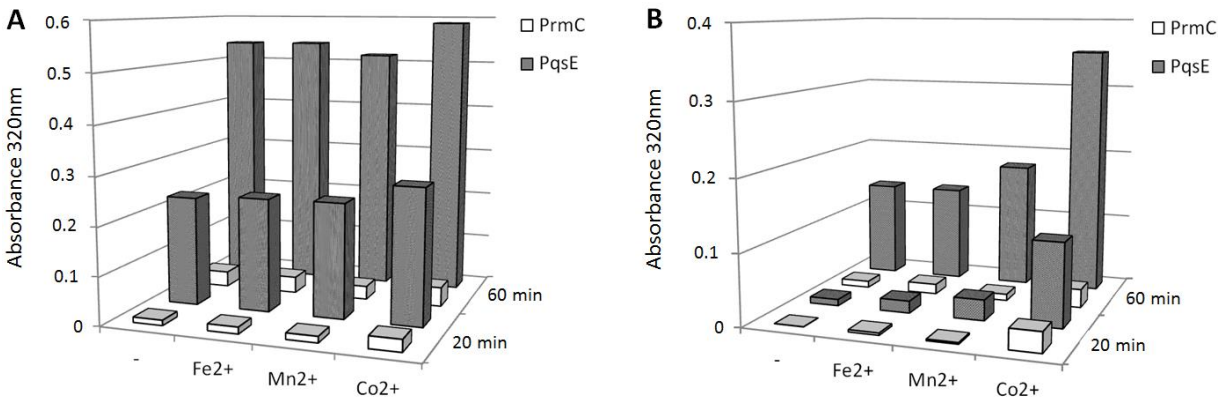

Figure 5.7: Potential chorismate mutase/prephenate dehydratase activity of PqsE. The *in vitro* conversion of 0.5 mM chorismate to prephenate and subsequently to phenylpyruvate by PqsE was monitored using 5 µM of freshly purified proteins using PrmC as a negative control. Formation of **(A)** prephenate, and **(B)** phenylpyruvate after 20 and 60 min of incubation at 37 °C was measured by absorbance at 320 nm, following a well-established protocol (282). Reactions were carried out in 50 µl of 50 mM NaH_2PO_4 pH 7.5, in the presence of 0.1 mM cofactor (Fe^{2+}, Mn^{2+} and Co^{2+}) as indicated on the X-axis. Presented data are representative of two independent experiments.

5.2.5 Phenylalanine catabolism is directly linked to pyocyanin production

Preliminary data suggest that PqsE might channel chorismate into the biosynthesis of the aromatic amino acid phenylalanine, similar to the ubiquitous bifunctional P-protein (PheA). If the main function of PqsE, besides putative binding of PQS, was to convert chorismate to ultimately phenylalanine one would assume that exogenous addition of either phenylpyruvate or phenylalanine should complement a pyocyanin-deficient *pqsE* mutant. Yet, repeated attempts to complement the *pqsE* mutant by addition of different concentrations of these aromatics in various media have been unsuccessful (data not shown). Nonetheless, it was striking that the wild-type strain produced significantly elevated levels of pyocyanin upon addition of phenylalanine, with only a minor additive effect on growth. While the presence of 0.1 mM phenylalanine did not affect pyocyanin synthesis, the PA14 wild-type strain secreted double the amount of phenazine with 1 mM phenylalanine supplementation (Fig. 5.8). Similar results were obtained when using phenylpyruvate.

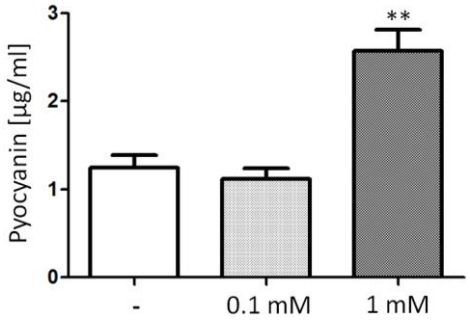

Figure 5.8: Effect of phenylalanine on the production of pyocyanin. The levels of pyocyanin were determined in the supernatants from overnight cultures of *P. aeruginosa* PA14 grown at 37 °C in BM2

minimal medium supplemented with 0.01% (w/v) casamino acids and indicated concentrations of phenylalanine. Statistical significance values of three biological replicates are stated (paired t-test).

The importance of phenylalanine on phenazine biosynthesis has already been described previously, but the reason for the observed induction is still unknown (283, 284). It is intriguing that this increase reflects just about the same effect as *pqsE* overexpression has on pyocyanin biosynthesis in the wild-type strain. Like *pqsE*, phenylalanine also had no major impact on the growth behavior of *P. aeruginosa*.To test if a direct correlation exists between a putative PheA-like activity of PqsE and pyocyanin production *in vivo*, a PA14Δ*pheA* transposon mutant was assayed for its ability to produce pyocyanin in dependence of *pqsE*. Interestingly, mutation of *pheA* is associated with both impaired growth and pyocyanin synthesis in BM2 minimal medium, but not in LB (data not shown). Noteworthy, supplementation with high levels of either phenylpyruvate or phenylalanine could complement the pyocyanin-deficient phenotype of the mutant in minimal medium (Fig. 5.9). Again, addition of 0.1 mM phenylpyruvate/phenylalanine had no significant effect on pyocyanin production but complemented growth of the *pheA* mutant. Intriguingly, a similar concentration-dependent pattern of pyocyanin production could be observed when overexpressing *pqsE* in the *pheA* mutant. While constitutive expression of *pqsE* with a *lac* promoter had no major impact on the phenotype (Fig. 5.9 pUCP20), *pqsE* expression placed under the control of the strong IPTG-inducible *tac* promoter partially restored pyocyanin production (Fig. 5.9 pME6032). This result is all the more remarkable because *pqsE* overexpression usually enhances phenazine biosynthesis regardless of the *P. aeruginosa* mutation status. However, unlike phenylpyruvate and phenylalanine, strong *pqsE* overexpression did not stimulate growth. This suggests that PqsE-produced phenylpyruvate is not majorly metabolized by the bacteria, but seems to be readily available to cells to stimulate phenazine biosynthesis.

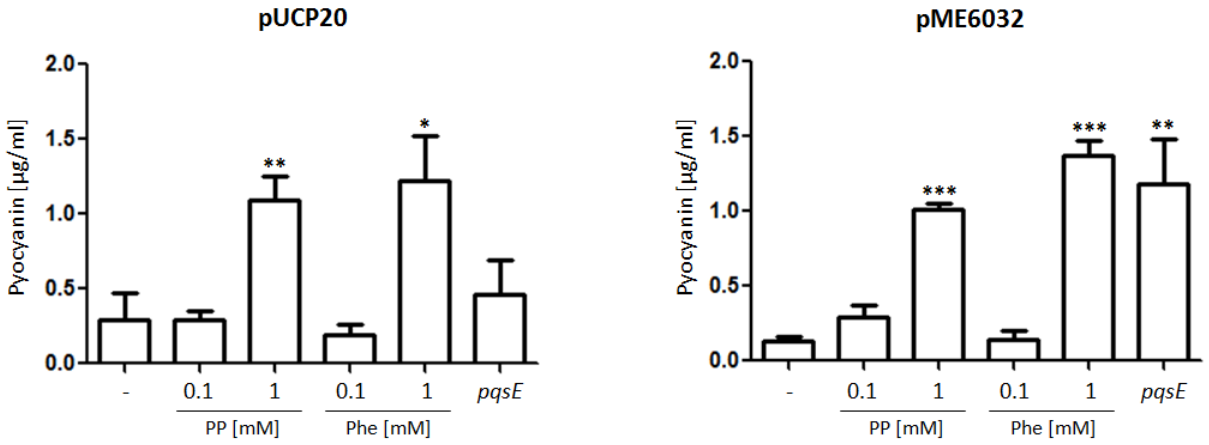

Figure 5.9: Strong overexpression of *pqsE* complements the pyocyanin-deficient phenotype of a PA14Δ*pheA* mutant. The pyocyanin production of a PA14Δ*pheA* transposon mutant was quantified in the supernatants from overnight cultures grown at 37 °C in BM2 minimal medium supplemented with 0.01 % (w/v) casamino acids and indicated concentrations of phenylpyruvate (PP) and phenylalanine (Phe), respectively. The *pheA* mutant harbored the following plasmids (as can be seen in the graphics): pUCP20 and pUCP20*pqsE* (indicated by *pqsE*), or pME6032 and pME6032*pqsE* (indicated by *pqsE*). Statistical significance values of three biological replicates are stated (paired t-test).

5.2.6 An Integrative –omics approach to investigate the 'off' status of the *pqsE* mutant to produce pyocyanin

To investigate the striking phenotype discrepancy between the *pqsE* mutant and the wild-type strain, I next performed an integrative transcriptome (RNA-Seq) and translatome (Ribo-Seq) analysis of the two strains grown in M9 minimal medium. On that account, I took advantage of the novel technique Ribo-Seq to investigate potential effects on post-transcriptional regulation. The samples were prepared from the same culture at the onset of stationary growth phase (OD_{600} of ~3.0). These growth conditions were used to allow for future comparison to a proteome analysis performed by Jonas Krüger at the Twincore (Hannover).

To reduce potential sources of bias and occurrence of false positives, only genes with a fold-change greater than or equal to five were included in this study. Further, given a difference in the number of mRNA sequencing reads obtained from both approaches, we used fitted minimum read depth cutoffs for RNA-Seq (normalized reads per gene ≥ 50) and Ribo-Seq (normalized reads per gene ≥ 20) samples. In total, 73 genes were downregulated and 15 were

found to be upregulated in the *pqsE* mutant using RNA- and Ribo-sequencing data (Fig. 5.10 A). Overall, the transcriptomic and translatomic data correlated well. This is a very interesting finding, considering that often the abundance ratio of an mRNA transcript is not necessarily reflected on the protein level. As reported in Tab. 5.1 and illustrated in Fig. 5.10 B, loss of *pqsE* led to a severe downregulation of the redundant phenazine operons *phzA-G1* and *phzA-G2*, which explains the inability of the mutant to produce pyocyanin. This downregulation was accompanied by reduced expression and translation of the *mexGHI-opmD* multidrug efflux pump, comprising a major part of the pyocyanin regulon (285). The pump, located just upstream of *phzA-G1* (Fig. 5.10 B), is required for virulence of *P. aeruginosa* via direct association with the AQ signaling system (189). Another striking, but unexpected finding was the negative effect of *pqsE* mutation on the protocatechuate branch of the beta-ketoadipate pathway (see Fig. 5.6). Several genes of this key metabolic pathway, involved in aromatic compound degradation, were transcriptionally and translatinally repressed in the mutant by more than 8-fold (*pobA*, *pcaGH*, *catI*, and *pcaJF*), including the transporter for 4-hydroxybenzoate and protocatechuate (PcaK). Another transporter of aromatic compounds (BenK) involved in uptake of compounds in the benzoate branch of the beta-ketoadipate pathway was likewise strongly repressed in the *pqsE* mutant. Among the strongly downregulated genes in RNA-Seq and Ribo-Seq were furthermore two 4-hydroxyphenylpyruvate dioxygenase genes, namely *hpd* and PA14_03000. Other downregulated genes included the juxtapositional operons PA14_48530-PA14_48590 and PA14_48600-PA14_48640 containing genes of unknown function. The first of these operon structures is under transcriptional control of LasR (286). Interestingly, mutation of the predicted trans-aconitate methyltransferase gene PA14_48590, the last gene of this operon, was shown to cause attenuated virulence in *C. elegans* (287). Further, the *pqsE* mutant was impaired in transcription and translation of the glucose-specific porin OprB (288), two putative MFS transporters (PA14_64750 and PA14_02990), and the methionine synthase (MetE) being part of the SAM cycle. Curiously, despite severe repression of the beta-ketoadipate pathway, the OprB glucose transport component, and other potential membrane transporters, the *pqsE* mutation had no significant effect on the growth behavior.

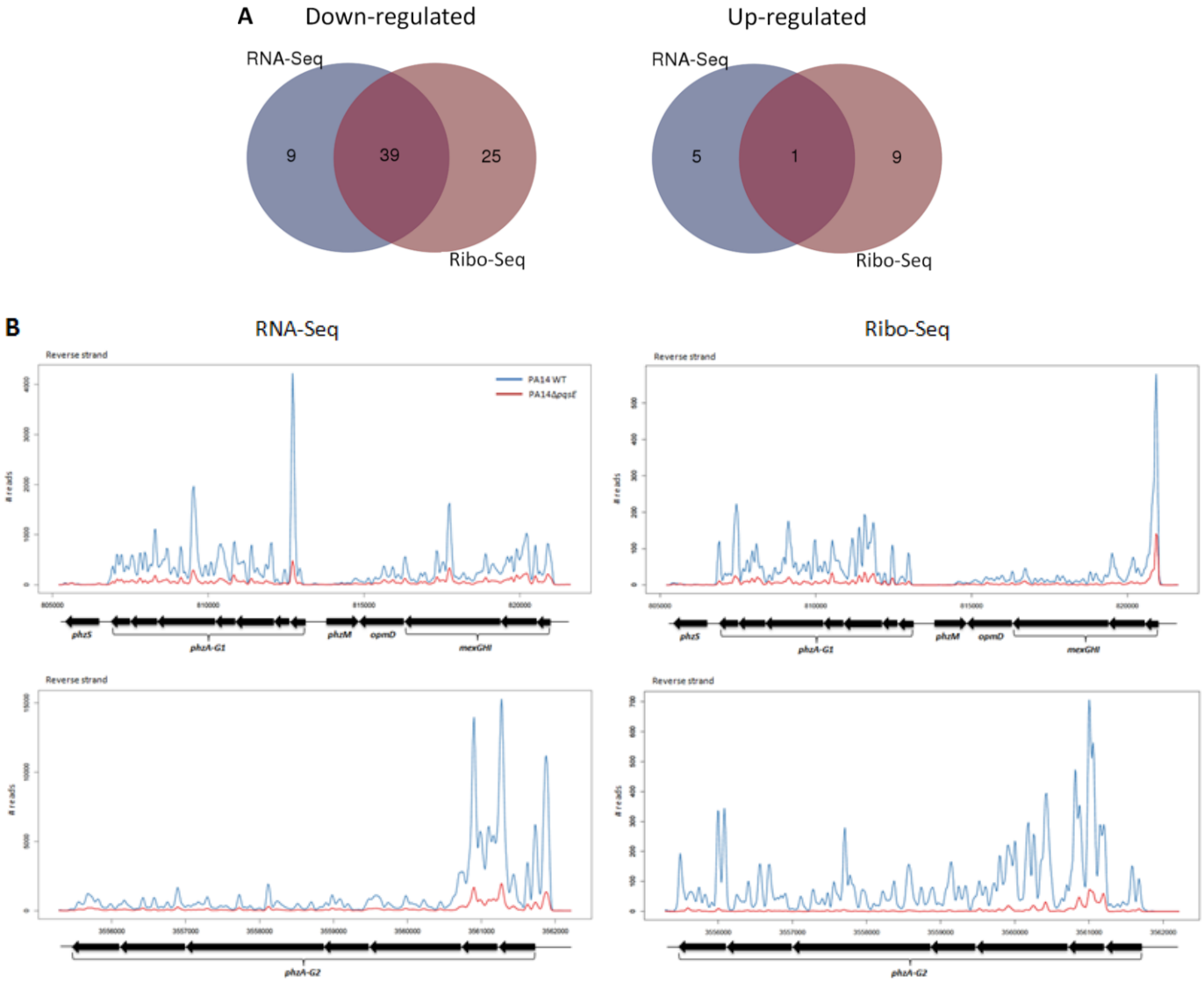

Figure 5.10: Analysis of PqsE-dependent efficiency of transcription and translation. (A) Venn diagram showing the distribution of strongly differentially regulated genes (≥5-fold change) in PA14Δ*pqsE* detected with the '-omic' approach. (B) Expression of the two phenazine biosynthetic loci and the *mexGHI-opmD* operon is shown for the PA14 wild-type and PA14Δ*pqsE* mutant (blue and red lines, respectively). Sequencing reads were mapped to a PA14 reference genome and smoothened using the 'locally weighted scatterplot smoothing' (LOESS) regression model.

While most of the genes were negatively affected by the loss of *pqsE* on a transcriptional and translational level, only a few were found to be upregulated by more than 5-fold in RNA-Seq and Ribo-Seq (Fig. 5.10 A). Common to both was upregulation of a putative effector of murein hydrolase (PA14_19690) encoded within a two-gene operon (PA14_19680 - PA14_19690). The second gene of the operon (PA14_19680) was also found to be increased

by ≥5-fold in PA14Δ*pqsE* in RNA-Seq, whose gene product shows structural features of the LrgA-like family. In *Staphylococcus aureus*, the homologous *lrgAB* operon was demonstrated to confer negative control on extracellular murein hydrolase activity, and to be involved in antibiotic tolerance and biofilm formation (289, 290). Intriguingly, carbohydrate metabolism was reported to have a dramatic impact on expression of *lrgAB* (291, 292), comparable to *pqsE* mutation. Surprisingly, and in contrast to previous transcriptomic analyses, none of the *pqs* biosynthetic genes was found among the set of highly abundant mRNAs in neither of the two approaches (133, 134). This, however, was due to the strict selection criteria used for data analysis. Expression of all biosynthetic genes (*phnAB* and *pqsA-D*) was found to be increased in the *pqsE* mutant by up to 5-fold.

Table 5.1: List of selected genes affected by PqsE identified in the itegrative –omics study.

			***pqsE* vs wt**[b]		
	PA14[a]	**Gene**[a]	**RNA-Seq**	**Ribo-Seq**	**Product name**[a]
Down-regulated	PA14_01150			-2.60	putative uncharacterized protein
	PA14_01900	***pcaH***	-5.680	-3.46	protocatechuate 3.4-dioxygenase. beta subunit
	PA14_01910	***pcaG***	-5.443	-4.05	protocatechuate 3.4-dioxygenase. alpha subunit
	PA14_02760	***catI***	-3.835	-5.61	putative CoA transferase. subunit A
	PA14_02770	***pcaJ***	-3.202	-5.27	putative CoA transferase. subunit B
	PA14_02790	***pcaF***	-3.070	-4.87	beta-ketoadipyl CoA thiolase PcaF
	PA14_02900	*pcaK*		-4.56	4-hydroxybenzoate transporter PcaK
	PA14_02990		-4.042	-10.53	putative MFS transporter
	PA14_03000		-4.485	-5.85	putative 4-hydroxyphenylpyruvate dioxygenase
	PA14_03010			-2.41	putative transcriptional regulator. TetR family
	PA14_03050	*pobA*		-5.36	p-hydroxybenzoate hydroxylase
	PA14_03290			-2.58	nd
	PA14_09410	***phzG1***	-2.818	-3.18	probable pyrodoxamine 5'-phosphate oxidase
	PA14_09420	*phzF1*	-2.912		phenazine biosynthesis protein PhzF1
	PA14_09440	***phzE1***	-2.989	-2.80	phenazine biosynthesis protein PhzE1
	PA14_09450	***phzD1***	-2.801	-2.40	phenazine biosynthesis protein PhzD1
	PA14_09460	***phzC1***	-3.126	-2.57	phenazine biosynthesis protein PhzC1
	PA14_09470	*phzB1*	-2.772		phenazine biosynthesis protein PhzB1
	PA14_09480	***phzA1***	-3.420	-2.82	phenazine biosynthesis protein PhzA1
	PA14_09500	*opmD*		-2.49	outer membrane protein
	PA14_09520	***mexI***	-2.457	-2.48	probable RND efflux transporter
	PA14_09530	***mexH***	-2.374	-2.91	RND efflux membrane fusion protein
	PA14_13130		-2.546		putative uncharacterized protein
	PA14_13140		-2.361		putative uncharacterized protein
	PA14_14320			-2.36	putative uncharacterized protein

PA14_14480			-2.54	putative transcriptional regulator
PA14_16310		-2.912	-3.31	putative MFS permease
PA14_21530			-2.35	putative ankyrin domain protein
PA14_22320			-2.55	putative membrane protein
PA14_22350	*actP*	-2.517		putative sodium/proline:solute symporter
PA14_23030	***oprB***	-2.380	-3.70	glucose/carbohydrate outer membrane porin OprB
PA14_24310			-2.65	putative BNR/Asp-box repeat protein
PA14_24790	*opdQ*	-2.364		putative outer membrane porin
PA14_24860	***snr1***	-2.339	-3.16	cytochrome c Snr1
PA14_31370	*tam*		-2.59	trans-aconitate 2-methyltransferase
PA14_32190			-2.70	putative transcriptional regulator
PA14_34870	*chiC*		-2.74	Chitinase ChiC
PA14_35160		-2.905	-2.80	putative uncharacterized protein
PA14_38360	*ugd*		-4.74	putative UDP-glucose 6-dehydrogenas
PA14_39590	***metE***	-2.662	-3.19	homocysteine methyltransferase MetE
PA14_39880	***phzG2***	-2.814	-4.92	probable pyridoxamine 5'-phosphate oxidase
PA14_39890	***phzF2***	-2.938	-5.17	phenazine biosynthesis protein PhzF2
PA14_39910	***phzE2***	-2.957	-5.29	phenazine biosynthesis protein PhzE2
PA14_39925	***phzD2***	-2.997	-5.57	phenazine biosynthesis protein PhzD2
PA14_39945	***phzC2***	-3.046	-4.25	phenazine biosynthesis protein PhzC2
PA14_39960	***phzB2***	-3.217	-3.12	phenazine biosynthesis protein PhzB2
PA14_39970	***phzA2***	-3.332	-4.37	phenazine biosynthesis protein PhzA2
PA14_40100			-2.97	putative uncharacterized protein
PA14_45410			-12.74	putative FlhB domain protein
PA14_46590			-7.64	putative AcrB/AcrD/AcrF family protein
PA14_46670			-4.44	putative uncharacterized protein
PA14_48530		-2.942		putative AMP-binding enzyme
PA14_48540		-2.576	-3.44	putative uncharacterized protein
PA14_48550		-2.745	-3.19	putative uncharacterized protein
PA14_48560		-2.741	-2.66	putative uncharacterized protein
PA14_48570		-2.682	-2.71	putative 2-isopropylmalate synthase
PA14_48590		-2.674	-2.61	putative uncharacterized protein
PA14_48600		-2.609	-3.31	putative AMP-binding enzyme
PA14_48610		-2.640	-2.90	putative sparagine synthase
PA14_48620		-2.437	-2.33	putative clavaminic acid synthetase
PA14_48630		-2.433	-2.65	putative MFS transporter
PA14_48640			-3.36	putative uncharacterized protein
PA14_52800	***acsA***	-2.666	-2.56	acetyl-coenzyme A synthetase (AcCoA synthetase)
PA14_53070	***hpd***	-2.726	-2.58	4-hydroxyphenylpyruvate dioxygenase
PA14_53300			-2.98	probable alkyl hydroperoxide reductase
PA14_55750		-2.430		putative chemotaxis transducer
PA14_63020	*fur*		-2.80	ferric uptake regulation protein
PA14_64750	***benK***	-2.647	-3.58	putative MFS transporter
PA14_69390	*algQ*		-2.36	alginate regulatory protein AlgQ
PA14_70670	***glcF***	-3.978	-8.94	glycolate oxidase. iron-sulfur subunit
PA14_70680	*glcE*		-2.81	glycolate oxidase subunit GlcE

	PA14_70690	*glcD*	-3.911		glycolate oxidase subunit GlcD
Up-regulated	PA14_11530			2.69	putative ABC transporter
	PA14_16010			2.69	putative ong-chain acyl-CoA thioester hydrolase
	PA14_16430	*wspA*		4.38	putative methyl-accepting chemotaxis transducer
	PA14_18820			5.66	putative uncharacterized protein
	PA14_19680		4.040		putative murein hydrolase exporter
	PA14_19690		4.296	2.34	putative murein hydrolase export regulator
	PA14_21150			2.37	probable ABC transporter permease component
	PA14_25620			2.72	putative uncharacterized protein
	PA14_30970	*bphR*		2.68	putative transcriptional regulator
	PA14_31150			2.76	putative uncharacterized protein
	PA14_32750			5.59	putative uncharacterized protein
	PA14_38580		3.255		putative H+/gluconate symporter
	PA14_38590	*bdhA*	2.654		3-hydroxybutyrate dehydrogenase
	PA14_38640	*scoB*	2.623		putative CoA transferase. subunit B
	PA14_38660	*scoA*	2.467		putative CoA transferase. subunit A

a. Gene number. gene name and product name are from the *Pseudomonas* genome project (193). **b**. log2-fold change (≥|5|-fold change) in gene expression of *P. aeruginosa* PA14Δ*pqsE* mutant compared with PA14 wild-type (wt). Differentially expressed genes from RNA- and Ribo-Seq data are highlighted in bold.

5.2.7 Monitoring global transcription and translation patterns in response to phenylalanine

To investigate why phenylalanine supplementation cannot complement the pyocyanin-deficient phenotype of the *pqsE* mutant but induces phenazine biosynthesis in the wild-type strain (Fig. 5.8), the integrative –omic approach was used to examine the route of metabolism in both strains. The growth conditions and analytical procedure were similar to the preceding experiment, except exogenous provision of 5 mM phenylalanine.

General effect of phenylalanine

In a previous study, the transcriptional response of *P. aeruginosa* to aromatic amino acids has already been studied in detail (284). In agreement with the study of Palmer and colleagues (284), almost exclusively genes participating in phenylalanine/tyrosine catabolism were among the most strongly induced (≥5-fold change) genes in the RNA-Seq and RiPro-Seq data of phenylalanine-treated cells, independent of *pqsE* (Fig. 5.11.). Together, in both methods, only 14 genes were found to be upregulated in the *pqsE* mutant and the wild-type including eight genes of the central catabolic pathway involved in the degradation of phenylalanine through the homogentisate pathway (*phhA*, *phhB*, *hpd*, *hmgA*, *maiA*, *fahA*, *scoA* and *scoB*)

(Fig. 5.6). These results suggest that both strains generally utilized exogenously supplemented phenylalanine in the same way. In both approaches, a putative transmembrane protein structurally homologous to amino acid efflux pumps of the RhtB/LysE family (PA14_58500) was the most upregulated gene in response to phenylalanine addition, but the physiological function of this protein is speculative and needs further investigation. On the other hand, no remarkable strain-independent downregulation of gene expression could be observed in response to phenylalanine. This was surprising since I at least would have expected that *pheA* and *hisC*, genes of the biosynthetic pathway of phenylalanine, were downregulated. In *E. coli*, for instance, *pheA* was shown to be subject to strong feedback inhibition by phenylalanine (293).

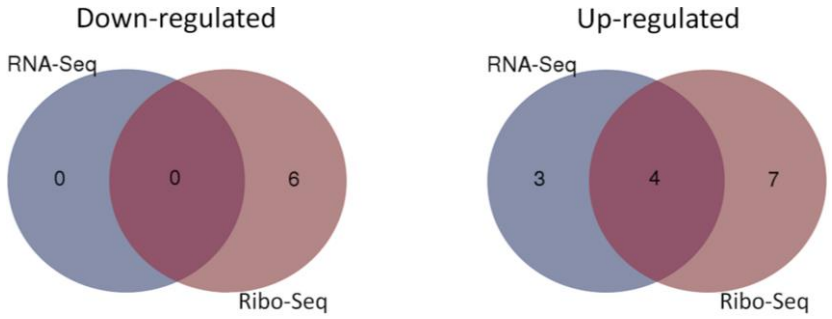

Figure 5.11: Strain-independent effect of phenylalanine on global efficiency of transcription and translation. Venn diagram showing the distribution of strongly differentially regulated genes (≥5-fold change) in the *pqsE* mutant and the wild-type strain upon supplementation with phenylalanine.

Strain-specific effects of phenylalanine

There were also unique features in the -omics analysis of the *pqsE* mutant and the wild-type strain indicating that phenylalanine served not only as a nutrient for *P. aeruginosa*, but also differentially affected several cellular pathways in a PqsE-dependent manner. We were particularly interested in genes and pathways that were inversely affected in both strains. The following criteria were used to determine this strain-dependent behavioral response to phenylalanine: (i) A minmum number of sequence reads per genes was required in any of the samples (wt vs *pqsE* mutant; with and without 5 mM phenylalanine): RNA-Seq (≥50 reads), and Ribo-Seq (≥20 reads). (ii) Genes for which no reads were detected in the samples were excluded from analysis. (iii) Only genes that displayed a greater than |2|-fold change in

transcription or translation efficiency during growth on phenylalanine were considered when they were inversely regulated in the two strains.

Interestingly, the effect of phenylalanine was most evident at the translational level. A particularly intriguing finding was the differential regulation of transcription and translation of genes involved in iron metabolism in both strains upon exogenous supplementation with phenylalanine (Tab. 5.2). PqsE is well known to play a crucial role in iron homeostasis (133, 134), and our data suggest that phenylalanine is an important factor to achieve effective iron homeostasis (Fig. 5.12). Translation of numerous iron-responsive genes was found to be inversely regulated in the wild-type and the *pqsE* mutant including *fpvB*, *pvdS*, *pvdL*, *pirA*, and *fur* (Tab. 5.2). As shown before, *fur* mRNA translation was reduced by ~ 7-fold in the *pqsE* mutant (Tab. 5.1). Interestingly, this PqsE-dependent post-transcriptional effect on *fur* was reversed upon growth in phenylalanine-rich medium. While the *fur* mRNA translation efficiency was increased by ~ 4-fold in the *pqsE* mutant, it was reduced by more than 5-fold in the wild-type strain (Tab. 5.2). The ferric uptake regulator (Fur) is a global transcriptional regulator of iron-responsive genes. In the presence of sufficiently high iron concentrations Fur binds to a conserved DNA motif of iron-regulated genes thus blocking their transcription. The gene encoding for the alternative sigma factor PvdS is one of the genes known to be under direct control of Fur. PvdS is required for initiation of transcription from pyoverdine (*pvd*) promoters like *pvdL*, which is crucial for the biosynthesis of the main siderophore of fluorescent *Pseudomonads* (155, 167, 294, 295). Other genes controlled by Fur include the PA14_58040-*fumC*-PA14_58010-*sodM* operon encoding fumarase C and manganese-cofactored superoxide dismutase. Both, FumC and SodM, were reported to increase in activity and expression under iron limiting conditions (296, 297). As with other aforementioned iron-responsive genes, translation of the PA14_58040-*fumC*-PA14_58010-*sodM* operon appeared to be inversely related to Fur levels, although there was no significant differential regulation detectable with RNA-Seq (except for *pvdL*). These results demonstrate that phenylalanine also interferes with the complex interplay between AQ signaling and iron metabolism in *P. aeruginosa*.

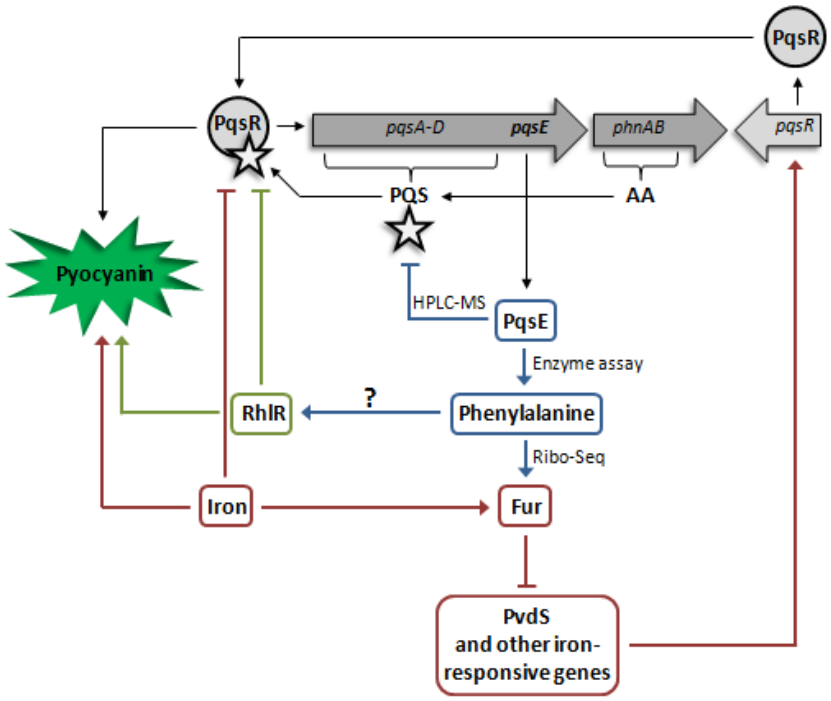

Figure 5.12: Proposed model to describe the role of PqsE and phenylalanine in iron homeostasis. In *P. aeruginosa* transcription of the *pqsA-E* operon was found to decrease with increasing iron concentrations (298). Conversely, iron induces pyocyanin and Fur synthesis. Simlar effects apply to PqsE and which might be linked to the PheA-like activity of PqsE described in the present study. While the positive impact of phenylalanine on *fur* mRNA translation was experimentally verified (Ribo-Seq), the correlation between pyocyanin and phenylalanine still remains to be determined. But given that PqsE functions via RhlR, it can be speculated that phenylalanine potentially enhances *rhl* signaling. The negative autoregulatory role of PqsE may arise from its probable ability to bind/interact with PQS. Alternatively, or in addition, this self-inhibitory role of PqsE could be correlated to promoting RhlR activity, thereby inhibiting PQS signaling in two different ways: (A) by inhibiting *pqsR* expression (129), and (B) by repressing *pqsA-E* mRNA translation (299). An additional layer of regulation could be the stimulating effect of phenylalanine on the global regulator Fur, which represses expression of several iron-responsive genes, including *pvds*. PvdS, in turn, is a positive transcriptional regulator of *pqsR* (300). AA, anthranilate.

Remarkably, translation of *phzD-G2* mRNA was consistently repressed in the wild-type strain grown on phenylalanine (Tab. 5.2). This actually contradicts the phenotype of increased pyocyanin production (Fig. 5.8). On the contrary, supplementation with phenylalanine resulted in a higher translation rate of the same *phz* transcripts in the *pqsE* mutant (Tab. 5.2). However, this inverse regulation of *phzD-G2* translation does not appear to have a significant

effect on phenazine biosynthesis, since exogenously added phenylalanine failed to induce pyocyanin production in the *pqsE* mutant.

Table 5.2: List of selected genes inversely affected by phenylalanine in the PA14 wild-type and PA14Δ*pqsE*.

			Phe effect[b]		
	PA14[a]	Gene[a]	wt	*pqsE*	Product name[a]
RNA-Seq	PA14_24790	*opdQ*	-1.02	1.29	putative outer membrane porin
	PA14_38580		1.81	-1.40	putative H+/gluconate symporter
	PA14_38590	*bdhA*	1.00	-1.99	3-hydroxybutyrate dehydrogenase
	PA14_33280	*pvdL*	1.18	-1.65	PvdL
Ribo-Seq	PA14_02230	*cheW*	-1.03	1.43	putative purine-binding chemotaxis protein
	PA14_02530		-1.01	1.60	putative esterase
	PA14_03290		-3.46	1.54	nd
	PA14_08680	*tufB*	-1.19	1.66	elongation factor Tu
	PA14_09970	*fpvB*	1.72	-2.24	type I ferripyoverdine receptor, FpvB
	PA14_11530		1.68	-2.15	putative ABC transporter
	PA14_12180		-1.47	1.30	putative uncharacterized protein
	PA14_13740	*narX*	-1.30	1.12	putative nitrate/nitrite sensor protein, NarX
	PA14_18820		3.42	-6.68	nd
	PA14_21150		1.80	-2.49	probable ABC transporter permease component
	PA14_22320		2.77	-1.26	putative membrane protein
	PA14_23030	*oprB*	-2.06	1.57	glucose/carbohydrate outer membrane porin OprB
	PA14_28970		1.11	-1.30	putative uncharacterized protein
	PA14_30020	*nuoA*	-1.67	2.26	NADH-quinone oxidoreductase subunit A 1
	PA14_30970	*bphR*	1.77	-1.16	putative transcriptional regulator
	PA14_32190		-1.23	1.78	putative transcriptional regulator
	PA14_32750		5.13	-4.24	putative uncharacterized protein
	PA14_32780		1.14	-1.38	putative uncharacterized protein
	PA14_33260	*pvdS*	1.12	-2.08	sigma factor PvdS
	PA14_33280	*pvdL*	1.10	-1.81	PvdL
	PA14_36620		-1.40	1.03	putative uncharacterized protein
	PA14_39420		1.27	-1.18	putative uncharacterized protein
	PA14_39880	*phzG2*	-1.55	1.01	probable pyridoxamine 5'-phosphate oxidase
	PA14_39890	*phzF2*	-2.28	1.46	phenazine biosynthesis protein PhzF2
	PA14_39910	*phzE2*	-1.58	1.57	phenazine biosynthesis protein PhzE2
	PA14_39925	*phzD2*	-1.72	2.32	phenazine biosynthesis protein PhzD2
	PA14_40340		-1.00	1.35	putative uncharacterized protein
	PA14_42200		-1.68	2.42	putative uncharacterized protein
	PA14_42950		1.46	-1.40	putative uncharacterized protein
	PA14_46670		-2.04	2.86	putative uncharacterized protein
	PA14_47400		1.01	-1.67	putative sigma-70 factor, ECF subfamily

PA14_49410		-1.65	1.41	probable cold-shock protein
PA14_51620		1.24	-1.60	possible transposase
PA14_52230	*pirA*	1.10	-1.49	siderophore receptor protein
PA14_55070		-1.25	1.18	putative uncharacterized protein
PA14_57990		1.78	-2.22	putative heavy-metal transporter
PA14_58000	*sodM*	1.24	-2.86	superoxide dismutase
PA14_58010		2.17	-1.72	putative uncharacterized protein
PA14_58030	*fumC*	1.12	-2.28	nd
PA14_58040		1.04	-3.17	putative uncharacterized protein
PA14_61040	*katB*	3.44	-1.12	catalase KatB
PA14_62300	*phuT*	1.44	-1.23	putative periplasmic binding protein
PA14_63020	*fur*	-2.74	2.08	ferric uptake regulation protein
PA14_64530		1.40	-2.12	putative uncharacterized protein
PA14_69390	*algQ*	-1.72	1.50	alginate regulatory protein AlgQ

a. Gene number. gene name and product name are from the *Pseudomonas* genome project (193). **b**. log2-fold change (≥|2|-fold change) in gene expression of *P. aeruginosa* PA14Δ*pqsE* mutant compared with PA14 wild-type (wt).

5.2.8 Metabolome analysis reveals a pivotal role for PqsE in controlling phenylalanine/ tyrosine catabolism in *P. aeruginosa*

To get an idea of the influence of PqsE on the biosynthetic pathway of the two aromatic aminoc acids phenylalanine and tyrosine in *P. aeruginosa in vivo*, we next performed a pilot study by metabolic profiling of a *pqsE* mutant and its complementant in collaboration with Dr. Raimo Franke (HZI – group chemical biology). Thereby, we initially focused on intracellular pools of the aromatics phenylpyruvate, phenylalanine, tyrosine as well as pyocyanin.

This time, cells were grown to mid-exponential growth phase in BM2 minimal medium at the onset of pyocyanin production. We hypothesized that the impact of PqsE on the metabolic landscape of *P. aeruginosa* is likely to be strongest at this stage. In accordance with our previous findings, PqsE had a consistent and significant positive effect on levels of all tested metabolites (Fig. 5.13). This effect was most evident in the *pqsE* mutant, where phenylpyruvate, phenylalanine and tyrosine levels were ≥2-fold lower than in the wild-type. A downregulation by 2-fold is a significant difference considering phenylalanine and tyrosine are essential amino acids. Not surprisingly, the amount of pyocyanin produced by PA14Δ*pqsE* was hardly detectable, neither intracellularly nor in the culture supernatant. As expected, all metabolites were inversely regulated in the *pqsE* complementant having, on

average, 1.5-fold higher levels of the tested aromatics than the wild-type. Given that there are no differences in growth behavior among the strains, our results suggest that phenylalanine may not be significantly metabolized at this stage and could be readily available to the cell.

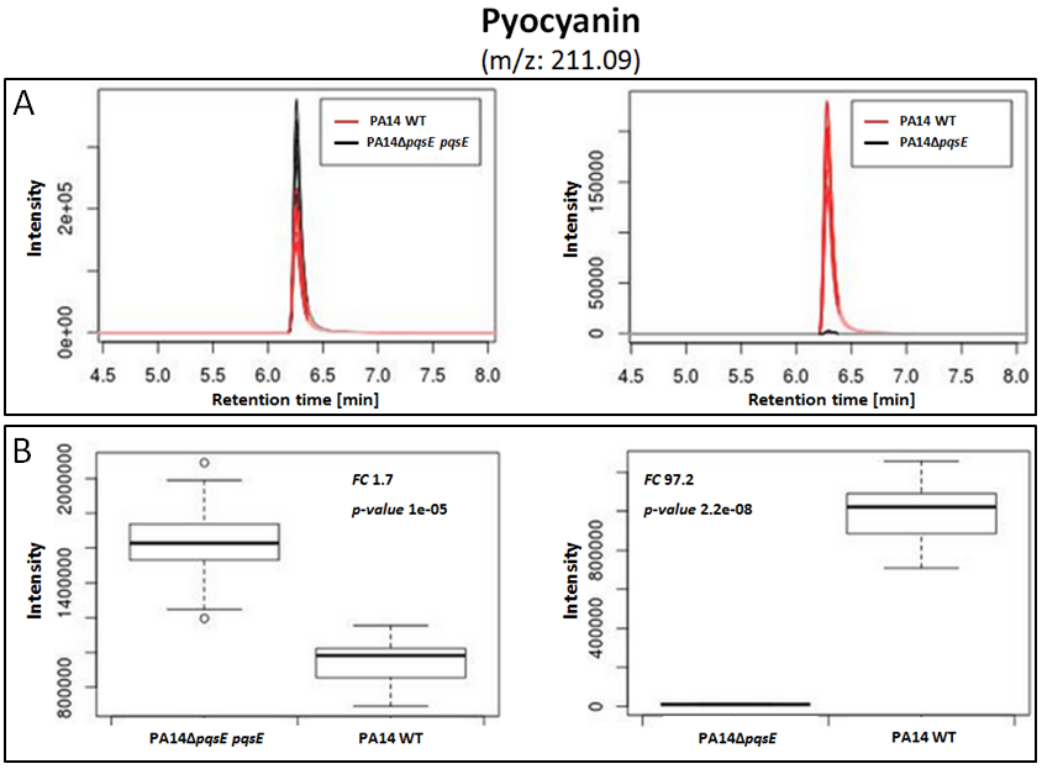

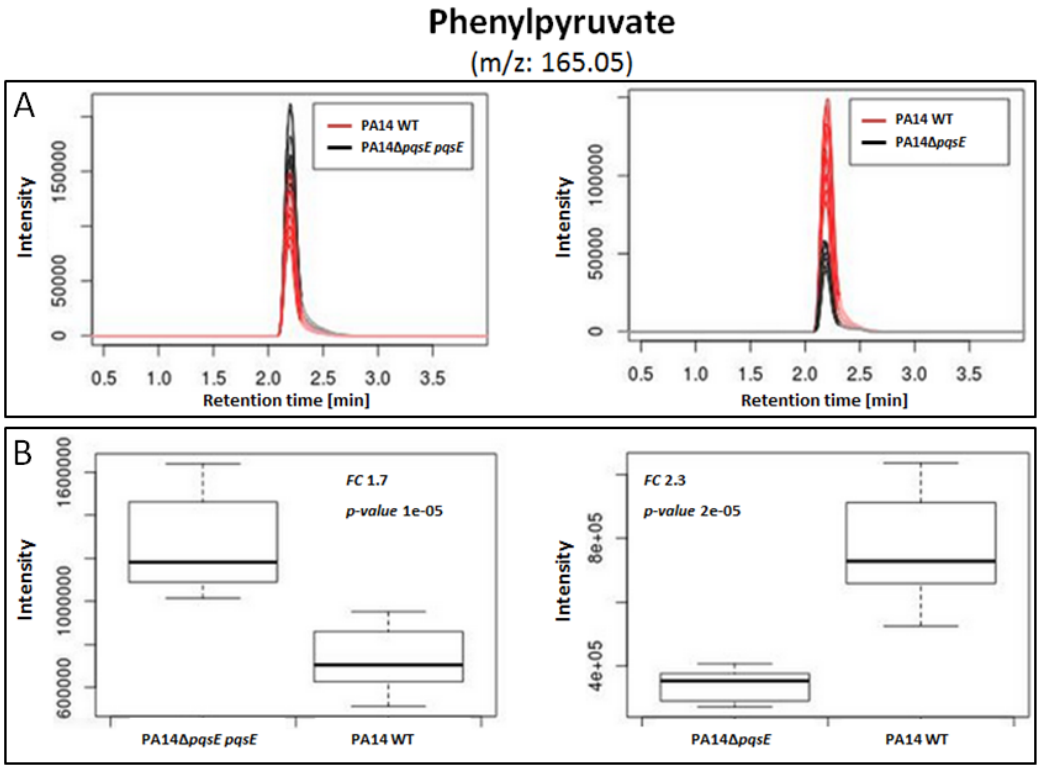

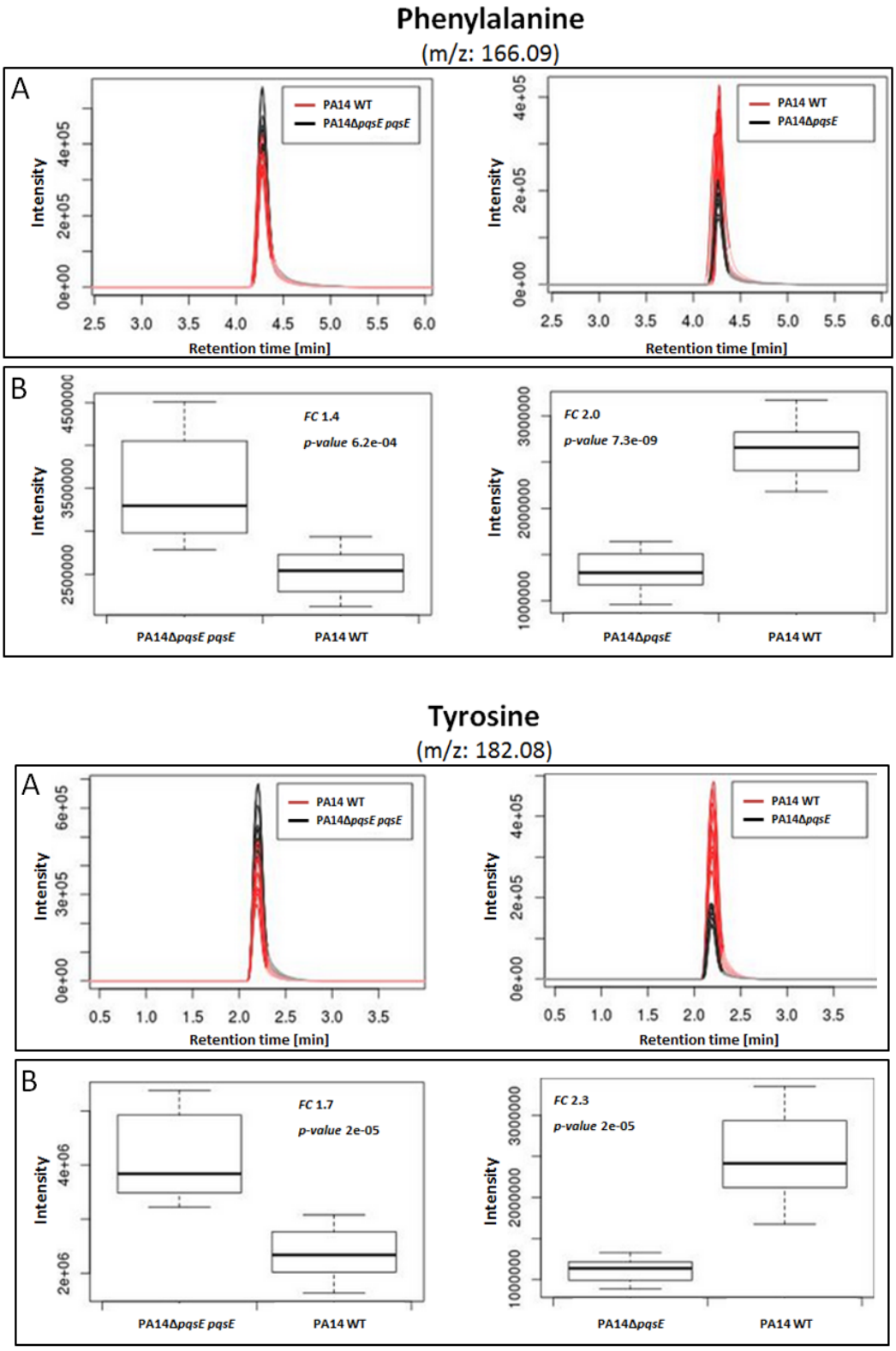

Figure 5.13: Metabolomic profiling of aromatic metabolites in dependence of *pqsE*. Intracellular metabolites of *P. aeruginosa* PA14 wild-type, a *pqsE* mutant and a complemented *pqsE* mutant carrying pUCP20*pqsE* were extracted during mid-exponential growth phase at an OD_{600} of 1.5. Bacteria were grown in BM2 minimal medium containing 0.01 % (w/v) casamino acids at 37 °C. (A)

Ultra high performance liquid chromatography for intracellular metabolite quantification. (B) Box-and-Whisker plot. p- and fold-change values in metabolite accumulation are shown in the box plot.

5.3 Discussion

QS in *P. aeruginosa* constitutes a sophisticated signaling network essential to the pathogenicity and exceptional ecologic success of this human opportunistic pathogen. The AQ system is a crucial part of this regulatory network. A prominent key component of the AQ signaling pathway is PqsE. Although not directly involved in AQ biosynthesis, PqsE is of undisputed importance in facilitating environmental adaptation and virulence of *P. aeruginosa*. Many attempts have been made to elucidate the molecular function of PqsE but have so far failed to identify the natural substrate of PqsE. The aim of this study was to gain insight into potential mechanisms of action that could explain the striking phenotype of a *pqsE* mutant strain.

A novel PqsE-dependent regulatory cascade to control phenazine biosynthesis?

In the present work, I performed for the first time a global integrative –omic study of a *pqsE* mutant strain which combined RNA-Seq and Ribo-Seq. We identifed PqsE as an important player in the regulation of gene expression of several catabolic pathways for aromatic compounds. In general translatomic data correlated well with the transcriptome. Primarily, PqsE was required for induction of the two phenazine biosynthetic operons, the *mexGHI-opmD* multidrug efflux pump, and the protocatechuate branch of the beta-ketoadipate pathway. It was shown previously that PqsE depends on the downstream acting transcriptional regulator RhlR to induce pyocyanin biosynthesis (134). Although no differential in *rhlI/R* expression was identified in the –omics study, I could demonstrate that PqsE enhances *rhl* signaling particularly during the early growth phase. For a better understanding of this relationship, we next seeked to elucidate the enzymatic activity of PqsE. Independent structural studies on the protein have co-crystallized PqsE in presence of a small chorismate-derived molecule in the active-site cavity (214, 275). In fact, the hydrophobic catalytic pocket of PqsE seems perfectly suited to such a compound. Additionally, the protein exhibits a unique C-terminal α-helical motif which potentially functions as a lid-like structure restricting entrance to the catalytic center (275). It could be shown that the lid was essential for the molecular function of PqsE because mutational variants of PqsE in this motif were

unable to restore the pyocyanin-deficient phenotype of a *pqsE* mutant. Interestingly, active site lid dynamics are also important for catalysis of *P. aeruginosa* isochorismate-pyruvate lyase (PchB) and other chorismate-utilizing enzymes (301).

Here, preliminary data indicate that PqsE may have catalytic activity similar to the bifunctional P-protein (PheA). Freshly purified PqsE exhibited activities of both chorismate mutase and prephenate dehydratase *in vitro* (Fig. 5.7). The latter activity could be strongly induced upon addition of cobalt as catalytic cofactor; this phenomenon was previously associated with a potential thioesterase activity of PqsE (214). In fact, proteins with chorismate mutase activity domains are widespread in bacteria and archaea. Often they are fused to other aromatic-pathway catalytic domains. A well-studied example is PchB whose physiological function is to produce salicylate and pyruvate from isochorismate, the second reaction in the pyochelin biosynthetic pathway in *P. aeruginosa* (302). Further, PchB displays weak chorismate mutase activity thus being able to catalyze two distinct pericyclic reactions. Another prominent example of such bifunctional proteins is the so called T-protein. The T-protein is encoded by the *tyrA* gene and it possesses catalytic domains for a chorismate mutase and for a prephenate dehydrogenase. In comparison to the ubiquitous and highly specific bifunctional P-protein, possession of the T-protein is limited to enteric bacteria and their closest phylogenetic neighbors (281, 303). It has proven to be a cyclohexadienyl dehydrogenase able to use prephenate and arogenate as alternative substrate for biosynthesis of tyrosine (304). Like other *Pseudomonads*, *P. aeruginosa* lacks *tyrA* and cytoplasmic biosynthesis of both phenylalanine and tyrosine relies exclusively on functional PheA. The importance of these two aromatic amino acids in respect of AQ signaling and antimicrobial activity of *P. aeruginosa* has been demonstrated by Palmer and colleagues who proposed a model where the presence of phenylalanine/tyrosine allows increased flux of chorismate into PQS biosynthesis, which in turn accounts for increased pyocyanin production (284). The presented results, however, suggest an alternative model for a number of reasons. First, a *pqsE* mutant itself produces elevated levels of PQS but is incapable to produce pyocyanin even in the presence of phenylalanine. Second, neither the addition of anthranilate nor tryptophane increase pyocyanin synthesis to a comparable level as phenylalanine does (data not shown), although both substances are notoriously better substrates for the AQ biosynthetic pathway. In fact, accumulation of anthranilate (e.g. caused by mutation of the *mexGHI-opmD* efflux pump) is postulated to repress pyocyanin production (189). Yet, addition of anthranilate to the wild-type strain can slightly induce pyocyanin biosynthesis. Third, the –

omics analysis showed no altered expression patterns of any of the genes involved in PQS synthesis albeit gene expression of phenylalanine/tyrosine catabolism was significantly induced. These findings suggest that there might be a different relationship between synthesis of aromatic amino acids and pyocyanin in *P. aeruginosa*.

It could be shown that the regulatory activity of PqsE requires RhlR for induction of pyocyanin (132, 133). RhlR is a transcriptional regulator which binds to the phenazine promoter region to activate phenazine biosynthesis (305). Farrow and colleagues reported that addition of large amounts of the AHL C_4-HSL to an isogenic PAO1Δ*pqsE* mutant restored pyocyanin production (132). However, this was not reproducible in PA14 cells (134), and all of my attempts to reproduce the measurements in both strains PAO1 and PA14 were likewise unsuccessful (data not shown). Still, overexpression of *rhlR* in a *pqsE* mutant had minor, but significant effects on pyocyanin production. Further I showed that the interaction between PqsE and the *rhl* system is time-dependent and presumably neglectable during late exponential phase of growth. Noteworthy, a metabolomics analysis during mid-exponential growth revealed a pivotal role of PqsE in regulating the intracellular pools of phenylpyruvate, phenylalanine, and tyrosine (Fig. 5.13), strengthening the results of our enzymatic assay. It is also interesting to note that in the genome of *P. aeruginosa* a cyclohexadienyl dehydratase (*pheC*), responsible for periplasmic phenylalanine biosynthesis, is located just adjacent to the *rhl* system. This could be a sheer coincidence; nevertheless, phenylalanine may well have a positive effect on *rhl* signaling. In the plant-beneficial bacterium *Pseudomonas chlororaphis*, for instance, phenylalanine was shown to stimulate both production of phenazines and the major autoinducer C_6-HSL (306). One can speculate now that in *P. aeruginosa* promoted pyocyanin levels could be coupled to an increased activity of RhlR due to elevated levels of C_4-HSL, which will be target for future experiments. Taken together, these findings highlight that it is quite reasonable that PqsE might direct carbon flow to phenylalanine synthesis and thereby increase/enable pyocyanin production in *P. aeruginosa*.

Admittedly, there are also arguments that could still speak against the validity of a potential PheA-like activity of PqsE. To begin with, rearrangement of chorismate to prephenate is a rare pericyclic Claisen rearrangement reaction with structural requirements for catalysis (307), and there is evidently no structural homology of PqsE to chorismate mutases. This, however, does not necessarily exclude such an activity since independent studies have co-purified a chorismate-derived molecule with PqsE (214, 275). Still, why is a *pqsE* mutant completely

deficient in pyocyanin production even after phenylalanine supplementation, if the main activity of PqsE was to ultimately synthetize this aromatic amino acid? Certainly a *pqsE* mutant appears to respond differently to exogenous phenylalanine addition than the wild-type strain. For example, expression of *rhlR* in a *pqsE* mutant *in trans* was not accompanied by elevated pyocyanin release upon exposure to this aromatic amino acid (data not shown). But why there has been no significant evidence for dysregulation of genes involved in phenylalanine catabolism in any of various -omic approaches? Conceivably this is a matter of time considering PqsE predominantly affects the *rhl* system during early growth, yet this hypothesis remains to be determined. It is possible that the PheA-like activity of PqsE may actually represent residual activity comparable to PchB. Still, it is very tempting to associate PqsE activity with phenylalanine/tyrosine catabolism given that both of them similarly induce pyocyanin production in *P. aeruginosa*.

The importance of the conversion of chorismate to phenylpyruvate in this nosocomial pathogen is known for quite some time (308, 309). In addition to the cytosolic activity of PheA, *P. aeruginosa* possesses a complete chorismate-to-phenylpyruvate pathway in the periplasm (281). The actual benefit of this 'hidden overflow pathway' is still unknown, but it nicely illustrates both the complexity and significance of phenylalanine catabolism in *P. aeruginosa*. Therefore it is easily conceivable that PqsE might as well be implicated in aromatic amino acid synthesis. In this respect it is noteworthy that strong overexpression of *pqsE* in a PA14Δ*pheA* transposon mutant was able to complement the mutant for pyocyanin production in BM2 minimal medium, similar to high concentrations of phenylpyruvate and phenylalanine (Fig. 5.9). Yet this influence of PqsE was limited to pyocyanin synthesis as *pqsE* did not stimulate growth of the mutant. Unfortunately, it is not possible to use heavy-isotope labeled chorismate to directly monitor the metabolic fate of this key intermediate in dependence of PqsE, as it is not efficiently imported into *P. aeruginosa*.

Another very significant finding of the integrative -omics approach, besides dysregulation of the phenazine biosynthetic genes, was the severely impaired expression of the *mexGHI-opmD* efflux pump. Located just upstream of the *phzA-G1* operon, it is described to be part of the pyocyanin regulon (285). Mutation of genes encoding this pump resulted in impaired cell-to-cell signaling, growth and virulence factor production (189). Most, if not all of these phenotypes were hypothesized to be attributable to accumulation of anthranilate (or a derivate), suggesting that *mexGHI-opmD* is involved in the excretion of these toxic

metabolites. Interestingly, despite severe downregulation of the pump, growth of the *pqsE* mutant is not affected at all compared to the wild-type. It is likely that accumulation of anthranilate in the *pqsE* mutant is relieved by directing the pool into AQ synthesis. This would likewise explain a significantly increased production of PQS in a *pqsE* mutant.

Furthermore, loss of *pqsE* lead to severely impaired expression of the 4-hydroxybenzoate (*pob*) and protocatechuate (*pca*) branches of the beta-ketoadipate pathway for aromatic degradation. In this respect, downregulation of PA14_02990 (putative MFS transporter) and PA14_03000 (hypothetical 4-hydroxyphenylpyruvate dioxygenase) could as well be associated with a sorely afflicted beta-ketoadipate pathway given their genomic proximity to *pob* and *pca* genes, comparable to the *qsu* operon of *Corynebacterium glutamicum* and the respective *qui* homologues in *Acinetobacter* species (310, 311). The protein products of these two genes might - hypothetically - deliver the substrate for the protocatechuate 3,4-dioxygenase (PcaGH) by channeling 3-Dehydroshikimate away from the shikimate pathway (see Fig. 5.6). In *P. aeruginosa*, little is known about the beta-ketoadipate pathway and no direct connection between the *pob* and *pca* branches and virulence has been established yet. The catechol branch of this pathway, on the other hand, was shown to be important for biofilm formation (312, 313). Under conditions which favor growth in biofilms, anthranilate can be used as carbon source and is degraded via the catechol branch instead of being used for the generation of AQs. The destination of anthranilate is thereby finely tuned by a growth-phase dependent antagonistic interplay of several QS regulators (314). Considering a hypothetical enzymatic activity of PqsE as chorismate mutase-prephenate dehydratase, it is conceivable that PqsE might affect the *pob* and *pca* branches of this metabolic pathway indirectly by diverting intracellular chorismate pools to phenylalanine synthesis, albeit addition of phenylalanine alone was not sufficient to chemically complement *pqsE* mutation. Attempts to restore pyocyanin production in the *pqsE*-negative strain by addition of 4-hydroxybenzoate in combination with phenylalanine also failed to complement the pyocyanin-deficient phenotype. The ability of the mutant to utilize both aromatic compounds was verified by testing growth in minimal medium containing the respective compound as sole carbon source. Nevertheless, a repressed beta-ketoadipate pathway in PA14Δ*pqsE* could be directly related to induced expression of two putative effectors of murein hydrolase activity (PA14_19680 and PA14_19690). This two-gene operon shows similarities to the *lrgAB* locus of *S. aureus*. LrgAB family proteins were found to play a central role in the regulation of membrane permeability and to interfere with murein hydrolase export (289–291). In *S.*

aureus, there are two regulatory pathways controlling *lrgAB* expression; one is dependent on weak acids like acetate and pyruvate and the other depends on proton motif force (291, 292). The same could apply for *P. aeruginosa* where PqsE evidently plays a crucial role in carbohydrate metabolism and thus may affect expression of PA14_19680 and PA14_19690 in a similar way. In general it is remarkable that mutation of *pqsE* does not majorly affect growth behavior considering the suppressed expression of the beta-ketoadipate pathway and other MFS transporters.

With its environmental versatility *P. aeruginosa* has great and highly complex metabolic network modularity as depicted in Fig. 5.6 (56, 57). Transitions in the network can affect timing and control of diverse biological processes. Consequently, the supply of nutrients can cause subtle reconfiguration of functional network organization to adjust to changes in the environment. Enzymatic activity and integrative -omic studies revealed that PqsE can be considered as a master regulator of metabolic flux of aromatic compounds. It is therefore not surprising that provision of exogenous aromatics not automatically results in a metabolic rescue of the *pqsE* mutant phenotype. It is entirely possible that loss of *pqsE* entail metabolic shifts inhibiting conversion of chorismate to pyocyanin. Accumulation of certain secondary compounds, for instance, can have severe effects on the activity of transcriptional regulators and modify their interaction profiles. In the nonpathogenic gram-positive bacterium *Corynebacterium glutamicum* accumulation of chorismate was shown to modulate carbon flow by serving as a direct effector of the LysR-type transcriptional regulator QsuR (317). The same is true for anthranilate, whose metabolism is complexly intertwined in the *P. aeruginosa* QS network. Like chorismate in *C. glutamicum*, accumulating anthranilate serves as an inducer for a LysR-type transcriptional regulator (AntR) which, in return, leads to degradation of anthranilate to catechol by an anthranilate dioxygenase complex encoded by *antABC* (166, 318). In both cases, the flow of carbon is diverted to generation of acetyl-CoA and succinyl-CoA and results in energy production via the TCA cycle. A possible increased activity of the LysR-type transcriptional regulator RhlR in the presence of phenylpyruvate/phenylalanine may constitute another, novel example of metabolic regulation in *P. aeruginosa*. This, however, is still a hypothesis that needs to be confirmed. These examples illustrate that carbon flow and regulation of aromatic biosynthesis is very significant and finely tuned in bacteria. It is certainly feasible that there are other metabolic signals for transcriptional regulators in a *pqsE* mutant preventing pyocyanin production. Much remains to be learned about how exactly PqsE facilitates regulatory function. Detailed metabolic

analysis of the mutant might help to gain deeper insight into the functional role of PqsE in controlling metabolic fluxes in *P. aeruginosa*.

The interaction between PqsE and PQS

Besides the proposed PheA-like activity, PqsE has an inhibitory autoregulatory function by repressing expression of the *pqs* biosynthetic genes including the *phnAB* operon (133, 134). Both functions of PqsE are known to be not directly interlinked since expression of *pqsE* in a *pqsA-E* knockout mutant can restore pyocyanin production despite the absence of AQs. How PqsE facilitates regulatory control on these pathways is still not fully characterized and understood, but the present data give preliminary evidence that PqsE might be a multifunctional moonlighting protein which both directly and indirectly shapes the metabolic network of *P. aeruginosa*. Moonlighting proteins have the capacity to perform more than one function and often they are involved in metabolic regulation or cell stress responses (319, 320). Remarkably, these proteins are known to be virulence determinants in infection disease in a range of important human pathogens (reviewed by (321)). In addition to enzymatic catalysis, moonlighting proteins generally have a secondary non-enzymatic function. The same could be true for PqsE: on the one hand, the main catalytic function of PqsE could be the stepwise conversion of chorismate into prephenate and phenylpyruvate analogous to the bifunctional P-protein (although this observation should still be treated with caution as results were obtained from a single batch of purified PqsE); on the other hand, PqsE appeared to be able to specifically bind PQS which could account for its described self-inhibition (133). The redox-stable Fe^{2+}/Fe^{3+} center in the active site of PqsE could thereby be of critical importance. It is not clear yet whether the Fe^{2+}/Fe^{3+} center of recombinant PqsE is just an artifact of heterologous expression (214), as metal composition under physiological conditions remains elusive. But the relevance of the two metal atoms in virulence of *P. aeruginosa* was illustrated recently (275). Surprisingly, the interaction of iron-binding chelators with the PqsE iron center has so far not been studied.

Here, I demonstrated that PqsE specifically lowered PQS levels of PA14 supernatant metabolite extracts *in vitro*. The same effect was observed when ferric iron was added to the extract. HPLC-MS analyses suggest now the following three plausible scenarios: (1) PqsE trapped PQS in its active site via complexation with the ferric iron atom; (2) PQS simply removed metal ions from the catalytic center of PqsE and was insoluble after re-extraction; or (3) the first two scenarios in the respective sequence of events, delayed in order. Undoubtedly,

PQS is a potent ferric iron chelator which generally forms a complex with a molar ratio of 3:1 (126). Possibly, PQS is able to physically capture the iron from PqsE by virtue of its superior binding strength. Irrespective of the scenario, PQS seemed to have entered the active site of recombinant PqsE either way whereas pyochelin, a theoretically equally efficient ferric iron chelator, presumably did not. Therefore it is tempting that we can explain the inhibitory function of PqsE as a potent repressor of AQ signaling by potentially sequestering and, thus, lowering intracellular available pools of PQS, an important signal molecule for the PqsR transcriptional regulator of the *pqs* system (109, 121, 274). It may as well account for a direct connection to differential expression of iron-responsive genes in the *pqsE* mutant as PQS is intimately intertwined in iron homeostasis (126, 273). Elevated concentrations of PQS have been shown to strongly induce production of the siderophore pyoverdine (273). Synthesis of this important iron-scavenger is under positive transcriptional control of the alternative sigma factor PvdS (322, 323), which in turn is under negative control of the global iron regulator Fur (300) (Fig. 5.12). It is conceivable that the upregulation of AQ biosynthetic genes in the *pqsE* mutant may be responsible for the observed repression of Fur at a post-transcriptional level resulting in enhanced expression of *pvdS*. In this context, as shown with the integrative –omic study, phenylalanine could again be a key factor modulating the efficiency of Fur production. Hence, the autoregulatory function of PqsE might as well be attributable to its enzymatic activity as chorismate-mutase/prephenate dehydratase. Further, repression of the *pqs* sytem could be achieved by the suggested activity-stimulating effect of phenylpyruvate/ phenylalanine on RhlR which, in turn, would result in suppressed translation efficiency of *pqs* mRNA (299).

For the moment, the nature of the interaction between PqsE and PQS remains unclear. A pull-down assay with immobilized PqsE and PQS might help to assess binding of PQS to the active site of PqsE. In this case, however, trapped PQS in the active-site cavity will most likely lead to the reduction or loss in the enzymatic activity of PqsE, which could be tested in the enzymatic activity assay. *In vivo*, such a scenario may be of temporal relevance to the pathogenesis of *P. aeruginosa* depending on environmental conditions.

5.4 Experimental procedures

Bacterial strains and growth conditions

Unless otherwise noted, bacterial strains listed in Tab. 5.3 were routinely grown in LB or BM2 minimal medium [7 mM $(NH_4)_2SO_4$, 40 mM K_2HPO_4 and 22 mM KH_2PO_4, 0.4 % glucose, 2 mM $MgSO_4$, 10 µM $FeSO_4$ and 0.01 % casamino acids] at 37°C and shaking at 180 rpm. Antibiotics were added at the following final concentrations [µg/ml]: for *E. coli*, kanamycin 50; ampicillin 100; tetracycline 12.5; for *P. aeruginosa*, carbenicillin 400; tetracaycline 100. IPTG was added to the medium at a concentration of 1 mM.

Table 5.3: Bacterial strains and plasmids.

Strain/plasmid	Relevant characteristics	Source
Strains		
E. coli DH5α	F$^-$ *endA1 gln*V44 *thi-1 recA1 relA1 gyr*A96 *deoR nupG* Φ80d*lacZ*ΔM15 Δ(*lacZYA-argF*) U169, *hsdR*17 ($r_K^-m_K^+$), λ-	(211)
E. coli BL21 [DE3]	F- *ompT hsdS*$_B$ (r_B^- m_B^-) gal dcm	Stratagene
PA14	Wild-type	(180)
PA14Δ*pqsE*	*pqsE* knockout mutant	Dr. Julia Gödeke (Twincore, Hannover)
PA14Δ*pqsR*	*pqsR* knockout mutant	(299)
PA14Δ*pchA-D*	*pchA-D* knockout mutant	Dr. Julia Gödeke (Twincore, Hannover)
Plasmids		
pUCP20	*Escherichia-Pseudomonas* shuttle vector with beta-lactamase (*bla*) and LacZ alpha peptide (*lacZ* alpha) genes, Amp^R/$Carb^R$	(213)
pUC20*pqsE*	pUCP20 containing PAO1 *pqsE*	(214)
pUCP20*rhlR*	pUCP20 containing PAO1 *rhlR*	Dr. Christian Pustelny (HZI)
pUCP20*rhlR*-GFP	pUCP20 containing 5' UTR + 20 codons of PA14 rhlR linked to gfpmut2	Dr. Julia Gödeke (Twincore, Hannover)
pME6032	pVS1-p15A shuttle expression vector, Tc^R	(215)
pME6032*pqsE*	pME6032 containing PAO1 pqsE	(133)
pET28a*pqsE*	pET28a containing PAO1 pqsE	(214)
pET28a*prmC*	pET28a containing PA14 pqsE	(221)

Protein purification

Both proteins PqsE and PrmC were purified as previously described (chapter 2), except using no DTT and 25 mM Tris-HCl and 150 mM NaCl pH 8.0 as buffer for PqsE. For enzyme activity assays, the proteins were adjusted to reaction conditions using Vivaspin® 4 Centrifugal Concentrator (Vivaproducts).

Preparation of concentrated P. aeruginosa PA14 metabolite extract

400 ml of LB was incoluated with PA14 and grown overnight at 37 °C and 180 rpm. After pelletation at 4 °C, culture supernatants were acidifed to a pH of ~2.0 using 30 ml of 1 N HCl. Metabolites were adsorbed from the acidified supernatants by stirring for 45 min with 10 g of XAD resin. After filtration, the metabolites were extracted from the XAD resin with sonication for 30 min in dichlormethane. Dichlormethane-soluble metabolites were evaporated to dryness under air, resuspended in 200 µl of methanol, and stored at -20 °C.

In vitro experiments with crude PA14 metabolite extracts

Prior to usage in the *in vitro* assay, PA14 extracts were serially diluted in the following order: (i) 1/5 in 80 % methanol, (ii) 1/5 in the reaction buffer [50 mM NaH_2PO_4 pH7.5], (iii) 1/16 in the reaction mixture with a final volume of 100 µl. The reaction mix contained purified PqsE and PrmC (negative control) using protein concentrations of 1, 2.5, and 5 µM. Samples were immediately transferred to a 96-well plate and fluorescence of the extracts was monitored at 37 °C under 320 nm excitation and 405 nm emission using an EnSpire Multimode Plate Reader (PerkinElmer).

Reporter rhlR-gfp fusion

To analyze post-transcriptional effects of PqsE on *rhlR* translation, Dr. Julia Gödeke constructed the vector pUCP20*rhlR-gfp* containing the 5' UTR and the fist 20 codons of *rhlR* linked to *gfp*mut2. This fragment was cloned in the opposite orientation to the *lac* promoter in pUCP20. The resulting plasmid pUCP20*rhlR-gfp* was transformed into a PA14Δ*pqsE* transposon mutant strain (180) harboring the empty vector pME6032, or pME6032*pqsE* respectively. *P. aeruginosa* cultures were grown in BM2 minimal medium supplemented with 1 mM IPTG at 37 °C and shaking at 180 rpm. At defined timepoints, 200 µl aliquots were transferred to a 96-well plate and fluorescence of GFP was measured using an EnSpire Multimode Plate Reader (PerkinElmer) under 488 nm excitation and 508 nm emmision.

Quantitative HPLC-MS analysis

Samples were mixed with an equal volume of dilute HCl solution (pH 3.0) and transferred onto a Strata-X 33u cartridge (polymeric reversed phase, 20 mg/ml). The cartridges were washed 3 – 4 times with 2 ml of dilute HCl solution (pH 3.0) under vacuum. After washing,

the metabolites were extracted using repetitive (3 – 4 times) elution with 2 ml ethyl acetate as organic solvent. The extracts were evaporized to dryness by means of a rotary evaporator and the residue was resuspended in 100 µl of 100 % methanol prior to HPLC-MS analysis.

All analyses were performed on Agilent 1260 Infinity Systems with diode array detector and C_{18} Acquity UPLC BEH column (2.1 × 50 mm, 1.7 µm) from Waters. Solvent A: H_2O + 0.1 % formic acid, solvent B: AcCN + 0.1 % formic acid, gradient system: 5 % B for 0.5 min increasing to 100 % B in 19.5 min, maintaining 100 % B for 5 min, flowrate = 0.6 ml/min, UV detection 200 − 600 nm. LC-MS spectra were recorded on an ion trap MS (amaZon speed™, Bruker) with an electrospray ionization source. Experiments were performed using positive and negative ionization modes.

Pyocyanin quantification

Pyocyanin levels were determined as previously described (chapter 2), using cell-free supernatants of *P. aeruginosa* cultures grown in BM2 minimal medium at 37 °C and 180 rpm.

Enzyme activity assay

Conversion of chorismate was monitored using a 10 mM stock of chorismate (Chorismic acid from *Enterobacter aerogenes* ≥80%, SIGMA-ALDRICH) solubilized in 1/10 deuterized dimethyl sulfoxide (DMSO-d 6)/reaction buffer [50 mM NaH_2PO_4 pH7.5]. The reaction mix contained 0.5 mM chorismate, 5 µM enzyme and 0.1 mM cofactor. Reactions were carried out at 37 °C in a thermocycler and aliquots of 50 µl were sampled at indicated timepoints. To measure the amount of prephenate produced in the samples, reactions were acidified with 25 µl of 1 N HCl, incubated for 15 min at 37 °C, and mixed with 175 µl of 2.5 N NaOH. For direct measurement of phenylpyruvate, the 50 µl aliquots were first diluted with 35 µl reaction buffer before being adjusted to an alkaline pH using 165 µl of 2.5 N NaOH. The samples (250 µl) were transferred to a 96-well plate and the absorbance was measured against a blank at 320 nm using an EnSpire Multimode Plate Reader (PerkinElmer).

Integrative –omics study

RNA- and Ribo-Seq data were generated as previously described (chapter 4). Bacterial cultures were grown to an OD_{600} of 3.0 in M9 minimal medium in the presence or absence of 5 mM phenylalanine.

Metabolome study

P. aeruginosa wild-type and mutants were cultivated in 50 ml BM2 medium with 0.01 % casamino acids in an erlenmeyer flask (37 °C, 160 rpm) until an OD_{600} of 1.5 (mid-exponential phase). 10 ml culture was transferred to a 50 ml falcon tube and centrifuged for 5 min (4 °C, 9000 G). The pellet was washed with 10 ml PBS and resuspended in 1 ml PBS to transfer the suspension in a 2 ml Eppendorf tube. After 5 min centrifugation (8000 rpm) the supernatant was removed and the residue stored at -70 °C. Metabolites were extracted with 1 ml cold (4 °C) methanol/water in the ratio 8/2 in an ice-cold ultrasonic bath (15 min). As internal standards 100 µg/ml trimethoprim and 100 µg/ml nortriptyline were spiked in the extraction solution. After centrifugation (20 min, 13000 rpm), 900 µl of the supernatant were dried using a speedvac and the residue was re-dissolved in 90 µl methanol/water 8/2 (with two spiked standards: caffeine and naproxen, 1 mg/ml). For an LC-MS analysis 1 µl was injected. For each condition (wild-type, knockout, complementant), 5 biological replicates were used (5 separate cultures) and of each culture two independent extractions were performed (2 technical replicates for each biological replicate) resulting in a total of 10 samples per condition.

Ultra high performance liquid chromatography was performed on a Dionex Ultimate 3000 UPLC by using a reverse-phase C_{18} column (Phenomenex Kinetex 1.7 µ C_{18}. 150 x 2.1 mm diameter column) with a flow rate of 300 µl/min. Water/acetonitrile was used as mobile phases with (a) water with 0.1 % formic acid, and (b) acetonitrile with 0.1 % formic acid. A linear gradient was used: 0 min: 1 % (b), 2 min: 1 % (b), 20 min: 100 % (b), 25 min: 100 % (b), 30 min: 1 % (b).

For untargeted profiling, samples were analyzed by electrospray ionization quadrupole time-of-flight mass spectrometry on a Bruker maXis HD QTof instrument.

Data were analyzed by using XCMSonline (324–327). Accurate masses were obtained by internal calibration using a sodium formiate cluster and lock mass calibration. Statistically significant regulated features were searched against metabolite databases (here: METLIN). Metabolite identifications was achieved by comparing the retention time and MS/MS fragmentation pattern of the metabolite of interest to that of a standard compound analyzed with identical conditions (except phenylpyruvate: here only a putative identification could be made by the exact mass).

6 General Discussion

The overall aim of the present study was to gain new insights into post-transcriptional regulation of virulence in the opportunistic nosocomial pathogen *P. aeruginosa*. As already discussed in detail in the chapters, we were able to identify previously unknown molecular mechanisms controlling the expression of important virulence determinants. Firstly, site-specific methylation of peptide chain release factors by the SAM-dependent methyltransferase PrmC was shown to be essential for the pathogenicity of *P. aeruginosa*. Methylation of a conserved GGQ motif of release factors had a global impact on gene expression of virulence determinants and enabled growth under anaerobic growth conditions, which caused attenuated virulence of a *prmC* mutant strain in a *G. mellonella* infection model. PrmC-mediated control of these processes could partially be explained by a reduced QS activity. The function and role of PrmC in pathogenicity has already been characterized in other bacteria (178, 179, 181, 182, 328), but the importance of this post-translational regulation mechanism was previously unknown for *P. aeruginosa*.

Secondly, we discovered an entirely novel post-transcriptional regulation mechanism in bacteria that is ubiquitous in eukaryotes - bacterial protein levels were found to be modulated via the production of different mRNA isoforms translated at variable efficiency. More precisely, the transcriptional regulator RhlR was proved to induce *pqsA* transcription from an alternative TSS, thus interfering with *pqs* signaling by forming a structure in the 5' UTR that restricts ribosome access to the SD element. We suggest that this regulatory QS cross-talk plays a central role in the delicate balance between *pqs* and *rhl* signaling in response to cell density and environmental stimuli.

Thirdly, we were able to shed light on the molecular activity of PqsE. By using a multi-methodological approach, we identified PqsE to possess a PheA-like enzymatic activity and to be involved in phenylalanine biosynthesis. Our data suggest that PqsE primarily diverts metabolic flux at the chorismate metabolic branch-point in aromatic biosynthesis. Evidently, phenylalanine catabolism is closely linked to phenazine production, and PqsE appears to exert control on the metabolic fate of phenylpyruvate and/or phenylalanine. Since PqsE activity is dependent on the downstream acting RhlR, there might exist a direct relation between phenylalanine catabolism and the activity of RhlR, a transcriptional regulator controlling the expression of multiple virulence factors. Like in *P. chlororaphis* (306), we suggest that in the presence of PqsE phenylpyruvate and/or phenylalanine might stimulate the production of

pyocyanin by increasing levels of the RhlR autoinducer C_4-HSL. Further, PqsE may represent a moonlighting protein whose iron centre specifically interacted with (bound to) PQS. This interaction could account for the negative autoregulatory role of PqsE. However, further analyses are needed to fully explore the molecular function of PqsE and to better understand the PqsE-triggered metabolic responses of *P. aeruginosa*.

Finally, we describe a protocol for Ribo-Seq, a new method that has great potential to be used to study translational regulation in *P. aeruginosa* on a genome-wide scale. Ribo-Seq is based on deep sequencing of ribosome-protected mRNA fragments generating a snapshot of the cellular translatome at a defined timepoint. Once optimized for cost-efficient high-throughput sequencing of multiplexed ribosomal footprints, this technique will allow reliable conclusions to be drawn from translational efficiency *in vivo*. Preliminary evidence has been provided that spatial patterns of ribosome occupancy on mRNAs can easily be determined using the established protocol. There is little doubt that Ribo-Seq will greatly improve our knowledge on the role of post-transcriptional regulation in the control of gene expression in *P. aeruginosa*. In addition, Ribo-Seq could find widespread application in assessing the mode of action of new antibacterial agents targeting the bacterial ribosome and/or translation, as recently shown for macrolides (241). It is equally conceivable that translational profiling will help to identify a number of novel coding elements in the *P. aeruginosa* genome, including micropeptide-encoding genes. Several hundred of these translated small ORFs have already previously been identified in vertebrates by using Ribo-Seq (329). As depicted in Fig. 6.1, it is planned to include Ribo-Seq routinely in mutlivariate data analysis of well-established –omic approaches to better understand genetic control and evolution of phenotypic plasticity in *P. aeruginosa*. Such an integrated approach might aid to determine functional properties of yet uncharacterized proteins.

With respect to the present thesis, footprinting of mRNA-ribosome complexes may also shed light on the alleged selective action of *P. aeruginosa* PrmC on translational read-through of virulence factor transcripts. Although PrmC affects translational termination efficiency, very few protein spots were found to be differentially expressed in a PA14Δ*prmC* transposon mutant - in spite of significant differences in gene expression. The surprisingly low level of correlation between protein and mRNA abundance, however, could be due to the comparably imprecise nature of 2D-PAGE. Ribo-Seq seems prefectly suited for the fine-scale mapping of genes affected by the loss of *prmC*. Footprint analysis in the C-terminal region of such genes

could reveal genetic features responsible for stop codon read-through. By using Ribo-Seq, Dunn and colleagues were the first to show that read-through is, in fact, an exquisitely regulated process in eukaryotes and only occurs in specific transcripts (330). It is particularly intersting to determine possible similarities and differences between prokaryotic and eukaryotic signals that trigger C-terminal extension by termination failure. Currently, there is still no clear empirical evidence why methylation of peptide chain release factors is so important for the virulence of bacterial pathogens.

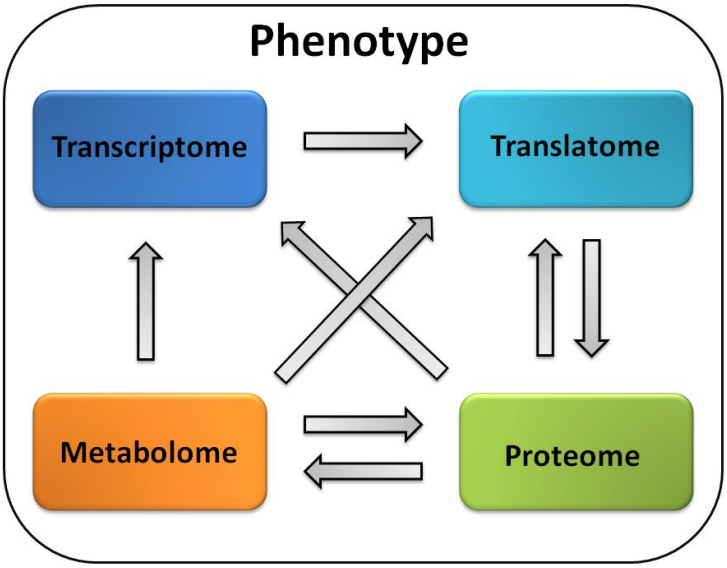

Figure 6.1: Global phenotypic characterization of *P. aeruginosa* by multi–omics analysis. The scheme illustrates the biological complexity and intertwined relationship of the four basic biochemical pillars of functional genomics. The influence of non-coding RNAs on phenotypic plasticity is not taken into account.

In conclusion, this thesis renders a significant contribution to the field of infection control in *P. aeruginosa*. We discovered novel regulatory mechanisms that control virulence factor production and, by establishing Ribo-Seq, we present a promising tool to gain deeper insight into the pathogenicity of this clinically relevant bacterial pathogen.

7 References

1. **Ozer EA, Allen JP, Hauser AR**. 2014. Characterization of the core and accessory genomes of *Pseudomonas aeruginosa* using bioinformatic tools Spine and AGEnt. BMC Genomics **15**:1–17.

2. **Kung VL, Ozer EA, Hauser AR**. 2010. The accessory genome of *Pseudomonas aeruginosa*. Microbiol. Mol. Biol. Rev. **74**:621–641.

3. **Stover CK, Pham XQ, Erwin AL, Mizoguchi SD, Warrener P, Hickey MJ, Brinkman FS, Hufnagle WO, Kowalik DJ, Lagrou M, Garber RL, Goltry L, Tolentino E, Westbrock-Wadman S, Yuan Y, Brody LL, Coulter SN, Folger KR, Kas A, Larbig K, Lim R, Smith K, Spencer D, Wong GK, Wu Z, Paulsen IT, Reizer J, Saier MH, Hancock RE, Lory S, Olson M V**. 2000. Complete genome sequence of *Pseudomonas aeruginosa* PAO1, an opportunistic pathogen. Nature **406**:959–964.

4. **Ramos GP, Rocha JL, Tuon FF**. 2013. Seasonal humidity may influence *Pseudomonas aeruginosa* hospital-acquired infection rates. Int. J. Infect. Dis. **17**.

5. **Koch C, Høiby N**. 2000. Diagnosis and treatment of cystic fibrosis. Respiration. **67**:239–247.

6. **Nair CG, Chao C, Ryall B, Williams HD**. 2013. Sub-lethal concentrations of antibiotics increase mutation frequency in the cystic fibrosis pathogen *Pseudomonas aeruginosa*. Lett. Appl. Microbiol. **56**:149–154.

7. **Fuqua WC, Winans SC, Greenberg EP**. 1994. Quorum sensing in bacteria: the LuxR-LuxI family of cell density-responsive transcriptional regulators. J. Bacteriol. **176**:269–275.

8. **Kropinski AMB, Lewis V, Berry D**. 1987. Effect of growth temperature on the lipids, outer membrane proteins, and lipopolysaccharides of *Pseudomonas aeruginosa* PAO. J. Bacteriol. **169**:1960–1966.

9. **Nishijyo T, Haas D, Itoh Y**. 2001. The CbrA-CbrB two-component regulatory system controls the utilization of multiple carbon and nitrogen sources in *Pseudomonas aeruginosa*. Mol. Microbiol. **40**:917–931.

10. **Line L, Alhede M, Kolpen M, KÃ¼hl M, Ciofu O, Bjarnsholt T, Moser C, Toyofuku M, Nomura N, HÃ¸iby N, Jensen PÃ**. 2014. Physiological levels of nitrate support anoxic growth by denitrification of *Pseudomonas aeruginosa* at growth rates reported in cystic fibrosis lungs and sputum. Front. Microbiol. **5**:1–11.

11. **Eschbach M, Schreiber K, Trunk K, Buer J, Jahn D, Schobert M**. 2004. Long-term anaerobic survival of the opportunistic pathogen *Pseudomonas aeruginosa* via pyruvate fermentation. J. Bacteriol. **186**:4596–4604.

12. **Schreiber K, Boes N, Eschbach M, Jaensch L, Wehland J, Bjarnsholt T, Givskov M, Hentzer M, Schobert M**. 2006. Anaerobic survival of *Pseudomonas aeruginosa* by pyruvate fermentation requires an Usp-type stress protein. J. Bacteriol. **188**:659–668.

13. **Mercenier A, Simon JP, Vander Wauven C, Haas D, Stalon V**. 1980. Regulation of enzyme synthesis in the arginine deiminase pathway of *Pseudomonas aeruginosa*. J. Bacteriol. **144**:159–163.

14. **Vander Wauven C, Piérard A, Kley-Raymann M, Haas D**. 1984. *Pseudomonas aeruginosa* mutants affected in anaerobic growth on arginine: evidence for a four-gene cluster encoding the arginine deiminase pathway. J. Bacteriol. **160**:928–934.

15. **Zimmermann A, Reimmann C, Galimand M, Haas D**. 1991. Anaerobic growth and cyanide synthesis of *Pseudomonas aeruginosa* depend on *anr*, a regulatory gene homologous with *fnr* of *Escherichia coli*. Mol. Microbiol. **5**:1483–1490.

16. **Benkert B, Quäck N, Schreiber K, Jaensch L, Jahn D, Schobert M**. 2008. Nitrate-responsive NarX-NarL represses arginine-mediated induction of the *Pseudomonas aeruginosa* arginine fermentation *arcDABC* operon. Microbiology **154**:3053–3060.

17. **Glasser NR, Kern SE, Newman DK**. 2014. Phenazine redox cycling enhances anaerobic survival in *Pseudomonas aeruginosa* by facilitating generation of ATP and a proton-motive force. Mol. Microbiol. **92**:399–412.

18. **Visca P, Imperi F, Lamont IL**. 2007. Pyoverdine siderophores: from biogenesis to biosignificance. Trends Microbiol. **15**:22-30.

19. **Sibley CD, Rabin H, Surette MG**. 2006. Cystic fibrosis: a polymicrobial infectious disease. Future Microbiol. **1**:53–61.

20. **Bradley DE**. 1980. A function of *Pseudomonas aeruginosa* PAO polar pili: twitching motility. Can. J. Microbiol. **26**:146–154.

21. **Whitchurch CB, Hobbs M, Livingston SP, Krishnapillai V, Mattick JS**. 1991. Characterisation of a *Pseudomonas aeruginosa* twitching motility gene and evidence for a specialised protein export system widespread in eubacteria. Gene **101**:33–44.

22. **Kohler T, Curty LK, Barja F, Van Delden C, Pechere JC**. 2000. Swarming of *Pseudomonas aeruginosa* is dependent on cell-to-cell signaling and requires flagella and pili. J. Bacteriol. **182**:5990–5996.

23. **Déziel E, Lépine F, Milot S, Villemur R**. 2003. *rhlA* is required for the production of a novel biosurfactant promoting swarming motility in *Pseudomonas aeruginosa*: 3-(3-hydroxyalkanoyloxy)alkanoic acids (HAAs), the precursors of rhamnolipids. Microbiology. **149**:2005-2013.

24. **Caiazza NC, Shanks RMQ, O'Toole GA**. 2005. Rhamnolipids modulate swarming motility patterns of *Pseudomonas aeruginosa*. J. Bacteriol. **187**:7351–7361.

25. **Arora SK, Ritchings BW, Almira EC, Lory S, Ramphal R**. 1998. The Pseudomonas aeruginosa flagellar cap protein, FliD, is responsible for mucin adhesion. Infect. Immun. **66**:1000–1007.

26. **O'Toole GA, Kolter R**. 1998. Flagellar and twitching motility are necessary for *Pseudomonas aeruginosa* biofilm development. Mol. Microbiol. **30**:295–304.

27. **Feldman M, Bryan R, Rajan S, Scheffler L, Brunnert S, Tang H, Prince A**. 1998. Role of flagella in pathogenesis of *Pseudomonas aeruginosa* pulmonary infection. Infect. Immun. **66**:43–51.

28. **Burrows LL**. 2012. Twitching Motility: Type IV Pili in Action. Annu. Rev. Microbiol. **66**:493-520.

29. **Conrad JC, Gibiansky ML, Jin F, Gordon VD, Motto DA, Mathewson MA, Stopka WG, Zelasko DC, Shrout JD, Wong GCL**. 2011. Flagella and pili-mediated near-surface single-cell motility mechanisms in *P. aeruginosa*. Biophys. J. **100**:1608–1616.

30. **Harshey RM**. 1994. Bees aren't the only ones: Swarming in gram-negative bacteria. Mol. Microbiol. **13**:389-394.

31. **Tremblay J, Déziel E**. 2010. Gene expression in *Pseudomonas aeruginosa* swarming motility. BMC Genomics **11**:587.

32. **Yeung ATY, Torfs ECW, Jamshidi F, Bains M, Wiegand I, Hancock REW, Overhage J**. 2009. Swarming of *Pseudomonas aeruginosa* is controlled by a broad spectrum of transcriptional regulators, including MetR. J. Bacteriol. **191**:5592–5602.

33. **Verstraeten N, Braeken K, Debkumari B, Fauvart M, Fransaer J, Vermant J, Michiels J**. 2008. Living on a surface: swarming and biofilm formation. Trends Microbiol. **16**:496-506.

34. **Henrici AT**. 1932. A direct microscopic technique. J. Bacteriol. 277–287.

35. **Heukelekian H, Heller a**. 1940. Relation between Food Concentration and Surface for Bacterial Growth. J. Bacteriol. **40**:547–558.

36. **Parsek MR, Tolker-Nielsen T**. 2008. Pattern formation in *Pseudomonas aeruginosa* biofilms. Curr. Opin. Microbiol. **11**:560-566.

37. **Klausen M, Gjermansen M, Kreft JU, Tolker-Nielsen T**. 2006. Dynamics of development and dispersal in sessile microbial communities: Examples from

Pseudomonas aeruginosa and *Pseudomonas putida* model biofilms. FEMS Microbiol. Lett. **261**:1-11.

38. **Aaron SD, Ferris W, Ramotar K, Vandemheen K, Chan F, Saginur R**. 2002. Single and combination antibiotic susceptibilities of planktonic, adherent, and biofilm-grown *Pseudomonas aeruginosa* isolates cultured from sputa of adults with cystic fibrosis. J. Clin. Microbiol. **40**:4172–4179.

39. **Drenkard E, Ausubel FM**. 2002. *Pseudomonas* biofilm formation and antibiotic resistance are linked to phenotypic variation. Nature **416**:740–743.

40. **Mah T-F, Pitts B, Pellock B, Walker GC, Stewart PS, O'Toole GA**. 2003. A genetic basis for *Pseudomonas aeruginosa* biofilm antibiotic resistance. Nature **426**:306–310.

41. **Hancock REW, Speert DP**. 2000. Antibiotic resistance in *Pseudomonas aeruginosa:* mechanisms and impact on treatment. Drug Resist. Updat. **3**:247–255.

42. **Lewis K**. 2010. Persister cells. Annu. Rev. Microbiol. **64**:357–372.

43. **Sauer K, Camper AK, Ehrlich GD, Costerton JW, Davies DG**. 2002. *Pseudomonas aeruginosa* displays multiple phenotypes during development as a biofilm. J. Bacteriol. **184**:1140–1154.

44. **Ma L, Conover M, Lu H, Parsek MR, Bayles K, Wozniak DJ**. 2009. Assembly and development of the *Pseudomonas aeruginosa* biofilm matrix. PLoS Pathog. **5**:e1000354.

45. **Davey ME, O'toole GA**. 2000. Microbial biofilms: from ecology to molecular genetics. Microbiol. Mol. Biol. Rev. **64**:847–867.

46. **Hentzer M, Eberl L, Givskov M**. 2005. Transcriptome analysis of *Pseudomonas aeruginosa* biofilm development: anaerobic respiration and iron limitation. Biofilms. **2**:37-61.

47. **Williamson KS, Richards LA, Perez-Osorio AC, Pitts B, McInnerney K, Stewart PS, Franklin MJ**. 2012. Heterogeneity in *Pseudomonas aeruginosa* biofilms includes expression of ribosome hibernation factors in the antibiotic-tolerant subpopulation and

hypoxia-induced stress response in the metabolically active population. J. Bacteriol. **194**:2062–2073.

48. **Kirisits MJ, Parsek MR**. 2006. Does *Pseudomonas aeruginosa* use intercellular signalling to build biofilm communities? Cell. Microbiol. **8**:1841-1849.

49. **Hengge R**. 2009. Principles of c-di-GMP signalling in bacteria. Nat. Rev. Microbiol. **7**:263–273.

50. **Müsken M, Di Fiore S, Dötsch A, Fischer R, Häussler S**. 2010. Genetic determinants of *Pseudomonas aeruginosa* biofilm establishment. Microbiology **156**:431–441.

51. **Wolcott R, Costerton JW, Raoult D, Cutler SJ**. 2013. The polymicrobial nature of biofilm infection. Clin. Microbiol. Infect. **19**:107-112.

52. **Venkataraman A, Rosenbaum MA, Werner JJ, Winans SC, Angenent LT**. 2014. Metabolite transfer with the fermentation product 2,3-butanediol enhances virulence by *Pseudomonas aeruginosa*. ISME J. **8**:1210–20.

53. **Davies D**. 2003. Understanding biofilm resistance to antibacterial agents. Nat. Rev. Drug Discov. **2**:114–122.

54. **König B, Jaeger KE, Sage AE, Vasil ML, König W**. 1996. Role of *Pseudomonas aeruginosa* lipase in inflammatory mediator release from human inflammatory effector cells (platelets, granulocytes, and monocytes). Infect. Immun. **64**:3252–3258.

55. **Leid JG, Willson CJ, Shirtliff ME, Hassett DJ, Parsek MR, Jeffers AK**. 2005. The exopolysaccharide alginate protects *Pseudomonas aeruginosa* biofilm bacteria from IFN-gamma-mediated macrophage killing. J. Immunol. **175**:7512–7518.

56. **Jensen PØ, Bjarnsholt T, Phipps R, Rasmussen TB, Calum H, Christoffersen L, Moser C, Williams P, Pressler T, Givskov M, Høiby N**. 2007. Rapid necrotic killing of polymorphonuclear leukocytes is caused by quorum-sensing-controlled production of rhamnolipid by *Pseudomonas aeruginosa*. Microbiology **153**:1329–1338.

57. **Alhede M, Bjarnsholt T, Jensen P, Phipps RK, Moser C, Christophersen L, Christensen LD, van Gennip M, Parsek M, Høiby N, Rasmussen TB, Givskov M**. 2009. *Pseudomonas aeruginosa* recognizes and responds aggressively to the presence of polymorphonuclear leukocytes. Microbiology **155**:3500–3508.

58. **Liu P V**. 1974. Extracellular toxins of *Pseudomonas aeruginosa*. J. Infect. Dis. **130 Suppl**:S94–S99.

59. **Berk RS, Brown D, Coutinho I, Meyers D**. 1987. In vivo studies with two phospholipase C fractions from *Pseudomonas aeruginosa*. Infect. Immun. **55**:1728–1730.

60. **Wozniak DJ, Hsu LY, Galloway DR**. 1988. His-426 of the *Pseudomonas aeruginosa* exotoxin A is required for ADP-ribosylation of elongation factor II. Proc. Natl. Acad. Sci. U. S. A. **85**:8880–8884.

61. **Armstrong S, Yates SP, Merrill AR**. 2002. Insight into the catalytic mechanism of *Pseudomonas aeruginosa* exotoxin A: Studies of toxin interaction with eukaryotic elongation factor-2. J. Biol. Chem. **277**:46669–46675.

62. **Barbieri JT, Sun J**. 2004. *Pseudomonas aeruginosa* ExoS and ExoT. Rev. Physiol. Biochem. Pharmacol. **152**:79–92.

63. **Yahr TL, Goranson J, Frank DW**. 1996. Exoenzyme S of *Pseudomonas aeruginosa* is secreted by a type III pathway. Mol. Microbiol. **22**:991–1003.

64. **Sato H, Frank DW, Hillard CJ, Feix JB, Pankhaniya RR, Moriyama K, Finck-Barbançon V, Buchaklian A, Lei M, Long RM, Wiener-Kronish J, Sawa T**. 2003. The mechanism of action of the *Pseudomonas aeruginosa*-encoded type III cytotoxin, ExoU. EMBO J. **22**:2959–2969.

65. **Goehring UM, Schmidt G, Pederson KJ, Aktories K, Barbieri JT**. 1999. The N-terminal domain of *Pseudomonas aeruginosa* exoenzyme S is a GTPase-activating protein for Rho GTPases. J. Biol. Chem. **274**:36369–36372.

66. **Krall R, Schmidt G, Aktories K, Barbieri JT**. 2000. *Pseudomonas aeruginosa* ExoT is a Rho GTPase-activating protein. Infect. Immun. **68**:6066–6068.

67. **Mavrodi D V, Blankenfeldt W, Thomashow LS**. 2006. Phenazine compounds in fluorescent *Pseudomonas spp*. biosynthesis and regulation. Annu. Rev. Phytopathol. **44**:417–445.

68. **Wilson R, Sykes DA, Watson D, Rutman A, Taylor GW, Cole PJ**. 1988. Measurement of *Pseudomonas aeruginosa* phenazine pigments in sputum and assessment of their contribution to sputum sol toxicity for respiratory epithelium. Infect. Immun. **56**:2515–2517.

69. **O'Malley YQ, Reszka KJ, Spitz DR, Denning GM, Britigan BE**. 2004. *Pseudomonas aeruginosa* pyocyanin directly oxidizes glutathione and decreases its levels in airway epithelial cells. Am. J. Physiol. Lung Cell. Mol. Physiol. **287**:L94–L103.

70. **Price-Whelan A, Dietrich LEP, Newman DK**. 2007. Pyocyanin alters redox homeostasis and carbon flux through central metabolic pathways in *Pseudomonas aeruginosa* PA14. J. Bacteriol. **189**:6372–6381.

71. **Blankenfeldt W, Parsons JF**. 2014. The structural biology of phenazine biosynthesis. Curr. Opin. Struct. Biol. **29**:26–33.

72. **Pierson LS, Pierson EA**. 2010. Metabolism and function of phenazines in bacteria: Impacts on the behavior of bacteria in the environment and biotechnological processes. Appl. Microbiol. Biotechnol. **86**:1659.1670.

73. **Mavrodi DV, Bonsall RF, Delaney SM, Soule MJ, Phillips G, Thomashow LS**. 2001. Functional analysis of genes for biosynthesis of pyocyanin and phenazine-1-carboxamide from *Pseudomonas aeruginosa* PAO1. J. Bacteriol. **183**:6454–6465.

74. **Recinos DA, Sekedat MD, Hernandez A, Cohen TS, Sakhtah H, Prince AS, Price-Whelan A, Dietrich LEP**. 2012. Redundant phenazine operons in *Pseudomonas aeruginosa* exhibit environment-dependent expression and differential roles in pathogenicity. Proc. Natl. Acad. Sci. U. S. A. **109**:19420–5.

75. **Lane JFA**. 1973. The logic of living systems: a history of heredity. English translation by Betty E. Spillman.Division of Penguin Books, Ltd.

76. **Engebrecht J, Nealson K, Silverman M**. 1983. Bacterial bioluminescence: isolation and genetic analysis of functions from *Vibrio fischeri*. Cell **32**:773–781.

77. **Mcfall-ngai MJ**. 1990. Crypsis in the pelagic environment. Integr. Comp. Biol. **30**:175–188.

78. **Schaefer AL, Val DL, Hanzelka BL, Cronan JE, Greenberg EP**. 1996. Generation of cell-to-cell signals in quorum sensing: acyl homoserine lactone synthase activity of a purified *Vibrio fischeri* LuxI protein. Proc. Natl. Acad. Sci. U. S. A. **93**:9505–9509.

79. **Parsek MR, Val DL, Hanzelka BL, Cronan JE, Greenberg EP**. 1999. Acyl homoserine-lactone quorum-sensing signal generation. Proc. Natl. Acad. Sci. U. S. A. **96**:4360–4365.

80. **Latifi A, Foglino M, Tanaka K, Williams P, Lazdunski A**. 1996. A hierarchical quorum-sensing cascade in *Pseudomonas aeruginosa* links the transcriptional activators LasR and RhlR (VsmR) to expression of the stationary-phase sigma factor RpoS. Mol. Microbiol. **21**:1137–1146.

81. **Schuster M, Greenberg EP**. 2006. A network of networks: quorum-sensing gene regulation in *Pseudomonas aeruginosa*. Int. J. Med. Microbiol. **296**:73–81.

82. **Medina G**. 2003. Transcriptional regulation of *Pseudomonas aeruginosa rhlR*, encoding a quorum-sensing regulatory protein. Microbiology **149**:3073–3081.

83. **Latifi A, Foglino M, Tanaka K, Williams P, Lazdunski A**. 1996. A hierarchical quorum-sensing cascade in *Pseudomonas aeruginosa* links the transcriptional activators LasR and RhIR (VsmR) to expression of the stationary-phase sigma factor RpoS. Mol. Microbiol. **21**:1137–1146.

84. **Schuster M, Greenberg EP**. 2006. A network of networks: Quorum-sensing gene regulation in *Pseudomonas aeruginosa*. Int. J. Med. Microbiol.

85. **Pearson J, Pesci E, Iglewski B**. 1997. Roles of *Pseudomonas aeruginosa las* and *rhl* quorum-sensing systems in control of elastase and rhamnolipid biosynthesis genes. J. Bacteriol. **179**:5756–5767.

86. **Williams P, Cámara M**. 2009. Quorum sensing and environmental adaptation in *Pseudomonas aeruginosa*: a tale of regulatory networks and multifunctional signal molecules. Curr. Opin. Microbiol. **12**:182–91.

87. **Nadal Jimenez P, Koch G, Thompson JA, Xavier KB, Cool RH, Quax WJ**. 2012. The multiple signaling systems regulating virulence in *Pseudomonas aeruginosa*. Microbiol. Mol. Biol. Rev. **76**:46-65.

88. **Albus AM, Pesci EC, Runyen-Janecky LJ, West SE, Iglewski BH**. 1997. Vfr controls quorum sensing in *Pseudomonas aeruginosa*. J. Bacteriol. **179**:3928–3935.

89. **Fuchs EL, Brutinel ED, Jones AK, Fulcher NB, Urbanowski ML, Yahr TL, Wolfgang MC**. 2010. The *Pseudomonas aeruginosa* Vfr regulator controls global virulence factor expression through cyclic AMP-dependent and -independent mechanisms. J. Bacteriol. **192**:3553–3564.

90. **Croda-García G, Grosso-Becerra V, Gonzalez-Valdez A, Servín-González L, Soberón-Chávez G**. 2011. Transcriptional regulation of *Pseudomonas aeruginosa rhlR*: Role of the CRP orthologue Vfr (virulence factor regulator) and quorum-sensing regulators LasR and RhlR. Microbiology **157**:2545–2555.

91. **Chugani SA, Whiteley M, Lee KM, D'Argenio D, Manoil C, Greenberg EP**. 2001. QscR, a modulator of quorum-sensing signal synthesis and virulence in *Pseudomonas aeruginosa*. Proc. Natl. Acad. Sci. U. S. A. **98**:2752–2757.

92. **Ledgham F, Ventre I, Soscia C, Foglino M, Sturgis JN, Lazdunski A**. 2003. Interactions of the quorum sensing regulator QscR: Interaction with itself and the other regulators of *Pseudomonas aeruginosa* LasR and RhlR. Mol. Microbiol. **48**:199–210.

93. **Chugani S, Greenberg EP**. 2014. An evolving perspective on the *Pseudomonas aeruginosa* orphan quorum sensing regulator QscR. Front. Cell. Infect. Microbiol. **4**:1–7.

94. **Oinuma KI, Greenberg EP**. 2011. Acyl-homoserine lactone binding to and stability of the orphan *Pseudomonas aeruginosa* quorum-sensing signal receptor QscR. J. Bacteriol. **193**:421–428.

95. **Liang H, Deng X, Ji Q, Sun F, Shen T, He C**. 2012. The *Pseudomonas aeruginosa* global regulator VqsR directly inhibits QscR to control quorum-sensing and virulence gene expression. J. Bacteriol. **194**:3098–3108.

96. **Dong YH, Zhang XF, Xu JL, Tan AT, Zhang LH**. 2005. VqsM, a novel AraC-type global regulator of quorum-sensing signalling and virulence in *Pseudomonas aeruginosa*. Mol. Microbiol. **58**:552–564.

97. **Liang H, Deng X, Li X, Ye Y, Wu M**. 2014. Molecular mechanisms of master regulator VqsM mediating quorum-sensing and antibiotic resistance in *Pseudomonas aeruginosa*. Nucleic Acids Res. **42**:10307–10320.

98. **Rampioni G, Bertani I, Zennaro E, Polticelli F, Venturi V, Leoni L**. 2006. The quorum-sensing negative regulator RsaL of *Pseudomonas aeruginosa* binds to the *lasI* promoter. J. Bacteriol. **188**:815–819.

99. **De Kievit T, Seed PC, Nezezon J, Passador L, Iglewski BH**. 1999. RsaL, a novel repressor of virulence gene expression in *Pseudomonas aeruginosa*. J. Bacteriol. **181**:2175–2184.

100. **Dieppois G, Ducret V, Caille O, Perron K**. 2012. The transcriptional regulator CzcR modulates antibiotic resistance and quorum sensing in *Pseudomonas aeruginosa*. PLoS One **7**:e0038148.

101. **Castang S, McManus HR, Turner KH, Dove SL**. 2008. H-NS family members function coordinately in an opportunistic pathogen. Proc. Natl. Acad. Sci. U. S. A. **105**:18947–18952.

102. **Fan H, Dong Y, Wu D, Bowler MW, Zhang L, Song H**. 2013. QsIA disrupts LasR dimerization in antiactivation of bacterial quorum sensing. Proc. Natl. Acad. Sci. U. S. A. **110**:20765–70.

103. **Siehnel R, Traxler B, An DD, Parsek MR, Schaefer AL, Singh PK**. 2010. A unique regulator controls the activation threshold of quorum-regulated genes in *Pseudomonas aeruginosa*. Proc. Natl. Acad. Sci. U. S. A. **107**:7916–7921.

104. **Köhler T, Ouertatani-Sakouhi H, Cosson P, Van Delden C**. 2014. QsrO a novel regulator of quorum-sensing and virulence in *Pseudomonas aeruginosa*. PLoS One **9**:e0087814.

105. **Pesci EC, Milbank JB, Pearson JP, McKnight S, Kende AS, Greenberg EP, Iglewski BH**. 1999. Quinolone signaling in the cell-to-cell communication system of *Pseudomonas aeruginosa*. Proc. Natl. Acad. Sci. U. S. A. **96**:11229–11234.

106. **Gallagher L a, McKnight SL, Kuznetsova MS, Pesci EC, Manoil C**. 2002. Functions required for extracellular quinolone signaling by *Pseudomonas aeruginosa*. J. Bacteriol. **184**:6472–6480.

107. **Cao H, Krishnan G, Goumnerov B, Tsongalis J, Tompkins R, Rahme LG**. 2001. A quorum sensing-associated virulence gene of *Pseudomonas aeruginosa* encodes a LysR-like transcription regulator with a unique self-regulatory mechanism. Proc. Natl. Acad. Sci. U. S. A. **98**:14613–14618.

108. **McGrath S, Wade DS, Pesci EC**. 2004. Dueling quorum sensing systems in *Pseudomonas aeruginosa* control the production of the *Pseudomonas* quinolone signal (PQS). FEMS Microbiol. Lett. **230**:27–34.

109. **Xiao G, Déziel E, He J, Lépine F, Lesic B, Castonguay M-H, Milot S, Tampakaki AP, Stachel SE, Rahme LG**. 2006. MvfR, a key *Pseudomonas aeruginosa* pathogenicity LTTR-class regulatory protein, has dual ligands. Mol. Microbiol. **62**:1689–1699.

110. **Diggle SP, Lumjiaktase P, Dipilato F, Winzer K, Kunakorn M, Barrett DA, Chhabra SR, Cámara M, Williams P**. 2006. Functional genetic analysis reveals a 2-Alkyl-4-quinolone signaling system in the human pathogen *Burkholderia pseudomallei* and related bacteria. Chem. Biol. **13**:701–710.

111. **Diggle SP, Winzer K, Chhabra SR, Worrall KE, Cámara M, Williams P**. 2003. The *Pseudomonas aeruginosa* quinolone signal molecule overcomes the cell density-dependency of the quorum sensing hierarchy, regulates *rhl*-dependent genes at the onset of stationary phase and can be produced in the absence of LasR. Mol. Microbiol. **50**:29–43.

112. **Häussler S, Becker T**. 2008. The *Pseudomonas* quinolone signal (PQS) balances life and death in *Pseudomonas aeruginosa* populations. PLoS Pathog. **4**:e1000166.

113. **Lépine F, Milot S, Déziel E, He J, Rahme LG**. 2004. Electrospray/mass spectrometric identification and analysis of 4-hydroxy-2-alkylquinolines (HAQs) produced by *Pseudomonas aeruginosa*. J. Am. Soc. Mass Spectrom. **15**:862–9.

114. **Coleman JP, Hudson LL, McKnight SL, Farrow JM, Calfee MW, Lindsey CA, Pesci EC**. 2008. *Pseudomonas aeruginosa* PqsA is an anthranilate-coenzyme A ligase. J. Bacteriol. **190**:1247–1255.

115. **Farrow JM, Pesci EC**. 2007. Two distinct pathways supply anthranilate as a precursor of the *Pseudomonas* quinolone signal. J. Bacteriol. **189**:3425–3433.

116. **Calfee MW, Coleman JP, Pesci EC**. 2001. Interference with *Pseudomonas* quinolone signal synthesis inhibits virulence factor expression by *Pseudomonas aeruginosa*. Proc. Natl. Acad. Sci. U. S. A. **98**:11633–11637.

117. **Bredenbruch F, Nimtz M, Wray V, Morr M, Müller R, Häussler S**. 2005. Biosynthetic pathway of *Pseudomonas aeruginosa* 4-hydroxy-2-alkylquinolines. J. Bacteriol. **187**:3630–3635.

118. **Bera AK, Atanasova V, Robinson H, Eisenstein E, Coleman JP, Pesci EC, Parsons JF**. 2009. Structure of PqsD, a *Pseudomonas* quinolone signal biosynthetic enzyme, in complex with anthranilate. Biochemistry **48**:8644–8655.

119. **Déziel E, Lépine F, Milot S, He J, Mindrinos MN, Tompkins RG, Rahme LG**. 2004. Analysis of *Pseudomonas aeruginosa* 4-hydroxy-2-alkylquinolines (HAQs) reveals a role for 4-hydroxy-2-heptylquinoline in cell-to-cell communication. Proc. Natl. Acad. Sci. U. S. A. **101**:1339–1344.

120. **Schertzer JW, Brown SA, Whiteley M**. 2010. Oxygen levels rapidly modulate *Pseudomonas aeruginosa* social behaviours via substrate limitation of PqsH. Mol. Microbiol. **77**:1527–1538.

121. **Wade DS, Calfee MW, Rocha ER, Ling E a, Engstrom E, Coleman JP, Pesci EC**. 2005. Regulation of *Pseudomonas* quinolone signal synthesis in *Pseudomonas aeruginosa*. J. Bacteriol. **187**:4372–4380.

122. **Lamarche MG, Déziel E**. 2011. MexEF-oprN efflux pump exports the *Pseudomonas* quinolone signal (PQS) precursor HHQ (4-hydroxy-2-heptylquinoline). PLoS One **6**:e0024310.

123. **Mashburn LM, Whiteley M**. 2005. Membrane vesicles traffic signals and facilitate group activities in a prokaryote. Nature **437**:422–425.

124. **Mashburn-Warren L, Howe J, Garidel P, Richter W, Steiniger F, Roessle M, Brandenburg K, Whiteley M**. 2008. Interaction of quorum signals with outer membrane lipids: Insights into prokaryotic membrane vesicle formation. Mol. Microbiol. **69**:491–502.

125. **Diggle SP, Matthijs S, Wright VJ, Fletcher MP, Chhabra SR, Lamont IL, Kong X, Hider RC, Cornelis P, Cámara M, Williams P**. 2007. The *Pseudomonas aeruginosa* 4-quinolone signal molecules HHQ and PQS play multifunctional roles in quorum sensing and iron entrapment. Chem. Biol. **14**:87–96.

126. **Bredenbruch F, Geffers R, Nimtz M, Buer J, Häussler S**. 2006. The *Pseudomonas aeruginosa* quinolone signal (PQS) has an iron-chelating activity. Environ. Microbiol. **8**:1318–29.

127. **Allesen-Holm M, Barken KB, Yang L, Klausen M, Webb JS, Kjelleberg S, Molin S, Givskov M, Tolker-Nielsen T**. 2006. A characterization of DNA release in *Pseudomonas aeruginosa* cultures and biofilms. Mol. Microbiol. **59**:1114–28.

128. **Hooi DSW, Bycroft BW, Chhabra SR, Williams P, Pritchard DI**. 2004. Differential immune modulatory activity of *Pseudomonas aeruginosa* quorum-sensing signal molecules. Infect. Immun. **72**:6463–6470.

129. **Xiao G, He J, Rahme LG**. 2006. Mutation analysis of the *Pseudomonas aeruginosa mvfR* and *pqsABCDE* gene promoters demonstrates complex quorum-sensing circuitry. Microbiology **152**:1679–1686.

130. **McKnight SL, Iglewski BH, Pesci EC**. 2000. The *Pseudomonas* quinolone signal regulates rhl quorum sensing in *Pseudomonas aeruginosa*. J. Bacteriol. **182**:2702–2708.

131. **Calfee MW, Shelton JG, McCubrey JA, Pesci EC**. 2005. Solubility and bioactivity of the *Pseudomonas* quinolone signal are increased by a *Pseudomonas aeruginosa*-produced surfactant. Infect. Immun. **73**:878–882.

132. **Farrow JM, Sund ZM, Ellison ML, Wade DS, Coleman JP, Pesci EC**. 2008. PqsE functions independently of PqsR-*Pseudomonas* quinolone signal and enhances the *rhl* quorum-sensing system. J. Bacteriol. **190**:7043–7051.

133. **Rampioni G, Pustelny C, Fletcher MP, Wright VJ, Bruce M, Rumbaugh KP, Heeb S, Cámara M, Williams P**. 2010. Transcriptomic analysis reveals a global alkyl-quinolone-independent regulatory role for PqsE in facilitating the environmental adaptation of *Pseudomonas aeruginosa* to plant and animal hosts. Environ. Microbiol. **12**:1659–1673.

134. **Hazan R, He J, Xiao G, Dekimpe V, Apidianakis Y, Lesic B, Astrakas C, Déziel E, Lépine F, Rahme LG**. 2010. Homeostatic interplay between bacterial cell-cell signaling and iron in virulence. PLoS Pathog. **6**:e1000810.

135. **Picard F, Dressaire C, Girbal L, Cocaign-Bousquet M**. 2009. Examination of post-transcriptional regulations in prokaryotes by integrative biology. Comptes Rendus - Biol.

136. **Arraiano CM, Maquat LE**. 2003. Post-transcriptional control of gene expression: Effectors of mRNA decay. Mol. Microbiol. **49**:267–276.

137. **Kozak M**. 2005. Regulation of translation via mRNA structure in prokaryotes and eukaryotes. Gene **361**:13–37.

138. **Geissmann T, Marzi S, Romby P**. 2009. The role of mRNA structure in translational control in bacteria. RNA Biol. **6**:153–160.

139. **Winkler WC, Breaker RR**. 2005. Regulation of bacterial gene expression by riboswitches. Annu. Rev. Microbiol. **59**:487–517.

140. **De Smit MH, van Duin J**. 1990. Secondary structure of the ribosome binding site determines translational efficiency: a quantitative analysis. Proc. Natl. Acad. Sci. U. S. A. **87**:7668–72.

141. **Kortmann J, Narberhaus F**. 2012. Bacterial RNA thermometers: molecular zippers and switches. Nat. Rev. Microbiol. **10**:255–65.

142. **Krajewski SS, Nagel M, Narberhaus F**. 2013. Short ROSE-like RNA thermometers control IbpA synthesis in *Pseudomonas* species. PLoS One **8**:e65168.

143. **Zielinski NA, Maharaj R, Roychoudhury S, Danganan CE, Hendrickson W, Chakrabarty AM**. 1992. Alginate synthesis in *Pseudomonas aeruginosa*: Environmental regulation of the *algC* promoter. J. Bacteriol. **174**:7680–7688.

144. **Fujiwara S, Chakrabarty AM**. 1994. Post-transcriptional regulation of the *Pseudomonas aeruginosa algC* gene. Gene **146**:1–5.

145. **Irie Y, Starkey M, Edwards AN, Wozniak DJ, Romeo T, Parsek MR**. 2010. *Pseudomonas aeruginosa* biofilm matrix polysaccharide Psl is regulated transcriptionally by RpoS and post-transcriptionally by RsmA. Mol. Microbiol. **78**:158–172.

146. **O'Toole GA, Gibbs KA, Hager PW, Phibbs P V., Kolter R**. 2000. The global carbon metabolism regulator Crc is a component of a signal transduction pathway required for biofilm development by *Pseudomonas aeruginosa*. J. Bacteriol. **182**:425–431.

147. **Linares JF, Moreno R, Fajardo A, Martínez-Solano L, Escalante R, Rojo F, Martínez JL**. 2010. The global regulator Crc modulates metabolism, susceptibility to

antibiotics and virulence in *Pseudomonas aeruginosa*. Environ. Microbiol. **12**:3196–3212.

148. **Milojevic T, Grishkovskaya I, Sonnleitner E, Djinovic-Carugo K, Bläsi U**. 2013. The *Pseudomonas aeruginosa* catabolite repression control protein Crc is devoid of RNA binding activity. PLoS One **8**:e0064609.

149. **Brumlik MJ, Storey DG**. 1998. Post-transcriptional control of *Pseudomonas aeruginosa lasB* expression involves the 5' untranslated region of the mRNA. FEMS Microbiol. Lett. **159**:233–239.

150. **Yu H, He X, Xie W, Xiong J, Sheng H, Guo S, Huang C, Zhang D, Zhang K**. 2014. Elastase LasB of *Pseudomonas aeruginosa* promotes biofilm formation partly through rhamnolipid-mediated regulation. Can. J. Microbiol. **60**:227–35.

151. **Balasubramanian D, Vanderpool CK**. 2013. New developments in post-transcriptional regulation of operons by small RNAs. RNA Biol. **10**:337–41.

152. **Livny J, Brencic A, Lory S, Waldor MK**. 2006. Identification of 17 *Pseudomonas aeruginosa* sRNAs and prediction of sRNA-encoding genes in 10 diverse pathogens using the bioinformatic tool sRNAPredict2. Nucleic Acids Res. **34**:3484–3493.

153. **Sonnleitner E, Sorger-Domenigg T, Madej MJ, Findeiss S, Hackermüller J, Hüttenhofer A, Stadler PF, Bläsi U, Moll I**. 2008. Detection of small RNAs in *Pseudomonas aeruginosa* by RNomics and structure-based bioinformatic tools. Microbiology **154**:3175–3187.

154. **Ferrara S, Brugnoli M, de Bonis A, Righetti F, Delvillani F, Dehò G, Horner D, Briani F, Bertoni G**. 2012. Comparative profiling of *Pseudomonas aeruginosa* strains reveals differential expression of novel unique and conserved small RNAs. PLoS One **7**:e0036553.

155. **Gómez-Lozano M, Marvig RL, Molin S, Long KS**. 2012. Genome-wide identification of novel small RNAs in *Pseudomonas aeruginosa*. Environ. Microbiol. **14**:2006–2016.

156. **Sonnleitner E, Romeo A, Bläsi U**. 2012. Small regulatory RNAs in *Pseudomonas aeruginosa*. RNA Biol.

157. **Sonnleitner E, Abdou L, Haas D**. 2009. Small RNA as global regulator of carbon catabolite repression in *Pseudomonas aeruginosa*. Proc. Natl. Acad. Sci. U. S. A. **106**:21866–21871.

158. **Deutscher J**. 2008. The mechanisms of carbon catabolite repression in bacteria. Curr. Opin. Microbiol. **11**:87-93.

159. **Görke B, Stülke J**. 2008. Carbon catabolite repression in bacteria: many ways to make the most out of nutrients. Nat. Rev. Microbiol. **6**:613–624.

160. **Sonnleitner E, Bläsi U**. 2014. Regulation of Hfq by the RNA CrcZ in *Pseudomonas aeruginosa* carbon catabolite repression. PLoS Genet. **10**:e1004440.

161. **Lapouge K, Schubert M, Allain FH-T, Haas D**. 2008. Gac/Rsm signal transduction pathway of gamma-proteobacteria: from RNA recognition to regulation of social behaviour. Mol. Microbiol. **67**:241–253.

162. **Pessi G, Williams F, Hindle Z, Heurlier K, Holden MT, Cámara M, Haas D, Williams P**. 2001. The global posttranscriptional regulator RsmA modulates production of virulence determinants and N-acylhomoserine lactones in *Pseudomonas aeruginosa*. J. Bacteriol. **183**:6676–6683.

163. **Heurlier K, Williams F, Heeb S, Dormond C, Pessi G, Singer D, Cámara M, Williams P, Haas D**. 2004. Positive control of swarming, rhamnolipid synthesis, and lipase production by the posttranscriptional RsmA/RsmZ system in *Pseudomonas aeruginosa* PAO1. J. Bacteriol. **186**:2936–2945.

164. **Sonnleitner E, Gonzalez N, Sorger-Domenigg T, Heeb S, Richter AS, Backofen R, Williams P, Hüttenhofer A, Haas D, Bläsi U**. 2011. The small RNA PhrS stimulates synthesis of the *Pseudomonas aeruginosa* quinolone signal. Mol. Microbiol. **80**:868–885.

165. **Wilderman PJ, Sowa N a, FitzGerald DJ, FitzGerald PC, Gottesman S, Ochsner UA, Vasil ML**. 2004. Identification of tandem duplicate regulatory small RNAs in *Pseudomonas aeruginosa* involved in iron homeostasis. Proc. Natl. Acad. Sci. U. S. A. **101**:9792–7.

166. **Oglesby AG, Farrow JM, Lee JH, Tomaras AP, Greenberg EP, Pesci EC, Vasil ML**. 2008. The influence of iron on *Pseudomonas aeruginosa* physiology: A regulatory link between iron and quorum sensing. J. Biol. Chem. **283**:15558–15567.

167. **Oglesby-Sherrouse AG, Vasil ML**. 2010. Characterization of a heme-regulated non-coding RNA encoded by the prrf locus of *Pseudomonas aeruginosa*. PLoS One **5**.

168. **Ferrara S, Carloni S, Fulco R, Falcone M, Macchi R, Bertoni G**. 2015. Post-transcriptional regulation of the virulence-associated enzyme AlgC by the σ 22 -dependent small RNA ErsA of *Pseudomonas aeruginosa*. Environ. Microbiol. **17**:199–214.

169. **Tipton KA., Coleman JP, Pesci EC**. 2015. Post-transcriptional regulation of gene PA5507 controls *Pseudomonas* quinolone signal concentration in *P. aeruginosa*. Mol. Microbiol. doi:10.1111/mmi.12963.

170. **Tipton KA, Coleman JP, Pesci EC**. 2013. QapR (PA5506) represses an operon that negatively affects the *Pseudomonas* quinolone signal in *Pseudomonas aeruginosa*. J. Bacteriol. **195**:3433–3411.

171. **Grosso-Becerra M V., Croda-Garcia G, Merino E, Servin-Gonzalez L, Mojica-Espinosa R, Soberon-Chavez G**. 2014. Regulation of *Pseudomonas aeruginosa* virulence factors by two novel RNA thermometers. Proc. Natl. Acad. Sci. **111**:15562–15567.

172. **Gupta R, Gobble TR, Schuster M**. 2009. GidA posttranscriptionally regulates *rhl* quorum sensing in *Pseudomonas aeruginosa*. J. Bacteriol. **191**:5785–5792.

173. **Yang N, Ding S, Chen F, Zhang X, Xia Y, Di H, Cao Q, Deng X, Wu M, Wong CCL, Tian X-X, Yang C-G, Zhao J, Lan L**. 2015. The Crc protein participates in

down-regulation of the *lon* gene to promote rhamnolipid production and *rhl* quorum sensing in *Pseudomonas aeruginosa*. Mol. Microbiol. doi:10.1111/mmi.12954.

174. **Jude F, Köhler T, Branny P, Perron K, Mayer MP, Comte R, Van Delden C**. 2003. Posttranscriptional control of quorum-sensing-dependent virulence genes by DksA in *Pseudomonas aeruginosa*. J. Bacteriol. **185**:3558–3566.

175. **Ingolia NT, Ghaemmaghami S, Newman JRS, Weissman JS**. 2009. Genome-wide analysis in vivo of translation with nucleotide resolution using ribosome profiling. Science **324**:218–223.

176. **Heurgué-Hamard V, Champ S, Engström Å, Ehrenberg M, Buckingham RH**. 2002. The *hemK* gene in *Escherichia coli* encodes the N5-glutamine methyltransferase that modifies peptide release factors. EMBO J. **21**:769–778.

177. **Nakahigashi K, Kubo N, Narita S, Shimaoka T, Goto S, Oshima T, Mori H, Maeda M, Wada C, Inokuchi H**. 2002. HemK, a class of protein methyl transferase with similarity to DNA methyl transferases, methylates polypeptide chain release factors, and *hemK* knockout induces defects in translational termination. Proc. Natl. Acad. Sci. U. S. A. **99**:1473–1478.

178. **Park Y, Yilmaz O, Jung I-Y, Lamont RJ**. 2004. Identification of *Porphyromonas gingivalis* genes specifically expressed in human gingival epithelial cells by using differential display reverse transcription-PCR. Infect. Immun. **72**:3752–3758.

179. **John M, Kudva IT, Griffin RW, Dodson AW, McManus B, Krastins B, Sarracino D, Progulske-Fox A, Hillman JD, Handfield M, Tarr PI, Calderwood SB**. 2005. Use of in vivo-induced antigen technology for identification of *Escherichia coli* O157:H7 proteins expressed during human infection. Infect. Immun. **73**:2665–2679.

180. **Liberati NT, Urbach JM, Miyata S, Lee DG, Drenkard E, Wu G, Villanueva J, Wei T, Ausubel FM**. 2006. An ordered, nonredundant library of *Pseudomonas aeruginosa* strain PA14 transposon insertion mutants. Proc. Natl. Acad. Sci. U. S. A. **103**:2833–8.

181. **Pannekoek Y, Heurgué-Hamard V, Langerak AAJ, Speijer D, Buckingham RH, Van Der Ende A**. 2005. The N5-glutamine S-adenosyl-L-methionine-dependent methyltransferase PrmC/HemK in *Chlamydia trachomatis* methylates class 1 release factors. J. Bacteriol. **187**:507–511.

182. **Garbom S, Olofsson M, Björnfot AC, Srivastava K, Robinson VL, Oyston PCF, Titball RW, Wolf-Watz H**. 2007. Phenotypic characterization of a virulence-associated protein, VagH, of *Yersinia pseudotuberculosis* reveals a tight link between VagH and the type III secretion system. Microbiology **153**:1464–1473.

183. **Dötsch A, Eckweiler D, Schniederjans M, Zimmermann A, Jensen V, Scharfe M, Geffers R, Häussler S**. 2012. The *Pseudomonas aeruginosa* transcriptome in planktonic cultures and static biofilms using RNA sequencing. PLoS One **7**:e31092.

184. **Cox CD**. 1980. Iron uptake with ferripyochelin and ferric citrate by *Pseudomonas aeruginosa*. J. Bacteriol. **142**:581–587.

185. **Ankenbauer RG, Quan HN**. 1994. FptA, the Fe(III)-pyochelin receptor of *Pseudomonas aeruginosa*: A phenolate siderophore receptor homologous to hydroxamate siderophore receptors. J. Bacteriol. **176**:307–319.

186. **Braun V**. 2001. Iron uptake mechanisms and their regulation in pathogenic bacteria. Int. J. Med. Microbiol. **291**:67–79.

187. **Folders J, Algra J, Roelofs MS, Van Loon LC, Tommassen J, Bitter W**. 2001. Characterization of *Pseudomonas aeruginosa* chitinase, a gradually secreted protein. J. Bacteriol. **183**:7044–7052.

188. **Arai H, Mizutani M, Igarashi Y**. 2003. Transcriptional regulation of the *nos* genes for nitrous oxide reductase in *Pseudomonas aeruginosa*. Microbiology. **149**:29-36.

189. **Aedekerk S, Diggle SP, Song Z, Høiby N, Cornelis P, Williams P, Cámara M**. 2005. The MexGHI-OpmD multidrug efflux pump controls growth, antibiotic susceptibility and virulence in *Pseudomonas aeruginosa* via 4-quinolone-dependent cell-to-cell communication. Microbiology **151**:1113–1125.

190. **Zumft WG, Kroneck PMH**. 2006. Respiratory transformation of nitrous oxide (N_2O) to dinitrogen by bacteria and archaea. Adv. Microb. Physiol. **52**:107-227.

191. **Engel J, Balachandran P**. 2009. Role of *Pseudomonas aeruginosa* type III effectors in disease. Curr. Opin. Microbiol. **12**:61-66.

192. **Hauser AR**. 2009. The type III secretion system of *Pseudomonas aeruginosa*: infection by injection. Nat. Rev. Microbiol. **7**:654–665.

193. **Winsor GL, Lam DKW, Fleming L, Lo R, Whiteside MD, Yu NY, Hancock REW, Brinkman FSL**. 2011. *Pseudomonas* Genome Database: Improved comparative analysis and population genomics capability for *Pseudomonas* genomes. Nucleic Acids Res. **39**. doi: 10.1093/nar/gkq869.

194. **Gething MJ, Sambrook J**. 1992. Protein folding in the cell. Nature **355**:33–45.

195. **Ochsner UA, Koch AK, Fiechter A, Reiser J**. 1994. Isolation and characterization of a regulatory gene affecting rhamnolipid biosurfactant synthesis in *Pseudomonas aeruginosa*. J. Bacteriol. **176**:2044–2054.

196. **Ochsner UA, Reiser J**. 1995. Autoinducer-mediated regulation of rhamnolipid biosurfactant synthesis in *Pseudomonas aeruginosa*. Proc. Natl. Acad. Sci. U. S. A. **92**:6424–6428.

197. **Glessner A, Smith RS, Iglewski BH, Robinson JB**. 1999. Roles of *Pseudomonas aeruginosa las* and *rhl* quorum-sensing systems in control of twitching motility. J. Bacteriol. **181**:1623–1629.

198. **Webb JS, Thompson LS, James S, Charlton T, Tolker-Nielsen T, Koch B, Givskov M, Kjelleberg S**. 2003. Cell death in *Pseudomonas aeruginosa* biofilm development. J. Bacteriol. **185**:4585–4592.

199. **Jander G, Rahme LG, Ausubel FM**. 2000. Positive correlation between virulence of *Pseudomonas aeruginosa* mutants in mice and insects. J. Bacteriol. **182**:3843–3845.

200. **Fedhila S, Daou N, Lereclus D, Nielsen-LeRoux C**. 2006. Identification of *Bacillus cereus* internalin and other candidate virulence genes specifically induced during oral infection in insects. Mol. Microbiol. **62**:339–355.

201. **Bergin D, Murphy L, Keenan J, Clynes M, Kavanagh K**. 2006. Pre-exposure to yeast protects larvae of *Galleria mellonella* from a subsequent lethal infection by *Candida albicans* and is mediated by the increased expression of antimicrobial peptides. Microbes Infect. **8**:2105–2112.

202. **Mylonakis E, Moreno R, El Khoury JB, Idnurm A, Heitman J, Calderwood SB, Ausubel FM, Diener A**. 2005. *Galleria mellonella* as a model system to study *Cryptococcus neoformans* pathogenesis. Infect. Immun. **73**:3842–3850.

203. **Shin YP, Kyoung MK, Joon HL, Sook JS, In HL**. 2007. Extracellular gelatinase of *Enterococcus faecalis* destroys a defense system in insect hemolymph and human serum. Infect. Immun. **75**:1861–1869.

204. **Aperis G, Burgwyn Fuchs B, Anderson CA, Warner JE, Calderwood SB, Mylonakis E**. 2007. *Galleria mellonella* as a model host to study infection by the *Francisella tularensis* live vaccine strain. Microbes Infect. **9**:729–734.

205. **Mukherjee K, Altincicek B, Hain T, Domann E, Vilcinskas A, Chakraborty T**. 2010. *Galleria mellonella* as a model system for studying *Listeria* pathogenesis. Appl. Environ. Microbiol. **76**:310–317.

206. **García-Lara J, Needham AJ, Foster SJ**. 2005. Invertebrates as animal models for *Staphylococcus aureus* pathogenesis: A window into host-pathogen interaction. FEMS Immunol. Med. Microbiol. **43**:311-323.

207. **Champion OL, Cooper IAM, James SL, Ford D, Karlyshev A, Wren BW, Duffield M, Oyston PCF, Titball RW**. 2009. *Galleria mellonella* as an alternative infection model for *Yersinia pseudotuberculosis*. Microbiology **155**:1516–1522.

208. **Miyata S, Casey M, Frank DW, Ausubel FM, Drenkard E**. 2003. Use of the *Galleria mellonella* caterpillar as a model host to study the role of the type III secretion system in *Pseudomonas aeruginosa* pathogenesis. Infect. Immun. **71**:2404–2413.

209. **Polevoda B, Span L, Sherman F**. 2006. The yeast translation release factors Mrf1p and Sup45p (eRF1) are methylated, respectively, by the methyltransferases Mtq1p and Mtq2p. J. Biol. Chem. **281**:2562–2571.

210. **Figaro S, Scrima N, Buckingham RH, Heurgué-Hamard V**. 2008. HemK2 protein, encoded on human chromosome 21, methylates translation termination factor eRF1. FEBS Lett. **582**:2352–2356.

211. **Woodcock DM, Crowther PJ, Doherty J, Jefferson S, DeCruz E, Noyer-Weidner M, Smith SS, Michael MZ, Graham MW**. 1989. Quantitative evaluation of *Escherichia coli* host strains for tolerance to cytosine methylation in plasmid and phage recombinants. Nucleic Acids Res. **17**:3469–3478.

212. **Altman, S., Brenner, S., and Smith JD**. 1971. Identification of an Ochre-suppressing Anticodon 195–197.

213. **West SEH, Schweizer HP, Dall C, Sample AK, Runyen-Janecky LJ**. 1994. Construction of improved *Escherichia-Pseudomonas* shuttle vectors derived from pUC18/19 and sequence of the region required for their replication in *Pseudomonas aeruginosa*. Gene **148**:81–86.

214. **Yu S, Jensen V, Seeliger J, Feldmann I, Weber S, Schleicher E, H??ussler S, Blankenfeldt W**. 2009. Structure elucidation and preliminary assessment of hydrolase activity of PqsE, the *Pseudomonas* quinolone signal (PQS) response protein. Biochemistry **48**:10298–10307.

215. **Heeb S, Blumer C, Haas D**. 2002. Regulatory RNA as mediator in GacA/RsmA-dependent global control of exoproduct formation in *Pseudomonas fluorescens* CHA0. J. Bacteriol. **184**:1046–1056.

216. **Xu H, Lin W, Xia H, Xu S, Li Y, Yao H, Bai F, Zhang X, Bai Y, Saris P, Qiao M**. 2005. Influence of *ptsP* gene on pyocyanin production in *Pseudomonas aeruginosa*. FEMS Microbiol. Lett. **253**:103–109.

217. **Wilhelm S, Gdynia A, Tielen P, Rosenau F, Jaeger KE**. 2007. The autotransporter esterase EstA of P*seudomonas aeruginosa* is required for rhamnolipid production, cell motility, and biofilm formation. J. Bacteriol. **189**:6695–6703.

218. **Hornef MW, Roggenkamp A, Geiger AM, Hogardt M, Jacobi CA, Heesemann J**. 2000. Triggering the ExoS regulon of *Pseudomonas aeruginosa*: A GFP-reporter analysis of exoenzyme (Exo) S, ExoT and ExoU synthesis. Microb. Pathog. **29**:329–343.

219. **Colson C**. 1977. Genetics of ribosomal protein methylation in *Escherichia coli*. I. A mutant deficient in methylation of protein L11. Mol. Gen. Genet. **154**:167–173.

220. **Do CB, Woods DA, Batzoglou S**. 2006. CONTRAfold: RNA secondary structure prediction without physics-based models. Bioinformatics **22**:e90–8.

221. **Pustelny C, Brouwer S, Müsken M, Bielecka A, Dötsch A, Nimtz M, Häussler S**. 2013. The peptide chain release factor methyltransferase PrmC is essential for pathogenicity and environmental adaptation of *Pseudomonas aeruginosa* PA14. Environ. Microbiol. **15**:597–609.

222. **Pesci EC, Milbank JBJ, Pearson JP, McKnight S, Kende AS, Greenberg EP, Iglewski BH**. 1999. Quinolone signaling in the cell-to-cell communication system of *Pseudomonas aeruginosa*. Proc. Natl. Acad. Sci. **96**:11229–11234.

223. **D'Argenio DA, Calfee MW, Rainey PB, Pesci EC**. 2002. Autolysis and autoaggregation in *Pseudomonas aeruginosa* colony morphology mutants. J. Bacteriol. **184**:6481–6489.

224. **Bredenbruch F, Nimtz M, Wray V, Morr M, Müller R, Häussler S**. 2005. Biosynthetic pathway of *Pseudomonas aeruginosa* 4-hydroxy-2-alkylquinolines. J. Bacteriol. **187**:3630–3635.

225. **Batey RT**. 2006. Structures of regulatory elements in mRNAs. Curr. Opin. Struct. Biol. **16**:299–306.

226. **Zafar MA, Carabetta VJ, Mandel MJ, Silhavy TJ**. 2014. Transcriptional occlusion caused by overlapping promoters. Proc. Natl. Acad. Sci. U. S. A. **111**:1557–61.

227. **Hughes TA**. 2006. Regulation of gene expression by alternative untranslated regions. Trends Genet. **22**:119–122.

228. **Hughes TA, Brady HJM**. 2005. Expression of axin2 is regulated by the alternative 5'-untranslated regions of its mRNA. J. Biol. Chem. **280**:8581–8588.

229. **Hughes TA, Brady HJM**. 2005. E2F1 up-regulates the expression of the tumour suppressor *axin2* both by activation of transcription and by mRNA stabilisation. Biochem. Biophys. Res. Commun. **329**:1267–1274.

230. **Sobczak K, Krzyzosiak WJ**. 2002. Structural determinants of BRCA1 translational regulation. J. Biol. Chem. **277**:17349–17358.

231. **Simon R, Priefer U, Pühler A**. 1983. A broad host range mobilization system for in vivo genetic engineering: Transposon mutagenesis in gram negative bacteria. Bio/Technology **1**:784-791.

232. **Hoang TT, Karkhoff-Schweizer RR, Kutchma AJ, Schweizer HP**. 1998. A broad-host-range Flp-FRT recombination system for site-specific excision of chromosomally-located DNA sequences: application for isolation of unmarked *Pseudomonas aeruginosa* mutants. Gene **212**:77–86.

233. **Blanka A, Schulz S, Eckweiler D, Franke R, Bielecka A, Nicolai T, Casilag F, Düvel J, Abraham W-R, Kaever V, Häussler S**. 2014. Identification of the alternative sigma factor SigX regulon and its implications for *Pseudomonas aeruginosa* pathogenicity. J. Bacteriol. **196**:345–56.

234. **Choi K-H, Gaynor JB, White KG, Lopez C, Bosio CM, Karkhoff-Schweizer RR, Schweizer HP**. 2005. A Tn7-based broad-range bacterial cloning and expression system. Nat. Methods **2**:443–8.

235. **Gödeke J, Heun M, Bubendorfer S, Paul K, Thormann KM**. 2011. Roles of two *Shewanella oneidensis* MR-1 extracellular endonucleases. Appl. Environ. Microbiol. **77**:5342–51.

236. **Choi K-H, Schweizer HP**. 2005. An improved method for rapid generation of unmarked *Pseudomonas aeruginosa* deletion mutants. BMC Microbiol. **5**:30.

237. **Greenfield NJ**. 2006. Using circular dichroism collected as a function of temperature to determine the thermodynamics of protein unfolding and binding interactions. Nat. Protoc. **1**:2527–35.

238. **Böhme K, Steinmann R, Kortmann J, Seekircher S, Heroven AK, Berger E, Pisano F, Thiermann T, Wolf-Watz H, Narberhaus F, Dersch P**. 2012. Concerted actions of a thermo-labile regulator and a unique intergenic RNA thermosensor control *Yersinia* virulence. PLoS Pathog. **8**:e1002518.

239. **Li G-W, Oh E, Weissman JS**. 2012. The anti-Shine–Dalgarno sequence drives translational pausing and codon choice in bacteria. Nature **484**:538-541.

240. **Oh E, Becker AH, Sandikci A, Huber D, Chaba R, Gloge F, Nichols RJ, Typas A, Gross CA, Kramer G, Weissman JS, Bukau B**. 2011. Selective ribosome profiling reveals the cotranslational chaperone action of trigger factor in vivo. Cell **147**:1295–1308.

241. **Kannan K, Kanabar P, Schryer D, Florin T, Oh E, Bahroos N, Tenson T, Weissman JS, Mankin AS**. 2014. The general mode of translation inhibition by macrolide antibiotics. Proc. Natl. Acad. Sci. **111**:15958–15963.

242. **Becker AH, Oh E, Weissman JS, Kramer G, Bukau B**. 2013. Selective ribosome profiling as a tool for studying the interaction of chaperones and targeting factors with nascent polypeptide chains and ribosomes. Nat. Protoc. **8**:2212–39.

243. **Dingwall C, Lomonossoff GP, Laskey RA**. 1981. High sequence specificity of micrococcal nuclease. Nucleic Acids Res. **9**:2659–2674.

244. **O'Connor PBF, Li GW, Weissman JS, Atkins JF, Baranov P V.** 2013. rRNA:mRNA pairing alters the length and the symmetry of mRNA-protected fragments in ribosome profiling experiments. Bioinformatics **29**:1488–1491.

245. **Plotkin JB, Kudla G**. 2011. Synonymous but not the same: the causes and consequences of codon bias. Nat. Rev. Genet. **12**:32–42.

246. **Gupta SK, Ghosh TC**. 2001. Gene expressivity is the main factor in dictating the codon usage variation among the genes in *Pseudomonas aeruginosa*. Gene **273**:63–70.

247. **Nakamura Y, Tabata S**. 1997. Codon-anticodon assignment and detection of codon usage trends in seven microbial genomes. Microb. Comp. Genomics **2**:299–312.

248. **Sharp PM, Li WH**. 1987. The codon adaptation index-a measure of directional synonymous codon usage bias, and its potential applications. Nucleic Acids Res. **15**:1281–1295.

249. **Shields DC, Sharp PM, Higgins DG, Wright F**. 1988. "Silent" sites in *Drosophila* genes are not neutral: evidence of selection among synonymous codons. Mol. Biol. Evol. **5**:704–716.

250. **Roymondal U, Das S, Sahoo S**. 2009. Predicting gene expression level from relative codon usage bias: An application to *Escherichia coli* genome. DNA Res. **16**:13–30.

251. **Jones PG, VanBogelen RA, Neidhardt FC**. 1987. Induction of proteins in response to low temperature in *Escherichia coli*. J. Bacteriol. **169**:2092–2095.

252. **Ermolenko DN, Makhatadze GI**. 2002. Bacterial cold-shock proteins. Cell. Mol. Life Sci. **59**:1902-1913.

253. **Lott BB, Wang Y, Nakazato T**. 2013. A comparative study of ribosomal proteins: linkage between amino acid distribution and ribosomal assembly. BMC Biophys. **6**:13.

254. **McCabe B**. 2010. Found in translation. Nat. Publ. Gr. **12**:238.

255. **Shah P, Ding Y, Niemczyk M, Kudla G, Plotkin JB**. 2013. Rate-limiting steps in yeast protein translation. Cell **153**:1589–601.

256. **Lackner DH, Beilharz TH, Marguerat S, Mata J, Watt S, Schubert F, Preiss T, Bähler J**. 2007. A network of multiple regulatory layers shapes gene expression in fission yeast. Mol. Cell **26**:145–155.

257. **Charneski CA, Hurst LD**. 2014. Positive charge loading at protein termini is due to membrane protein topology, not a translational ramp. Mol. Biol. Evol. **31**:70–84.

258. **Tuller T, Waldman YY, Kupiec M, Ruppin E**. 2010. Translation efficiency is determined by both codon bias and folding energy. Proc. Natl. Acad. Sci. U. S. A. **107**:3645–3650.

259. **Bailey TL, Elkan C**. 1994. Fitting a mixture model by expectation maximization to discover motifs in biopolymers. Proc. Int. Conf. Intell. Syst. Mol. Biol. **2**:28–36.

260. **De Smit MH, van Duin J**. 1994. Translational initiation on structured messengers. Another role for the Shine-Dalgarno interaction. J. Mol. Biol. **235**:173–184.

261. **Ringquist S, Shinedling S, Barrick D, Green L, Binkley J, Stormo GD, Gold L**. 1992. Translation initiation in *Escherichia coli*: sequences within the ribosome-binding site. Mol. Microbiol. **6**:1219–1229.

262. **Ishihama A**. 1997. Adaptation of gene expression in stationary phase bacteria. Curr. Opin. Genet. Dev. **7**:582-588.

263. **Ishihama A**. 1999. Modulation of the nucleoid, the transcription apparatus, and the translation machinery in bacteria for stationary phase survival. Genes to Cells **4**:135-143.

264. **Ma J, Campbell A, Karlin S**. 2002. Correlations between Shine-Dalgarno sequences and gene features such as predicted expression levels and operon structures. J. Bacteriol. **184**:5733–5745.

265. **Whiteley M, Bangera MG, Bumgarner RE, Parsek MR, Teitzel GM, Lory S, Greenberg EP**. 2001. Gene expression in *Pseudomonas aeruginosa* biofilms. Nature **413**:860–864.

266. **Han Y, Gao X, Liu B, Wan J, Zhang X, Qian S-B**. 2014. Ribosome profiling reveals sequence-independent post-initiation pausing as a signature of translation. Cell Res. **24**:842–51.

267. **Wada A, Yamazaki Y, Fujita N, Ishihama A**. 1990. Structure and probable genetic location of a "ribosome modulation factor" associated with 100S ribosomes in stationary-phase *Escherichia coli* cells. Proc. Natl. Acad. Sci. U. S. A. **87**:2657–2661.

268. **Wada A, Mikkola R, Kurland CG, Ishihama A**. 2000. Growth phase-coupled changes of the ribosome profile in natural isolates and laboratory strains of *Escherichia coli*. J. Bacteriol. **182**:2893–2899.

269. **Yoshida H, Maki Y, Kato H, Fujisawa H, Izutsu K, Wada C, Wada A**. 2002. The ribosome modulation factor (RMF) binding site on the 100S ribosome of *Escherichia coli*. J. Biochem. **132**:983–989.

270. **Kato T, Yoshida H, Miyata T, Maki Y, Wada A, Namba K**. 2010. Structure of the 100S ribosome in the hibernation stage revealed by electron cryomicroscopy. Structure **18**:719–724.

271. **Olshen AB, Hsieh AC, Stumpf CR, Olshen RA, Ruggero D, Taylor BS**. 2013. Assessing gene-level translational control from ribosome profiling. Bioinformatics **29**:2995–3002.

272. **Michel AM, Fox G, M. Kiran A, De Bo C, O'Connor PBF, Heaphy SM, Mullan JPA, Donohue CA, Higgins DG, Baranov P V.** 2014. GWIPS-viz: Development of a ribo-seq genome browser. Nucleic Acids Res. **42**:doi: 10.1093/nar/gkt1035.

273. **Diggle SP, Matthijs S, Wright VJ, Fletcher MP, Chhabra SR, Lamont IL, Kong X, Hider RC, Cornelis P, C??mara M, Williams P**. 2007. The *Pseudomonas aeruginosa* 4-Quinolone Signal Molecules HHQ and PQS Play Multifunctional Roles in Quorum Sensing and Iron Entrapment. Chem. Biol. **14**:87–96.

274. **McGrath S, Wade DS, Pesci EC**. 2004. Dueling quorum sensing systems in *Pseudomonas aeruginosa* control the production of the *Pseudomonas* quinolone signal (PQS). FEMS Microbiol. Lett. **230**:27–34.

275. **Folch B, Déziel E, Doucet N**. 2013. Systematic mutational analysis of the putative hydrolase PqsE: Toward a deeper molecular understanding of virulence acquisition in *Pseudomonas aeruginosa*. PLoS One **8**:e0073727.

276. **Rampioni G, Schuster M, Greenberg EP, Bertani I, Grasso M, Venturi V, Zennaro E, Leoni L**. 2007. RsaL provides quorum sensing homeostasis and functions as a global regulator of gene expression in *Pseudomonas aeruginosa*. Mol. Microbiol. **66**:1557–1565.

277. **Brandel J, Humbert N, Elhabiri M, Schalk IJ, Mislin GL a., Albrecht-Gary A-M**. 2012. Pyochelin, a siderophore of *Pseudomonas aeruginosa*: Physicochemical characterization of the iron(iii), copper(ii) and zinc(ii) complexes. Dalt. Trans. **41**:2820.

278. **Zaborin A, Romanowski K, Gerdes S, Holbrook C, Lepine F, Long J, Poroyko V, Diggle SP, Wilke A, Righetti K, Morozova I, Babrowski T, Liu DC, Zaborina O, Alverdy JC**. 2009. Red death in *Caenorhabditis elegans* caused by *Pseudomonas aeruginosa* PAO1. Proc. Natl. Acad. Sci. U. S. A. **106**:6327–6332.

279. **Kim K, Kim YU, Koh BH, Hwang SS, Kim SH, Lépine F, Cho YH, Lee GR**. 2010. HHQ and PQS, two *Pseudomonas aeruginosa* quorum-sensing molecules, down-regulate the innate immune responses through the nuclear factor-κB pathway. Immunology **129**:578–588.

280. **Dosselaere F, Vanderleyden J**. 2001. A metabolic node in action: chorismate-utilizing enzymes in microorganisms. Crit. Rev. Microbiol. **27**:75–131.

281. **Calhoun DH, Bonner CA, Gu W, Xie G, Jensen RA**. 2001. The emerging periplasm-localized subclass of AroQ chorismate mutases, exemplified by those from *Salmonella typhimurium* and *Pseudomonas aeruginosa*. Genome Biol. **2**:research0030-research0030.16.

282. **Euverink GJ, Wolters DJ, Dijkhuizen L**. 1995. Prephenate dehydratase of the actinomycete *Amycolatopsis methanolica*: purification and characterization of wild-type and deregulated mutant proteins. Biochem. J. **308**:313–320.

283. **Palmer KL, Aye LM, Whiteley M**. 2007. Nutritional cues control *Pseudomonas aeruginosa* multicellular behavior in cystic fibrosis sputum. J. Bacteriol. **189**:8079–8087.

284. **Palmer GC, Palmer KL, Jorth PA, Whiteley M**. 2010. Characterization of the *Pseudomonas aeruginosa* transcriptional response to phenylalanine and tyrosine. J. Bacteriol. **192**:2722–2728.

285. **Dietrich LEP, Price-Whelan A, Petersen A, Whiteley M, Newman DK**. 2006. The phenazine pyocyanin is a terminal signalling factor in the quorum sensing network of *Pseudomonas aeruginosa*. Mol. Microbiol. **61**:1308–21.

286. **Wurtzel O, Yoder-Himes DR, Han K, Dandekar AA, Edelheit S, Greenberg EP, Sorek R, Lory S**. 2012. The single-nucleotide resolution transcriptome of *Pseudomonas aeruginosa* grown in body temperature. PLoS Pathog. **8**:e1002945.

287. **Feinbaum RL, Urbach JM, Liberati NT, Djonovic S, Adonizio A, Carvunis AR, Ausubel FM**. 2012. Genome-wide identification of *Pseudomonas aeruginosa* virulence-related genes using a *Caenorhabditis elegans* infection model. PLoS Pathog. **8**:11.

288. **Wylie JL, Worobec EA**. 1995. The OprB porin plays a central role in carbohydrate uptake in *Pseudomonas aeruginosa*. J. Bacteriol. **177**:3021–3026.

289. **Groicher KH, Firek BA, Fujimoto DF, Bayles KW**. 2000. The *Staphylococcus aureus lrgAB* operon modulates murein hydrolase activity and penicillin tolerance. J. Bacteriol. **182**:1794–1801.

290. **Ranjit DK, Endres JL, Bayles KW**. 2011. *Staphylococcus aureus* CidA and LrgA proteins exhibit holin-like properties. J. Bacteriol. **193**:2468–2476.

291. **Rice KC, Nelson JB, Patton TG, Yang SJ, Bayles KW**. 2005. Acetic acid induces expression of the *Staphylococcus aureus cidABC* and *lrgAB* murein hydrolase regulator operons. J. Bacteriol. **187**:813–821.

292. **Patton TG, Yang SJ, Bayles KW**. 2006. The role of proton motive force in expression of the *Staphylococcus aureus cid* and *lrg* operons. Mol. Microbiol. **59**:1395–1404.

293. **Nelms J, Edwards RM, Warwick J, Fotheringham I**. 1992. Novel mutations in the *pheA* gene of *Escherichia coli* K-12 which result in highly feedback inhibition-resistant variants of chorismate mutase/prephenate dehydratase. Appl. Environ. Microbiol. **58**:2592–2598.

294. **Merrell DS, Thompson LJ, Kim CC, Mitchell H, Tompkins LS, Lee A, Falkow S**. 2003. Growth phase-dependent response of *Helicobacter pylori* to iron starvation. Infect. Immun. **71**:6510–6525.

295. **Leoni L, Ciervo A, Orsi N, Visca P**. 1996. Iron-regulated transcription of the *pvdA* gene in *Pseudomonas aeruginosa*: Effect of fur and PvdS on promoter activity. J. Bacteriol. **178**:2299–2313.

296. **Polack B, Dacheux D, Delic-Attree I, Toussaint B, Vignais PM**. 1996. The *Pseudomonas aeruginosa fumC* and *sodA* genes belong to an iron-responsive operon. Biochem. Biophys. Res. Commun. **226**:555–560.

297. **Hassett DJ, Howell ML, Sokol PA, Vasil ML, Dean GE**. 1997. Fumarase C activity is elevated in response to iron deprivation and in mucoid, alginate-producing *Pseudomonas aeruginosa*: Cloning and characterization *fumC* and purification of native *fumC*. J. Bacteriol. **179**:1442–1451.

298. **Yang L, Barken KB, Skindersoe ME, Christensen AB, Givskov M, Tolker-Nielsen T**. 2007. Effects of iron on DNA release and biofilm development by *Pseudomonas aeruginosa*. Microbiology **153**:1318–1328.

299. **Brouwer S, Pustelny C, Ritter C, Klinkert B, Narberhaus F, Haussler S**. 2014. The PqsR and RhlR transcriptional regulators determine the level of *Pseudomonas* quinolone signal synthesis in *Pseudomonas aeruginosa* by producing two different *pqsABCDE* mRNA Isoforms. J. Bacteriol. **196**:4163–4171.

300. **Ochsner UA, Wilderman PJ, Vasil AI, Vasil ML**. 2002. GeneChip® expression analysis of the iron starvation response in *Pseudomonas aeruginosa*: Identification of novel pyoverdine biosynthesis genes. Mol. Microbiol. **45**:1277–1287.

301. **Luo Q, Meneely KM, Lamb AL**. 2011. Entropic and enthalpic components of catalysis in the mutase and lyase activities of pseudomonas aeruginosa PchB. J. Am. Chem. Soc. **133**:7229–7233.

302. **Gaille C, Kast P, Dieter H**. 2002. Salicylate biosynthesis in *Pseudomonas aeruginosa*. Purification and characterization of PchB, a novel bifunctional enzyme displaying isochorismate pyruvate-lyase and chorismate mutase activities. J. Biol. Chem. **277**:21768–21775.

303. **Ahmad S, Weisburg WG, Jensen RA**. 1990. Evolution of aromatic amino acid biosynthesis and application to the fine-tuned phylogenetic positioning of enteric bacteria. J. Bacteriol. **172**:1051–1061.

304. **Ahmad S, Jensen RA**. 1987. The prephenate dehydrogenase component of the bifunctional T-protein in enteric bacteria can utilize L-arogenate. FEBS Lett. **216**:133–139.

305. **Latifi A, Winson MK, Foglino M, Bycroft BW, Stewart GSAB, Lazdunski A, Williams P**. 1995. Multiple homologues of LuxR and LuxI control expression of virulence determinants and secondary metabolites through quorum sensing in *Pseudomonas aeruginosa* PAO1. Mol. Microbiol. **17**:333–343.

306. **Van Rij ET, Wesselink M, Chin-A-Woeng TFC, Bloemberg G V, Lugtenberg BJJ**. 2004. Influence of environmental conditions on the production of phenazine-1-carboxamide by *Pseudomonas chlororaphis* PCL1391. Mol. Plant. Microbe. Interact. **17**:557–566.

307. **Lamb AL**. 2011. Pericyclic reactions catalyzed by chorismate-utilizing enzymes. Biochemistry.

308. **Patel N, Pierson DL, Jensen RA**. 1977. Dual enzymatic routes to L-tyrosine and L-phenylalanine via pretyrosine in *Pseudomonas aeruginosa*. J. Biol. Chem. **252**:5839–5846.

309. **Fiske MJ, Whitaker RJ, Jensen RA**. 1983. Hidden overflow pathway to L-phenylalanine in *Pseudomonas aeruginosa*. J. Bacteriol. **154**:623–631.

310. **Shen XH, Zhou NY, Liu SJ**. 2012. Degradation and assimilation of aromatic compounds by *Corynebacterium glutamicum*: Another potential for applications for this bacterium? Appl. Microbiol. Biotechnol. **95**:77-89.

311. **Elsemore DA, Ornston LN**. 1994. The *pca-pob* supraoperonic cluster of *Acinetobacter calcoaceticus* contains *quiA*, the structural gene for quinate-shikimate dehydrogenase. J. Bacteriol. **176**:7659–7666.

312. **Costaglioli P, Barthe C, Claverol S, Brözel VS, Perrot M, Crouzet M, Bonneu M, Garbay B, Vilain S**. 2012. Evidence for the involvement of the anthranilate degradation pathway in *Pseudomonas aeruginosa* biofilm formation. Microbiologyopen **3**:326-339.

313. **Kim S, Park H, Lee J**. 2015. Anthranilate deteriorates biofilm structure of *Pseudomonas aeruginosa* and antagonizes the biofilm-enhancing indole effect. Appl. Environ. Microbiol. doi: 10.1128/AEM.03551-14.

314. **Choi Y, Park HY, Park SJ, Park SJ, Kim SK, Ha C, Im SJ, Lee JH**. 2011. Growth phase-differential quorum sensing regulation of anthranilate metabolism in *Pseudomonas aeruginosa*. Mol. Cells **32**:57–65.

315. **Kreimer A, Borenstein E, Gophna U, Ruppin E**. 2008. The evolution of modularity in bacterial metabolic networks. Proc. Natl. Acad. Sci. U. S. A. **105**:6976–6981.

316. **Grüning NM, Lehrach H, Ralser M**. 2010. Regulatory crosstalk of the metabolic network. Trends Biochem. Sci.

317. **Kubota T, Tanaka Y, Takemoto N, Watanabe A, Hiraga K, Inui M, Yukawa H**. 2014. Chorismate-dependent transcriptional regulation of quinate/shikimate utilization

genes by LysR-type transcriptional regulator QsuR in *Corynebacterium glutamicum*: Carbon flow control at metabolic branch point. Mol. Microbiol. **92**:356–368.

318. **Kim SK, Im SJ, Yeom DH, Lee JH**. 2012. AntR-mediated bidirectional activation of *antA* and *antR*, anthranilate degradative genes in *Pseudomonas aeruginosa*. Gene **505**:146–152.

319. **Jeffery CJ**. 1999. Moonlighting proteins. Trends Biochem. Sci. **24**:8-11.

320. **Copley SD**. 2003. Enzymes with extra talents: Moonlighting functions and catalytic promiscuity. Curr. Opin. Chem. Biol. **7**:265-272.

321. **Henderson B, Martin A**. 2011. Bacterial virulence in the moonlight: Multitasking bacterial moonlighting proteins are virulence determinants in infectious disease. Infect. Immun. **79**:3476-3491.

322. **Cunliffe HE, Merriman TR, Lamont IL**. 1995. Cloning and characterization of *pvdS*, a gene required for pyoverdine synthesis in *Pseudomonas aeruginosa*: PvdS is probably an alternative sigma factor. J. Bacteriol. **177**:2744–2750.

323. **Wilson MJ, McMorran BJ, Lamont IL**. 2001. Analysis of promoters recognized by PvdS, an extracytoplasmic-function sigma factor protein from *Pseudomonas aeruginosa*. J. Bacteriol. **183**:2151–2155.

324. **Rinehart D, Johnson CH, Nguyen T, Ivanisevic J, Benton HP, Lloyd J, Arkin AP, Deutschbauer AM, Patti GJ, Siuzdak G**. 2014. Metabolomic data streaming for biology-dependent data acquisition. Nat. Biotechnol. **32**:524–7.

325. **Gowda H, Ivanisevic J, Johnson CH, Kurczy ME, Benton HP, Rinehart D, Nguyen T, Ray J, Kuehl J, Arevalo B, Westenskow PD, Wang J, Arkin AP, Deutschbauer AM, Patti GJ, Siuzdak G**. 2014. Interactive XCMS online: Simplifying advanced metabolomic data processing and subsequent statistical analyses. Anal. Chem. **86**:6931–6939.

326. **Benton HP, Ivanisevic J, Mahieu NG, Kurczy ME, Johnson CH, Franco L, Rinehart D, Valentine E, Gowda H, Ubhi BK, Tautenhahn R, Gieschen A, Fields**

MW, Patti GJ, Siuzdak G. 2015. Autonomous metabolomics for rapid metabolite identification in global profiling. Anal. Chem. **87**:884–891.

327. **Tautenhahn R, Patti GJ, Rinehart D, Siuzdak G**. 2012. XCMS online: A web-based platform to process untargeted metabolomic data. Anal. Chem. **84**:5035–5039.

328. **Garbom S, Forsberg Å, Wolf-Watz H, Kihlberg BM**. 2004. Identification of novel virulence-associated genes via genome analysis of hypothetical genes. Infect. Immun. **72**:1333–1340.

329. **Bazzini AA, Johnstone TG, Christiano R, MacKowiak SD, Obermayer B, Fleming ES, Vejnar CE, Lee MT, Rajewsky N, Walther TC, Giraldez AJ**. 2014. Identification of small ORFs in vertebrates using ribosome footprinting and evolutionary conservation. EMBO J. **33**:981–993.

330. **Dunn JG, Foo CK, Belletier NG, Gavis ER, Weissman JS**. 2013. Ribosome profiling reveals pervasive and regulated stop codon readthrough in *Drosophila melanogaster*. eLife **2**:e01179.

8 Acknowledgment

I would like to thank my PhD supervisor Prof. Susanne Häußler who provided excellent guidance and gave me the opportunity to perform this exciting project. Her optimism and inventiveness were contagious and often helped to find the appropriate solution. Especially I need to thank Dr. Christian Pustelny for his never-ending help, fruitful discussions and to find and maintain a perfect balance between work life and social life. I am glad you were around during my PhD!

Further thanks go to my first referee and mentor Prof. Michael Steinert and Prof. Dietmar Schomburg for being member of the examination committee.

Many thanks to all members of the group MOBA, for the ideal coordination of the work, the nice working atmosphere and the great help by providing ideas and materials to perform my experiments. It has been a great pleasure working with all of you throughout the years, and I sincerely hope that we can stay in touch.

In addition to the aforementioned colleagues, I would also like to thank all of the collaborators who contributed to this thesis, as well as the side projects that I have been involved with over the years. In particular, I would like to thank Dr. Ariane Khaledi for her contribution to the establishment of Ribo-Seq.

Thanks go to the members of my thesis committees, Prof. Irene Wagner-Döbler and Dr. Max Schomburg, for their interest in my project and for inspiring discussions.

A deep thank at the end to all my relatives for everything they have done for me. It is important to point out my great parents as I am grateful, that they always supported me in all of my endeavors. Thank you so much for being there when I needed a helping hand!